



## MOLECULAR TOOLS FOR THE RAPID AND COST-EFFECTIVE DETECTION OF SMALL MOLECULES

Xhensila Shkempi

**ADVERTIMENT.** L'accés als continguts d'aquesta tesi doctoral i la seva utilització ha de respectar els drets de la persona autora. Pot ser utilitzada per a consulta o estudi personal, així com en activitats o materials d'investigació i docència en els termes establerts a l'art. 32 del Text Refós de la Llei de Propietat Intel·lectual (RDL 1/1996). Per altres utilitzacions es requereix l'autorització prèvia i expressa de la persona autora. En qualsevol cas, en la utilització dels seus continguts caldrà indicar de forma clara el nom i cognoms de la persona autora i el títol de la tesi doctoral. No s'autoritza la seva reproducció o altres formes d'explotació efectuades amb finalitats de lucre ni la seva comunicació pública des d'un lloc aliè al servei TDX. Tampoc s'autoritza la presentació del seu contingut en una finestra o marc aliè a TDX (framing). Aquesta reserva de drets afecta tant als continguts de la tesi com als seus resums i índexs.

**ADVERTENCIA.** El acceso a los contenidos de esta tesis doctoral y su utilización debe respetar los derechos de la persona autora. Puede ser utilizada para consulta o estudio personal, así como en actividades o materiales de investigación y docencia en los términos establecidos en el art. 32 del Texto Refundido de la Ley de Propiedad Intelectual (RDL 1/1996). Para otros usos se requiere la autorización previa y expresa de la persona autora. En cualquier caso, en la utilización de sus contenidos se deberá indicar de forma clara el nombre y apellidos de la persona autora y el título de la tesis doctoral. No se autoriza su reproducción u otras formas de explotación efectuadas con fines lucrativos ni su comunicación pública desde un sitio ajeno al servicio TDR. Tampoco se autoriza la presentación de su contenido en una ventana o marco ajeno a TDR (framing). Esta reserva de derechos afecta tanto al contenido de la tesis como a sus resúmenes e índices.

**WARNING.** Access to the contents of this doctoral thesis and its use must respect the rights of the author. It can be used for reference or private study, as well as research and learning activities or materials in the terms established by the 32nd article of the Spanish Consolidated Copyright Act (RDL 1/1996). Express and previous authorization of the author is required for any other uses. In any case, when using its content, full name of the author and title of the thesis must be clearly indicated. Reproduction or other forms of for profit use or public communication from outside TDX service is not allowed. Presentation of its content in a window or frame external to TDX (framing) is not authorized either. These rights affect both the content of the thesis and its abstracts and indexes.



UNIVERSITAT  
ROVIRA i VIRGILI

# **Molecular tools for the rapid and cost-effective detection of small molecules**

**Xhensila Shkempi**

**Doctoral Thesis 2021**

# Doctoral Thesis

## Molecular tools for the rapid and cost-effective detection of small molecules

**XHENSILA SHKEMBI**

**Supervised by: Prof. Ciara K. O'Sullivan**

**Dr. Vasoula Skouridou**

**Doctoral Programme in Nanoscience, Materials and Chemical Engineering**

**Departament d'Enginyeria Química**

**INTERFIBIO group**



**UNIVERSITAT ROVIRA I VIRGILI**

**Tarragona**

**2021**



## DEPARTAMENT D'ENGINYERIA QUÍMICA

Universitat Rovira i Virgili

Av. Països Catalans 26

43007 Tarragona, Spain

Tel: 977 55 96 58

Fax: 977 55 96 67

### CERTIFY:

That the doctoral thesis entitled: "Molecular tools for the rapid and cost-effective detection of small molecules" submitted by Xhensila Shkempi in order to achieve the Degree of Doctor, has been carried out under our supervision, at Department of Chemical Engineering at Universitat Rovira i Virgili and that it fulfils all the requirements to be eligible for the Doctorate Award.

Tarragona, September 1<sup>st</sup>, 2021

### Doctoral Thesis Supervisors



Prof. Ciara K. O'Sullivan



Dr. Vasoula Skouridou

## Acknowledgments

During these years of my PhD, I get to know a lot of people, each of them give me support, love, and their time and no words can express the gratitude and the love that my heart feels for every person during my PhD journey.

First of all, I would like to express my sincere acknowledgement to my director of my thesis **Prof. Ciara K. O'Sullivan**, for giving me the opportunity to undertake this research for my doctoral thesis in her group. She was very patient and gave me thoughtful advice throughout this project with her advice and support. It has been a very enriching experience in many aspects, beyond the scientific and academic field. Thank you for everything.

To my supervisors **Marketa** and **Vasso**, thank you for every support in my everyday challenges in the lab, but also for every personal support and kind word, you have always been there for me and helping take this research to a level that may not have otherwise been possible

I would also like to thank all the technical and scientific help that I have received from **Miriam, Mayreli, Tete, Carmen, and Mary Luz**, you were always there for my questions and curiosity. Thank you also for your positivity and good sense of humor in every moment.

To **Bàrbara** and **Núria** for all the help received in bureaucratic issues and for being there in any situation.

During my Ph.D. I've met many wonderful people. I started the trip with some of them, others have already left and others will continue long after I leave, but all of them will always have a special place on my memories.

Thank you **Nihad, Nasif, Julio**, for sharing the same trip with me, **Zaida** for always being there in our early working hours, for your jokes and your beautiful heart.

Thank you **Cristoph, Shaira, Sharmaine, Emelina, Nerissa, Keylin, Melike, and Eoaden and Cathrine** for all the shared moments.

Thank you, **Valerie**, my SELEX mate, for your love, for late night working hours to select our aptamers. Thank you, Tine, for being there when I needed the most, for being my right arm, when I couldn't use mine 😊, we started together some years ago and now I wish you all the best in your PhD trip.

Thank you, **Ivan** and **Laura**, for being my "Musketees", for the support, for the friendship, advice, and for everything we have done together. You are special to me, thank you for being part of my life. You were there from the begging,,like a family,,you will always be in my heart.

To **Cansu** and **Evelin**, for the beautiful moments that we had at lab, for the tears and jokes, for the love, and hugs in these last months of my PhD. You are beautiful people, and you deserve the best.

To all members of **INTERFIBIO** group, thank you for everything.

To my friends that I had the chance to meet in Tarragona, **Elena, Antonio, Carlos, Ceride, Hava, Hande, Mohsen, Koorosh, Ayda, Abdelal, Wassima, Nasibe, Elena, Betul, Noelia, Katerina** and **Vasilis** thank you for the beautiful moments.

*“What can you do to promote world peace? Go home and love your family.”* That’s what our beloved Mother Teresa used to say.

I am blessed to share every second of this journey with my family and to feel their unconditional love. I am indebted to the unconditional love and support of my family. I especially thank my mother **Fatmira** for nurturing my curiosity and being by my side throughout all these years of my education. My brother **Klevis**, my biggest support, who even in distance was always there for me, in bad and good times. My father **Maksi** who always takes care of me with his enormous sacrifices and wisdom words that I always will use in my life. Without their sacrifices and honesty, my longing to become a scientist would have only been a dream. I thank my **grandmother** and my **uncle**, you are not among us today, but I know that wherever you are proud of me.

Finally, I would like to thank my fiancé, **Albenc**, my biggest support in this road, he showed me the right way to science and life, with his patience and unconditional love he was always there by my side.

I love you all and my heart belongs to you!

Thank you all from the bottom of my heart!

## Contents

Chapter 1 .....	15
1.1 Aptamers as biorecognition molecules .....	15
1.1.1 Aptamers <i>versus</i> antibodies .....	16
1.1.2 Disadvantages of aptamers .....	18
SELEX process .....	18
1.1.1 Designing the library pool.....	19
1.2.2 Selection rounds of SELEX .....	21
1.2.2.1 Co-incubation .....	21
1.2.2.2 Partition.....	22
1.2.2.3 Elution.....	23
1.2.2.4 Amplification .....	24
1.2.2.5 Preparation of single-stranded DNA .....	25
1.1.2 Monitoring of SELEX process .....	25
1.1.3 Cloning and sequencing.....	26
1.2.5 The characterization and validation of selected aptamers .....	26
Different types of SELEX .....	27
1.3.1 CE-SELEX .....	27
1.3.2 Microfluidic SELEX .....	28
1.3.3 High-throughput Sequencing SELEX .....	29
1.3.4 <i>In vivo</i> SELEX .....	29
1.3.5 Cell SELEX.....	30
1.4 SELEX type focused more on small molecules .....	32
1.4.1 Problems associated with small- molecule binding aptamers .....	32
1.4.2 Magnetic beads-based SELEX .....	34
1.4.3 GO-SELEX .....	36
1.4.4 Capture SELEX.....	38
Characterization of aptamers for small molecules .....	40
1.5.1 Enzyme linked aptamer assay (ELAA).....	40
1.5.2 Surface plasmon resonance (SPR) .....	41
1.5.3 Microscale Thermophoresis (MST).....	41
1.5.4 Apta-PCR affinity assay (APPA).....	42
1.5.5 Isothermal Titration Calorimetry (ITC) .....	42
1.5.6 Biolayer interferometry (BLI).....	42

1.5.7 Equilibrium filtration or dialysis .....	43
1.5.8 Fluorescent binding assay .....	43
Aptamer-based biosensors.....	44
1.6.1 Optical-based aptasensors .....	44
1.6.2 Electrochemical aptasensors.....	46
1.7 Lateral flow aptamer assays .....	47
1.7.1 Sandwich aptamer lateral flow assay .....	48
1.7.2 Competitive lateral flow aptamer assay.....	49
References.....	52
2.1. Introduction.....	70
2.2. Experimental section .....	73
2.2.1. Materials.....	73
2.2.2. Capture-SELEX process .....	74
2.2.3. Next Generation Sequencing (NGS) and data analysis.....	74
2.2.4. Determination of affinity dissociation constants ( $K_D$ ) .....	75
2.2.5. Hybrid antibody-aptamer sandwich assay for TTX determination .....	75
2.2.6. Fish samples and TTXs extraction.....	76
2.2.7. Detection of TTX in puffer fish.....	76
2.3. Results and Discussion.....	77
2.3.1. Selections.....	77
2.3.2. NGS and identification of aptamer candidates .....	78
2.3.3. Screening of the aptamer candidates .....	81
2.3.4. Binding properties of the aptamer candidates .....	81
2.3.5. TTX detection with a hybrid antibody-aptamer sandwich assay .....	82
2.3.6. Application of the assay to puffer fish analysis.....	84
2.4 Conclusions.....	85
2.5. References .....	86
2.6 Supplementary information .....	91
2.6.1. Selection process.....	91
2.6.2. NGS analysis .....	93
2.6.3. Characterization of aptamer candidates.....	100
2.6.3.1 Immobilization of TTX on magnetic beads for affinity assays .....	100
2.6.3.2 Initial screening of the aptamer candidates.....	100
2.6.4. TTX detection.....	102
2.6.4.1 Magnetic bead-based colorimetric immunoassay for TTX detection .....	103
2.6.5. References .....	105

3.1. Introduction.....	108
3.2. Materials and methods .....	110
3.2.1. Chemicals and reagents.....	110
3.2.2 Oligonucleotide sequences .....	111
3.2.3 Development of the dipstick assay for TTX.....	111
3.2.4 Preparation of gold nanoparticle labelled reporter aptamer conjugates.....	112
3.2.5 Calibration Curve .....	112
3.2.6 Sensitivity and specificity of the dipstick assay.....	112
3.2.7 Fish extracts for TTX detection.....	113
3.3. Results and discussions .....	113
3.3.1 Optimization of the dipstick assay .....	113
3.3.2 Cross-reactivity studies. ....	117
3.3.2 Analysis of TTX in puffer fish samples .....	117
3.4. Conclusions.....	118
3.5. References .....	119
4. 1. Introduction.....	123
4. 2. Experimental.....	125
4. 2. 1 Materials.....	125
4. 2. 2 <i>In vitro</i> selection .....	126
4. 2.3 Next Generation Sequencing (NGS) and identification of aptamer candidates.....	126
4. 2. 4 Apta-PCR affinity assay (APAA).....	127
4. 2. 5 Bead-Enzyme Linked Aptamer Assay (bead-ELAA).....	127
4. 2. 6 Enzyme Linked Aptamer Assay (ELAA) .....	127
4. 2. 7 Gold nanoparticles (AuNPs)-aptamer assay for NAND detection .....	128
4. 3. Results and Discussion.....	128
4. 3. 1 Selection process .....	128
4. 3. 2 NGS and identification of aptamer candidates .....	129
4. 3. 3 Affinity and specificity of the aptamers.....	130
4. 3. 4 AuNP-aptamer assay for NAND detection.....	132
4. 5. Conclusions.....	134
4.6 References.....	135
4.6 Supplementary information .....	139
4.6.1. Materials and methods .....	139
4.6.1.1 Structures of the molecules .....	139
4.6.1.2 Preparation of carboxymethyloxime (CMO) derivatives of steroids.....	139
4.6.1.3 Preparation of sepharose media for negative and counter selection steps .....	140

4.6.1.4 Preparation of steroid-magnetic beads.....	140
4.6.1.5 Immobilization of nandrolone on microtiter plates for binding studies.....	141
4.6. 2. Next Generation Sequencing for aptamer identification.....	141
4.6.3. Aptamer characterization.....	145
4.6.4 AuNPs-aptamer assay for NAND detection.....	147
4.6.5 References.....	148

## **Summary**

In recent years, the interest in developing biosensors for the detection and monitoring of low molecular weight targets is increased. These small molecules play important roles in human health, environmental, food, and biomedical field, including different groups such as antibiotics, toxin, ions, drugs, steroids, and different chemicals. In this thesis work we studied and evaluate the possible novel methods of detection for two different small molecules, tetrodotoxin, part of marine toxins and nandrolone, an anabolic steroid.

Tetrodotoxin (TTX) is a paralytic marine neurotoxin causing seafood poisoning after the ingestion of contaminated marine food such as puffer fish and shellfish. Its paralytic toxic effects derive from its selective binding to voltage-gated sodium channels and ultimately interfering with neural transmission. Symptoms of TTX intoxication include numbness sensation in the mouth, headache, vomiting, muscle weakness, and even fatal respiratory or heart failure. Puffer fish poisoning is typical of warm waters and was regarded as a problem confined to Asian countries, but in recent years, TTX has been reported and detected in seafood in many different European countries including Spain, Greece, United Kingdom, France and Italy. The high toxicity and the increase incidence requires fast and cost-effective detection techniques.

The second target that we studied, nandrolone, is an androgenic anabolic steroid (AAS) functioning as a growth promoting agent which helps to gain muscle weight. Its AAS properties have led to its exploitation as a doping agent in sports and horse racing, whereas it is also used as an animal feed additive on the other hand, several studies report the presence of nandrolone in dietary supplements as a cross-contaminant and consumption of such supplements could lead to accidental doping. Adverse side effects are associated with nandrolone accumulation in the body such as endocrine, cardiovascular, skin and psychiatric disorders. It is therefore evident that monitoring the presence of nandrolone in human and animal biological fluids, meat products and nutritional supplements is essential to protect public health and discourage doping practices in sports.

For both types of these molecules, liquid or gas chromatography-mass spectroscopy is routinely used for laboratory-based analysis of field samples. Competitive immunoassays have also been developed and are available in the market for their detection. Aptamers are biorecognition molecules considered as alternative to antibodies which are suitable for the detection of any type of target and have great potential in analytical applications. They are artificial synthetic nucleic acids (RNA/DNA) that bind specifically to their target, and they are selected through an *in vitro* iterative process called Systematic Evolution of Ligands by Exponential enrichment (SELEX). The development of aptamers for small molecules is a challenging task, especially when you deal with small molecules as they lack the multiple binding sites in their structures. Although, in our work we sought to develop novel aptamers binding to TTX and Nandrolone and exploit them for their detection in different assays.

For TTX aptamers identification was used a variation of SELEX suitable for small molecules (Capture-SELEX), while nandrolone aptamers were identified using a classical SELEX

process with nandrolone-Sepharose resin. Both selections were done in combination with high-throughput Next Generation Sequencing and binding properties of the selected aptamers were characterized.

Finally for the best identified aptamer 2 different types of assays were developed. For TTX was developed a highly sensitive and user-friendly antibody-aptamer sandwich dipstick format assay which was successfully applied for the detection of TTX in puffer fish extracts. For Nandrolone a label-free colorimetric assay was finally developed using the aptamer for its detection based on gold nanoparticles and their aggregation in the presence of target molecules after salt addition.

In my thesis it is discussed the general objectives and subobjectives of this work. Chapter 1 includes a detailed introduction of the state of art of the research area. It provides a brief information about aptamers and their methods of selection against different types of small molecules by using different types of selection. Moreover, is given a general view of different types of aptasensor used for small molecules detection.

The detailed selection process of the TTX aptamers isolation is detailed in Chapter 2. Capture SELEX is implemented for immobilizing ssDNA on the surface of streptavidin magnetic beads and TTX target is free in the solution throughout selection process. The affinity of the selected aptamers was confirmed by two different methodologies, APAA and Bead-ELAA. Finally, one of the aptamer selected was used hybrid antibody-aptamer sandwich assay for TTX detection in puffer fish extracts.

Chapter 3 describes the proof of concept of a highly specific and sensitive dipstick format assay for point of care devices, and its application in real puffer fish sample detection including gonads, muscle, skin and liver extracts. Finally, the specificity of this format was also evaluated, by analyzing the interference of other marine toxins which can be present in the same sample.

In Chapter 4 is reported the selection performed for the identification of nandrolone aptamers and their characterization of the binding properties. Moreover, an easy and rapid colorimetric assay was developed for nandrolone detection using the adsorption of aptamer on gold nanoparticle which prevent their aggregation, while in the presence of nandrolone, aptamer is bind to nandrolone and gold nanoparticles aggregate after the salt addition.

## **Resum**

L'interès per la detecció de molècules amb un baix pes molecular s'ha incrementat els darrers anys. Monitoritzar els nivells de molècules petites amb activitat biològica, com ara els antibiòtics, toxines, marcadors moleculars, ions metàl·lics, medicaments i esteroides entre altres, es molt important en el camp de la biomedicina, la monitorització ambiental i el control i la seguretat alimentària. Els assajos analítics i els biosensors amb alta sensibilitat, especificitat, assequibles i portàtils capaços de detectar aquest tipus de molècules petites son necessaris per a assegurar la salut pública. En aquesta tesis, s'han escollit dues molècules diana: la tetrodotoxina (toxina marina) i la nandrolona (esteroide anabòlic).

La Tetrodotoxina (TTX) es una neurotoxina marina paralitzant que pot causar intoxicació alimentària després d'ingerir aliments contaminats com ara el peix globus o mariscs. Els seus efectes tòxics es deriven de la seva afinitat als canals de sodi cel·lulars, interferint amb la transmissió neuronal. Els símptomes per intoxicació amb TTX inclouen sensació de adormiment de la boca, mal de cap, vòmits, debilitat muscular, i fins i tot aturades cardío-respiratòries. La intoxicació per la ingesta de peix globus es comuna en aigües càlides i ha estat típicament un problema associat als països asiàtics. No obstant, i en els darrers anys, s'han detectat aliments marins contaminats amb TTX en diferents països Europeus, incloent Espanya, Grècia, El Regne Unit, França i Itàlia. La gran toxicitat i l'augment en la incidència d'intoxicacions per TTX requereix tècniques de detecció ràpides i assequibles.



# Chapter 1

---

## Introduction

## Chapter 1

### 1.1 Aptamers as biorecognition molecules

Molecular recognition is a specific biological interaction between two or more molecules which exhibit molecular complementarity via non-covalent bonding including hydrogen bonding, hydrophobic forces<sup>1</sup>, van der Waals forces,  $\pi$ - $\pi$  interactions, and electrostatic interactions<sup>2</sup>. At the cellular level, these molecular recognition or binding events may occur between proteins and small molecules to induce signalling processes<sup>3</sup>, between proteins and nucleic acids, such as in DNA/histone interactions<sup>4</sup>, and between nucleic acids and small molecules, such as those displayed by riboswitches<sup>5</sup>. Taking advantages of these recognition principles, researchers have developed target detection methods as well as therapeutics for countless diseases. While antibodies have been the gold standard for recognition for several decades, aptamers are emerging as an attractive alternative for the specific detection of a wide range of target molecules.

Aptamers are a class of single-stranded DNA (ssDNA) or RNA oligonucleotides, which form three-dimensional structures enabling their specific binding with a target. Aptamers are selected from large library pools using an iterative selection process termed Systematic Evolution of Ligands by Exponential Enrichment (SELEX). The word aptamer stems from the Latin “*aptus*”-meaning “*to fit*”, and the Greek word “*meros*”-meaning “*part*”. Aptamers were first reported by Ellington & Szostak and Tuerk & Gold, who independently developed techniques to select RNA aptamers against specific organic dyes and T4 DNA polymerase, respectively<sup>6,7</sup> and since then there has been an exponential growth in the number of publications detailing the selection and applications of aptamers (Figure 1.1).

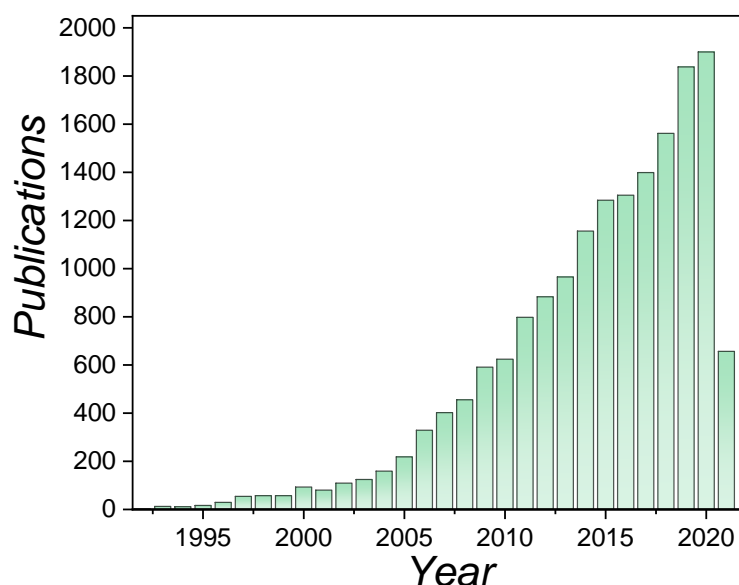


**Figure 1.1.** Number of publications as a function of the years involving the research in aptamers. (Data extracted from PubMed).

The ability of aptamers to fold into distinct 3D conformations characterised by stems, loops, hairpins, bulges, triplexes, and quadruplexes facilitates the high affinity binding and selectivity to their target (Figure 1.2). Aptamers bind selectively to their target through intermolecular interactions, such as van der Waals forces, hydrogen bonding, electrostatic interactions between charged groups, and  $\pi$ - $\pi$  stacking of “flat-structured” aromatic moieties<sup>8</sup>, which allow them to interact with a wide variety of target molecules from single molecules to complex target mixtures or even whole cells with dissociation constants ( $K_D$ ) typically in the low nanomolar range, comparable to those observed for monoclonal antibodies<sup>9</sup>.

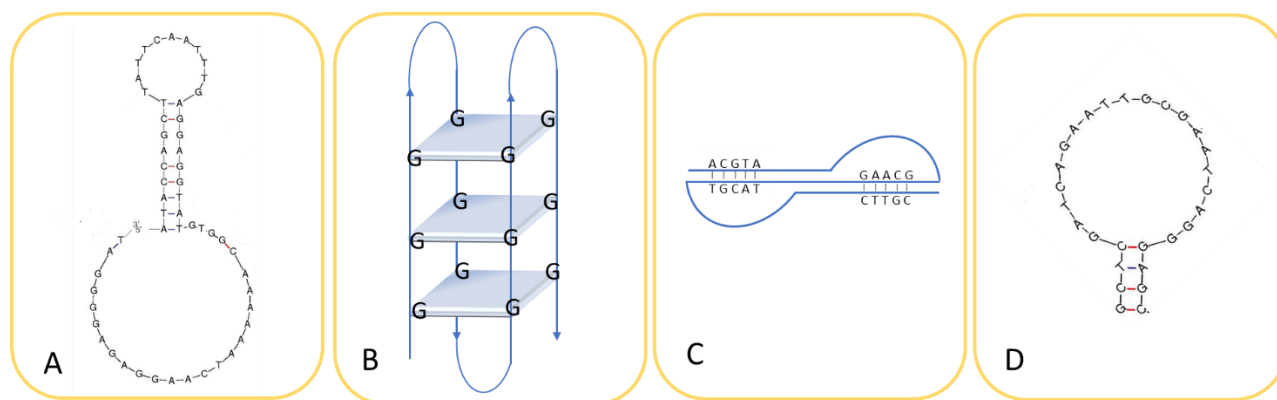


**Figure 1.2.** (A) stem-loop/ bulge (RNA ligand for ATP), (B) G-quartet (DNA ligand for thrombin), (C) Pseudoknot (RNA ligand for HIV-1 reverse transcriptase), (D) hairpin (RNA ligand for Bacteriophage T4 polymerase)<sup>10</sup>.

### 1.1.1 Aptamers *versus* antibodies

Aptamers possess similar affinity and specificity as monoclonal antibodies. Despite that, they offer multiple advantages including a relative ease of large-scale synthesis at affordable costs with no batch-to-batch variation, physical stability, and facile chemical modification<sup>11,12</sup> (Table 1.1). Aptamers can be selected against toxic and non-immunogenic compounds, whereas antibodies cannot be developed due to lethal damage of these toxic molecules on the host animals prior to the production of antibodies. Further, the production of these antibodies, requires sacrificing the host animal and in addition, antibodies are relatively expensive compared to aptamers<sup>13</sup>. On the other hand, aptamers are not immunogenic or toxic in *in vivo* levels as nucleic acids are not typically recognised by the human immune system as foreign agents<sup>14,15</sup>. Pegaptanib, the first aptamer approved by the US Food and Drug Administration agency (FDA) against wet Age-related Macular Degeneration (AMD) displayed no immunogenicity in either preclinical evaluation in animals or clinical trials in patients<sup>16</sup>. Due to their relatively small sizes, even compared to antibodies, aptamers can penetrate easily through tissues and even cells<sup>17</sup>. Aptamers have binding affinities that are comparable to, and in some examples, even surpass those of monoclonal antibodies. Due to the inclusion of counter selection steps in SELEX they are inherently extremely specific, as demonstrated by the theophylline aptamer developed by Jenison *et al.*, which showed an affinity for its cognate ligand that is 10,000-fold higher than that for caffeine, which differs from theophylline by only a single methyl group at nitrogen atom N-7<sup>18</sup>. The arginine aptamer

developed by Geiger *et al.* showed a 12,000 fold stronger affinity with L-arginine than with D-arginine<sup>19</sup>. These properties position aptamers as ideal candidates for therapeutics and diagnostics.

Furthermore, once the aptamers sequence is identified, they can be synthesized with high purity, reproducibly and at a relatively low cost as compared to antibodies (Table 1.1). Aptamers can be easily chemically modified with various chemical tags including fluorescence probes, quenchers, electrochemical indicators, nanoparticles, or enzymes. These modifications can allow the immobilization of aptamers on various solid supports, provide stability against nucleases, and allow the incorporation of labels for use in various methods of detection.

**Table 1.1.** Characteristics for antibodies and aptamers.

	Aptamer	Antibody
<b>Stability &amp; Storage</b>	<ul style="list-style-type: none"> <li>➤ Long shelf life at room temperature</li> <li>➤ Remains stable after multiple freeze thaws</li> <li>➤ Can be designed to resist enzymes</li> <li>➤ Can be stored digitally and re-synthesized at low cost</li> </ul>	<ul style="list-style-type: none"> <li>➤ Long shelf life when frozen</li> <li>➤ Degrades after multiple freeze thaws</li> <li>➤ Cannot be designed to resist enzymes</li> <li>➤ Hybridoma storage and maintenance required</li> </ul>
<b>Development &amp; Scalability</b>	<ul style="list-style-type: none"> <li>➤ 3-5 months (selection and sequencing)</li> <li>➤ No animals required</li> <li>➤ &lt; 1 week to replenish</li> <li>➤ Very low batch-to-batch variability</li> </ul>	<ul style="list-style-type: none"> <li>➤ 6-9 months (immunization and hybridoma development)</li> <li>➤ Animals required</li> <li>➤ 3-4 weeks to replenish</li> <li>➤ Low to moderate batch-to-batch variability</li> </ul>
<b>Target Molecule</b>	<ul style="list-style-type: none"> <li>➤ Any target may be used</li> <li>➤ Poor immunogens or small molecules: no conjugation required to enhance selection</li> </ul>	<ul style="list-style-type: none"> <li>➤ Target limit to immunogenic, non-toxic molecules</li> <li>➤ Poor immunogens or small molecules: carrier protein molecules to enhance immunogenicity</li> </ul>
<b>Modification</b>	<ul style="list-style-type: none"> <li>➤ Easy conjugated to proteins, peptides, drugs and other small molecules</li> <li>➤ Can be modified with fluorescent dyes</li> <li>➤ Inexpensive to biotinylate (~100\$/mg)</li> </ul>	<ul style="list-style-type: none"> <li>➤ Poor immunogens or small molecules: carrier protein molecules to enhance immunogenicity</li> <li>➤ Easy conjugated to proteins, peptides, drugs and other small molecules</li> <li>➤ Can be modified with fluorescent dyes</li> <li>➤ Expensive to biotinylate (~1000\$/mg)</li> </ul>
<b>Cost</b>	<ul style="list-style-type: none"> <li>➤ Individual aptamer selection: 4000\$</li> <li>➤ Once selected cost 100 \$</li> </ul>	<ul style="list-style-type: none"> <li>➤ Monoclonal antibody: 4000\$</li> <li>➤ Polyclonal antibody: 1000\$</li> </ul>

### 1.1.2 Disadvantages of aptamers

Nowadays, a large number of aptamers have been selected and exploited in different applications for a wide range of targets as bacteria/pathogens<sup>20,21</sup>, proteins<sup>22</sup>, toxins<sup>23</sup>, viruses<sup>19</sup>, cells<sup>24</sup>, and tissues<sup>25</sup>. However, the process of aptamer production, SELEX, is still a long labour-intensive, repetitive process that requires trained personnel. Robots have been developed for the automation of SELEX, but conditions and parameters (selection buffer, pH, concentrations), need to be optimized per each specific target. Notably, at the *in vitro* level, the rate of the successful selection of the aptamers does not exceed 30%<sup>26</sup>.

Aptamers, despite displaying high specificity in *in vitro* levels, may fail to efficiently bind to the specific target when used *in vivo*. This drawback arises due to their specific chemistry which renders them hydrophilic. In addition, non-modified RNA aptamers particularly, can degrade in the presence of nucleases circulating in blood. A possible solution to overcome this drawback is linked to the modification in the DNA or RNA backbone or modified nucleotides<sup>27</sup>. Nevertheless, one should account for the fact that aptamer modifications are sequence-dependent, and may affect the folding and formation of the structures of aptamers, resulting in a loss of their functions<sup>28</sup>. Meanwhile, drawbacks may arise also from their compositions. Aptamers are typically composed of four nucleic acids, resulting in a lower diversity of secondary and tertiary structures, whose environment-dependent functionalities add to the limitations. To overcome this, modified nucleotides can be incorporated to increase the chemical diversity and rigidity of the aptamers<sup>29</sup>. Aptamers are also characterised by a short *in vivo* circulating half-time followed by rapid renal clearance. For this reason, aptamers are combined with polyethylene glycol (PEG), in order to increase the hydrodynamic/molecular weight of aptamers above the renal filtration cut off<sup>30</sup>.

Considering the widespread application of aptamers in biosensors and diagnostic reagents, it is predicted that aptamers are one of the fastest-growing biotechnology areas in diagnostics and therapeutics<sup>31</sup>. A comprehensive description of the future perspectives of aptamers was published by Research and Markets<sup>32</sup> in a report entitled "Global aptamers market-segmented by type of products and applications-growth, trends and forecasts (2018-2023)". They reported the potential advantages of aptamers over antibodies in the fields of therapeutics and diagnostics and the market value is estimated to reach 401.30 billion \$ in 2023 and is expected to register a compound annual growth rate of 17.89% during the forecast period 2018 to 2023<sup>32</sup>.

### SELEX process

As stated above, the standard procedure to synthesize and identify aptamers is known as 'Systematic Evolution of Ligands by Exponential Enrichment' (SELEX). Target-binding oligonucleotides are selected from a random library pool of different oligonucleotides ( $10^{13}$ - $10^{15}$ ) through reiterative cycles of affinity separation and amplification<sup>7,33</sup>.

Standard SELEX consist of the following five main steps:

- a) designing an aptamer library pool;
- b) performing the SELEX cycle/round;
- c) monitoring the SELEX progression;
- d) cloning of the enriched library and sequencing of selection rounds for characterization and structural analyses
- e) characterisation of aptamer candidates.

These steps are generally applicable to most aptamer selections. In general, aptamer sequences can be obtained with high affinity and specificity after 8-20 rounds of screening. SELEX typically also includes negative and counter selection steps, to eliminate matrix binders and sequences that binding to potential interferents, respectively<sup>34-36</sup>.

### 1.1.1 Designing the library pool

The starting point of the SELEX process is a chemically synthesized random library. This library consists of random ssDNA sequences ( $\sim 10^{15}$  molecules). Most libraries are designed to be around 70-120 bases in length with a central random region of 20-80 random bases, flanked by two fixed sequences, (17-21 bases), that provide primer hybridization sites for PCR amplification, ssDNA production and enzyme digestion (Figure 1.3)<sup>37</sup>. An aptamer library is chemically synthesised by multiple couplings of adenine (A), thymine (T), guanine (G) and cytosine (C) through phosphoramidite chemistry<sup>38</sup>. This random region should contain all four bases in an equal distribution. Many researchers reported that an equal distribution increases the sequence space and consequently an enhanced possibility to select aptamers with the desired binding properties<sup>39</sup>.

Amplification of the oligonucleotide random library at the beginning and throughout SELEX is of considerable importance, as the correct choice of library and efficient PCR amplification of the random library contribute to the success of aptamer selection. The diversity within the library is determined by the length of the random core region. Generally, as the length of the random region increases, the structural diversity within the library also increases. This increase in diversity allows for the presence of more complex 3D structures, which are more likely to have high-affinity moieties<sup>40</sup>.

Modified nucleotides can not only improve the nuclease resistance and thermal stability of aptamers structure, but also contribute to the diversity of the library. Some nucleotide modifications include the modification of pyrimidines at the 5' position with I, Br, Cl, NH<sub>3</sub> and N<sub>3</sub> and the 2' position with NH<sub>2</sub>, F and OCH<sub>3</sub><sup>41</sup> and with NH<sub>3</sub>, F or 2-OCH<sub>3</sub> groups<sup>42</sup>, 2' fluoropyrimidines<sup>43,44</sup>, 2' O-methyl nucleotides<sup>45,46</sup>, position 5 of pyrimidines<sup>47</sup> and position 4 of pyrimidines using thiol UTP and CTP<sup>48</sup>.

The primer binding regions should not contain regions of internal complementary sequences in order to avoid hairpin structures and primer-dimer formation<sup>49</sup>. Some strategies purposely avoid the primer binding regions being part of the target binding sequence, such as tailored<sup>50</sup> and dual SELEX<sup>51</sup>. These strategies use conserved sequences (7-10 nucleotides), which are sequestered by self-complementary sequences, thus minimizing the risk that they become part of the target binding motif. An alternative strategy is primer-free DNA aptamer selection<sup>52</sup>, which employs endonuclease cleavage of the doubled stranded DNA template. The library is reconstituted after selection by ligation with primer annealing sites. This protocol was used to isolate aptamers against HIV reverse transcriptase<sup>53</sup>.

A further important parameter to consider is the size of the target molecule. The molecular size difference between proteins such as bovine serum albumin (~66 kD) and small molecules such as cocaine (~0.30 kD) is broad. Therefore, the surface area available for an aptamer to interact with the target varies significantly between different classes of molecules. An appropriate length of the random region should strike a balance between the structural diversity required for selecting high affinity aptamers and an appropriate surface coverage of the target molecule<sup>54</sup>. Increasingly, the design of an aptamer library is driven by the structural traits of its cognate target. This may incorporate the application of computational analyses of aptamer-target interactions<sup>55</sup>. Furthermore, when designing an aptamer library, the random core region can be either a complete randomisation or a partial (doped) randomisation<sup>56</sup>. Based on the critical motif responsible for binding with the target molecule, a doped aptamer library can be synthesised to reselect optimal aptamers, with the aim of improving their affinity and specificity to the target<sup>57,58</sup>.

Finally, an aptamer library in-solution normally forms energy efficient secondary structures by self-folding and this may obstruct the availability of nucleotide bases to interact with the target molecule<sup>59</sup>. To overcome this, the aptamer library at the start of every SELEX round is normally heat-denatured<sup>13,60</sup>. Following this heat denaturing process, the linearised oligonucleotides can interact more freely with the target molecule.

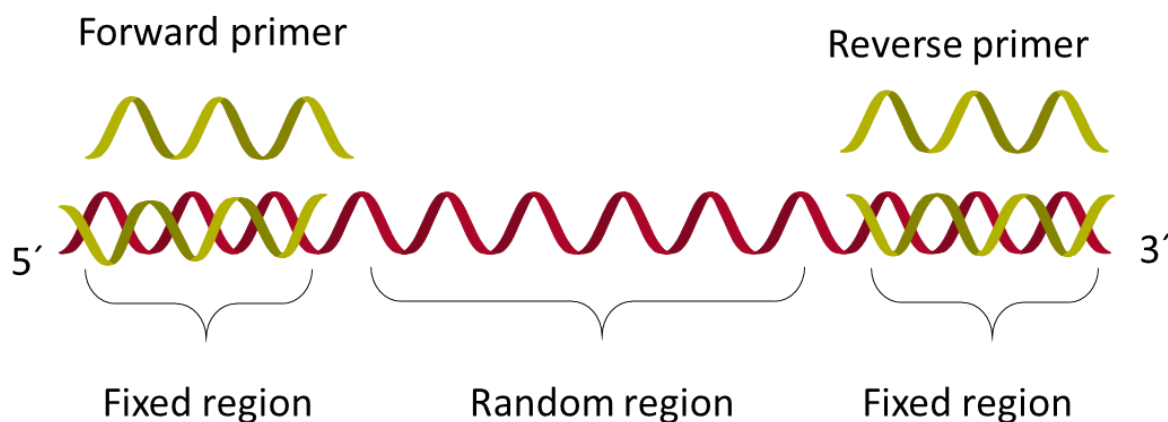


**Figure 1.3.** A schematic diagram of ssDNA oligonucleotide.

## 1.2.2 Selection rounds of SELEX

Each SELEX round or cycle involves 5 important steps (Figure 1.4):

- co-incubation of library pool with the target of interest to form nucleic acid-target complexes,
- partition of unbound sequences from the bound sequence-target complex,
- Elution of the bound sequences,
- amplification of the eluted sequences,
- preparation of the enriched ssDNA sequences for the next round of SELEX.

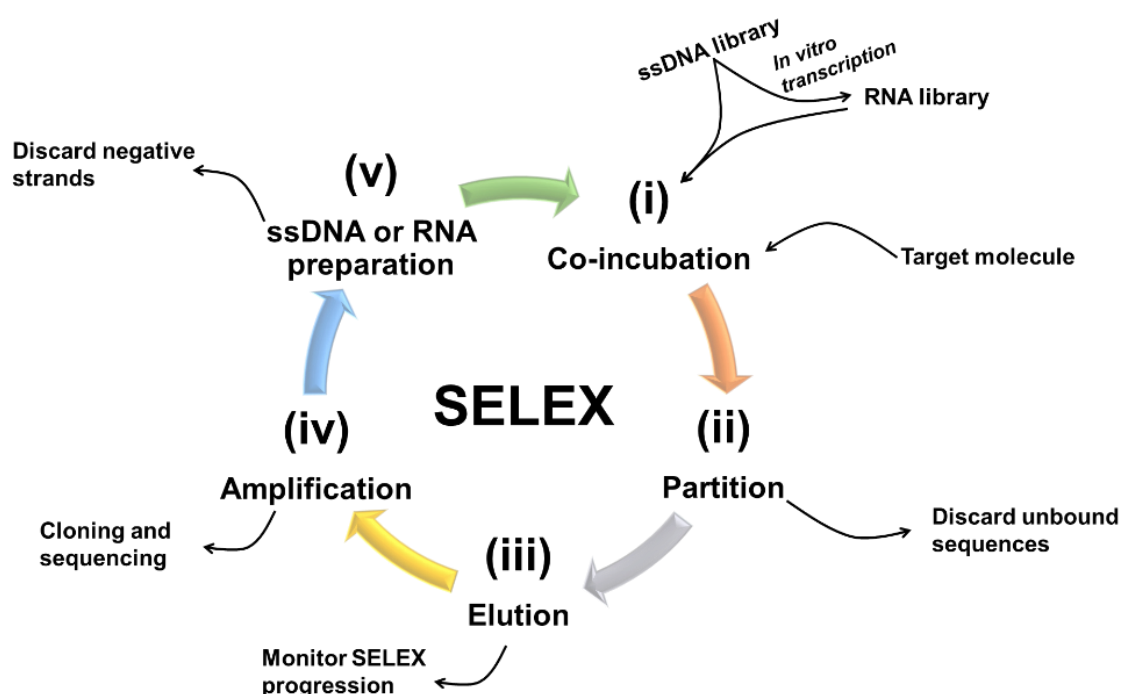


**Figure 1.4.** Schematic overview of SELEX cycle.

### 1.2.2.1 Co-incubation

The first step of SELEX process is the incubation of the library pool with the target in an appropriate buffer solution and with the proper incubation conditions. Binding of an aptamer with the target relies on electrostatic, H-bonds, hydrophilic or  $\pi$ - $\pi$  stacking interaction, which cause the conformational change within the aptamer by forming different 3D structures aiming the binding to the target<sup>61</sup>. Determining the appropriate *in vitro* conditions is guided primarily by the final planned application of the aptamer. It is generally recommended that

these conditions remain constant throughout the selection process so optimal binding efficiency can be achieved.

This aptamer-target binding can be affected by physicochemical properties such as temperature, pH, and ionic strength<sup>62</sup>. Nevertheless, ionic composition *i.e.* sodium (Na<sup>+</sup>), magnesium (Mg<sup>2+</sup>), calcium (Ca<sup>2+</sup>) and potassium (K<sup>+</sup>) of the buffering system can strongly affect the oligonucleotide 3D structure<sup>63</sup>. Nucleic acids are polyanionic molecules and negative-negative charge repulsion may inhibit the formation of complex structures and thus impede binding with the target without the presence of these counterions. For instance, the divalent ions Mg<sup>2+</sup> and Ca<sup>2+</sup> can influence the degree of DNA folding. A study from Carothers *et al.*<sup>64</sup> indicated that carrying out SELEX under low Mg<sup>2+</sup> concentrations (1-2,5 mM), increased the stringency of selection, leading to the production of high-affinity binding aptamers. Other ions such as Na<sup>+</sup> are effective in neutralizing negative charges of the phosphate molecules on the DNA backbone. Cruz-Aguado and Penner<sup>23</sup> demonstrated that the binding affinity of the aptamer selected against ochratoxin (OTA), was increased in the presence of Ca<sup>2+</sup> ions.

G-rich aptamers that form G-quadruplexes (G4) have several advantages compared to unstructured sequences. They are thermodynamically and chemically stable and resistant to serum nucleases and they have twice negatively charged density per unit length as compared to duplex DNA<sup>65</sup>. A number of G-rich aptamers have been developed, such as the thrombin binding aptamer<sup>66</sup>, as well as aptamers selected against hematoporphyrin<sup>67</sup>, and HIV-1 integrase<sup>68</sup>. The generation of these aptamers was performed in the presence of K<sup>+</sup> in the buffer solution, as K<sup>+</sup> is required to stabilise G-rich sequences to fold into the G4.

#### 1.2.2.2 Partition

The partition step is the most critical step of SELEX and involves the separation of bound sequences to the target from weakly or unbound sequences. There are numerous methods for performing this phase, and one of the first methods used was separation via nitrocellulose membrane of controlled pore sizes, where nucleic acid sequences bound to the target cannot pass through these pores, whereas unbound sequences pass through<sup>69</sup>. However, in membrane SELEX there is a high degree of non-specific binding of the nucleic acid sequences to the membrane itself, and thus other strategies were pursued.

The use of affinity columns where the target molecule was immobilised via covalent interactions has been widely reported<sup>70,71</sup> where partitioning is effectively achieved via elution of the unbound sequences, followed by release of the bound sequences using affinity elution or pH change<sup>72</sup>. Ciesiolka *et al.* performed the selection of Zn<sup>2+</sup> binding aptamer by immobilization of metal ion on iminodiacetic acid group-Sepharose column<sup>73</sup>.

Microtiter plates have also been used for target immobilisation, where the target is immobilised on the surface of the wells of the microtiter plate (polystyrene/streptavidin-coated/maleimide activated/amine activated), and partitioning is achieved via removal of the supernatant following incubation of the library with the immobilised target. The advantage of microtiter plates is that a fresh aliquot of target is used every cycle of SELEX, avoiding

problems of denaturation/desorption of the target during the SELEX process. Examples of this include the selection of aptamers for *Trichomonas vaginalis*<sup>74</sup> and shiga toxin<sup>75</sup>.

One of the most commonly used methods for partitioning is the use of magnetic beads. As with the microtiter plates, there are a wide range of magnetic beads of diverse sizes ranging from nanometre to micrometre, with different functionalities e.g. carboxyl, amine, maleimide, streptavidin, Ni<sup>2+</sup>. There are multiple examples of this type of partitioning, including cholera toxin<sup>76</sup>, okadaic acid<sup>77</sup>, testosterone<sup>78</sup>, histamine<sup>79</sup>, estradiol, progesterone, testosterone<sup>80</sup>.

Electrophoresis-based partition methods have been used to identify aptamers binders to proteins such as IgE<sup>81</sup>, neuropeptide Y<sup>82</sup>, and Muts protein<sup>83</sup>. Electrophoresis-based partitioning take advantage of the size-based difference in mobility of an analyte when an electrical field is applied, thus facilitating separation of target bound and unbound sequences. However, this method of partitioning is only useful for large molecules as efficient separation is generally not feasible with small molecules.

Whilst some of the above techniques can be used for partitioning when carrying out SELEX against small molecules, immobilisation can be challenging as few binding sites are available and can also result in a conformational change in the structure of the target. However, there are many examples of SELEX carried out via immobilisation of the small molecule target, as detailed in Section 1.4.

Apart from these conventional methods, other partitioning techniques have been reported, such as the use of affinity tags<sup>84</sup>, centrifugation<sup>85</sup>, flow cytometry<sup>86</sup>, and electrophoretic mobility shift assays<sup>87</sup>. Several of these partitioning methods for aptamer selection have been reviewed in detail by Gopinath *et al.*<sup>88</sup>. Further emerging techniques for effective partitioning when carrying out SELEX against small molecules include that of capture SELEX, where the library rather than the target is immobilised, and GO-SELEX, where a graphene oxide matrix has a high affinity for the single stranded sequences not bound to the target. These approaches are explained in further detail in Section 1.4.

The use of negative and counter SELEX steps is routinely used. Negative SELEX involves incubation of the nucleic acid library with the matrix to be used for partitioning e.g., nitrocellulose membrane, microtiter plates, magnetic beads, affinity columns, and this step removes any matrix binders. Counter SELEX is carried out after negative SELEX and involves incubation with molecules that could potentially interfere in the final application of the aptamer. Counter SELEX can be carried out sequentially with each of these potentially interferents<sup>79</sup>, or with a combination of them together<sup>78,89</sup>. This ability to eliminate binders to closely related structures/potential interferents facilitates a careful tuning of the specificity of the aptamer, which is not possible with antibodies, where the antibodies generated are dependent on the physiological response of the animal host.

### 1.2.2.3 Elution

Following removal of the unbound part of the library, bound oligonucleotides are generally eluted from the ssDNA/target complex. Interactions between the bound sequences and the target of interest are noncovalent in nature, and so several methods are possible for eluting these sequences. Methods used for elution include heat treatment<sup>76,90</sup>, affinity elution<sup>91</sup>, changes in ionic strength or pH of, and the use of denaturing substances such sodium dodecyl sulfate (SDS), ethylenediaminetetraacetic acid (EDTA), NaOH and urea, to disrupt hydrophobic stacking of DNA bases or chelation of aptamer-target complexes<sup>19,69,91</sup>. It is also worth noting that complete elution of bound sequences may not always be achievable. Some sequences possessing extremely high affinity to the target molecule are often difficult to elute, and can be lost during elution<sup>92</sup>.

An alternative strategy for obtaining bound sequences is to use aptamer-target complexes directly as the template for PCR amplification, providing the binding complexes do not interfere with the Taq polymerase used in PCR. This strategy has been applied successfully in generating histamine-specific aptamers<sup>79</sup>, progesterone and estradiol aptamer<sup>80</sup>, and testosterone aptamer<sup>78</sup>. In this approach, the bound target aptamers dissociate from the aptamer-bound matrix during the denaturation step of the PCR cycle, and become freely available for primers to bind, thereby initiating the amplification process.

#### 1.2.2.4 Amplification

The isolated oligonucleotides molecules are subsequently amplified to increase the enriched amount of selected aptamer. An effective SELEX procedure must be accompanied by efficient PCR amplification to obtain the proper length of amplicons and to retain those sequences that form stable secondary structures during the cycles of amplification in order to obtain high-affinity aptamers. The most conventional and effective technique for the amplification process is done by performing polymerase chain reaction for the ssDNA selected or reverse transcription-PCR for RNA sequences after the elution step. When using PCR for the aptamer selection, the random DNA or RNA is used as PCR template, and the diversity of template sequences can cause non-specific by-products amplicons during PCR due to stem-loop secondary structures formation of GC regions. These structures can promote polymerase jumping during PCR and generate PCR products of smaller sizes and thus prevent evolution to the desired aptamer sequence and structure<sup>93,94</sup>.

Although optimising PCR conditions, such as primer concentration, annealing temperature, and the number of amplification cycles can, moderately, reduce the amount of PCR by-product formation, it is not always effective. One of the common methods to improve the PCR amplification is the addition of DMSO, betadine, glycerol, or formamide to the reaction mixture<sup>76,95</sup>. Moreover, some advanced PCR techniques, such as real-time PCR and emulsion PCR have been used in SELEX<sup>96,97</sup>. Real-time PCR allows the detection of amplification in real time by introducing a fluorescent dye such as SYBR green. As SYBR green dye binds to double stranded DNA, the intensity of the fluorescent emission increases as the reaction progresses<sup>98</sup>. Other approaches used in RT-PCR include the use of molecular

beacons, Taqman probes and Light-cycler probes. The use of RT-PCR is useful as it avoids the over amplification, which sometimes can form PCR by-products, reducing the efficiency of aptamer enrichment<sup>99</sup>.

#### 1.2.2.5 Preparation of single-stranded DNA

In final step of normal PCR, the final product obtained is double stranded DNA (dsDNA), thus requiring the generation of single stranded DNA prior to the next cycle of SELEX. One of most commonly used methods for the generation of single stranded is the use of biotinylated forward or reverse primers, resulting in a biotinylated amplicon, and streptavidin coated magnetic beads<sup>62-64</sup>. The biotinylated dsDNA binds to the streptavidin magnetic beads, the duplex is then denatured via low/high pH or heating, and following magnetic separation, the unlabelled strand for use in the next cycle of SELEX is found in the supernatant. An alternative approach for the generation of ssDNA is the use of asymmetric PCR, which exploits a huge excess of one primer over the other, resulting in a mixture of single and double stranded DNA. Following amplification, these are separated using gel electrophoresis and the single stranded DNA is excised from the gel and purified<sup>68,69</sup>. The use of enzymes of exonucleases such as lambda exonucleases<sup>49,100</sup> and T7 Gene 6 exonuclease<sup>101</sup> is another alternative. During PCR amplification, a 5'-phosphate group is incorporated into one strand of the dsDNA by using a 5'-phosphorylated primer. Lambda exonuclease transforms dsDNA into ssDNA through digestion from the end containing 5'-phosphate, preferentially digesting one strand. Finally, based separation methods can be used, where DNA strands of unequal size are produced as a result of chemical or structural modifications of one of the PCR primers. The incorporation of a chemical spacer such as hexaethylene glycol (HEGL)<sup>102</sup>; constrained Nucleic Acids (CNA)<sup>103</sup> or a GC-rich stem loop structure<sup>104</sup> at the 5' end of the primer and downstream of poly-nucleotide extension, act as terminators of DNA polymerization. This leads to the production of a PCR amplicon that is partially double stranded, with two strands of unequal size that can be separated using gel electrophoresis.

#### 1.1.2 Monitoring of SELEX process

Monitoring of the aptamer's evolution is critical to ensure the selection of target-specific aptamers and to determine if the conditions used during SELEX are appropriate. These methods can be classified as direct and indirect methods. In direct methods the evolution of aptamers is evaluated in each round using techniques such as surface plasmon resonance (SPR), filter-binding assay, enzyme-linked oligonucleotide assay (ELONA), electrophoretic mobility shift assay (EMSA), and fluorescence-activated cell sorting (FACS)<sup>105-109</sup>.

Indirect methods for monitoring SELEX mostly rely on assessing the gradual reduction of the sequence diversity of aptamer pools. The advances in next-generation sequencing have provided the possibility of massive parallelised sequencing of aptamer populations of each round during the selection process<sup>110</sup>. Moreover, the diversity and structure of aptamer

populations can be monitored by methods such as denaturing HPLC, melting and remelting curve analysis in real-time PCR-restriction, fragment length polymorphism (PCR-RFLP), and nuclear magnetic resonance (NMR)<sup>110–114</sup>. In comparison with other methods, real-time PCR, allows the detection of very low amount of eluted ssDNA. Nevertheless, due to the heterogeneity of the SELEX library, particular optimization of different significant parameters is crucial to minimize by-product formation during the amplification step. In addition, this technique does not provide information regarding changes of binding affinity during selection rounds. In other approaches Eastern and dot blot techniques can be used by combining nitrocellulose membrane and the nucleic acids that are modified with a fluorophore or biotin molecule<sup>115,116</sup>.

In an affinity column-based SELEX, affinity column elution is used to monitor the evolution of SELEX<sup>73,117,118</sup>. In this approach, the target is bound on the column, and the nucleic acids are labelled with a radioisotope or fluorescent tag. The amount of nucleic acids eluted is analysed and compared with the amount of nucleic acids added to the column, and good evolution would result in less and less labelled nucleic acids eluting from the column.

### 1.1.3 Cloning and sequencing

After several selection rounds of SELEX when the affinity saturation of an enriched library has been achieved, previously the final oligonucleotide pool was cloned into bacterial vectors and individual colonies (30-100) and Sanger-sequencing carried out to<sup>119</sup>. However nowadays, next generation sequence (NGS) is widely used, and this enables the sequencing and analyses of thousands of sequences instead of just a hundred. Subsequently the identified sequences of each individual aptamer can be evaluated and analysed using bioinformatic tools such as Galaxy, Clustal Omega, AptaSuite and Geneious<sup>120–123</sup>. The data from each pool of the selection rounds are then compared and analysed, with the aim of finding the sequences with high affinity and specificity for the target. The identified sequences can also be evaluated using mFold program to predict their two-dimensional (2D) structures<sup>124</sup>, that can be further analysed to identify key motifs that are potentially critical for aptamer-target interaction.

### 1.2.5 The characterization and validation of selected aptamers

Following sequencing, the next step is the characterization and validation of the selected aptamer candidates, including (a) assessing binding affinity and specificity of each sequence, (b) determining  $K_D$  values, and (c) confirming in-solution binding capability. Aptamer candidates can be chemically synthesised and modified to perform target binding assays. Once the binding assays are completed, the binding affinity of each aptamer is ranked, and aptamers with low affinity are excluded from further studies. The  $K_D$  values of the high affinity aptamers are determined to evaluate the strength of aptamer-target interactions and can vary from  $\mu\text{M}$  to  $\text{pM}$  range. The  $K_D$  is calculated as the value that describes the ratio of unbound and bound aptamers, expressed in molar units (M). In order to determine the  $K_D$  value, the concentration of one of the two variables (*i.e.* aptamer or target

molecule) is kept constant while the other is successively varied, followed by the measurement of the amount of aptamer-target complexes formed over a range of starting concentrations. General methods used for determining the  $K_D$  value include: (a) surface plasmon resonance (SPR)<sup>118</sup>, (b) enzyme Linked Aptamer Assay (ELONA)<sup>125</sup>, (c) fluorescent binding assay<sup>90</sup>, (d) MicroScale Thermophoresis (MST), and Equilibrium filtration or dialysis<sup>19,126</sup>. More details per each of the techniques can be found in Section 1.5.

## Different types of SELEX

In the past 30 years, the selection of aptamers has been achieved for a variety of different molecules, with applications in biology, chemistry, medicine, bioinformatics, environment, and food safety sciences. However, the efficiency of conventional SELEX in the discovery of aptamers is sometimes more challenging in terms of its cost effectiveness, limited partition capability and target limitations. In the first work, Ellington and Szostak *et al.* and Tuerk and Gold *et al.*<sup>6,7</sup> used nitrocellulose filters, affinity columns and gel columns for the separation of complex and the unbound sequences. Since that time, various modifications of SELEX have been developed (Table 1.2).

To date, more than 32 kinds of SELEX variations have been introduced, however, a standard SELEX protocol suitable for all targets or the experimental settings does not exist<sup>127</sup>. Significant improvements have been achieved in some critical points of SELEX: the design of the nucleic acid library (e.g. chemical modifications, high fidelity-SELEX, genomic-SELEX)<sup>128</sup>, target preparation (e.g. cell-SELEX)<sup>129</sup>, library/target co-incubation (e.g. atomic force microscopy SELEX, capture SELEX)<sup>130</sup>, complex separation (e.g. capillary electrophoresis-SELEX, magnetic bead-SELEX, graphene oxide-SELEX (GO-SELEX), SPR-SELEX, on-chip SELEX)<sup>131,132</sup>, PCR amplification (e.g. real time-PCR, emulsion PCR, digital PCR)<sup>133</sup>, sequencing methods (high throughput sequencing-SELEX)<sup>134</sup> and entirely novel SELEX protocols (*in vivo* SELEX, robotic SELEX and *in silico* SELEX)<sup>131</sup>.

Although the main principles of the SELEX process remain the same, these variants have greatly improved the initial SELEX, resulting in more effective methods for the selection of aptamers.

### 1.3.1 CE-SELEX

Capillary electrophoresis (CE) SELEX was firstly introduced in 2004 by Mendonsa *et al.*<sup>81,135</sup>, who selected an aptamer against human Immunoglobulin E (IgE). CE is a separation technique that separates the charged molecules based on size due to their different rates of migration in an electric field<sup>136</sup>. CE-SELEX uses this mechanism in order to differentiate the target bound oligonucleotides from the unbound oligonucleotides due to the difference in their electrophoretic mobility, which makes it a very efficient separation method<sup>37</sup>. Regardless of their size the nonbinding sequences migrate through the capillary with the same mobility and

are collected separately from the target-sequence complex. In the next step the bound sequences are amplified, purified and ssDNA generated for use in the next selection round<sup>138</sup>. This method enables the selection of optimal candidates with high affinity and specificity, and can markedly reduce the required number selection rounds<sup>138</sup>. The efficiency and simplicity of the selection is attributed to some advantages of this method; (a) as some of the targets are rare or expensive CE-SELEX require less sample and use of reagents<sup>139</sup>; (b) both target and sequences are free in solution (not bound on any support matrix), and in this way their natural structure is maintained when they bind to the nucleic acids<sup>140</sup>; (c) CE is not just a separation tool, but also an analytical technique, which can monitor the sequence enrichment and quality in every selection round. Tang *et al.*<sup>141</sup> compared the selection efficiency using CE and affinity chromatography, CE showed two-fold improvement of nearly 87.2% binding while affinity chromatography with only 38.5%<sup>141</sup>. CE-SELEX has been used for aptamer generation against several targets, achieving low nanomolar dissociation constants<sup>141</sup>, but has a significant limitation in that the target should be large to allow for efficient separation between bound and unbound sequences. Yang *et al.* did, however, perform a CE-SELEX against porphyrin (580 kD), but the selection was not as effective as that achieved with larger targets<sup>173</sup>.

In order to improve the selection procedure and to avoid PCR amplification, an alternative CE-based method, called non-SELEX, selects an aptamer without amplification; e.g. non-Equilibrium Capillary Electrophoresis of Equilibrium Mixtures (NECEEM)<sup>142</sup>, equilibrium capillary electrophoresis of equilibrium mixtures (ECEEM)<sup>83,143</sup>. In ECEEM the components of the equilibrium mixture, which is injected into a capillary prefilled, are separated by capillary electrophoresis while equilibrium mixture is maintained between the target and the aptamers. Here differences in aptamer  $K_D$ , results in different fractions of aptamers migration with different mobilities. This SELEX technique collected these different fractions and generated smart aptamers with different and predefined  $K_D$  values in only three rounds of selection.

However, CE-SELEX displays some drawbacks, for example, a very small amount of library is allowed to be injected to maintain an adequate resolution. This small quantity limits the number of sequences that can be assessed. Further drawbacks are related to the fraction collection as the abundance of aptamers in early rounds is often below the limit of detection and variability in mobilities requires collection windows to be adjusted. To overcome the relatively limited size of the library<sup>135</sup> ( $\sim 10^{12}$  sequences), Jing *et al.*<sup>144</sup> modified this method by using micro Free Flow Electrophoresis ( $\mu$ FFE), where the starting library reaches up to  $\sim 10^{14}$ .

### 1.3.2 Microfluidic SELEX

Combing conventional SELEX with microfluidics, Hybarger *et al.*<sup>145</sup> developed a fully automated system called Microfluidic SELEX (M-SELEX) for the selection of an RNA aptamer against lysosome. In contrast with conventional SELEX cycle, using the microfluidic chip facilitated the achievement of each SELEX cycle in just an hour, whilst also requiring less

sample and reagents. Luo *et al.*<sup>146</sup>, combined magnetic bead SELEX with microfluidics in a continuous-flow magnetic activated chip-based separation, for aptamer selection against the recombinant botulinium neurotoxin. This aptamer showed high affinity but the aggregation of magnetic beads in the microchannel resulted in low aptamer purity and recovery. To overcome these disadvantages Qian *et al.*<sup>147</sup>, improved the process by integrating ferromagnetic structures in the microfluid channel chip, resulting in a successful aptamer selection against streptavidin. An alternative microfluidic SELEX method was suggested by Park *et al.*<sup>148</sup> to obtain a prostate-specific antigen-binding aptamer based on an acoustophoresis technique using a nanos porous sol-gel microarray material. M-SELEX has become a versatile and automated method for the rapid generation of aptamers and recently other modified techniques have been established to enhance the efficiency of the selected aptamers, including protein microarray-microfluidic chip SELEX<sup>149</sup>, capillary electrophoresis microfluidic SELEX<sup>139</sup>, and bead-based microfluidic SELEX<sup>150</sup>. A new platform integrating magnetic separation, micropumps, micromixers and temperature control systems for enzymatic amplification reactions for aptamers against the influenza A/H1N1 virus was recently reported<sup>151</sup>.

### 1.3.3 High-throughput Sequencing SELEX

In conventional SELEX the method to identify the individual sequences of the enriched libraries was based on Sanger sequencing analysis. However, in most cases the final library consists of thousands of sequences, making it difficult to identify the best aptamer. In addition, the best sequences with highest affinity and specificity, are not always those with the highest frequencies and thus it is important to apply clustering of related sequences. High-throughput-sequencing (HTS) was recently introduced to SELEX, facilitating the sequencing of the library through the selection rounds<sup>152</sup>. Hence, the enriched sequences are visible in earlier rounds giving information about the evolution of SELEX. Using HTS, the huge amount of raw data from sequencing is analysed in terms of counting sequences and ranking them in order of frequency. These sequences can be analysed, ranked, and filtered by cut-off read numbers to select candidate aptamers for further testing. Additionally, the use of bioinformatic tools can facilitate the characterization of aptamers, structure prediction, aptamer-target interaction<sup>153</sup>. Since the first HTS performed on 2010 by Cho *et al.*<sup>152</sup>, several aptamers against different targets have been selected using this approach<sup>24,121,154,155</sup>.

### 1.3.4 *In vivo* SELEX

Aptamers selected *in vitro* sometimes may not be functional *in vivo* due to localised environment conditions such as temperature, ion atmosphere, pH, and other variables, that determine the affinity and specificity of the aptamer. To address this, researchers have developed an *in vivo*-based SELEX method to select tissue-penetrating aptamers directly within animal models. Mi *et al.*<sup>156</sup> performed whole-organism *in vivo* SELEX in a model of intrahepatic colorectal cancer (CRC) metastases. After 14 rounds of selection collecting the aptamer that bound to liver metastases, they generated an aptamer that bound to oncogenic

helicase p68. In another work Chen *et al.* identified an aptamer capable of crossing the blood brain barrier<sup>157</sup>. Despite the fact that these examples demonstrate the successful generation of aptamers using live animal model, still, the main concern is that nucleic acids are susceptible to enzymatic degradation. Moreover, when aptamers are injected systematically, elimination through the liver and clearance in the kidney is inevitable.

### 1.3.5 Cell SELEX

Cell-SELEX employs whole live cells as targets. As in conventional SELEX even here two types of screening are done, the oligonucleotide library is primarily incubated with non-target cells (counter SELEX) and then with the target cells (positive SELEX). Compared to *in vitro* SELEX, in cell SELEX molecular targets are in their native conformation and different receptors molecules can be screened simultaneously. Cell SELEX was first published in 2003 by Daniels *et al.*<sup>158</sup> where they successfully selected an aptamer against tenascin-C using a glioblastoma-derived cell line, U251. Ara *et al.*<sup>159</sup> successfully screened tumour cell surface antigen aptamers, that can be used as molecular and diagnostic markers as well as for cancer treatment. Lin *et al* generated an aptamer that can distinguish the glioma cells from the human astrocytes<sup>160</sup>. Several other cell SELEX-based studies have been published such as TECS SELEX<sup>161</sup>, FACS-SELEX<sup>129,162</sup>, 3D cell SELEX<sup>163</sup>, cell internalization SELEX<sup>164,165</sup>. Currently, cell-SELEX is mainly used for cancer-related biomarkers. In general, cell-SELEX requires a higher number of cycles, and is considerably longer than conventional SELEX and there is a risk of failure due to the damage of fragile cells<sup>166</sup>.

**Table 1.2.** List of some modified SELEX methods which are commonly used.

Method	Advantages	Limitations	Ref.
<b>Nitrocellulose filter binding SELEX</b>	Relative ease of selection No special equipment required Equilibrium, in solution aptamer-target binding Potential for parallel aptamer selections for multiple targets Can be used as medium-throughput binding assay	Large number of selections rounds necessary (8–20 rounds) Relative abundance and rapid enrichment of filter-binding aptamers High amount of non-specific binding of library to membrane	167
<b>Bead-based SELEX</b>	Applicable to most targets (small-molecules, peptides, proteins, and cells) Potential for serial and parallel aptamer selections for multiple targets Rapid selection of aptamers (1-6 rounds of selection)	Target or aptamer immobilization: restricted interaction surface Nonequilibrium, flow binding (if used with fluidic devices) Fabrication of fluidic devices, and electronic instruments and flow pumps required for operation Density-dependent co-operativity for non-specific interactions	168

	Equilibrium, in-solution binding Ease in fine-tuning selection stringency		
<b>Microfluidic SELEX</b>	Potential for serial and/or parallel aptamer selections for multiple targets Both equilibrium, in-solution and nonequilibrium, flow binding systems are available Rapid selection of aptamers (1–6 rounds of selection)	Target immobilization or encapsulation required Fabrication of fluidic devices, and electronic instruments and flow pumps required for operation	169
<b>Microarray SELEX</b>	Equilibrium binding with in-solution target and immobilized aptamer Can be used as a large-scale binding assay	Limited capacity for aptamer library (<10 <sup>5</sup> sequences) Currently limited to ssDNA aptamers Aptamer sequences need to be pre-determined (designed or derived from a pre-selected aptamer library) Relatively large number of selection rounds are necessary (~9 rounds) Costly and time consuming due to fabrication of a microarray with different sequences unique for each target Single target selections Prone to artifactual results due to design of sequences Requires microarray scanner to measure binding	170
<b>Microscopic SELEX</b>	Single-round selection reported	Limited capacity for aptamer library (<10 <sup>8</sup> sequences) Requires expensive and specialized instrument (i.e., Atomic Force Microscopy system) Immobilization of either target or aptamer is required Non-equilibrium binding	171
<b>Cell SELEX</b>	Biomarker discovery Therapeutic potential of selected aptamers Target in native state Selection against cell	Restricted to molecules presented on cell surface Prone to artifacts due to dead cells in population Target(s) of the selected aptamers are unknown Selection of aptamers to an unintended target is very likely	109
<b><i>In vivo</i> SELEX</b>	Selection of <i>in vivo</i> functional aptamers	Limited capacity for aptamer library (~10 <sup>4</sup> sequences) Relatively large number of selection rounds are necessary (up to 14 rounds) Selection of aptamers to an unintended target is very likely	172

<b>Small molecule SELEX</b>	Equilibrium, in solution binding No immobilization of small-molecule target	Complications of aptamer capture sequence within aptamer library random region Relatively large number of selection rounds are necessary (~13 rounds) Depends on target binding-induced conformational change on aptamer for its release	
<b>Capillary electrophoresis SELEX</b>	Separate aptamers-target complexes from free aptamers according to their electrophoretic mobility with capillary electrophoresis Could effectively identify high affinity aptamers in few rounds	Restricted to targets that cause a shift in aptamer electrophoretic mobility pattern	138
<b>Capillary Electrophoresis SELEX</b>	Equilibrium, in-solution binding Rapid partitioning of target-bound and unbound aptamers	Limited capacity for aptamer library (~10 <sup>12</sup> sequences) Restricted to targets that cause an electrophoretic shift on nucleic acid aptamers Capillary-electrophoresis instrument or fabrication of micro-electrophoresis devices are required	173
<b><i>In silico</i> SELEX</b>	Could be used to predict aptamer affinity, specificity, 3D structure and aptamer-target interaction by computer prior to experimental characterizations Employ computational docking	Small size of starting library Complex computational methods and programs	166

## 1.4 SELEX type focused more on small molecules

### 1.4.1 Problems associated with small- molecule binding aptamers

As can be seen in Figure 1.5 only 19% of existing aptamers have been generated for small molecules targets. Originally SELEX was presented as a very effective methodology for the selection of aptamers for small molecules. However, other larger targets such as proteins or cells have more functional groups and structural motifs, implicating higher probability for the successful selection of aptamers with high affinity and specificity. On the other hand, small molecules play important roles in many fields and the demand for their detection is of increasing interest. These molecules include cell signalling molecules, toxins, drugs, heavy metals, antibiotics, ions, and pesticides<sup>97-100</sup>.

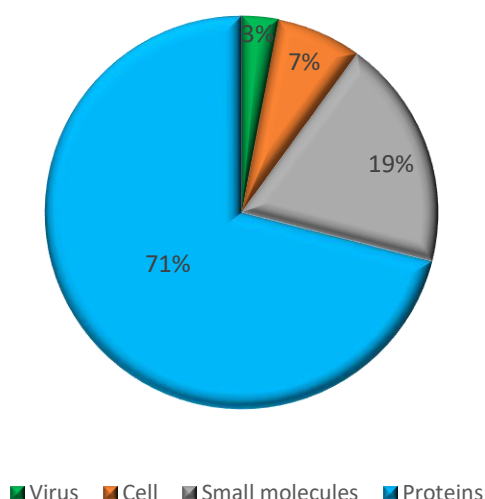


**Figure 1.5.** A chart that represents the selected aptamer per each target type<sup>174</sup>.

Considering their importance conventional SELEX protocols have been modified to develop new and improved protocols aimed at the successful selection of specific aptamers against small molecules, and approaches where target small molecules have been immobilised on diverse matrices (Table 1.3) as well as approaches where the target small molecules are free in solution, have been developed. In the case of small molecules, the number of functional groups is limited, and when the selection is not performed with the target free in the solution, one of its functional groups will have to be used for the immobilization, thus potentially decreasing the amount of possible interaction with the aptamer candidate. Moreover, the binding of the target to the matrix for the selection is often carried out in a conjugate form rather than for the target alone, and this can negatively affect the applications when the target is free in the solution. For example, the aptamer selected for sulforhodamine, displayed weaker binding to the target when in solution compared to when the target was immobilized on the matrix used for the selection<sup>175</sup>. In some other studies, the pool library is exposed to target, linked to protein carrier molecules such as bovine serum albumin (BSA), ovalbumin (OVA), and keyhole limpet hemocyanin (KLH)<sup>176</sup>. However, this promotes the aptamer selection against a conjugate or linker molecule rather than the unmodified original target. To overcome these disadvantages, alternative SELEX methodologies have been developed, such as GO-SELEX<sup>177</sup> and capture SELEX<sup>178</sup>, where the target does not need to be immobilised.

**Table 1.3.** Commercially available chemically modified matrixes used for the immobilization of small molecules for their aptamer selection.

Chemical moiety of ligand	Matrix chemistry	Magnetic bead	Agarose
<b>COOH CHO</b>	hydrazine		Adipic acid dihydrazide Agarose
<b>COOH CHO (EAH Sepharose only)</b>	amine	M-270 Amine	EAH Sepharose 4B Affi-Gel 102 Gel CH sepharose 4B Carboxy Link Coupling Resin
<b>NH<sub>2</sub></b>	aldehyde		AminoLink PlusCoupling Resin AminoLink Coupling Resin
<b>NH<sub>2</sub></b>	cyanogen bromide		CNBr-Activated Sepharose 4B CNBr-Activated Sepharose 6 MB
<b>NH<sub>2</sub></b>	N-hydroxy succinimide (NHS)		NHS-Activated Sepharose E Fast Flow Affi-Gel 10 Affi-Gel 15 Pierce NHS-Activated Agarose
<b>NH<sub>2</sub> N-nucleophiles</b>	carbonyl diimidazole		Pierce CDI activated Agarose Resin
<b>NH<sub>2</sub> SH</b>	tosylactivated	M-280 Tosylactivated MyOne Tosylactivated	
<b>NH<sub>2</sub> SH (Dynabeads only)</b>	Carboxylic acid	M-270 CarboxylicAcid MyOne CarboxylicAcid	ECH Sepharose 4B
<b>NH<sub>2</sub> SH OH (Sepharose only)</b>	epoxy	M-270 epoxy	Epoxy-Activated Sepharose 6B
<b>SH</b>	iodoacetyl		SulfoLink Coupling Resin
<b>SH heavy metal ions alkyl and aryl</b>	thiol		Activated Thiol Sepharose 4B
<b>Halides addition to C=O C=C N=N</b>			Thiopropyl Sepharose 6B

#### 1.4.2 Magnetic beads-based SELEX

One of the main challenges of performing SELEX with a small molecule target is the partitioning of bound and unbound sequences. Magnetic beads are the most widely used solid matrix for the selection of aptamers against small molecules, that simplify the separation

process of target-ssDNA and unbound-ssDNA through the aid of a magnet rack. These beads are super magnetic spherical polymers with a uniform size and a define surface allowing a variety of chemistries for the coupling reaction with different molecules (Table 1.3). The use of magnetic beads reduces the volumes needed to perform aptamer selection, additionally, since magnetic beads are thermally, they can be used directly in PCR to amplify the target bund DNA, avoiding any potential loss of sequences during elution. Many different aptamers have been selected against small molecules using magnetic beads. Kiani *et al.*<sup>179</sup> have used streptavidin-coated magnetic beads to isolate digoxin aptamer, Duan *et al.*<sup>180</sup> and Mairal *et al.*,<sup>79</sup> used carboxylic beads for chloramphenicol and histamine aptamer isolation, respectively. Bruno and Kiel *et al.*<sup>76</sup> and Lin *et al.*<sup>77</sup> have used tosylactivated magnetic beads for the selection of an aptamer against biotoxin and okadaic acid-mAb respectively.

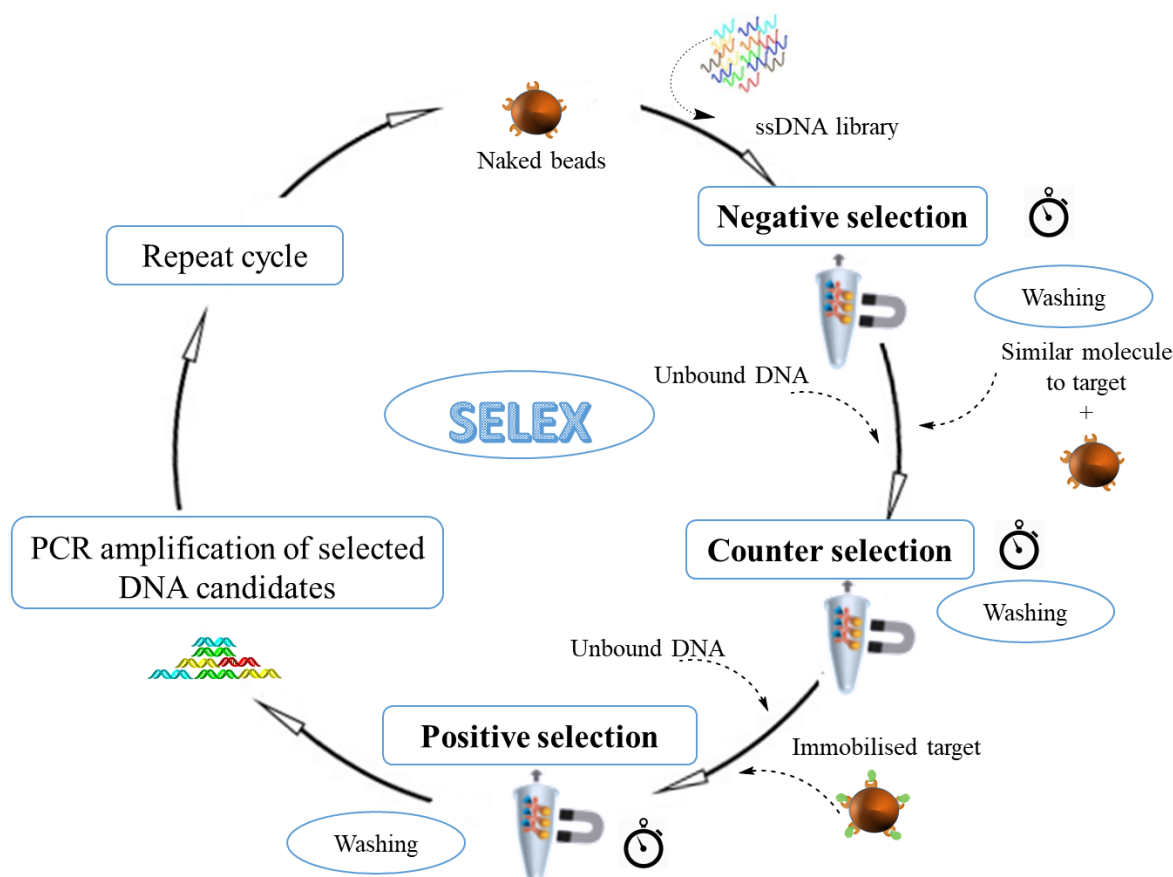


**Figure 1.6.** Schematic representation of Magnetic bead-based SELEX.

Briefly, as in SELEX with large molecules, the first step involves the immobilization of the target molecule through interaction of functional groups on the bead surface and the functional group of the target (Figure 1.6). Sequences that bind the target are separated from those they do not bind via multiple washes whilst the magnetic beads are separated from the supernatant by placing close to magnetic stand. The sequences are amplified for the next cycle of SELEX. As previously mentioned, a critical component of SELEX to increase the aptamer specificity, is the introduction of negative and counter selection steps. Negative

selection is the selection against non-target components that are present in the target sample, such components include selection buffer and unmodified matrix (naked or activated magnetic beads). Counter selection is performed against molecules structurally similar to the target, as well as potential interferents that may be present in the sample where the aptamer will finally be applied.

An interesting one-pot SELEX approach was developed by Jauset-Rubio *et al.*<sup>80</sup> using the benefits of counter-SELEX and next generation sequencing for the simultaneous identification of aptamers against the steroids estradiol, progesterone, and testosterone. Results of binding studies showed nanomolar affinity of the aptamers toward the specific targets, with reasonable specificity given the structural similarity of the target molecules.

### 1.4.3 GO-SELEX

Graphene oxide (GO), chemically exfoliated from oxidized graphite, is considered as a promising material for SELEX for small molecules. The novel approach of using GO in SELEX was first described by Park *et al.*<sup>177</sup> who selected an aptamer against the Nampt protein. In principle, oligonucleotides are bound to the GO surface through  $\pi$ - $\pi$  stacking interactions between the nucleobases and  $sp^2$  atoms of GO. Adsorption of dsDNA on GO is very weak due to the shielding of nucleobases by the phosphate backbone, whilst ssDNA binds very strongly<sup>181</sup>. In one approach, the oligonucleotides of a random library are adsorbed on GO and incubated with the target, and high affinity binders are desorbed from the GO and then extracted, amplified, and subsequently re-adsorbed to the GO for the next round of SELEX. Another approach is where the target is pre-incubated with the ssDNA/RNA library, and following incubation, added to the GO, and the unbound ssDNA binds to the GO, and centrifugation used to separate the GO-bound ssDNA from the target bound ssDNA. Alternatively, a combination of these approaches can be used, where the library is primarily incubated with the counter targets, and then added to the GO. ssDNA bound to the target is separated from the ssDNA bound to the GO via centrifugation, and the target is then added to the GO, and high affinity binders are desorbed from the GO via interaction with the target molecule (Figure 1.7).

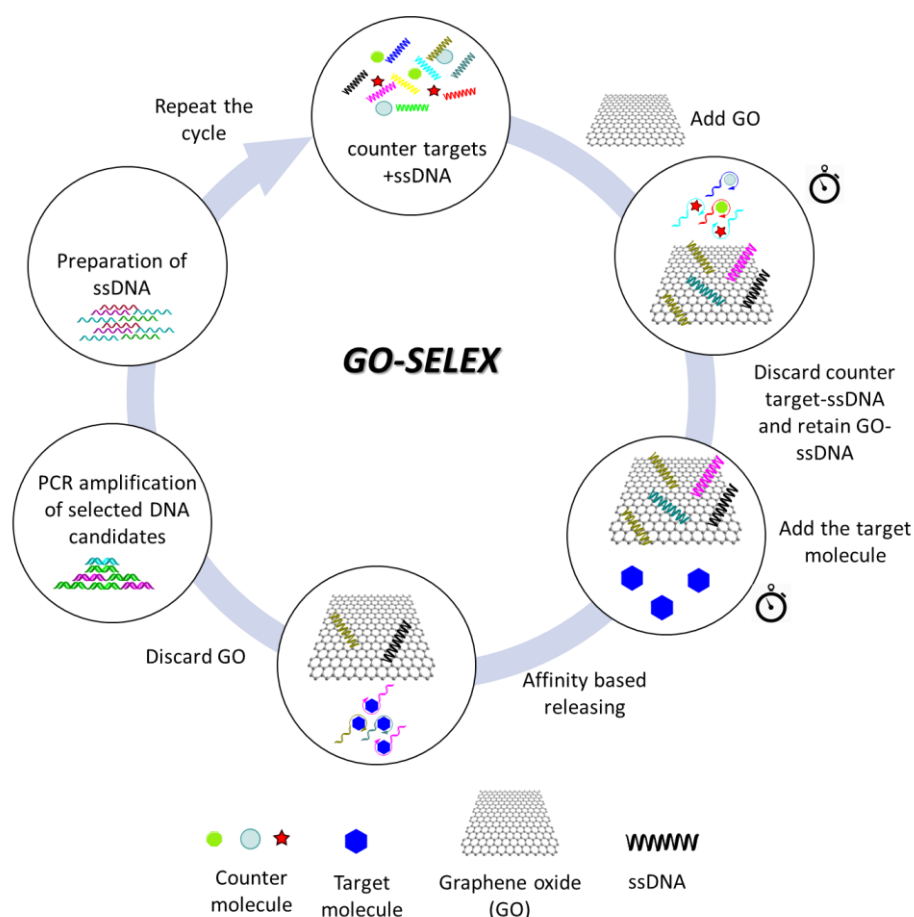


**Figure 1.2.** Schematic representation of GO-SELEX.

Nguyen *et al.*<sup>182</sup> developed multiple GO-SELEX selection of aptamers against different types of pesticides; tebuconazole, inabenfide, and mefenacet. In another selection done by Gu *et al.*<sup>183</sup>, three different screening processes were used to obtain aptamers against okadaic acid (OA). In the first step the ssDNA was firstly incubated with the target (OA) than with GO. In latest rounds a negative selection step was introduced in order to disqualify weakly bound ssDNA. Moreover, they performed an important step for increasing the aptamer specificity, which is the involvement of counter molecules which may co-exist with the target in a heterogeneous environment. In this work, the  $K_d$  values for aptamer selected against Okadaic acid were slightly lower than that of the aptamer screened by Eissa *et al.*<sup>184</sup>, who used immobilized okadaic magnetic beads for the aptamer selection. Comparing these 2 types of selection, the use of graphene oxide method allows the target to be free in the solution throughout the selection, enhancing the successful application of these aptamers in detecting contaminated samples with OA in its native conformation state<sup>183</sup>. Another successful aptamer selected using GO SELEX, was against the mycotoxins, patulin (PAT),<sup>185</sup> and T-2 toxin<sup>186</sup>.

#### 1.4.4 Capture SELEX

Capture SELEX was originally designed by Stoltenburg *et al.*<sup>178</sup>, and in this approach the library rather than the target molecule is immobilised. The nucleic acids used in the library generally have the format of fixed sequence for primer binding (20-25nt), random sequences (30-40nt), fixed docking probe sequence (8-12nt), random sequences (5-20nt), fixed sequence for primer binding (20-25nt). As always, the library is amplified and ssDNA generated, and the generated ssDNA is then immobilised onto a solid matrix such as agarose<sup>187</sup> or magnetic beads<sup>178</sup> (Figure 1.8). Streptavidin coated beads are normally used, and these are functionalised with a biotinylated probe complementary to the docking probe, thus achieving immobilisation of the library. Pre-elution and background elution steps are used to remove any unbound or weakly bound sequences. A counter SELEX step can then be introduced, incubating the functionalised beads with the counter molecules. Sequences with affinity to the counter molecules are displaced and this displaced DNA separated, and the beads then incubated with the target molecule. Sequences with affinity to the target molecule are effectively displaced, and this displaced DNA is then amplified, ssDNA generated and again immobilised on a fresh set of beads, and the process repeated until evolution has been completed (Figure 1.8).

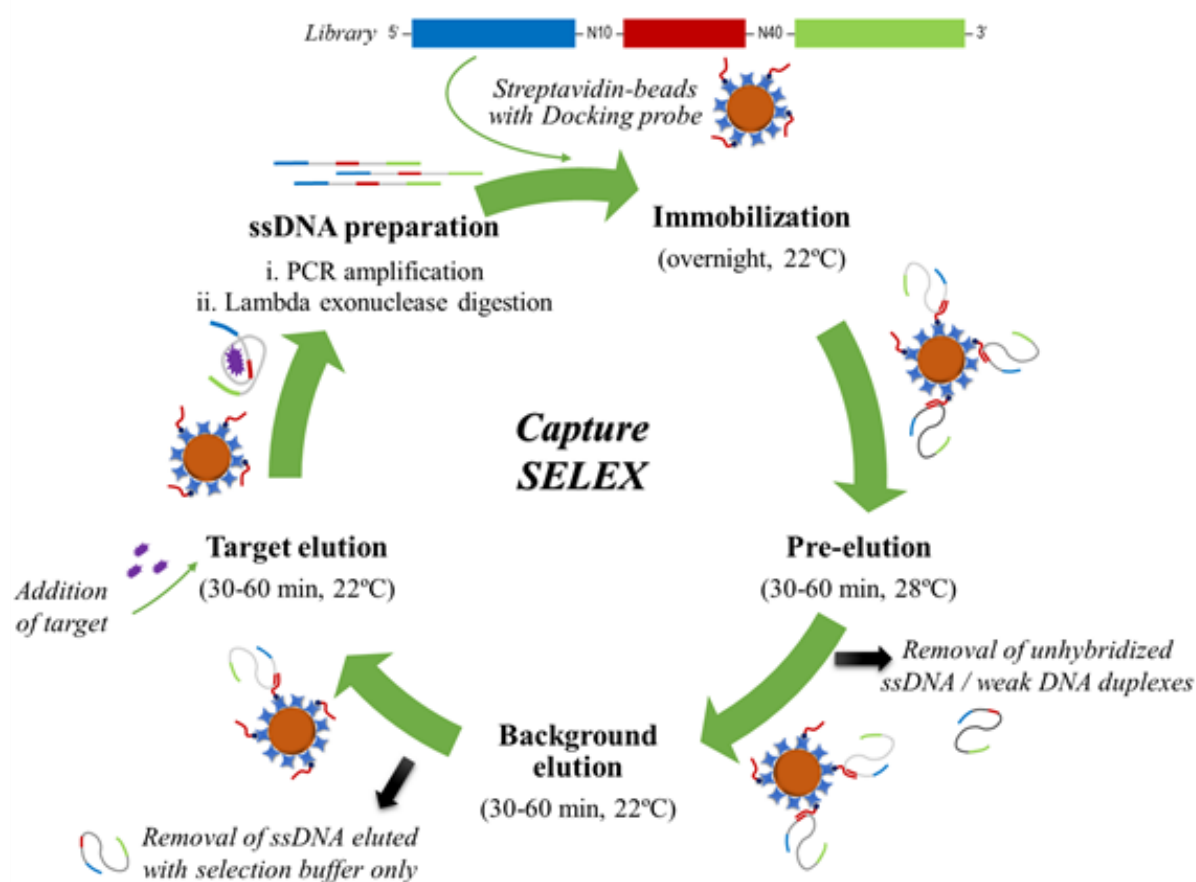


**Figure 1.8.** Schematic representation of Capture-SELEX.

In the case of agarose beads the library usually needs to be packed in an affinity chromatography column, and the target-binding-library need to be separated using centrifugation, which is not as gentle as separation through the magnetic rack in the case of magnetic beads. However, the cleaning process of magnetic beads is laborious, and if the cleaning is incomplete, some non-specific library sequences may remain.

Capture SELEX facilitates immobilisation-free SELEX and has been used successfully to select both DNA and RNA aptamers against small molecules<sup>188</sup>, including cadmium<sup>189</sup>, penicillin<sup>190</sup>, quinolone<sup>191</sup>, lipopolysaccharide<sup>192</sup>, amongst others (Table 1.4). However, capture SELEX requires careful optimisation of experimental conditions such as buffer composition, temperature and time of incubation<sup>130</sup>, and typically requires a high number of cycles to complete evolution.

**Table 1.4.** Example of different specific aptamers selected via Capture SELEX.

<b>Aptamer targets</b>	<b>Target type</b>	<b>Library sequence (5' to 13')</b>	<b><math>K_D</math></b>	<b>Ref.</b>
<b>ATP, GTP</b>	Phosphate compounds	CCTGCCACGCTCCGCAAGCTT-N10- CTGCAGCGATTCTTGATCG-N20- TAAGCTTGGCACCCGCATCGT	N.A	193
<b>Zinc</b>	Metal ions	CATCAGTTAGTCATTACGCTTACG-N50- ATTGTGAAGTCGTGTCCCTATAGTGAGTCG TATTAGAA	15 $\mu$ M	194
<b>Human <math>\alpha</math>-thrombin</b>	Serine protease	Forward PCR prime site-N17- TTTTGTGGGTAGGGCGGGTTGGTTTT-N17- Reverse PCR prime site	70 nM	195
<b>Acetamiprid</b>	Pesticide	CCTGCCACGCTCCGCAAGCTT-N10- CTGCAGCGATTCTTGATCG-N20- TAAGCTTGGCACCCGCATCGT	4.98 $\mu$ M	196
<b>Kanamycin A</b>	Aminoglycoside antibiotic	ATACCAGCTTATTCAATT-N10- TGAGGCTCGATC-N40- AGATAGTAAGTGCAATCT	3.9 $\mu$ M	178
<b>Phorate, profenofos, isocarbophos and omethoateas</b>	Organophosphorus pesticides	CCTGCCACGCTCCGCAAGCTT-N10- CTGCAGCGATTCTTGATCG-N20- TAAGCTTGGCACCCGCATCGT	0.8-2.5 $\mu$ M	187
<b>Cadmium</b>	Toxic metal	ACCGACCGTGCTGGACTCT-N30- AGTATGAGCGAGCGTTGCG	34.5 nM	189
<b>Cortisol</b>	Glucocorticoid hormone	GAATGGATCCACATCCATGG-N40- TTCAGTGCAGACTTGACGAAGCTTGACGAA	6.9 $\pm$ 2.8 $\mu$ M	197
<b>Tobramycin</b>	Aminoglycoside antibiotics	GGAATGGATCCACATCTACGA-N60- TTCAGTGCAGACTTGACGAA	200 nM	198
<b>Quinolones</b>	Antibiotics	ATACCAGCTTATTCAATT-N10- TGAGGCTCGATC-N40- ACAATCGTAATCAGTTAG	0.1-56.9 nM	191
<b>Clenbuterol hydrochloride</b>	$\beta$ -agonist	AGCAGCACAGAGGTCAGATG-N40- CCTATGCGTGCTACCGTGAA	76.61 $\pm$ 12.70 nM	199

<b>Lipopolysaccharides</b>	Outer membranes of Gram negative bacteria	ATAGGAGTCACGACGACCAG-N40-TATGTGCGTCTACCTCTTGA	102 ± 17 nM	192
<b>Ractopamine</b>	β-adrenergic agonists	AGCAGCACAGAGGTCAGATG-N40-CCTATGCGTGCTACCGTGAA	54.22 ± 8.02 nM	200
<b>Vanillin</b>	Flavoring	CGACCAGCTCATTCCCTCA-N10-GGAGTCTCGATG-N40-GGATCCGAGCTCACCAGTC	(9 ± 3) × 10 <sup>-7</sup> M	201
<b>Penicillin</b>	β-lactam antibiotics	GGGAGGACGAAGCGGAAC-N10-TGAGGCTCGATC-N40-CAGAAGACACGCCGACA	0.4-1000 µg L <sup>-1</sup>	190
<b>Atrazine</b>	Herbicide	TGTACCGTCTGAGCGATTCGTAC-N34-AGCCAGTCAGTGTTAAGGAGTGC	3.7 nM	202
<b>Zearalenone</b>	Nonsteroidal estrogenic mycotoxin	ATACCAGCTTATTCAATT-N10-TGAGGCTCGATC-N40-ACAATCGTAATCAGTTAG	15.2 ± 3.4 nM	203
<b>Spermine</b>	Polyamine	AGCAGCACAGAGGTCAGATG-N40-CCTATGCGTGCTACCGTGAA	9.648 ± 0.896 nM	204
<b>Paromomycin</b>	Aminoglycoside antibiotic	GGGCACUCCA AGCUAGAUCUACCGGU-N40-CUACUGGCUUCUA-N10-AAA AUGGCUAGCAAAGGAGAAGAACUUUUCACU	20 nM	205
<b>Di(2-ethylhexyl) phthalate</b>	Plasticizer	ATTGGCACTCCACGCATAGG-N40-CCTATGCGTGCTACCGTGAA	2.26 ± 0.06 nM	206

## Characterization of aptamers for small molecules

Following completion of SELEX, next generation sequencing and bioinformatics data analysis, the best aptamer candidates are selected and chemically synthesised for the further analyses.

The assays that are currently used for the characterisation of aptamers against small molecules include the apta-PCR affinity assay (APAA), enzyme linked aptamer assay (ELAA), surface plasmon resonance (SPR), isothermal titration calorimetry (ITC), capillary electrophoresis (CE), and AuNPs colorimetric assay. Each of these assays have some limitations and are not suitable for every target. Furthermore, the successful performance in one assay does not guarantee their functionality in another one. In the work of McKeague *et al.*<sup>207</sup>, an inconsistency in the binding affinities in different assays tested when using the same aptamer for ochratoxin A (OTA) detection was observed.

### 1.5.1 Enzyme linked aptamer assay (ELAA)

Enzyme linked aptamer assay (ELAA) is an alternative of the conventional enzyme linked immunosorbent assay (ELISA) where antibodies are replaced with aptamers as biorecognition element. In some studies both bead and plate-ELAA approaches have been

used<sup>80</sup>. In most cases, this assay is performed by coating a fixed amount of target on a microtiter plate or magnetic beads, followed by the incubation with a range of concentrations of biotinylated aptamer candidates. Following thorough washing to remove any unbound aptamers streptavidin-horse radish peroxidase (SA-HRP) is added, and after a further washing, the enzyme substrate 3,3',5,5'-Tetramethylbenzidine (TMB) is added followed by acid, and the generated colour measured. A binding isotherm is plotted and the  $K_D$  value elucidated from the plot. ELAA assay has not only been utilised to determine the  $K_D$  values for different molecules<sup>125,208</sup>, but has also been used in many bioanalytical applications for the target-specific detection of okadaic acid<sup>183</sup>, steroids<sup>80</sup>, dopamine<sup>209</sup>, OTA<sup>210</sup>, and deoxynivalenol (DON)<sup>211</sup>. However, the assay procedure usually involves multiple binding and washing steps, which can be time consuming.

### 1.5.2 Surface plasmon resonance (SPR)

SPR technology offers label-free detection and real time quantitative analysis and provides binding constant determination<sup>212</sup>. Briefly, when polarized light strikes an electrically conducted surface of a metal (gold or silver), at a particular angle, it can excite electrons on the metal surface, causing an electro density wave to propagate along the surface. Bioreceptors can be immobilised on the metal surface directly via chemisorption or on polymer coated metals via chemical crosslinking, and the change in the plasmons resonance upon interaction between the immobilised bioreceptor and its cognate target, measured. SPR has been used extensively to monitor evolution and for the determination of  $K_D$  for a wide range of molecules including vascular endothelial growth factor<sup>213</sup>, tubulin<sup>214</sup>, thrombin and thyroid transcription factor 1<sup>95</sup>, prostate-specific antigen<sup>215</sup>, and retinol binding protein 4<sup>216</sup>, and has also found application for small molecules, including kanamycin B<sup>217</sup>, codein<sup>218</sup>, S-adenosyl-L-homocysteine<sup>219</sup>, adenosine and alpha toxin<sup>220</sup>.

Because of the low refractive change index of the molecule interaction of some small molecules, it is difficult to detect these interactions only by conventional SPR techniques and AuNPs have been combined with SPR sensor for adenosine detection<sup>221</sup>, whilst Luo *et al.* developed a method using the salt-induced AuNPs aggregation and SPR for bisphenol A detection<sup>222</sup>. Although SPR is useful tool that shows in real time the binding kinetics of the interaction, the instrumentation associated with SPR technology is quite expensive and needs trained personnel, which narrows its use in many laboratories.

### 1.5.3 Microscale Thermophoresis (MST)

MST is another useful method for the characterisation and determination of the interaction between aptamers and small molecules. MST measures the motion of molecules along microscopic temperature gradients and detects changes in their molecular size, charge, and hydration shell when the target is bound to the aptamer. The thermophoretic movement is measured in thin glass capillaries through  $\mu\text{m}$  sized temperature gradients. Entzian and Schubert<sup>223</sup> used this method to determine the  $K_D$  of an adenosine triphosphate (ATP)

aptamer using a range of aptamer concentrations from pM to mM and the  $K_D$  was found to be  $34.4 \pm 4.4 \mu\text{M}$ . MST is a useful immobilization-free technique that can be used with small molecules, such as  $17\beta$  estradiol<sup>224</sup>, testosterone<sup>78</sup>.

#### 1.5.4 Apta-PCR affinity assay (APPA)

Apta-PCR Affinity Assay (APPA) is a simple method based on the PCR amplification of an aptamer that is bound to the target molecule, which in turn is immobilized on the surface of the matrix and offers rapid information regarding the affinity and specificity of studied aptamers. The use of this assay for analysing aptamer small molecule interactions has already been demonstrated<sup>78,224</sup>. In this assay the target is immobilised on a solid matrix (magnetic beads), usually the same one that is used during the selection process or a different one to demonstrate the absence of matrix participation in the binding event<sup>80</sup>. The process is followed by the incubation with different concentrations of unmodified aptamer, PCR amplification of the complex bead-target-aptamer, followed by gel electrophoresis. The intensity of the bands is measured using Image J, and isotherm plotted and used to determine the  $K_D$ .

#### 1.5.5 Isothermal Titration Calorimetry (ITC)

Isothermal Titration Calorimetry (ITC) is a widely used biophysical technique used for the measurement of affinity based on the enthalpies of affinity interactions<sup>225</sup>. ITC determines the enthalpy change occurring upon molecular interaction at a constant temperature where only the thermal effect is measured. ITC provides the stoichiometry of interaction and a set of thermodynamic binding parameters: the equilibrium binding constant ( $K_D$ ) and the change in enthalpy ( $\Delta H$ ) and entropy ( $\Delta S$ ) of the binding. One of drawbacks limiting the use of ITC is the need for a high amount of the interacting materials, and, furthermore, these molecules need to be soluble in water and stable in the solution.

ITC has been used for analysing large molecules like thrombin<sup>226</sup> but recently it has been used for characterisation of the specificity of an aptamer selected against cocaine, measuring the interaction between the aptamer and cocaine and its metabolites, ecgonine, benzoyl ecgonine, ecgonine methyl ester and norcocain<sup>227</sup>.

#### 1.5.6 Biolayer interferometry (BLI)

An interesting real-time optical analytical method for characterizing the binding of aptamer with small molecules is biolayer interferometry (BLI)<sup>228</sup>. BLI signal is based on target conformation, hydration, and dipole moment using a microfluidic chip, a charge coupled device (CCD) array, and a helium-neon laser. This method uses fibre optic biosensors to monitor changes in the optical thickness of the sensor layer that occur with biological binding events. Briefly, the laser irradiates the sample, the beam is reflected and refracted within the channel followed by detection with the CCD array, interaction between aptamer and the

molecule, causes a wavelength shift in the interference spectrum of the reflected light<sup>229</sup>. In recent years BLI has been used for quantitative determination of  $K_D$  for proteins<sup>230</sup> as well as with small molecules including toxins<sup>229</sup>, antibiotics tenofovir, ampicillin, tetracycline<sup>231</sup>, hormone norepinephrine<sup>232,233</sup>, and dinophysistoxin-1<sup>234</sup>.

### 1.5.7 Equilibrium filtration or dialysis

Equilibrium filtration or dialysis has been demonstrated as a very useful method to study the affinity of aptamers for small molecules. In both approaches, a target and its aptamer are mixed in a series of microfuge tubes, in which the amount of aptamer is kept constant, but the amount of target is linearly increased until the samples reach equilibrium. Thereafter, separation of aptamer-target complexes from unbound target molecules is performed by applying a molecular weight cut-off membrane such as a size exclusion filter or a dialysis chamber. Both methods utilise radio-isotope labelled target molecule, and the exact amount of unbound target is quantified by measuring the amount of radioactivity inside the filter or dialysis chamber using a scintillation counter<sup>235</sup>. Since input concentrations of the aptamer and target analyte are known, a series of numbers that describes the amount of aptamer bound at each target concentration can be calculated in order to determine the binding capacity of the aptamer.

Equilibrium-based methods have been applied in many aptamer studies, messenger adenosine 3',5'-cyclic monophosphate (cAMP-1)<sup>126</sup>, analysing L-arginine specific aptamer<sup>19</sup>. However, equilibrium-based methods assume free movement of small molecules across a membrane, which may not always be the case for some molecules, such as ATP. A study by Huizenga and Szostak demonstrated an incomplete passing of ATP through the membrane<sup>236</sup>. Moreover, both methods utilise radioisotope labelled targets, thus a radioisotope certified laboratory is required to undertake these assays which is not always available.

### 1.5.8 Fluorescent binding assay

Mann *et al.*<sup>90</sup> described fluorescent binding assays for the selection of ethanolamine-binding aptamers. The assay utilises convenient chemical synthesis and modification of oligonucleotides. By labelling an aptamer with a fluorophore, such as FAM<sup>237</sup>, Alexa 488<sup>238</sup> or Cy3<sup>239</sup>, quantification of aptamers can be achieved through the measurement of fluorescent intensity. The assay requires the immobilisation of a target molecule to a solid support (*i.e.* polystyrene microtiter plates, magnetic beads, agarose beads and sepharose beads). Then, a constant amount of the immobilised target can be incubated with a range of fluorophore-labelled aptamer concentrations. Following incubation, any excess unbound aptamers are removed by multiple washing steps, and bound aptamers are then eluted from aptamer-target complexes using denaturing substances such as SDS, EDTA or urea. Fluorescent intensity of the eluted aptamers can then be determined by fluorometry using appropriate excitation and emission wavelengths corresponding to the fluorophore used for aptamer labelling, followed by the calculation of saturation curves by using fluorophore

calibration plots. Due to simplicity, low cost, and user-friendly features, the method has been used to determine the binding features for aptamers targeting small molecules such as, chloramphenicol<sup>240</sup>, L-tryptophan<sup>241</sup>, polychlorinated biphenyls<sup>242</sup>, and okadaic acid<sup>184</sup>.

## Aptamer-based biosensors

Thousands of DNA or RNA aptamers have been identified for various targets, such as proteins, peptides, amino acids, antibiotics, viruses, whole or part of cells, metal ions, and even small chemicals, with high specificity and affinity, and they have been applied in therapeutics and analysis<sup>243</sup>.

A biosensor is an analytical device that detects changes in biological processes and converts them into an electrical signal by using as recognition element enzymes, antibodies, nucleic acids or aptamers. An aptasensor is a class of biosensor where the biological recognition element is a DNA or RNA aptamer, in which the aptamer recognizes the molecular target against which it was previously *in vitro* selected. The aptamer-target reaction is independent of both the type of detection system and the kind of transducer employed. Aptasensors can be easily multiplexed to detect a variety of aptamer-target reactions simultaneously<sup>244</sup>. According to their transducing element biosensors can be divided into (a) optical transduction, (b) electrochemical detection and (c) mass sensitive detection. Several aptasensors for the detection of different targets ranging from small ion molecules to large proteins have been reported, using optical transduction, mass-sensitive or electrochemical detection<sup>245,246</sup>. Within the following section, examples of aptasensors that have been developed for the detection of small molecules are detailed.

### 1.6.1 Optical-based aptasensors

Because of their chemical and physical properties, ability to absorb and scattered the light with high efficiency in a wide range of colours, AuNPs are widely used as labels in sensing. Moreover, the phenomena of physical or chemical adsorption between aptamers and AuNPs has been very well studied<sup>247,248</sup>.

In gold nanoparticle aggregation colorimetric assays, the aptamer is adsorbed onto the surface of AuNPs thus preventing their aggregation and maintaining the red colour of non-aggregated gold nanoparticles. Upon the target introduction, the aptamers are displaced from the surface of the AuNPs, and following addition of salt, the AuNPs aggregate, resulting in a change in colour to blue-purple<sup>249</sup>.

This technique has been widely used for detection of different small molecules including histamine<sup>250</sup>, metal ions, Hg<sup>2+</sup><sup>251</sup>, cocaine<sup>252</sup>, theophylline<sup>253</sup>, aminoglycosides<sup>254</sup>, serotonin<sup>255</sup>, malathion pesticide<sup>256</sup>, streptomycin detection in blood serum and milk<sup>257</sup>,

Ochratoxin A in red wine, as well as cocaine in spiked synthetic urine and saliva, respectively<sup>258</sup>.

AuNPs are very effective quenchers of fluorescence, and Chen *et al.* exploited this for the determination of Kanamycin A in milk samples. Dye-labelled aptamer was adsorbed onto the surface of AuNPs resulting in fluorescence quenching. Upon addition of Kanamycin A, the dye-labelled aptamer was displaced from the surface of AuNPs and the recovery of fluorescence intensity<sup>259</sup>.

AuNPs have also been used to enhance the sensitivity and selectivity of the resonance scattering (RS) in detection of tetracycline in milk<sup>260</sup>, and metal ions<sup>261</sup>. In this work, an aptamer-modified nanogold resonance scattering (RS) probe (AussDNA) is used for the detection of Hg<sup>2+</sup>. In principle, in the presence of Hg<sup>2+</sup>, nanogold particles aggregate to large nanogold clusters, generating a linear increase of RS intensity at 540 nm. Whenever the large nanogold clusters are removed by membrane filtration, the excess AussDNA in the filtrate solution exhibits a catalytic effect on the new Cu<sub>2</sub>O particle reaction between NH<sub>2</sub>OH and Cu<sup>2+</sup>-EDTA complex at 60 °C. In the addition of Hg<sup>2+</sup>, the excess AussDNA is decreased, resulting in the decrease of Cu<sub>2</sub>O particle RS intensity at 602 nm in a linear response to Hg<sup>2+</sup> concentration in the range of 0.1-400 nM, with a detection limit of 0.03 nM Hg<sup>2+</sup><sup>261</sup>.

Overall, the aforementioned studies demonstrate AuNPs aptasensors are suitable for the on-site detection of small molecules, due to its excellent simplicity, but its accuracy and reproducibility is slightly low, because the interaction between aptamers and AuNPs is rather delicate depending on the sensing environments. Therefore, this method is more for qualitative rather than quantitative analysis. Another limitation of AuNP-based colorimetric assays is the tendency of AuNPs to aggregate non-specifically in the presence of salt and other molecules present in the complex biological fluids<sup>248,262</sup>.

Other types of optical aptasensors require conjugation of the aptamer with an optically active molecule. Applying fluorescent probes such as quantum dots (QDs), nanoclusters, carbon, and fluorescent dyes, which show enhanced or quenched fluorescence intensity along with the binding between aptamers and their targets, fluorescent aptasensors achieve quantitative determination of target molecules based on the variation of fluorescence signal intensity<sup>263</sup>.

GO is one of the quencher nanomaterials that has the capability to capture the radiative energy emitted by the fluorophores. Using this advantage, Wang *et al.*<sup>264</sup> developed an experiment where simultaneously labelled aptamer with two different fluorophores were used for the detection of two different mycotoxins, ochratoxin and zearalenone. In the presence of the dual targets, the labelled aptamers were released, and form GO and the fluorescence in different lengths were measured. In other studies the combination of the fluorescent dye FAM with magnetic reduced GO also exhibits excellent sensitivity and has been applied to the detection of patulin<sup>265</sup>, deoxynivalenol<sup>211</sup>, and cylindrospermopsin<sup>266</sup>. Apart from GO, molybdenum carbide nanotubes are used for the fluorescence quenching of bisphenol A detection<sup>267</sup>. A simple ratiometric fluorescent sensing platform was proposed by Ahmadi *et al.*<sup>268</sup> for detection of patulin using target-induced strand displacement composed of two fluorescent dyes, FAM and Carboxytetramethylrhodamine (TAMRA).

Sabet *et al.*<sup>269</sup> apply a fluorescence quenching-based method, in which aptamer-conjugated quantum dots (QDs) are adsorbed to AuNPs, thus quenching the fluorescence of the QDs, which is restored upon addition of AFB1 due to displacement of the aptamers from the

AuNPs. Wang *et al.*<sup>270</sup> developed FRET aptasensor for the simultaneous determination of AFB1 and FB1 levels using quantum dots with different emission peaks (GQDs and RQDs) and magnetic GO/Fe<sub>3</sub>O<sub>4</sub> as the single acceptor.

Wu *et al.*<sup>271</sup> use two pyrenes molecules instead of one so to increase the fluorescence intensity in cocaine detection. The cocaine aptamer was split in 2 parts, each of them labelled with a pyrene, and the binding was measured by time-resolved fluorescence.

SPR technology is commonly utilised for the study of molecular binding interactions between free analyte molecules in solution and probe molecules which are linked to or immobilised onto the sensor surface in real time<sup>272-274</sup>. Although SPR has been widely used in biological analytes it is still a challenge for its detection of small biomolecules as the binding of small molecules with its aptamer causes too little change in refractive index for detection. In order to overcome this drawback, AuNPs have been combined with SPR aptasensor to enhance the signal, as in the case of adenosine detection which produce a detection range from  $1 \times 10^{-9}$  to  $1 \times 10^{-6}$  M<sup>221</sup>. Additionally, a GO-AuNPs composites SPR aptasensor in combination with a split aptamer was used for signal amplification in adenosine detection<sup>275</sup>.

### 1.6.2 Electrochemical aptasensors

Electrochemical aptasensors are classified in impedimetric, amperometric/voltammetric, and potentiometric sensors, and have been demonstrated to be useful tools for detection of biological small molecules including neurotransmitters, metabolites, vitamins, amino acids, dietary minerals<sup>246</sup>, antibiotics<sup>276-278</sup>, mycotoxin<sup>279</sup>, and alkaline metals<sup>280</sup>. In order to enhance the specificity and sensitivity of the electrochemical aptasensors for small molecules, nanomaterials such as are carbon nanotubes (CNTs), graphene, quantum dots (QDs), conducting polymers (CPs), and metal nanoparticles (MNPs), and AuNPs<sup>281</sup>. For example, incorporation of AuNPs can assist in improving their electrochemical signal in using two different approaches. The first approach is the enlargement of electrode surface by attachment of AuNPs on electrode, which might increase the amount of capture probes on electrode thus the electrochemical signal intensity can be enhanced.

Several electrochemical aptasensors have been developed for the detection of cocaine<sup>282</sup>. Li and co-workers developed a sensitive electrochemical aptasensor for cocaine detection using AuNPs self-assembled on a gold electrode<sup>283</sup>. Following the same principle Zhu *et al.*<sup>284</sup>, reported kanamycin detection conducting polymer-Au nanocomposite on screen-printed electrode (SPE). In another study AuNP was combined with multiwalled carbon-nanotubes-reduced graphene oxide nanoribbon for the detection of insecticide acetamiprid in soil, water and food samples through impedimetric aptasensor<sup>285</sup>. Omidina *et al.*<sup>286</sup> developed an aptasensor for phenylalanine detection using the electrochemical transduction method where 5-thiol-terminated aptamer is covalently attached onto a gold electrode. Other examples include 17 $\beta$ -estradiol detection<sup>287</sup>, l-histidine based on the switching structure of aptamer and gold nanoparticles-graphene nanosheets (GNPs-GNSs) composite<sup>288</sup>.

Other studies were focused on the detection of neurotransmitters such as serotonin<sup>289</sup>. The aptamer which was previously immobilized on a gold electrode through gold-thiol binding was

labelled my methylene blue in two different positions, where the aptasensor intermediate-labelled methylene site has the higher response in comparison to terminal methylene labelled site.

Cyclic voltammetry and electrochemical impedance spectroscopy were used for measuring the aptasensor signal in every step. Dopamine detection has been studied in different aptasensors<sup>290</sup>. An amperometric aptasensor for dopamine was fabricated on the basis of the electrostatic interactions between a negatively charged RNA specific aptamer and a positively charged cysteamine-modified gold electrode<sup>291</sup>. Moreover, the aptasensor specificity and stability when use in serum ,was improved via regulating the electrostatic immobilization of the aptamer in the next work from the same group<sup>292</sup>.

### 1.7 Lateral flow aptamer assays

The majority of before mention techniques require trained personnel, expensive instrumentation and are often laboratory based, limiting their use at point of care settings. In recent years, lateral flow assays (LFA) have gained significant attention due to their ease of use and high sensitivity. LFAs were first reported in 1956 by Plotz and Singer, and since then, hundreds of LFAs have been developed for the detection of a wide range of targets as it is summarized in Table 1.6.

Low development costs and ease of production of LFAs have resulted in the expansion of its applications to multiple fields in which rapid tests are required (Table 1.5). LFA is a paper based platform composed of a membrane such as nitrocellulose, which consists of a sample pad, conjugate pad, test and control line, and the absorbance pad, all assembled on a plastic backing pad which provides mechanical support<sup>293</sup>. LFA is based on affinity interaction, the sample is added to the sample pad and later migrates towards the conjugation pad via capillary action. The liquid in the sample hydrates a detection label in the pad consisting of a molecular recognition element (antibody or aptamer) coupled to a reporter molecule, which is always present in excess amount. If the target is present, it will form a complex that results in an appropriate response on the test line, while a response on the control line indicates the proper liquid flow through the strip. The read-out, represented by the lines appearing with different intensities, can be assessed by eye or using a dedicated reader<sup>294,295</sup>.

Although there are different applications of LFA for different targets, still, the device has a complex architecture, and many critical elements need to be considered during instrumental design to improve the sensitivity and the cost of the format.

**Table 1.5.** The advantages and limitations of lateral flow assay.

<b>Advantages</b>	<b>Limitations</b>
Low cost	Speed of capillary action cannot be controlled
Fast analysis of results	Generally qualitative or semi-quantitative
User-friendly	Batch reproducibility can vary
Microfluidic	Cross-reactivity can occur

Generally, does not require sample pre-treatment	Hook effect
No or little requirement for electricity	Can be difficult to construct a successful conjugate
Wide range of applications	Optimization is difficult
Can be multiplexed	

Different lateral flow assay formats have been reported exploiting aptamers as the bio affinity element as detailed below.

### 1.7.1 Sandwich aptamer lateral flow assay

The sandwich assay format is the most commonly used format for testing large molecules, which have multiple binding sites, and can exploit dual aptamers, a combination of antibodies and aptamer or split aptamer.

#### a) Sandwich aptamer lateral flow assay using pair of aptamers

Ahmad Raston *et al.*<sup>296</sup> used the vaspin dual aptamer (V1 and V49) in the paired aptamers lateral flow assay format, by using a AuNPs-secondary aptamer (V49) aptamer as a reporter molecule. The streptavidin-biotinylated aptamer V1 was used in test lined while the streptavidin-biotinylated complementary sequence to V49 aptamer was immobilized on the control line. In the presence of vaspin, the complex between the target and V491-AuNPs is captured by the V1 aptamer immobilised on the test line and a red band is observed. For the control experiment, complementary V49 aptamer on the control zone will capture the remaining AuNPs-V49 aptamer resulting in a second red band, the control line, demonstrating that the assay was working properly. Other examples of targets analysed in sandwich assay format, with some differences in bioconjugate preparation, are Ramon cancer cells<sup>297</sup> and arboviruses, including the Chikungunya and the Tick-borne encephalitis virus<sup>298</sup>.

#### b) Sandwich aptamer lateral flow assay using split aptamer

To overcome the absence of dual aptamers in LFA development, sandwich assay format using split aptamer fragments is used as an alternative solution. Zhu *et al.*<sup>299</sup> developed this novel assay by using two DNA probes that only assemble in the presence of the target ATP. One thiolated split aptamer (aptamer part 1) was chemisorbed on AuNPs and the other split aptamer was biotinylated (aptamer part 2) and immobilised on the nitrocellulose membrane by streptavidin-biotin interactions. DNA probe complementary to the aptamer part 1 AuNP bioconjugate was immobilised (DNA1) on the control line. In the presence of ATP, a complex between aptamer part 1AuNP/ATP/biotinylated aptamer part 2 was formed on the test line giving a red band. Excess aptamer part 1 AuNP was captured on the control line by hybridisation with DNA1.

#### c) Sandwich aptamer lateral flow assay using a combination of antibodies and aptamers

As dual aptamer selection can be challenging for some types of molecules, especially those with limited binding domains for aptamer binding, a different approach of sandwich assay consists in combination of 2 different biorecognition molecules, antibodies and aptamer, that bind to different sites of the target. One example is the detection of salivary  $\alpha$ -amylase (sAA). In this case, AMYm1 aptamer was modified with biotin and linked to streptavidin-AuNPs (aptamer-Biotin-SA-AuNP). On the test line anti-sAA antibody was immobilised and sAA protein was immobilised on the control line. In the presence of sAA, the complex between the target and aptamer-Biotin-SA-AuNP was captured by the antibody immobilised on the test line and the excess of bio conjugate (aptamer-Biotin-SA-AuNP) was captured on the control line, resulting in two red bands. In the absence of target, the bioconjugate was captured on the control line and only one band was observed<sup>300</sup>.

### 1.7.2 Competitive lateral flow aptamer assay

As low molecular weight molecules often lack a second binding site for the use of sandwich format, competition or inhibition assays are mostly used for their detection<sup>293,301</sup>. Differently from the sandwich format, in competition assay the presence of control and test line indicate the absence of the target, while the presence of only control line indicates the presence of the target. In the case of competitive LFAs, a decreasing intensity of the band at the test line with increasing concentration of the target analyte in the sample is observed. In competitive assays two different scenarios are employed, in the first, target in the sample solution that will be analysed will compete with the immobilized target on the test line for binding to AuNPs-aptamer conjugate<sup>302</sup>, in the second scenario, DNA, partially complementary to the aptamer-AuNP conjugate, is immobilised on the test line and competes against the target analyte to bind to the gold nanoparticle labelled aptamer<sup>303</sup>. Various solutions have been proposed for the control line including the inclusion of additional bases to the aptamer for subsequent hybridisation with the complementary to these bases immobilised at the control line. Moreover, a great importance should be given to the design of the DNA probe. If the sequence of the DNA probe is too short, the binding affinity to the aptamer can be weak, and this can lead to problems with specificity. Conversely, if the DNA probe is too long, the binding affinity can be too strong, resulting in reduced competition.

A simple and sensitive aptamer-based lateral flow test strip for zearalenone (ZEN) was successfully developed by Wu *et al.*<sup>304</sup> using the competitive format. Under the optimized conditions, the visual limit of detection of the strip was as low as 20 ng/mL. This format was based on the competition between the complementary sequence DNA1 on the test line and ZEN in the sample for binding to AuNPs-Aptamer. In the absence of ZEN, AuNPs-Aptamer is bind through complementary base pairing to DNA 1 on the test line and DNA 2 on the control line, resulting in two red lines. When ZEN is present, the complex AuNPs-Aptamer preferentially binds to ZEN and as result the test line is decreased or diminished. Other examples of small molecule application in lateral flow are summarized in Table 1.6.

**Table 1.6.** Aptamers in lateral flow (adapted from reference 324)

Target	LOD	Format	Test line	Control line	Bioconjugate	Ref.
Adenosine/Cocaine	20 $\mu$ M Adenosine 10 $\mu$ M cocaine	Direct assay (2 AuNP-conjugates)	SA	-	AuNPs-DNA 1 + Biotin-DNA 2-AuNPs-DNA 2 +Aptamer	305
Aflatoxin B1 (AFB1)	0.32 nM	Competitive assay	SA	Anti-Cy5 antibody	-	306
Arbovirus (Chikungunya virus and TBEV)	-	Sandwich assay (Pair of aptamers)	SA-biotin-aptamer	-	AuNPs-SA-biotin-DNA complementary	298
ATP	0.5 $\mu$ M	Sandwich assay (Split aptamer)	SA-biotin-split aptamer 2	SA-biotin DNA probe	AuNPs-split aptamer 1	299
ATP	69 $\mu$ M	Competition assay	Aptamer gated silica nanoparticles loaded rhodamine B dye	Mutated aptamer gated nanoparticles loaded rhodamine B dye	-	307
<i>E. coli</i> O157:H7	10 CFU/mL	Strand displacement amplification assay	SA-Biotin-DNA probe	SA-Biotin-DNA probe	AuNPs-DNA probe	308
<i>E.coli</i> O157:H7	3000 live cells	Sandwich assay	Amino-aptamer 2	Anti-digoxigenin antibody	QD-aptamer 1-digoxigenin	309
<i>E.coli</i> 8739	6000 live cells	Sandwich assay	Amino-aptamer 2	Anti-digoxigenin antibody	QD-aptamer 1-digoxigenin	309
IgE	0.7 pM	Sandwich assay	Anti-IgE antibody	Anti-M13 antibody	Aptamer-phage	310
Ochratoxin A (OTA)	4.7 nM	Competitive assay	SA-biotin-cDNA	SA-biotin-poly T	QD-aptamer	303
Ochratoxin A (OTA)	2.48 nM; 0.45 nM (strip reader)	Competitive assay	SA-biotin-cDNA	SA-biotin-poly T	AuNPs-aptamer	311
Ochratoxin A (OTA) in <i>Astragalus membranaceus</i>	2.48 nM	Competitive assay	SA-biotin-cDNA	SA-biotin-poly A	AuNPs-aptamer	312
Ramos cells	4000 Ramos cells visual and 800 Ramos cells in strip	Sandwich assay (Pair of aptamers)	SA-biotin-TE02 aptamer	SA-biotin-Control DNA	AuNPs-aptamer	297
Salivary $\alpha$ -amilase (sAA)	-	Sandwich assay (Antibody/aptamer pair)	Anti-sAA antibody	sAA protein	AuNPs-SA-biotin-aptamer	300
<i>Salmonella enteritidis</i>	10 <sup>1</sup> CFU/ml	Strand displacement	SA-Biotin-DNA probe	SA-Biotin-DNA probe	AuNPs-DNA probe	313

		amplification assay				
Thrombin	2.5 nM	Sandwich assay (Pair of aptamers)	SA-biotin-aptamer	SA-biotin-DNA complementary primary aptamer	AuNPs-primary aptamer	314
Thrombin	0.25 nM	Sandwich assay (2 AuNPs-conjugates)	Anti-thrombin antibody	SA-biotin-poly A	AuNPs-DNA 1/DNA 2-AuNPs-Aptamer	315
Thrombin	6.4 pM visual; 4.9 pM strip reader	Aptamer-cleavage + enzymatic reaction	SA	SA-Biotin-cDNA 1	AuNPs-DNA 1/Biotin-DNA 2-AuNPs-HRP	316
Vaspin	0.137 nM	Sandwich assay (Pair of aptamers)	SA-biotin-aptamer	SA-biotin-DNA complementary aptamer	AuNPs-aptamer	296
$\beta$ -conglutinin	55 pM	Competitive assay	$\beta$ -conglutinin	SA-biotin full DNA complementary aptamer	AuNPs-aptamer	302
$\beta$ -conglutinin	9 fM	Competitive assay + recombinase polymerase amplification	SA-Biotin-DNA probe	SA-biotin-DNA probe	AuNPs-DNA probe	302
Cortisol	2.7 nM	Lateral flow	Immobilized cysteamine	Cysteamine	AuNPs-aptamer	317
Zearalenone	20 ng/mL	Competitive assay	SA-DNA1	SA-DNA2	AuNPs-aptamer	304
Dopamine	50 ng/mL	Lateral flow	SA-Biotin-DNA probe	Streptavidin-DNA	AuNPs-aptamer	318
Ochratoxin A	1 ng/mL	Lateral flow	SA-Biotin-DNA probe	Streptavidin-DNA	AuNPs-aptamer	312
HER2	10 nM	Lateral flow	SA-Biotin-DNA probe	SA-DNA probe	AuNPs-aptamer	319
Ampicillin	185 mg/L	Competitive assay	Biotin-CRP	$\alpha$ -mouse antibody	AuNPs-aptamer	320
Creatine kinase MB	0.63 ng/mL	Fluorometric lateral flow assay	Streptavidin-C.Apt.21	Streptavidin-DNA probe	SA-fluorescencemicroparticles-C.Apt.30	321
Kanamycin	50 nM	Competitive assay	Streptavidin-biotin-capDNA1	Streptavidin-biotin-capDNA2	AuNPs-DNA1	322
Mercury	0.13 ng/mL	Competitive assay	Fluorescence microspheres-BSA	Fluorescence microspheres-BSA	AuNPs-aptamer	323

## References

- (1) Lockett, M. R.; Lange, H.; Breiten, B.; Heroux, A.; Sherman, W.; Rappoport, D.; Yau, P. O.; Snyder, P. W.; Whitesides, G. M. The Binding of Benzoarylsulfonamide Ligands to Human Carbonic Anhydrase Is Insensitive to Formal Fluorination of the Ligand. *Angew. Chemie - Int. Ed.* **2013**.
- (2) Cosic, I. Macromolecular Bioactivity: Is It Resonant Interaction Between Macromolecules?—Theory and Applications. *IEEE Trans. Biomed. Eng.* **1994**.
- (3) Shaaya, M.; Fauser, J.; Karginov, A. V. Optogenetics: The Art of Illuminating Complex Signaling Pathways. *Physiology* **2021**.
- (4) Henikoff, S.; Ahmad, K. ASSEMBLY OF VARIANT HISTONES INTO CHROMATIN. *Annu. Rev. Cell Dev. Biol.* **2005**.
- (5) Serganov, A.; Nudler, E. A Decade of Riboswitches. *Cell.* 2013, Pages .
- (6) Ellington, A. D.; Szostak, J. W. In Vitro Selection of RNA Molecules That Bind Specific Ligands. *Nature* **1990**.
- (7) Tuerk, C.; Gold, L. Systematic Evolution of Ligands by Exponential Enrichment: RNA Ligands to Bacteriophage T4 DNA Polymerase. *Science (80- )*. **1990**.
- (8) Hermann, T.; Patel, D. J. Adaptive Recognition by Nucleic Acid Aptamers. *Science.* 2000, Pages .
- (9) Stoltenburg, R.; Reinemann, C.; Strehlitz, B. SELEX-A (r)Evolutionary Method to Generate High-Affinity Nucleic Acid Ligands. *Biomolecular Engineering.* 2007, Pages .
- (10) McGown, L. B.; Joseph, M. J.; Pitner, J. B.; Vonk, G. P.; Linn, C. P. The Nucleic Acid Ligand. A New Tool for Molecular Recognition. *Anal. Chem.* **1995**.
- (11) Zhang, Y.; Lai, B. S.; Juhas, M. Recent Advances in Aptamer Discovery and Applications. *Molecules.* 2019, Pages .
- (12) Iliuk, A. B.; Hu, L.; Tao, W. A. Aptamer in Bioanalytical Applications. *Analytical Chemistry.* 2011, Pages .
- (13) Jayasena, S. D. Aptamers: An Emerging Class of Molecules That Rival Antibodies in Diagnostics. *Clin. Chem.* **1999**.
- (14) Keefe, A. D.; Pai, S.; Ellington, A. Aptamers as Therapeutics. *Nature Reviews Drug Discovery.* 2010, Pages .
- (15) Jayasena, S. D. Aptamers: An Emerging Class of Molecules That Rival Antibodies in Diagnostics. *Clin. Chem.* **1999**.
- (16) Ng, E. W. M.; Shima, D. T.; Calias, P.; Cunningham, E. T.; Guyer, D. R.; Adamis, A. P. Pegaptanib, a Targeted Anti-VEGF Aptamer for Ocular Vascular Disease. *Nature Reviews Drug Discovery.* 2006, Pages .
- (17) Xiang, D.; Shigdar, S.; Qiao, G.; Wang, T.; Kouzani, A. Z.; Zhou, S. F.; Kong, L.; Li, Y.; Pu, C.; Duan, W. Nucleic Acid Aptamer-Guided Cancer Therapeutics and Diagnostics: The next Generation of Cancer Medicine. *Theranostics.* 2015, Pages .
- (18) Jenison, R. D.; Gill, S. C.; Pardi, A.; Polisky, B. High-Resolution Molecular Discrimination by RNA. *Science (80- )*. **1994**.
- (19) Geiger, A.; Burgstaller, P.; Von der Eltz, H.; Roeder, A.; Famulok, M. RNA Aptamers That Bind L-Arginine with Sub-Micromolar Dissociation Constants and High Enantioselectivity. *Nucleic Acids Res.* **1996**.
- (20) Kurt, H.; Yüce, M.; Hussain, B.; Budak, H. Dual-Excitation Upconverting Nanoparticle and Quantum Dot Aptasensor for Multiplexed Food Pathogen Detection. *Biosens. Bioelectron.* **2016**.
- (21) Yüce, M.; Kurt, H.; Hussain, B.; Ow-Yang, C. W.; Budak, H. Exploiting Stokes and Anti-Stokes Type Emission Profiles of Aptamer-Functionalized Luminescent Nanoprobes for Multiplex Sensing Applications. *ChemistrySelect* **2018**.
- (22) Kurt, H.; Eyüpoğlu, A. E.; Sütlü, T.; Budak, H.; Yüce, M. Plasmonic Selection of SsDNA Aptamers against Fibroblast Growth Factor Receptor. *ACS Comb. Sci.* **2019**.

- (23) Cruz-Aguado, J. A.; Penner, G. Determination of Ochratoxin A with a DNA Aptamer Cruz-Aguado, J. A., & Penner, G. (2008). Determination of Ochratoxin A with a DNA Aptamer. [Http://Doi.Org/10.1021/Jf801957h](http://doi.org/10.1021/Jf801957h). *J. Agric. Food Chem.* **2008**.
- (24) Scoville, D. J.; Uhm, T. K. B.; Shallcross, J. A.; Whelan, R. J. Selection of DNA Aptamers for Ovarian Cancer Biomarker CA125 Using One-Pot SELEX and High-Throughput Sequencing. *J. Nucleic Acids* **2017**.
- (25) Zamay, G. S.; Ivanchenko, T. I.; Zamay, T. N.; Grigorieva, V. L.; Glazyrin, Y. E.; Kolovskaya, O. S.; Garanzha, I. V.; Barinov, A. A.; Krat, A. V.; Mironov, G. G.; Gargaun, A.; Veprintsev, D. V.; Bekuzarov, S. S.; Kirichenko, A. K.; Zukov, R. A.; Petrova, M. M.; Modestov, A. A.; Berezovski, M. V.; Zamay, A. S. DNA Aptamers for the Characterization of Histological Structure of Lung Adenocarcinoma. *Mol. Ther. - Nucleic Acids* **2017**.
- (26) Gold, L.; Ayers, D.; Bertino, J.; Bock, C.; Bock, A.; Brody, E. N.; Carter, J.; Dalby, A. B.; Eaton, B. E.; Fitzwater, T.; Flather, D.; Forbes, A.; Foreman, T.; Fowler, C.; Gawande, B.; Goss, M.; Gunn, M.; Gupta, S.; Halladay, D.; Heil, J.; Heilig, J.; Hicke, B.; Husar, G.; Janjic, N.; Jarvis, T.; Jennings, S.; Katilius, E.; Keeney, T. R.; Kim, N.; Koch, T. H.; Kraemer, S.; Kroiss, L.; Le, N.; Levine, D.; Lindsey, W.; Lollo, B.; Mayfield, W.; Mehan, M.; Mehler, R.; Nelson, S. K.; Nelson, M.; Nieuwlandt, D.; Nikrad, M.; Ochsner, U.; Ostroff, R. M.; Otis, M.; Parker, T.; Pietrasiewicz, S.; Resnicow, D. I.; Rohloff, J.; Sanders, G.; Sattin, S.; Schneider, D.; Singer, B.; Stanton, M.; Sterkel, A.; Stewart, A.; Stratford, S.; Vaught, J. D.; Vrkljan, M.; Walker, J. J.; Watrobka, M.; Waugh, S.; Weiss, A.; Wilcox, S. K.; Wolfson, A.; Wolk, S. K.; Zhang, C.; Zichi, D. Aptamer-Based Multiplexed Proteomic Technology for Biomarker Discovery. *PLoS One* **2010**.
- (27) Mayer, G. The Chemical Biology of Aptamers. *Angewandte Chemie - International Edition*. 2009, Pages .
- (28) Odeh, F.; Nsairat, H.; Alshaer, W.; Ismail, M. A.; Esawi, E.; Qaqish, B.; Bawab, A. Al; Ismail, S. I. Aptamers Chemistry: Chemical Modifications and Conjugation Strategies. *Molecules*. 2020, Pages .
- (29) Vaught, J. D.; Bock, C.; Carter, J.; Fitzwater, T.; Otis, M.; Schneider, D.; Rolando, J.; Waugh, S.; Wilcox, S. K.; Eaton, B. E. Expanding the Chemistry of DNA for in Vitro Selection. *J. Am. Chem. Soc.* **2010**.
- (30) Pieve, C. Da; Williams, P.; Haddleton, D. M.; Palmer, R. M. J.; Missailidis, S. Modification of Thiol Functionalized Aptamers by Conjugation of Synthetic Polymers. *Bioconjug. Chem.* **2010**.
- (31) Dhiman, A.; Kalra, P.; Bansal, V.; Bruno, J. G.; Sharma, T. K. Aptamer-Based Point-of-Care Diagnostic Platforms. *Sensors and Actuators, B: Chemical*. 2017, Pages .
- (32) Research, M. *Global Aptamers Market-Segmented by Type of Products and Applications-Growth, Trends and Forecasts (2018-2023)*; 2018; Pages .
- (33) Blank, M.; Blind, M. Aptamers as Tools for Target Validation. *Current Opinion in Chemical Biology*. 2005, Pages .
- (34) Ellington, A. D.; Szostak, J. W. Selection in Vitro of Single-Stranded DNA Molecules That Fold into Specific Ligand-Binding Structures. *Nature* **1992**.
- (35) Cox, J. C.; Ellington, A. D. Automated Selection of Anti-Protein Aptamers. *Bioorganic Med. Chem.* **2001**.
- (36) Berezovski, M.; Musheev, M.; Drabovich, A.; Krylov, S. N. Non-SELEX Selection of Aptamers. *J. Am. Chem. Soc.* **2006**.
- (37) Ma, H.; Liu, J.; Ali, M. M.; Mahmood, M. A. I.; Labanieh, L.; Lu, M.; Iqbal, S. M.; Zhang, Q.; Zhao, W.; Wan, Y. Nucleic Acid Aptamers in Cancer Research, Diagnosis and Therapy. *Chemical Society Reviews*. 2015, Pages .
- (38) Peng, C. K.; Buldyrev, S. V.; Havlin, S.; Simons, M.; Stanley, H. E.; Goldberger, A. L. Mosaic Organization of DNA Nucleotides. *Phys. Rev. E* **1994**.
- (39) Blind, M.; Blank, M. Aptamer Selection Technology and Recent Advances. *Molecular Therapy - Nucleic Acids*. 2015, Pages .
- (40) Luo, X.; Mckeague, M.; Pitre, S.; Dumontier, M.; Green, J.; Golshani, A.; Derosa, M. C.; Dehne, F. Computational Approaches toward the Design of Pools for the in Vitro Selection of Complex Aptamers. *RNA* **2010**.
- (41) Wolfgang Pieken, Diane Tasset, Nebojsa Janjic, Larry Gold, G. P. K. High Affinity Nucleic Acid Ligands Containing Modified Nucleotides. **1999**.

- (42) Barry Polisky, Robert D. Jenison, L. G. High Affinity Nucleic Acid Ligands That Discriminate between Theophylline and Caffeine, 1996.
- (43) Biesecker, G.; Dihel, L.; Enney, K.; Bendele, R. A. Derivation of RNA Aptamer Inhibitors of Human Complement C5. In *Immunopharmacology*; 1999; Pages .
- (44) P. Rusconi, E. Scardino, J. Layzer, G. A. Pitoc, T. L. Ortel, D. M. and B. A. S. The Chemical Biology of Nucleic Acids; 2002; Pages .
- (45) Burmeister, P. E.; Lewis, S. D.; Silva, R. F.; Preiss, J. R.; Horwitz, L. R.; Pendergrast, P. S.; McCauley, T. G.; Kurz, J. C.; Epstein, D. M.; Wilson, C.; Keefe, A. D. Direct in Vitro Selection of a 2'-O-Methyl Aptamer to VEGF. *Chem. Biol.* **2005**.
- (46) Burmeister, P. E.; Wang, C.; Killough, J. R.; Lewis, S. D.; Horwitz, L. R.; Ferguson, A.; Thompson, K. M.; Pendergrast, P. S.; McCauley, T. G.; Kurz, M.; Diener, J.; Cload, S. T.; Wilson, C.; Keefe, A. D. 2'-Deoxy Purine, 2'-O-Methyl Pyrimidine (DRmY) Aptamers as Candidate Therapeutics. *Oligonucleotides* **2006**.
- (47) Latham, J. A.; Johnson, R.; Toole, J. J. The Application of a Modified Nucleotide in Aptamer Selection: Novel Thrombin Aptamers Containing -(1 -Pentynyl)-2'-Deoxyuridine. *Nucleic Acids Res.* **1994**.
- (48) Kato, Y.; Minakawa, N.; Komatsu, Y.; Kamiya, H.; Ogawa, N.; Harashima, H.; Matsuda, A. New NTP Analogs: The Synthesis of 4'-ThioUTP and 4'-ThioCTP and Their Utility for SELEX. *Nucleic Acids Res.* **2005**.
- (49) Avci-Adali, M.; Paul, A.; Wilhelm, N.; Ziemer, G.; Wendel, H. P. Upgrading SELEX Technology by Using Lambda Exonuclease Digestion for Single-Stranded DNA Generation. *Molecules* **2010**.
- (50) Vater, A. Short Bioactive Spiegelmers to Migraine-Associated Calcitonin Gene-Related Peptide Rapidly Identified by a Novel Approach: Tailored-SELEX. *Nucleic Acids Res.* **2003**.
- (51) Jarosch, F.; Buchner, K.; Klussmann, S. In Vitro Selection Using a Dual RNA Library That Allows Primerless Selection. *Nucleic Acids Res.* **2006**.
- (52) Pan, W.; Xin, P.; Patrick, S.; Dean, S.; Keating, C.; Clawson, G. Primer-Free Aptamer Selection Using a Random DNA Library. *J. Vis. Exp.* **2010**.
- (53) Lai, Y. T.; DeStefano, J. J. A Primer-Free Method That Selects High-Affinity Single-Stranded DNA Aptamers Using Thermostable RNA Ligase. *Anal. Biochem.* **2011**.
- (54) Marshall, K. A.; Ellington, A. D. [14] In Vitro Selection of RNA Aptamers. *Methods in Enzymology*. 2000, Pages .
- (55) Tianjiao, W.; Hoy, J. A.; Lamm, M. H.; Nilsen-Hamilton, M. Computational and Experimental Analyses Converge to Reveal a Coherent yet Malleable Aptamer Structure That Controls Chemical Reactivity. *J. Am. Chem. Soc.* **2009**.
- (56) Santosh, B.; Yadava, P. K. Nucleic Acid Aptamers: Research Tools in Disease Diagnostics and Therapeutics. *BioMed Research International*. 2014, Pages .
- (57) Duclair, S.; Gautam, A.; Ellington, A.; Prasad, V. R. High-Affinity RNA Aptamers Against the HIV-1 Protease Inhibit Both in Vitro Protease Activity and Late Events of Viral Replication. *Mol. Ther. - Nucleic Acids* **2015**.
- (58) Lennarz, S.; Alich, T. C.; Kelly, T.; Blind, M.; Beck, H.; Mayer, G. Selective Aptamer-Based Control of Intraneuronal Signaling. *Angew. Chemie - Int. Ed.* **2015**.
- (59) Fabrizio, E. F.; Nadim, A.; Sterling, J. D. Resolution of Multiple SsDNA Structures in Free Solution Electrophoresis. *Anal. Chem.* **2003**.
- (60) Kim, Y. S.; Gu, M. B. Advances in Aptamer Screening and Small Molecule Aptasensors. *Adv. Biochem. Eng. Biotechnol.* **2014**.
- (61) Förster, U.; Weigand, J. E.; Trojanowski, P.; Suess, B.; Wachtveitl, J. Conformational Dynamics of the Tetracycline-Binding Aptamer. *Nucleic Acids Res.* **2012**.
- (62) Hianik, T.; Ostatná, V.; Sonlajtnerova, M.; Grman, I. Influence of Ionic Strength, PH and Aptamer Configuration for Binding Affinity to Thrombin. *Bioelectrochemistry* **2007**.
- (63) Baaske, P.; Wienken, C. J.; Reineck, P.; Duhr, S.; Braun, D. Optical Thermophoresis for Quantifying the Buffer

Dependence of Aptamer Binding. *Angew. Chemie - Int. Ed.* **2010**.

- (64) Carothers, J. M.; Goler, J. A.; Kapoor, Y.; Lara, L.; Keasling, J. D. Selecting RNA Aptamers for Synthetic Biology: Investigating Magnesium Dependence and Predicting Binding Affinity. *Nucleic Acids Res.* **2010**.
- (65) Gatto, B.; Palumbo, M.; Sissi, C. Nucleic Acid Aptamers Based on the G-Quadruplex Structure: Therapeutic and Diagnostic Potential. *Curr. Med. Chem.* **2009**.
- (66) Paborsky, L. R.; McCurdy, S. N.; Griffin, L. C.; Toole, J. J.; Leung, L. L. K. The Single-Stranded DNA Aptamer-Binding Site of Human Thrombin. *J. Biol. Chem.* **1993**.
- (67) Okazawa, A.; Maeda, H.; Fukusaki, E.; Katakura, Y.; Kobayashi, A. In Vitro Selection of Hematoporphyrin Binding DNA Aptamers. *Bioorganic Med. Chem. Lett.* **2000**.
- (68) De Soultrait, V. R.; Lozach, P. Y.; Altmeyer, R.; Tarrago-Litvak, L.; Litvak, S.; Andréola, M. L. DNA Aptamers Derived from HIV-1 RNase H Inhibitors Are Strong Anti-Integrase Agents. *J. Mol. Biol.* **2002**.
- (69) Bianchini, M.; Radrizzani, M.; Brocardo, M. G.; Reyes, G. B.; Gonzalez Solveyra, C.; Santa-Coloma, T. A. Specific Oligobodies against ERK-2 That Recognize Both the Native and the Denatured State of the Protein. *J. Immunol. Methods* **2001**.
- (70) Joeng, C. B.; Niazi, J. H.; Lee, S. J.; Gu, M. B. SsDNA Aptamers That Recognize Diclofenac and 2-Anilinophenylacetic Acid. *Bioorganic Med. Chem.* **2009**.
- (71) Jo, M.; Ahn, J. Y.; Lee, J.; Lee, S.; Hong, S. W.; Yoo, J. W.; Kang, J.; Dua, P.; Lee, D. K.; Hong, S.; Kim, S. Development of Single-Stranded DNA Aptamers for Specific Bisphenol a Detection. *Oligonucleotides* **2011**.
- (72) Hedayati Ch, M.; Amani, J.; Sedighian, H.; Amin, M.; Salimian, J.; Halabian, R.; Imani Fooladi, A. A. Isolation of a New SsDNA Aptamer against Staphylococcal Enterotoxin B Based on CNBr-Activated Sepharose-4B Affinity Chromatography. *J. Mol. Recognit.* **2016**.
- (73) Ciesiolka, J.; Gorski, J.; Yarus, M. Selection of an RNA Domain That Binds Zn<sup>2+</sup>. *RNA* **1995**.
- (74) Espiritu, C. A. L.; Justo, C. A. C.; Rubio, M. J.; Svobodova, M.; Bashammakh, A. S.; Alyoubi, A. O.; Rivera, W. L.; Rollon, A. P.; O'Sullivan, C. K. Aptamer Selection against a Trichomonas Vaginalis Adhesion Protein for Diagnostic Applications. *ACS Infect. Dis.* **2018**, 4 (9), 1306–1315.
- (75) Challa, S.; Tzipori, S.; Sheoran, A. Selective Evolution of Ligands by Exponential Enrichment to Identify Rna Aptamers against Shiga Toxins. *J. Nucleic Acids* **2014**.
- (76) Bruno, J. G.; Kiel, J. L. Use of Magnetic Beads in Selection and Detection of Biotxin Aptamers by Electrochemiluminescence and Enzymatic Methods. *Biotechniques* **2002**.
- (77) Lin, C.; Liu, Z. S.; Wang, D. X.; Li, L.; Hu, P.; Gong, S.; Li, Y. S.; Cui, C.; Wu, Z. C.; Gao, Y.; Zhou, Y.; Ren, H. L.; Lu, S. Y. Generation of Internal-Image Functional Aptamers of Okadaic Acid via Magnetic-Bead SELEX. *Mar. Drugs* **2015**.
- (78) Skouridou, V.; Jauset-Rubio, M.; Ballester, P.; Bashammakh, A. S.; El-Shahawi, M. S.; Alyoubi, A. O.; O'Sullivan, C. K. Selection and Characterization of DNA Aptamers against the Steroid Testosterone. *Microchim. Acta* **2017**.
- (79) Mairal Lerga, T.; Jauset-Rubio, M.; Skouridou, V.; Bashammakh, A. S.; El-Shahawi, M. S.; Alyoubi, A. O.; O'Sullivan, C. K. High Affinity Aptamer for the Detection of the Biogenic Amine Histamine. *Anal. Chem.* **2019**.
- (80) Jauset-Rubio, M.; Botero, M. L.; Skouridou, V.; Aktas, G. B.; Svobodova, M.; Bashammakh, A. S.; El-Shahawi, M. S.; Alyoubi, A. O.; O'Sullivan, C. K. One-Pot SELEX: Identification of Specific Aptamers against Diverse Steroid Targets in One Selection. *ACS Omega* **2019**.
- (81) Mendonsa, S. D.; Bowser, M. T. In Vitro Selection of High-Affinity DNA Ligands for Human IgE Using Capillary Electrophoresis. *Anal. Chem.* **2004**.
- (82) Mendonsa, S. D.; Bowser, M. T. In Vitro Selection of Aptamers with Affinity for Neuropeptide Y Using Capillary Electrophoresis. *J. Am. Chem. Soc.* **2005**.
- (83) Drabovich, A.; Berezovski, M.; Krylov, S. N. Selection of Smart Aptamers by Equilibrium Capillary Electrophoresis of Equilibrium Mixtures (ECEEM). *J. Am. Chem. Soc.* **2005**.

- (84) Dobbelstein, M.; Shenk, T. In Vitro Selection of RNA Ligands for the Ribosomal L22 Protein Associated with Epstein-Barr Virus-Expressed RNA by Using Randomized and CDNA-Derived RNA Libraries. *J. Virol.* **1995**.
- (85) Rhie, A.; Kirby, L.; Sayer, N.; Wellesley, R.; Disterer, P.; Sylvester, I.; Gill, A.; Hope, J.; James, W.; Tahiri-Alaoui, A. Characterization of 2'-Fluoro-RNA Aptamers That Bind Preferentially to Disease-Associated Conformations of Prion Protein and Inhibit Conversion. *J. Biol. Chem.* **2003**.
- (86) Davis, J. H.; Szostak, J. W. Isolation of High-Affinity GTP Aptamers from Partially Structured RNA Libraries. *Proc. Natl. Acad. Sci. U. S. A.* **2002**.
- (87) Tsai, R. Y. L.; Reed, R. R. Identification of DNA Recognition Sequences and Protein Interaction Domains of the Multiple-Zn-Finger Protein Roaz. *Mol. Cell. Biol.* **1998**.
- (88) Gopinath, S. C. B. Methods Developed for SELEX. *Anal. Bioanal. Chem.* **2007**.
- (89) Gu, H.; Duan, N.; Xia, Y.; Hun, X.; Wang, H.; Wang, Z. Magnetic Separation-Based Multiple SELEX for Effectively Selecting Aptamers against Saxitoxin, Domoic Acid, and Tetrodotoxin. *J. Agric. Food Chem.* **2018**.
- (90) Mann, D.; Reinemann, C.; Stoltenburg, R.; Strehlitz, B. In Vitro Selection of DNA Aptamers Binding Ethanolamine. *Biochem. Biophys. Res. Commun.* **2005**.
- (91) Bridonneau, P.; Chang, Y. F.; Buvoli, A. V. B.; O'Connell, D.; Parma, D. Site-Directed Selection of Oligonucleotide Antagonists by Competitive Elution. *Antisense Nucleic Acid Drug Dev.* **1999**.
- (92) Liu, J.; Stormo, G. D. Combining SELEX with Quantitative Assays to Rapidly Obtain Accurate Models of Protein-DNA Interactions. *Nucleic Acids Res.* **2005**.
- (93) Viswanathan, V. K.; Krcmarik, K.; Cianciotto, N. P. Template Secondary Structure Promotes Polymerase Jumping during PCR Amplification. *Biotechniques* **1999**.
- (94) Liu, Z.; Sun, J.; Zhao, G.; Xiong, S.; Ma, Y.; Zheng, M. Transient Stem-Loop Structure of Nucleic Acid Template May Interfere with Polymerase Chain Reaction through Endonuclease Activity of Taq DNA Polymerase. *Gene* **2021**.
- (95) Murphy, M. B.; Fuller, S. T.; Richardson, P. M.; Doyle, S. A. An Improved Method for the in Vitro Evolution of Aptamers and Applications in Protein Detection and Purification. *Nucleic Acids Res.* **2003**.
- (96) Hünninger, T.; Wessels, H.; Fischer, C.; Paschke-Kratzin, A.; Fischer, M. Just in Time -Selection: A Rapid Semiautomated SELEX of DNA Aptamers Using Magnetic Separation and BEAMing. *Anal. Chem.* **2014**.
- (97) Yufa, R.; Krylova, S. M.; Bruce, C.; Bagg, E. A.; Schofield, C. J.; Krylov, S. N. Emulsion PCR Significantly Improves Nonequilibrium Capillary Electrophoresis of Equilibrium Mixtures-Based Aptamer Selection: Allowing for Efficient and Rapid Selection of Aptamer to Unmodified ABH2 Protein. *Anal. Chem.* **2015**.
- (98) WANG Xian-Liang, WANG Xiao-Li, SU Yan-Hua, ZHANG Chi, ZHANG Li-Jun, LI Fang, LI Bai-Sheng, LI Xiao-Bo, XU Shu-Lei, LI Yuan-Yuan, X. S.-Q. A High-Sensitive New Method to Detect Proteins Based on DNA Aptamers and Exonuclease I. **2005**.
- (99) Tolle, F.; Wilke, J.; Wengel, J.; Mayer, G. By-Product Formation in Repetitive PCR Amplification of DNA Libraries during SELEX. *PLoS One* **2014**.
- (100) Jones, L. A.; Clancy, L. E.; Rawlinson, W. D.; White, P. A. High-Affinity Aptamers to Subtype 3a Hepatitis C Virus Polymerase Display Genotypic Specificity. *Antimicrob. Agents Chemother.* **2006**.
- (101) Nikiforov, T. T.; Rendle, R. B.; Kotewicz, M. L.; Rogers, Y. H. The Use of Phosphorothioate Primers and Exonuclease Hydrolysis for the Preparation of Single-Stranded PCR Products and Their Detection by Solid-Phase Hybridization. *PCR Methods Appl.* **1994**.
- (102) Williams, K. P.; Bartel, D. P. PCR Product with Strands of Unequal Length. *Nucleic Acids Res.* **1995**.
- (103) Martínez, O.; Ecochard, V.; Mahéo, S.; Gross, G.; Bodin, P.; Teissié, J.; Escudier, J. M.; Paquereau, L.  $\alpha,\beta$ -D-Constrained Nucleic Acids Are Strong Terminators of Thermostable DNA Polymerases in Polymerase Chain Reaction. *PLoS One* **2011**.
- (104) Cao, X.; Li, S.; Chen, L.; Ding, H.; Xu, H.; Huang, Y.; Li, J.; Liu, N.; Cao, W.; Zhu, Y.; Shen, B.; Shao, N. Combining Use of a Panel of SsDNA Aptamers in the Detection of Staphylococcus Aureus. *Nucleic Acids Res.* **2009**.

- (105) Heiat, M.; Ranjbar, R.; Latifi, A. M.; Rasaei, M. J. Selection of a High-Affinity and in Vivo Bioactive SsDNA Aptamer against Angiotensin II Peptide. *Peptides* **2016**.
- (106) Jing, D.; Agnew, J.; Patton, W. F.; Hendrickson, J.; Beechem, J. M. A Sensitive Two-Color Electrophoretic Mobility Shift Assay for Detecting Both Nucleic Acids and Protein in Gels. In *Proteomics*; 2003; Pages .
- (107) Di Primo, C.; Lebars, I. Determination of Refractive Index Increment Ratios for Protein-Nucleic Acid Complexes by Surface Plasmon Resonance. *Anal. Biochem.* **2007**.
- (108) Ellenbecker, M.; Sears, L.; Li, P.; Lanchy, J. M.; Stephen Lodmell, J. Characterization of RNA Aptamers Directed against the Nucleocapsid Protein of Rift Valley Fever Virus. *Antiviral Res.* **2012**.
- (109) Haghighi, M.; Khanahmad, H.; Palizban, A. Selection and Characterization of Single-Stranded DNA Aptamers Binding Human B-Cell Surface Protein CD20 by Cell-SELEX. *Molecules* **2018**.
- (110) Schütze, T.; Wilhelm, B.; Greiner, N.; Braun, H.; Peter, F.; Mörl, M.; Erdmann, V. A.; Lehrach, H.; Konthur, Z.; Menger, M.; Arndt, P. F.; Glökler, J. Probing the SELEX Process with Next-Generation Sequencing. *PLoS One* **2011**.
- (111) Müller, J.; El-Maarri, O.; Oldenburg, J.; Pötzsch, B.; Mayer, G. Monitoring the Progression of the in Vitro Selection of Nucleic Acid Aptamers by Denaturing High-Performance Liquid Chromatography. *Anal. Bioanal. Chem.* **2008**.
- (112) Mencin, N.; Šmuc, T.; Vraničar, M.; Mavri, J.; Hren, M.; Galeša, K.; Krkoč, P.; Ulrich, H.; Šolar, B. Optimization of SELEX: Comparison of Different Methods for Monitoring the Progress of in Vitro Selection of Aptamers. *J. Pharm. Biomed. Anal.* **2014**.
- (113) Vanbrabant, J.; Leirs, K.; Vanschoenbeek, K.; Lammertyn, J.; Michiels, L. Remelting Curve Analysis as a Tool for Enrichment Monitoring in the SELEX Process. *Analyst* **2014**.
- (114) Amano, R.; Aoki, K.; Miyakawa, S.; Nakamura, Y.; Kozu, T.; Kawai, G.; Sakamoto, T. NMR Monitoring of the SELEX Process to Confirm Enrichment of Structured RNA. *Sci. Rep.* **2017**.
- (115) Navani, N. K.; Mok, W. K.; Yingfu, L. In Vitro Selection of Protein-Binding DNA Aptamers as Ligands for Biosensing Applications. *Methods Mol. Biol.* **2009**.
- (116) Jun, S. L.; McNatty, K. P. Aptamer-Based Regionally Protected PCR for Protein Detection. *Clin. Chem.* **2009**.
- (117) Stoltenburg, R.; Reinemann, C.; Strehlitz, B. FluMag-SELEX as an Advantageous Method for DNA Aptamer Selection. *Anal. Bioanal. Chem.* **2005**.
- (118) Tombelli, S.; Minunni, M.; Luzi, E.; Mascini, M. Aptamer-Based Biosensors for the Detection of HIV-1 Tat Protein. In *Bioelectrochemistry*; 2005; Pages .
- (119) Hoon, S.; Zhou, B.; Janda, K. D.; Brenner, S.; Scolnick, J. Aptamer Selection by High-Throughput Sequencing and Informatic Analysis. *Biotechniques* **2011**.
- (120) Alam, K. K.; Chang, J. L.; Burke, D. H. FASTAptamer: A Bioinformatic Toolkit for High-Throughput Sequence Analysis of Combinatorial Selections. *Mol. Ther. - Nucleic Acids* **2015**.
- (121) Thiel, W. H. Galaxy Workflows for Web-Based Bioinformatics Analysis of Aptamer High-Throughput Sequencing Data. *Mol. Ther. - Nucleic Acids* **2016**.
- (122) Larkin, M. A.; Blackshields, G.; Brown, N. P.; Chenna, R.; McGettigan, P. A.; McWilliam, H.; Valentin, F.; Wallace, I. M.; Wilm, A.; Lopez, R.; Thompson, J. D.; Gibson, T. J.; Higgins, D. G. Clustal W and Clustal X Version 2.0. *Bioinformatics* **2007**.
- (123) Kearse, M.; Moir, R.; Wilson, A.; Stones-Havas, S.; Cheung, M.; Sturrock, S.; Buxton, S.; Cooper, A.; Markowitz, S.; Duran, C.; Thierer, T.; Ashton, B.; Meintjes, P.; Drummond, A. Geneious Basic: An Integrated and Extendable Desktop Software Platform for the Organization and Analysis of Sequence Data. *Bioinformatics* **2012**.
- (124) Zuker, M. Mfold Web Server for Nucleic Acid Folding and Hybridization Prediction. *Nucleic Acids Res.* **2003**.
- (125) Woo, H. M.; Kim, K. S.; Lee, J. M.; Shim, H. S.; Cho, S. J.; Lee, W. K.; Ko, H. W.; Keum, Y. S.; Kim, S. Y.; Pathinayake, P.; Kim, C. J.; Jeong, Y. J. Single-Stranded DNA Aptamer That Specifically Binds to the Influenza Virus NS1 Protein Suppresses Interferon Antagonism. *Antiviral Res.* **2013**.

- (126) Koizumi, M.; Breaker, R. R. Molecular Recognition of CAMP by an RNA Aptamer. *Biochemistry* **2000**.
- (127) Svobodová, M.; Pinto, A.; Nadal, P.; O' Sullivan, C. K. Comparison of Different Methods for Generation of Single-Stranded DNA for SELEX Processes. *Anal. Bioanal. Chem.* **2012**.
- (128) Röthlisberger, P.; Hollenstein, M. Aptamer Chemistry. *Adv. Drug Deliv. Rev.* **2018**.
- (129) Mayer, G.; Ahmed, M. S. L.; Dolf, A.; Endl, E.; Knolle, P. A.; Famulok, M. Fluorescence-Activated Cell Sorting for Aptamer SELEX with Cell Mixtures. *Nat. Protoc.* **2010**.
- (130) Wang, T.; Chen, C.; Larcher, L. M.; Barrero, R. A.; Veedu, R. N. Three Decades of Nucleic Acid Aptamer Technologies: Lessons Learned, Progress and Opportunities on Aptamer Development. *Biotechnology Advances*. 2019, Pages .
- (131) Bayat, P.; Nosrati, R.; Alibolandi, M.; Rafatpanah, H.; Abnous, K.; Khedri, M.; Ramezani, M. SELEX Methods on the Road to Protein Targeting with Nucleic Acid Aptamers. *Biochimie*. 2018, Pages .
- (132) Darmostuk, M.; Rimpelova, S.; Gbelcova, H.; Ruml, T. Current Approaches in SELEX: An Update to Aptamer Selection Technology. *Biotechnology Advances*. 2014, Pages .
- (133) Sun, H.; Zu, Y. A Highlight of Recent Advances in Aptamer Technology and Its Application. *Molecules*. 2015, Pages .
- (134) Zhuo, Z.; Yu, Y.; Wang, M.; Li, J.; Zhang, Z.; Liu, J.; Wu, X.; Lu, A.; Zhang, G.; Zhang, B. Recent Advances in SELEX Technology and Aptamer Applications in Biomedicine. *International Journal of Molecular Sciences*. 2017, Pages .
- (135) Mendonsa, S. D.; Bowser, M. T. In Vitro Evolution of Functional DNA Using Capillary Electrophoresis. *J. Am. Chem. Soc.* **2004**.
- (136) Jorgenson, J. W.; Lukacs, K. D. A. Zone Electrophoresis in Open-Tubular Glass Capillaries. *Anal. Chem.* **1981**.
- (137) Yang, Y.; Yang, D.; Schluesener, H. J.; Zhang, Z. Advances in SELEX and Application of Aptamers in the Central Nervous System. *Biomolecular Engineering*. 2007, Pages .
- (138) Mosing, R. K.; Mendonsa, S. D.; Bowser, M. T. Capillary Electrophoresis-SELEX Selection of Aptamers with Affinity for HIV-1 Reverse Transcriptase. *Anal. Chem.* **2005**.
- (139) Nie, H.; Chen, Y.; Lü, C.; Liu, Z. Efficient Selection of Glycoprotein-Binding DNA Aptamers via Boronate Affinity Monolithic Capillary. *Anal. Chem.* **2013**.
- (140) Mosing, R. K.; Bowser, M. T. Isolating Aptamers Using Capillary Electrophoresis-SELEX (CE-SELEX). *Methods Mol. Biol.* **2009**.
- (141) Tang, J.; Xie, J.; Shao, N.; Yan, Y. The DNA Aptamers That Specifically Recognize Ricin Toxin Are Selected by Two in Vitro Selection Methods. *Electrophoresis* **2006**.
- (142) Berezovski, M.; Drabovich, A.; Krylova, S. M.; Musheev, M.; Okhonin, V.; Petrov, A.; Krylov, S. N. Nonequilibrium Capillary Electrophoresis of Equilibrium Mixtures: A Universal Tool for Development of Aptamers. *J. Am. Chem. Soc.* **2005**.
- (143) Drabovich, A.; Krylov, S. N. Single-Stranded DNA-Binding Protein Facilitates Gel-Free Analysis of Polymerase Chain Reaction Products in Capillary Electrophoresis. In *Journal of Chromatography A*; 2004; Pages .
- (144) Jing, M.; Bowser, M. T. Isolation of DNA Aptamers Using Micro Free Flow Electrophoresis. *Lab Chip* **2011**.
- (145) Hybarger, G.; Bynum, J.; Williams, R. F.; Valdes, J. J.; Chambers, J. P. A Microfluidic SELEX Prototype. *Analytical and Bioanalytical Chemistry*. 2006, Pages .
- (146) Lou, X.; Qian, J.; Xiao, Y.; Viel, L.; Gerdon, A. E.; Lagally, E. T.; Atzberger, P.; Tarasow, T. M.; Heeger, A. J.; Soh, H. T. Micromagnetic Selection of Aptamers in Microfluidic Channels. *Proc. Natl. Acad. Sci. U. S. A.* **2009**.
- (147) Qian, J.; Lou, X.; Zhang, Y.; Xiao, Y.; Tom Soh, H. Generation of Highly Specific Aptamers via Micromagnetic Selection. *Anal. Chem.* **2009**.

- (148) Park, J. W.; Lee, S. J.; Ren, S.; Lee, S.; Kim, S.; Laurell, T. Acousto-Microfluidics for Screening of SsDNA Aptamer. *Sci. Rep.* **2016**.
- (149) Liu, X.; Li, H.; Jia, W.; Chen, Z.; Xu, D. Selection of Aptamers Based on a Protein Microarray Integrated with a Microfluidic Chip. *Lab Chip* **2017**.
- (150) Wang, Q.; Liu, W.; Xing, Y.; Yang, X.; Wang, K.; Jiang, R.; Wang, P.; Zhao, Q. Screening of DNA Aptamers against Myoglobin Using a Positive and Negative Selection Units Integrated Microfluidic Chip and Its Biosensing Application. *Anal. Chem.* **2014**.
- (151) Lai, H. C.; Wang, C. H.; Liou, T. M.; Lee, G. Bin. Influenza A Virus-Specific Aptamers Screened by Using an Integrated Microfluidic System. *Lab Chip* **2014**.
- (152) Cho, M.; Xiao, Y.; Nie, J.; Stewart, R.; Csordas, A. T.; Oh, S. S.; Thomson, J. A.; Soh, H. T. Quantitative Selection of DNA Aptamers through Microfluidic Selection and High-Throughput Sequencing. *Proc. Natl. Acad. Sci. U. S. A.* **2010**.
- (153) Quang, N. N.; Perret, G.; Ducongé, F. Applications of High-Throughput Sequencing for in Vitro Selection and Characterization of Aptamers. *Pharmaceuticals*. 2016, Pages .
- (154) Eaton, R. M.; Shallcross, J. A.; Mael, L. E.; Mears, K. S.; Minkoff, L.; Scoville, D. J.; Whelan, R. J. Selection of DNA Aptamers for Ovarian Cancer Biomarker HE4 Using CE-SELEX and High-Throughput Sequencing. *Anal. Bioanal. Chem.* **2015**.
- (155) Takahashi, M.; Wu, X.; Ho, M.; Chomchan, P.; Rossi, J. J.; Burnett, J. C.; Zhou, J. High Throughput Sequencing Analysis of RNA Libraries Reveals the Influences of Initial Library and PCR Methods on SELEX Efficiency. *Sci. Rep.* **2016**.
- (156) Mi, J.; Liu, Y.; Rabbani, Z. N.; Yang, Z.; Urban, J. H.; Sullenger, B. A.; Clary, B. M. In Vivo Selection of Tumor-Targeting RNA Motifs. *Nat. Chem. Biol.* **2010**.
- (157) Cheng, C.; Chen, Y. H.; Lennox, K. A.; Behlke, M. A.; Davidson, B. L. In Vivo SELEX for Identification of Brain-Penetrating Aptamers. *Mol. Ther. - Nucleic Acids* **2013**.
- (158) Daniels, D. A.; Chen, H.; Hicke, B. J.; Swiderek, K. M.; Gold, L. A Tenascin-C Aptamer Identified by Tumor Cell SELEX: Systematic Evolution of Ligands by Exponential Enrichment. *Proc. Natl. Acad. Sci. U. S. A.* **2003**.
- (159) Ara, M. N.; Hyodo, M.; Ohga, N.; Hida, K.; Harashima, H. Development of a Novel DNA Aptamer Ligand Targeting to Primary Cultured Tumor Endothelial Cells by a Cell-Based SELEX Method. *PLoS One* **2012**.
- (160) Lin, N.; Wu, L.; Xu, X.; Wu, Q.; Wang, Y.; Shen, H.; Song, Y.; Wang, H.; Zhu, Z.; Kang, D.; Yang, C. Aptamer Generated by Cell-SELEX for Specific Targeting of Human Glioma Cells. *ACS Appl. Mater. Interfaces* **2020**.
- (161) Ohuchi, S. P.; Ohtsu, T.; Nakamura, Y. Selection of RNA Aptamers against Recombinant Transforming Growth Factor- $\beta$  Type III Receptor Displayed on Cell Surface. *Biochimie* **2006**.
- (162) Kim, J. W.; Kim, E. Y.; Kim, S. Y.; Byun, S. K.; Lee, D.; Oh, K. J.; Kim, W. K.; Han, B. S.; Chi, S. W.; Lee, S. C.; Bae, K. H. Identification of DNA Aptamers toward Epithelial Cell Adhesion Molecule via Cell-SELEX. *Mol. Cells* **2014**.
- (163) Souza, A. G.; Marangoni, K.; Fujimura, P. T.; Alves, P. T.; Silva, M. J.; Bastos, V. A. F.; Goulart, L. R.; Goulart, V. A. 3D Cell-SELEX: Development of RNA Aptamers as Molecular Probes for PC-3 Tumor Cell Line. *Exp. Cell Res.* **2016**.
- (164) Thiel, W. H.; Thiel, K. W.; Flenker, K. S.; Bair, T.; Dupuy, A. J.; Mc namara, J. O.; Miller, F. J.; H. Giangrande, P. Cell-Internalization SELEX: Method for Identifying Cell- Internalizing RNA Aptamers for Delivering SiRNAs to Target Cells. *Methods Mol. Biol.* **2015**.
- (165) Yan, A.; Levy, M. Cell Internalization SELEX: In Vitro Selection for Molecules That Internalize into Cells. *Methods Mol. Biol.* **2014**.
- (166) Chushak, Y.; Stone, M. O. In Silico Selection of RNA Aptamers. *Nucleic Acids Res.* **2009**.
- (167) Yang, C.; Wang, Y.; Ge, M. H.; Fu, Y. J.; Hao, R.; Islam, K.; Huang, P.; Chen, F.; Sun, J.; Hong, D. F.;

- Naranmandura, H. Rapid Identification of Specific DNA Aptamers Precisely Targeting CD33 Positive Leukemia Cells through a Paired Cell-Based Approach. *Biomater. Sci.* **2019**.
- (168) Davydova, A.; Vorobyeva, M.; Bashmakova, E.; Vorobjev, P.; Krasheninina, O.; Tupikin, A.; Kabilov, M.; Krasitskaya, V.; Frank, L.; Venyaminova, A. Development and Characterization of Novel 2'-F-RNA Aptamers Specific to Human Total and Glycated Hemoglobins. *Anal. Biochem.* **2019**.
- (169) Sinha, A.; Gopinathan, P.; Chung, Y. Da; Lin, H. Y.; Li, K. H.; Ma, H. P.; Huang, P. C.; Shiesh, S. C.; Lee, G. Bin. An Integrated Microfluidic Platform to Perform Uninterrupted SELEX Cycles to Screen Affinity Reagents Specific to Cardiovascular Biomarkers. *Biosens. Bioelectron.* **2018**.
- (170) Yu, F.; Li, H.; Sun, W.; Xu, D.; He, F. Rapid Selection of Aptamers Based on Protein Microarray. *RSC Adv.* **2019**.
- (171) Miyachi, Y.; Shimizu, N.; Ogino, C.; Kondo, A. Selection of DNA Aptamers Using Atomic Force Microscopy. *Nucleic Acids Res.* **2009**.
- (172) Coulter, L. R.; Landree, M. A.; Cooper, T. A. Identification of a New Class of Exonic Splicing Enhancers by in Vivo Selection. *Mol. Cell. Biol.* **1997**.
- (173) Yang, J.; Bowser, M. T. Capillary Electrophoresis-SELEX Selection of Catalytic DNA Aptamers for a Small-Molecule Porphyrin Target. *Anal. Chem.* **2013**.
- (174) Cruz-Toledo, J.; McKeague, M.; Zhang, X.; Giamberardino, A.; McConnell, E.; Francis, T.; DeRosa, M. C.; Dumontier, M. Aptamer Base: A Collaborative Knowledge Base to Describe Aptamers and SELEX Experiments. *Database* **2012**.
- (175) Wilson, C.; Szostak, J. W. Isolation of a Fluorophore-Specific DNA Aptamer with Weak Redox Activity. *Chem. Biol.* **1998**.
- (176) Handy, S. M.; Yakes, B. J.; DeGrasse, J. A.; Campbell, K.; Elliott, C. T.; Kanyuck, K. M.; DeGrasse, S. L. First Report of the Use of a Saxitoxin-Protein Conjugate to Develop a DNA Aptamer to a Small Molecule Toxin. *Toxicon* **2013**.
- (177) Park, J. W.; Tatavarty, R.; Kim, D. W.; Jung, H. T.; Gu, M. B. Immobilization-Free Screening of Aptamers Assisted by Graphene Oxide. *Chem. Commun.* **2012**.
- (178) Stoltenburg, R.; Nikolaus, N.; Strehlitz, B. Capture-SELEX: Selection of DNA Aptamers for Aminoglycoside Antibiotics. *J. Anal. Methods Chem.* **2012**.
- (179) Kiani, Z.; Shafiei, M.; Rahimi-Moghaddam, P.; Karkhane, A. A.; Ebrahimi, S. A. In Vitro Selection and Characterization of Deoxyribonucleic Acid Aptamers for Digoxin. *Anal. Chim. Acta* **2012**.
- (180) Duan, Y.; Gao, Z.; Wang, L.; Wang, H.; Zhang, H.; Li, H. Selection and Identification of Chloramphenicol-Specific DNA Aptamers by Mag-SELEX. *Appl. Biochem. Biotechnol.* **2016**.
- (181) He, S.; Song, B.; Li, D.; Zhu, C.; Qi, W.; Wen, Y.; Wang, L.; Song, S.; Fang, H.; Fan, C. A Graphene Nanoprobe for Rapid, Sensitive, and Multicolor Fluorescent DNA Analysis. *Adv. Funct. Mater.* **2010**.
- (182) Nguyen, V. T.; Kwon, Y. S.; Kim, J. H.; Gu, M. B. Multiple GO-SELEX for Efficient Screening of Flexible Aptamers. *Chem. Commun.* **2014**.
- (183) Gu, H.; Duan, N.; Wu, S.; Hao, L.; Xia, Y.; Ma, X.; Wang, Z. Graphene Oxide-Assisted Non-Immobilized SELEX of Okadaic Acid Aptamer and the Analytical Application of Aptasensor. *Sci. Rep.* **2016**.
- (184) Eissa, S.; Ng, A.; Siaj, M.; Tavares, A. C.; Zourob, M. Selection and Identification of DNA Aptamers against Okadaic Acid for Biosensing Application. *Anal. Chem.* **2013**.
- (185) Wu, S.; Duan, N.; Zhang, W.; Zhao, S.; Wang, Z. Screening and Development of DNA Aptamers as Capture Probes for Colorimetric Detection of Patulin. *Anal. Biochem.* **2016**.
- (186) Chen, X.; Huang, Y.; Duan, N.; Wu, S.; Xia, Y.; Ma, X.; Zhu, C.; Jiang, Y.; Wang, Z. Screening and Identification of DNA Aptamers against T-2 Toxin Assisted by Graphene Oxide. *J. Agric. Food Chem.* **2014**.
- (187) Wang, L.; Liu, X.; Zhang, Q.; Zhang, C.; Liu, Y.; Tu, K.; Tu, J. Selection of DNA Aptamers That Bind to Four Organophosphorus Pesticides. *Biotechnol. Lett.* **2012**.

- (188) Lauridsen, L. H.; Doessing, H. B.; Long, K. S.; Nielsen, A. T. A Capture-SELEX Strategy for Multiplexed Selection of RNA Aptamers against Small Molecules. In *Methods in Molecular Biology*; 2018; Pages .
- (189) Wu, Y.; Zhan, S.; Wang, L.; Zhou, P. Selection of a DNA Aptamer for Cadmium Detection Based on Cationic Polymer Mediated Aggregation of Gold Nanoparticles. *Analyst* **2014**.
- (190) Paniel, N.; Istamboulié, G.; Triki, A.; Lozano, C.; Barthelmebs, L.; Noguer, T. Selection of DNA Aptamers against Penicillin G Using Capture-SELEX for the Development of an Impedimetric Sensor. *Talanta* **2017**.
- (191) Reinemann, C.; Freiin von Fritsch, U.; Rudolph, S.; Strehlitz, B. Generation and Characterization of Quinolone-Specific DNA Aptamers Suitable for Water Monitoring. *Biosens. Bioelectron.* **2016**.
- (192) Ye, H.; Duan, N.; Wu, S.; Tan, G.; Gu, H.; Li, J.; Wang, H.; Wang, Z. Orientation Selection of Broad-Spectrum Aptamers against Lipopolysaccharides Based on Capture-SELEX by Using Magnetic Nanoparticles. *Microchim. Acta* **2017**.
- (193) Nutiu, R.; Li, Y. In Vitro Selection of Structure-Switching Signaling Aptamers. *Angew. Chemie - Int. Ed.* **2005**.
- (194) Rajendran, M.; Ellington, A. D. Selection of Fluorescent Aptamer Beacons That Light up in the Presence of Zinc. *Anal. Bioanal. Chem.* **2008**.
- (195) Oh, S. S.; Plakos, K.; Lou, X.; Xiao, Y.; Soh, H. T. In Vitro Selection of Structure-Switching, Self-Reporting Aptamers. *Proc. Natl. Acad. Sci. U. S. A.* **2010**.
- (196) He, J.; Liu, Y.; Fan, M.; Liu, X. Isolation and Identification of the DNA Aptamer Target to Acetamidiprid. *J. Agric. Food Chem.* **2011**.
- (197) Martin, J. A.; Chávez, J. L.; Chushak, Y.; Chapleau, R. R.; Hagen, J.; Kelley-Loughnane, N. Tunable Stringency Aptamer Selection and Gold Nanoparticle Assay for Detection of Cortisol. *Anal. Bioanal. Chem.* **2014**.
- (198) Spiga, F. M.; Maietta, P.; Guiducci, C. More DNA-Aptamers for Small Drugs: A Capture-SELEX Coupled with Surface Plasmon Resonance and High-Throughput Sequencing. *ACS Comb. Sci.* **2015**.
- (199) Duan, N.; Gong, W.; Wu, S.; Wang, Z. Selection and Application of SsDNA Aptamers against Clenbuterol Hydrochloride Based on SsDNA Library Immobilized SELEX. *J. Agric. Food Chem.* **2017**.
- (200) Duan, N.; Gong, W.; Wu, S.; Wang, Z. An SsDNA Library Immobilized SELEX Technique for Selection of an Aptamer against Ractopamine. *Anal. Chim. Acta* **2017**.
- (201) Kuznetsov, A.; Komarova, N.; Andrianova, M.; Grudtsov, V.; Kuznetsov, E. Aptamer Based Vanillin Sensor Using an Ion-Sensitive Field-Effect Transistor. *Microchim. Acta* **2018**.
- (202) Abraham, K. M.; Roueifar, M.; Ponce, A. T.; Lussier, M. E.; Benson, D. B.; Hong, K. L. In Vitro Selection and Characterization of a Single-Stranded DNA Aptamer Against the Herbicide Atrazine. *ACS Omega* **2018**.
- (203) Zhang, Y.; Lu, T.; Wang, Y.; Diao, C.; Zhou, Y.; Zhao, L.; Chen, H. Selection of a DNA Aptamer against Zearalenone and Docking Analysis for Highly Sensitive Rapid Visual Detection with Label-Free Aptasensor. *J. Agric. Food Chem.* **2018**.
- (204) Tian, H.; Duan, N.; Wu, S.; Wang, Z. Selection and Application of SsDNA Aptamers against Spermine Based on Capture-SELEX. *Anal. Chim. Acta* **2019**.
- (205) Boussebayle, A.; Torcka, D.; Ollivaud, S.; Braun, J.; Bofill-Bosch, C.; Dombrowski, M.; Groher, F.; Hamacher, K.; Suess, B. Next-Level Riboswitch Development-Implementation of Capture-SELEX Facilitates Identification of a New Synthetic Riboswitch. *Nucleic Acids Res.* **2019**.
- (206) Lu, Q.; Liu, X.; Hou, J.; Yuan, Q.; Li, Y.; Chen, S. Selection of Aptamers Specific for DEHP Based on SsDNA Library Immobilized SELEX and Development of Electrochemical Impedance Spectroscopy Aptasensor. *Molecules* **2020**.
- (207) McKeague, M.; De Girolamo, A.; Valenzano, S.; Pascale, M.; Ruscito, A.; Velu, R.; Frost, N. R.; Hill, K.; Smith, M.; McConnell, E. M.; DeRosa, M. C. Comprehensive Analytical Comparison of Strategies Used for Small Molecule Aptamer Evaluation. *Anal. Chem.* **2015**.
- (208) Tan, Y.; Shi, Y. S.; Wu, X. D.; Liang, H. Y.; Gao, Y. B.; Li, S. J.; Zhang, X. M.; Wang, F.; Gao, T. M. DNA Aptamers That Target Human Glioblastoma Multiforme Cells Overexpressing Epidermal Growth Factor Receptor Variant III In

*Vitro. Acta Pharmacol. Sin.* **2013**.

- (209) Park, H.; Paeng, I. R. Development of Direct Competitive Enzyme-Linked Aptamer Assay for Determination of Dopamine in Serum. *Anal. Chim. Acta* **2011**.
- (210) Barthelmebs, L.; Jonca, J.; Hayat, A.; Prieto-Simon, B.; Marty, J. L. Enzyme-Linked Aptamer Assays (ELAAs), Based on a Competition Format for a Rapid and Sensitive Detection of Ochratoxin A in Wine. *Food Control* **2011**.
- (211) Mingwei Qin, Xiaomeng Zhang, Xinyue Zhao, Yuzhu Song, J. Z.; Han, X. X. & Q. Complementary Chain Competition and Fluorescence Quenching Detection of Deoxynivalenol and Analytical Applications Using a Novel Aptamer. *CYTA – J. FOOD*.
- (212) Di Primo, C.; Dausse, E.; Toulmé, J. J. Surface Plasmon Resonance Investigation of RNA Aptamer-RNA Ligand Interactions. *Methods Mol. Biol.* **2011**.
- (213) Li, Y.; Lee, H. J.; Corn, R. M. Detection of Protein Biomarkers Using RNA Aptamer Microarrays and Enzymatically Amplified SPR Imaging. *Anal. Chem.* **2008**.
- (214) Fukusaki, E. ichiro; Hasunuma, T.; Kajiyama, S. ichiro; Okazawa, A.; Itoh, T. J.; Kobayashi, A. SELEX for Tubulin Affords Specific T-Rich DNA Aptamers. *Bioorganic Med. Chem. Lett.* **2001**.
- (215) Svobodova, M.; Bunka, D. H. J.; Nadal, P.; Stockley, P. G.; O'Sullivan, C. K. Selection of 2'F-Modified RNA Aptamers against Prostate-Specific Antigen and Their Evaluation for Diagnostic and Therapeutic Applications. *Anal. Bioanal. Chem.* **2013**.
- (216) Su, J. L.; Youn, B. S.; Ji, W. P.; Niazi, J. H.; Yeon, S. K.; Man, B. G. SsDNA Aptamer-Based Surface Plasmon Resonance Biosensor for the Detection of Retinol Binding Protein 4 for the Early Diagnosis of Type 2 Diabetes. *Anal. Chem.* **2008**.
- (217) Kwon, M.; Chun, S. M.; Jeong, S.; Yu, J. In Vitro Selection of RNA against Kanamycin B. *Mol. Cells* **2001**.
- (218) Win, M. N.; Klein, J. S.; Smolke, C. D. Codeine-Binding RNA Aptamers and Rapid Determination of Their Binding Constants Using a Direct Coupling Surface Plasmon Resonance Assay. *Nucleic Acids Res.* **2006**.
- (219) Gebhardt, K.; Shokraei, A.; Babaie, E.; Lindqvist, B. H. RNA Aptamers to S-Adenosylhomocysteine: Kinetic Properties, Divalent Cation Dependency, and Comparison with Anti-S-Adenosylhomocysteine Antibody. *Biochemistry* **2000**.
- (220) Hong, K. L.; Battistella, L.; Salva, A. D.; Williams, R. M.; Sooter, L. J. In Vitro Selection of Single-Stranded DNA Molecular Recognition Elements against S. Aureus Alpha Toxin and Sensitive Detection in Human Serum. *Int. J. Mol. Sci.* **2015**.
- (221) Wang, J.; Zhou, H. S. Aptamer-Based Au Nanoparticles-Enhanced Surface Plasmon Resonance Detection of Small Molecules. *Anal. Chem.* **2008**.
- (222) Luo, Z.; Zhang, J.; Wang, Y.; Chen, J.; Li, Y.; Duan, Y. An Aptamer Based Method for Small Molecules Detection through Monitoring Salt-Induced AuNPs Aggregation and Surface Plasmon Resonance (SPR) Detection. *Sensors Actuators, B Chem.* **2016**.
- (223) Entzian, C.; Schubert, T. Studying Small Molecule-Aptamer Interactions Using MicroScale Thermophoresis (MST). *Methods* **2016**.
- (224) Svobodová, M.; Skouridou, V.; Botero, M. L.; Jauset-Rubio, M.; Schubert, T.; Bashammakh, A. S.; El-Shahawi, M. S.; Alyoubi, A. O.; O'Sullivan, C. K. The Characterization and Validation of 17 $\beta$ -Estradiol Binding Aptamers. *J. Steroid Biochem. Mol. Biol.* **2017**.
- (225) Jayanthi, S. The Versatility of Isothermal Titration Calorimetry in Modern Biology. *J. Anal. Bioanal. Tech.* **2015**.
- (226) Lin, P. H.; Chen, R. H.; Lee, C. H.; Chang, Y.; Chen, C. S.; Chen, W. Y. Studies of the Binding Mechanism between Aptamers and Thrombin by Circular Dichroism, Surface Plasmon Resonance and Isothermal Titration Calorimetry. *Colloids Surfaces B Biointerfaces* **2011**.
- (227) Slavkovic, S.; Altunisik, M.; Reinstein, O.; Johnson, P. E. Structure-Affinity Relationship of the Cocaine-Binding Aptamer with Quinine Derivatives. *Bioorganic Med. Chem.* **2015**.

- (228) Concepcion, J.; Witte, K.; Wartchow, C.; Choo, S.; Yao, D.; Persson, H.; Wei, J.; Li, P.; Heidecker, B.; Ma, W.; Varma, R.; Zhao, L.-S.; Perillat, D.; Carricato, G.; Recknor, M.; Du, K.; Ho, H.; Ellis, T.; Gamez, J.; Howes, M.; Phi-Wilson, J.; Lockard, S.; Zuk, R.; Tan, H. Label-Free Detection of Biomolecular Interactions Using BioLayer Interferometry for Kinetic Characterization. *Comb. Chem. High Throughput Screen.* **2009**.
- (229) Gao, S.; Zheng, X.; Hu, B.; Sun, M.; Wu, J.; Jiao, B.; Wang, L. Enzyme-Linked, Aptamer-Based, Competitive Biolayer Interferometry Biosensor for Palytoxin. *Biosens. Bioelectron.* **2017**.
- (230) Gao, S.; Zheng, X.; Wu, J. A Biolayer Interferometry-Based Enzyme-Linked Aptamer Sorbent Assay for Real-Time and Highly Sensitive Detection of PDGF-BB. *Biosens. Bioelectron.* **2018**.
- (231) Kammer, M. N.; Olmsted, I. R.; Kussrow, A. K.; Morris, M. J.; Jackson, G. W.; Bornhop, D. J. Characterizing Aptamer Small Molecule Interactions with Backscattering Interferometry. *Analyst* **2014**.
- (232) Shunxiang Gao 1, Bo Hu 2, Xin Zheng 3, Ying Cao 4, Dejing Liu 1, Mingjuan Sun 1, Binghua Jiao 5, L. W. 6. Gonyautoxin 1/4 Aptamers with High-Affinity and High-Specificity: From Efficient Selection to Aptasensor Application. *Biosens. Bioelectron.*
- (233) Shunxiang Gao 1, Bo Hu 2, Xin Zheng 3, Dejing Liu 1, Mingjuan Sun 1, Jiaxiang Qin 4, Hao Zhou 5, Binghua Jiao 2, L. W. 1. Study of the Binding Mechanism between Aptamer GO18-T-d and Gonyautoxin 1/4 by Molecular Simulation.
- (234) Zhen Li† ORCID logoa, Bo Hu†ab, Rong Zhou†ORCID logoa, Xiaojuan Zhang†ad, Ruizhe Wangc, Yun Gaoa, Mingjuan Suna, B. J. and L. W. Selection and Application of Aptamers with High-Affinity and High-Specificity against Dinophysistoxin-1. *R. Soc. Chem.* **2020**.
- (235) Samokhvalov, A. V.; Safenkova, I. V.; Eremin, S. A.; Zherdev, A. V.; Dzantiev, B. B. Measurement of (Aptamer-Small Target) KD Using the Competition between Fluorescently Labeled and Unlabeled Targets and the Detection of Fluorescence Anisotropy. *Anal. Chem.* **2018**.
- (236) Huizenga, D. E.; Szostak, J. W. A DNA Aptamer That Binds Adenosine and ATP. *Biochemistry* **1995**.
- (237) Bing, T.; Chang, T.; Yang, X.; Mei, H.; Liu, X.; Shangguan, D. G-Quadruplex DNA Aptamers Generated for Systemin. *Bioorganic Med. Chem.* **2011**.
- (238) Choi, J. S.; Kim, S. G.; Lahousse, M.; Park, H. Y.; Park, H. C.; Jeong, B.; Kim, J.; Kim, S. K.; Yoon, M. Y. Screening and Characterization of High-Affinity SsDNA Aptamers against Anthrax Protective Antigen. *J. Biomol. Screen.* **2011**.
- (239) Choi, J. H.; Chen, K. H.; Strano, M. S. Aptamer-Capped Nanocrystal Quantum Dots: A New Method for Label-Free Protein Detection. *J. Am. Chem. Soc.* **2006**.
- (240) Mehta, J.; Van Dorst, B.; Rouah-Martin, E.; Herrebout, W.; Scippo, M. L.; Blust, R.; Robbens, J. In Vitro Selection and Characterization of DNA Aptamers Recognizing Chloramphenicol. *J. Biotechnol.* **2011**.
- (241) Yang, X.; Bing, T.; Mei, H.; Fang, C.; Cao, Z.; Shangguan, D. Characterization and Application of a DNA Aptamer Binding to L-Tryptophan. *Analyst* **2011**.
- (242) Mehta, J.; Rouah-Martin, E.; Van Dorst, B.; Maes, B.; Herrebout, W.; Scippo, M. L.; Dardenne, F.; Blust, R.; Robbens, J. Selection and Characterization of PCB-Binding DNA Aptamers. *Anal. Chem.* **2012**.
- (243) Muhammad, M.; Huang, Q. A Review of Aptamer-Based SERS Biosensors: Design Strategies and Applications. *Talanta.* 2021, Pages .
- (244) Piro, B.; Shi, S.; Reisberg, S.; Noël, V.; Anquetin, G. Comparison of Electrochemical Immunosensors and Aptasensors for Detection of Small Organic Molecules in Environment, Food Safety, Clinical and Public Security. *Biosensors.* 2016, Pages .
- (245) Evtugyn, G.; Hianik, T. Electrochemical DNA Sensors and Aptasensors Based on Electropolymerized Materials and Polyelectrolyte Complexes. *TrAC - Trends in Analytical Chemistry.* 2016, Pages .
- (246) Hasanzadeh, M.; Shadjou, N.; de la Guardia, M. Aptamer-Based Assay of Biomolecules: Recent Advances in Electro-Analytical Approach. *TrAC - Trends in Analytical Chemistry.* 2017, Pages .
- (247) Li, H.; Rothberg, L. Colorimetric Detection of DNA Sequences Based on Electrostatic Interactions with Unmodified

Gold Nanoparticles. *Proc. Natl. Acad. Sci. U. S. A.* **2004**.

- (248) Huang, C. C.; Huang, Y. F.; Cao, Z.; Tan, W.; Chang, H. T. Aptamer-Modified Gold Nanoparticles for Colorimetric Determination of Platelet-Derived Growth Factors and Their Receptors. *Anal. Chem.* **2005**.
- (249) Zhao, W.; Chiunan, W.; Lam, J. C. F.; McManus, S. A.; Chen, W.; Cui, Y.; Pelton, R.; Brook, M. A.; Li, Y. DNA Aptamer Folding on Gold Nanoparticles: From Colloid Chemistry to Biosensors. *J. Am. Chem. Soc.* **2008**.
- (250) Lerga, T. M.; Skouridou, V.; Bermudo, M. C.; Bashammakh, A. S.; El-Shahawi, M. S.; Alyoubi, A. O.; O'Sullivan, C. K. Gold Nanoparticle Aptamer Assay for the Determination of Histamine in Foodstuffs. *Microchim. Acta* **2020**.
- (251) Lee, J. S.; Han, M. S.; Mirkin, C. A. Colorimetric Detection of Mercuric Ion (Hg<sup>2+</sup>) in Aqueous Media Using DNA-Functionalized Gold Nanoparticles. *Angew. Chemie - Int. Ed.* **2007**.
- (252) Shi, Y.; Dai, H.; Sun, Y.; Hu, J.; Ni, P.; Li, Z. Fluorescent Sensing of Cocaine Based on a Structure Switching Aptamer, Gold Nanoparticles and Graphene Oxide. *Analyst* **2013**.
- (253) Jiang, H.; Ling, K.; Tao, X.; Zhang, Q. Theophylline Detection in Serum Using a Self-Assembling RNA Aptamer-Based Gold Nanoparticle Sensor. *Biosens. Bioelectron.* **2015**.
- (254) Derbyshire, N.; White, S. J.; Bunka, D. H. J.; Song, L.; Stead, S.; Tarbin, J.; Sharman, M.; Zhou, D.; Stockley, P. G. Toggled RNA Aptamers against Aminoglycosides Allowing Facile Detection of Antibiotics Using Gold Nanoparticle Assays. *Anal. Chem.* **2012**.
- (255) Chávez, J. L.; Hagen, J. A.; Kelley-Loughnane, N. Fast and Selective Plasmonic Serotonin Detection with Aptamer-Gold Nanoparticle Conjugates. *Sensors (Switzerland)* **2017**.
- (256) Abnous, K.; Danesh, N. M.; Ramezani, M.; Alibolandi, M.; Emrani, A. S.; Lavaee, P.; Taghdisi, S. M. A Colorimetric Gold Nanoparticle Aggregation Assay for Malathion Based on Target-Induced Hairpin Structure Assembly of Complementary Strands of Aptamer. *Microchim. Acta* **2018**.
- (257) Emrani, A. S.; Danesh, N. M.; Lavaee, P.; Ramezani, M.; Abnous, K.; Taghdisi, S. M. Colorimetric and Fluorescence Quenching Aptasensors for Detection of Streptomycin in Blood Serum and Milk Based on Double-Stranded DNA and Gold Nanoparticles. *Food Chem.* **2016**.
- (258) Soh, J. H.; Lin, Y.; Rana, S.; Ying, J. Y.; Stevens, M. M. Colorimetric Detection of Small Molecules in Complex Matrixes via Target-Mediated Growth of Aptamer-Functionalized Gold Nanoparticles. *Anal. Chem.* **2015**.
- (259) Chen, J.; Li, Z.; Ge, J.; Yang, R.; Zhang, L.; Qu, L. B.; Wang, H. Q.; Zhang, L. An Aptamer-Based Signal-on Bio-Assay for Sensitive and Selective Detection of Kanamycin A by Using Gold Nanoparticles. *Talanta* **2015**.
- (260) Luo, Y.; He, L.; Zhan, S.; Wu, Y.; Liu, L.; Zhi, W.; Zhou, P. Ultrasensitive Resonance Scattering (RS) Spectral Detection for Trace Tetracycline in Milk Using Aptamer-Coated Nanogold (ACNG) as a Catalyst. *J. Agric. Food Chem.* **2014**.
- (261) Jiang, Z.; Fan, Y.; Chen, M.; Liang, A.; Liao, X.; Wen, G.; Shen, X.; He, X.; Pan, H.; Jiang, H. Resonance Scattering Spectral Detection of Trace Hg<sup>2+</sup> Using Aptamer-Modified Nanogold as Probe and Nanocatalyst. *Anal. Chem.* **2009**.
- (262) Kumar Sharma, T.; Ramanathan, R.; Weerathunge, P.; Mohammadtaheri, M.; Kumar Daima, H.; Shukla, R.; Bansal, V. Aptamer-Mediated "Turn-off/Turn-on" Nanozyme Activity of Gold Nanoparticles for Kanamycin Detection. *Chem. Commun.* **2014**, 50 (100).
- (263) Lan, L.; Yao, Y.; Ping, J.; Ying, Y. Recent Progress in Nanomaterial-Based Optical Aptamer Assay for the Detection of Food Chemical Contaminants. *ACS Applied Materials and Interfaces*. 2017, Pages .
- (264) Wang, Q.; Yang, Q.; Wu, W. Graphene-Based Steganographic Aptasensor for Information Computing and Monitoring Toxins of Biofilm in Food. *Front. Microbiol.* **2020**.
- (265) Ma, L.; Guo, T.; Pan, S.; Zhang, Y. A Fluorometric Aptasensor for Patulin Based on the Use of Magnetized Graphene Oxide and DNase I-Assisted Target Recycling Amplification. *Microchim. Acta* **2018**.
- (266) Chinnappan, R.; AlZabn, R.; Fataftah, A. K.; Alhoshani, A.; Zourob, M. Probing High-Affinity Aptamer Binding Region and Development of Aptasensor Platform for the Detection of Cylindrospermopsin. *Anal. Bioanal. Chem.* **2020**.
- (267) He, M. Q.; Wang, K.; Wang, J.; Yu, Y. L.; He, R. H. A Sensitive Aptasensor Based on Molybdenum Carbide

Nanotubes and Label-Free Aptamer for Detection of Bisphenol A. *Anal. Bioanal. Chem.* **2017**.

- (268) Ahmadi, A.; Danesh, N. M.; Ramezani, M.; Alibolandi, M.; Lavaee, P.; Emrani, A. S.; Abnous, K.; Taghdisi, S. M. A Rapid and Simple Ratiometric Fluorescent Sensor for Patulin Detection Based on a Stabilized DNA Duplex Probe Containing Less Amount of Aptamer-Involved Base Pairs. *Talanta* **2019**.
- (269) Sabet, F. S.; Hosseini, M.; Khabbaz, H.; Dadmehr, M.; Ganjali, M. R. FRET-Based Aptamer Biosensor for Selective and Sensitive Detection of Aflatoxin B1 in Peanut and Rice. *Food Chem.* **2017**.
- (270) Wang, C.; Huang, X.; Tian, X.; Zhang, X.; Yu, S.; Chang, X.; Ren, Y.; Qian, J. A Multiplexed FRET Aptasensor for the Simultaneous Detection of Mycotoxins with Magnetically Controlled Graphene Oxide/Fe<sub>3</sub>O<sub>4</sub> as a Single Energy Acceptor. *Analyst* **2019**.
- (271) Wu, C.; Yan, L.; Wang, C.; Lin, H.; Wang, C.; Chen, X.; Yang, C. J. A General Excimer Signaling Approach for Aptamer Sensors. *Biosens. Bioelectron.* **2010**.
- (272) Homola, J.; Yee, S. S.; Gauglitz, G. Surface Plasmon Resonance Sensors: Review. *Sensors Actuators, B Chem.* **1999**.
- (273) Green, R. J.; Frazier, R. A.; Shakesheff, K. M.; Davies, M. C.; Roberts, C. J.; Tendler, S. J. B. Surface Plasmon Resonance Analysis of Dynamic Biological Interactions with Biomaterials. *Biomaterials*. 2000, Pages .
- (274) Singh, P. *Surface Plasmon Resonance*; 2014; Pages .
- (275) Li, Q.; Wang, Q.; Yang, X.; Wang, K.; Zhang, H.; Nie, W. High Sensitivity Surface Plasmon Resonance Biosensor for Detection of MicroRNA and Small Molecule Based on Graphene Oxide-Gold Nanoparticles Composites. *Talanta* **2017**.
- (276) Zhao, J.; Guo, W.; Pei, M.; Ding, F. GR-Fe<sub>3</sub>O<sub>4</sub>NPs and PEDOT-AuNPs Composite Based Electrochemical Aptasensor for the Sensitive Detection of Penicillin. *Anal. Methods* **2016**.
- (277) Lee, A. Y.; Ha, N. R.; Jung, I. P.; Kim, S. H.; Kim, A. R.; Yoon, M. Y. Development of a SsDNA Aptamer for Detection of Residual Benzylpenicillin. *Anal. Biochem.* **2017**.
- (278) Rowe, A. A.; Miller, E. A.; Plaxco, K. W. Reagentless Measurement of Aminoglycoside Antibiotics in Blood Serum via an Electrochemical, Ribonucleic Acid Aptamer-Based Biosensor. *Anal. Chem.* **2010**.
- (279) Jalalian, S. H.; Ramezani, M.; Danesh, N. M.; Alibolandi, M.; Abnous, K.; Taghdisi, S. M. A Novel Electrochemical Aptasensor for Detection of Aflatoxin M1 Based on Target-Induced Immobilization of Gold Nanoparticles on the Surface of Electrode. *Biosens. Bioelectron.* **2018**.
- (280) Miao, P.; Tang, Y.; Wang, B.; Han, K.; Chen, X.; Sun, H. An Aptasensor for Detection of Potassium Ions Based on RecJf Exonuclease Mediated Signal Amplification. *Analyst* **2014**.
- (281) Wang, L.; Peng, X.; Fu, H.; Huang, C.; Li, Y.; Liu, Z. Recent Advances in the Development of Electrochemical Aptasensors for Detection of Heavy Metals in Food. *Biosensors and Bioelectronics*. 2020, Pages .
- (282) Baker, B. R.; Lai, R. Y.; Wood, M. S.; Doctor, E. H.; Heeger, A. J.; Plaxco, K. W. An Electronic, Aptamer-Based Small-Molecule Sensor for the Rapid, Label-Free Detection of Cocaine in Adulterated Samples and Biological Fluids. *J. Am. Chem. Soc.* **2006**.
- (283) Li, X.; Qi, H.; Shen, L.; Gao, Q.; Zhang, C. Electrochemical Aptasensor for the Determination of Cocaine Incorporating Gold Nanoparticles Modification. *Electroanalysis* **2008**.
- (284) Zhu, Y.; Chandra, P.; Song, K. M.; Ban, C.; Shim, Y. B. Label-Free Detection of Kanamycin Based on the Aptamer-Functionalized Conducting Polymer/Gold Nanocomposite. *Biosens. Bioelectron.* **2012**.
- (285) Fei, A.; Liu, Q.; Huan, J.; Qian, J.; Dong, X.; Qiu, B.; Mao, H.; Wang, K. Label-Free Impedimetric Aptasensor for Detection of Femtomole Level Acetaminophen Using Gold Nanoparticles Decorated Multiwalled Carbon Nanotube-Reduced Graphene Oxide Nanoribbon Composites. *Biosens. Bioelectron.* **2015**.
- (286) Omidinia, E.; Shadjou, N.; Hasanzadeh, M. Aptamer-Based Biosensor for Detection of Phenylalanine at Physiological PH. *Appl. Biochem. Biotechnol.* **2014**.
- (287) Kim, Y. S.; Jung, H. S.; Matsuura, T.; Lee, H. Y.; Kawai, T.; Gu, M. B. Electrochemical Detection of 17 $\beta$ -Estradiol

Using DNA Aptamer Immobilized Gold Electrode Chip. *Biosens. Bioelectron.* **2007**.

- (288) Liang, J.; Chen, Z.; Guo, L.; Li, L. Electrochemical Sensing of L-Histidine Based on Structure-Switching DNazymes and Gold Nanoparticle-Graphene Nanosheet Composites. *Chem. Commun.* **2011**.
- (289) Geng, X.; Zhang, M.; Long, H.; Hu, Z.; Zhao, B.; Feng, L.; Du, J. A Reusable Neurotransmitter Aptasensor for the Sensitive Detection of Serotonin. *Anal. Chim. Acta* **2021**.
- (290) Li, B. R.; Hsieh, Y. J.; Chen, Y. X.; Chung, Y. T.; Pan, C. Y.; Chen, Y. T. An Ultrasensitive Nanowire-Transistor Biosensor for Detecting Dopamine Release from Living Pc12 Cells under Hypoxic Stimulation. *J. Am. Chem. Soc.* **2013**.
- (291) Farjami, E.; Campos, R.; Nielsen, J. S.; Gothelf, K. V.; Kjems, J.; Ferapontova, E. E. RNA Aptamer-Based Electrochemical Biosensor for Selective and Label-Free Analysis of Dopamine. *Anal. Chem.* **2013**.
- (292) Álvarez-Martos, I.; Ferapontova, E. E. Electrochemical Label-Free Aptasensor for Specific Analysis of Dopamine in Serum in the Presence of Structurally Related Neurotransmitters. *Anal. Chem.* **2016**.
- (293) Sajid, M.; Kawde, A. N.; Daud, M. Designs, Formats and Applications of Lateral Flow Assay: A Literature Review. *J. Saudi Chem. Soc.* **2015**.
- (294) Mansfield, M. A.; Diagnostics, O.; Millipore, E.; Bedford, M. Design Considerations for Lateral Flow Test Strips.
- (295) Koczula, K. M.; Gallotta, A. Lateral Flow Assays. *Essays Biochem.* **2016**.
- (296) Ahmad Raston, N. H.; Nguyen, V. T.; Gu, M. B. A New Lateral Flow Strip Assay (LFSA) Using a Pair of Aptamers for the Detection of Vaspin. *Biosens. Bioelectron.* **2017**.
- (297) Liu, G.; Mao, X.; Phillips, J. A.; Xu, H.; Tan, W.; Zeng, L. Aptamer-Nanoparticle Strip Biosensor for Sensitive Detection of Cancer Cells. *Anal. Chem.* **2009**.
- (298) J.G., B.; M.P., C.; A.M., R.; T., P.; C., A.; J.S., L. Development, Screening, and Analysis of DNA Aptamer Libraries Potentially Useful for Diagnosis and Passive Immunity of Arboviruses. *BMC Res. Notes* **2012**.
- (299) Zhu, C.; Zhao, Y.; Yan, M.; Huang, Y.; Yan, J.; Bai, W.; Chen, A. A Sandwich Dipstick Assay for ATP Detection Based on Split Aptamer Fragments. *Anal. Bioanal. Chem.* **2016**.
- (300) Minagawa, H.; Onodera, K.; Fujita, H.; Sakamoto, T.; Akitomi, J.; Kaneko, N.; Shiratori, I.; Kuwahara, M.; Horii, K.; Waga, I. Selection, Characterization and Application of Artificial DNA Aptamer Containing Appended Bases with Sub-Nanomolar Affinity for a Salivary Biomarker. *Sci. Rep.* **2017**.
- (301) Schüling, T.; Eilers, A.; Scheper, T.; Walter, J. Aptamer-Based Lateral Flow Assays. *AIMS Bioeng.* **2018**.
- (302) Jauset-Rubio, M.; Svobodová, M.; Mairal, T.; McNeil, C.; Keegan, N.; El-Shahawi, M. S.; Bashammakh, A. S.; Alyoubi, A. O.; O'Sullivan, C. K. Aptamer Lateral Flow Assays for Ultrasensitive Detection of  $\beta$ -Conglutin Combining Recombinase Polymerase Amplification and Tailed Primers. *Anal. Chem.* **2016**.
- (303) Wang, L.; Chen, W.; Ma, W.; Liu, L.; Ma, W.; Zhao, Y.; Zhu, Y.; Xu, L.; Kuang, H.; Xu, C. Fluorescent Strip Sensor for Rapid Determination of Toxins. *Chem. Commun.* **2011**.
- (304) Wu, S.; Liu, L.; Duan, N.; Li, Q.; Zhou, Y.; Wang, Z. Aptamer-Based Lateral Flow Test Strip for Rapid Detection of Zearalenone in Corn Samples. *J. Agric. Food Chem.* **2018**.
- (305) Liu, J.; Mazumdar, D.; Lu, Y. A Simple and Sensitive "Dipstick" Test in Serum Based on Lateral Flow Separation of Aptamer-Linked Nanostructures. *Angew. Chemie - Int. Ed.* **2006**.
- (306) Shim, W. B.; Kim, M. J.; Mun, H.; Kim, M. G. An Aptamer-Based Dipstick Assay for the Rapid and Simple Detection of Aflatoxin B1. *Biosens. Bioelectron.* **2014**.
- (307) Özalp, V. C.; Çam, D.; Hernandez, F. J.; Hernandez, L. I.; Schäfer, T.; Öktem, H. A. Small Molecule Detection by Lateral Flow Strips via Aptamer-Gated Silica Nanopores. *Analyst* **2016**.
- (308) Wu, W.; Zhao, S.; Mao, Y.; Fang, Z.; Lu, X.; Zeng, L. A Sensitive Lateral Flow Biosensor for Escherichia Coli O157: H7 Detection Based on Aptamer Mediated Strand Displacement Amplification. *Anal. Chim. Acta* **2015**.

- (309) Bruno, J. G. Application of DNA Aptamers and Quantum Dots to Lateral Flow Test Strips for Detection of Foodborne Pathogens with Improved Sensitivity versus Colloidal Gold. *Pathogens* **2014**.
- (310) Adhikari, M.; Strych, U.; Kim, J.; Goux, H.; Dhamane, S.; Poongavanam, M. V.; Hagström, A. E. V.; Kourentzi, K.; Conrad, J. C.; Willson, R. C. Aptamer-Phage Reporters for Ultrasensitive Lateral Flow Assays. *Anal. Chem.* **2015**.
- (311) Wang, L.; Ma, W.; Chen, W.; Liu, L.; Ma, W.; Zhu, Y.; Xu, L.; Kuang, H.; Xu, C. An Aptamer-Based Chromatographic Strip Assay for Sensitive Toxin Semi-Quantitative Detection. *Biosens. Bioelectron.* **2011**.
- (312) Zhou, W.; Kong, W.; Dou, X.; Zhao, M.; Ouyang, Z.; Yang, M. An Aptamer Based Lateral Flow Strip for On-Site Rapid Detection of Ochratoxin A in *Astragalus Membranaceus*. *J. Chromatogr. B Anal. Technol. Biomed. Life Sci.* **2016**.
- (313) Fang, Z.; Wu, W.; Lu, X.; Zeng, L. Lateral Flow Biosensor for DNA Extraction-Free Detection of Salmonella Based on Aptamer Mediated Strand Displacement Amplification. *Biosens. Bioelectron.* **2014**.
- (314) Xu, H.; Mao, X.; Zeng, Q.; Wang, S.; Kawde, A. N.; Liu, G. Aptamer-Functionalized Gold Nanoparticles as Probes in a Dry-Reagent Strip Biosensor for Protein Analysis. *Anal. Chem.* **2009**.
- (315) Shen, G.; Zhang, S.; Hu, X. Signal Enhancement in a Lateral Flow Immunoassay Based on Dual Gold Nanoparticle Conjugates. *Clin. Biochem.* **2013**.
- (316) Qin, C.; Wen, W.; Zhang, X.; Gu, H.; Wang, S. Visual Detection of Thrombin Using a Strip Biosensor through Aptamer-Cleavage Reaction with Enzyme Catalytic Amplification. *Analyst* **2015**.
- (317) Dalirirad, S.; Steckl, A. J. Aptamer-Based Lateral Flow Assay for Point of Care Cortisol Detection in Sweat. *Sensors Actuators, B Chem.* **2019**.
- (318) Dalirirad, S.; Steckl, A. J. Lateral Flow Assay Using Aptamer-Based Sensing for on-Site Detection of Dopamine in Urine. *Anal. Biochem.* **2020**.
- (319) Ranganathan, V.; Srinivasan, S.; Singh, A.; DeRosa, M. C. An Aptamer-Based Colorimetric Lateral Flow Assay for the Detection of Human Epidermal Growth Factor Receptor 2 (HER2). *Anal. Biochem.* **2020**.
- (320) Kaiser, L.; Weisser, J.; Kohl, M.; Deigner, H. P. Small Molecule Detection with Aptamer Based Lateral Flow Assays: Applying Aptamer-C-Reactive Protein Cross-Recognition for Ampicillin Detection. *Sci. Rep.* **2018**.
- (321) Zhang, J.; Lv, X.; Feng, W.; Li, X.; Li, K.; Deng, Y. Aptamer-Based Fluorometric Lateral Flow Assay for Creatine Kinase MB. *Microchim. Acta* **2018**.
- (322) Ou, Y.; Jin, X.; Liu, J.; Tian, Y.; Zhou, N. Visual Detection of Kanamycin with DNA-Functionalized Gold Nanoparticles Probe in Aptamer-Based Strip Biosensor. *Anal. Biochem.* **2019**.
- (323) Wu, Z.; Shen, H.; Hu, J.; Fu, Q.; Yao, C.; Yu, S.; Xiao, W.; Tang, Y. Aptamer-Based Fluorescence-Quenching Lateral Flow Strip for Rapid Detection of Mercury (II) Ion in Water Samples. *Anal. Bioanal. Chem.* **2017**.
- (324) Jauset-Rubio, M.; El-Shahawi, M. S.; Bashammakh, A. S.; Alyoubi, A. O.; O'Sullivan, C. K. Advances in Aptamers-Based Lateral Flow Assays. *TrAC - Trends in Analytical Chemistry*. 2017, Pages .



# Chapter 2

---

## **Hybrid antibody-aptamer assay for detection of tetrodotoxin in puffer fish**

## Chapter 2

### Abstract

The marine toxin tetrodotoxin (TTX) poses a great risk to public health safety due to its severe paralytic effects after ingestion. Seafood poisoning caused by the consumption of contaminated marine species like puffer fish expanding in non-endemic areas has increased the need for fast and reliable detection of the toxin to effectively implement prevention strategies. Liquid chromatography-mass spectrometry is considered as the most accurate method whereas competitive immunoassays have also been reported. In this work, we sought to develop an aptamer-based assay for the rapid, sensitive and cost-effective detection of TTX detection in puffer fish. Using capture-SELEX combined with Next Generation Sequencing, novel aptamers were identified, and their binding properties were evaluated. Finally, a highly sensitive and user-friendly hybrid antibody-aptamer sandwich assay was developed with superior performance compared to several assays reported in the literature and commercial immunoassay kits. The assay was successfully applied to the quantification of TTX in puffer fish extracts, and the results obtained correlated very well with a competitive magnetic bead-based immunoassay performed in parallel for comparison. This is one of the very few works reported in the literature of such hybrid assays for small molecule analytes whose compatibility with field samples is also demonstrated. Ongoing work is focused on the development of a lateral flow assay exploiting this sandwich format which will facilitate the rapid on-site screening of samples.

### 2.1. Introduction

Tetrodotoxin (TTX) is a very potent neurotoxin produced by marine bacteria and it is associated with severe seafood poisoning after consumption of puffer fish (Tetraodontidae family)<sup>1</sup>. Its paralytic toxic effects derive from its selective binding to voltage-gated sodium channels and ultimately interfering with neural transmission<sup>2</sup>. Symptoms of TTX intoxication include numbness sensation in the mouth, headache, vomiting and muscle weakness<sup>3</sup>, and fatal respiratory or heart failure have also been reported<sup>4</sup>. This low molecular weight toxin (319.3 g/mol) was originally isolated from puffer fish in 1909<sup>5,6</sup> and was later also found in other marine<sup>7</sup> and terrestrial<sup>8</sup> species. Even though it was initially believed that TTX was produced by the pufferfish itself, marine bacterial species have been postulated to be able to produce TTX<sup>9</sup> suggesting that symbiotic marine bacteria could be the primary source of TTX that bioaccumulates in puffer fish and other marine species, and finally reaches humans through the food chain. As recently reported, there are more than 30 different bacteria genera capable

of producing TTX that have been isolated among which the most common is *Vibrio* sp.<sup>10</sup>. To date, however, there is still some discussion regarding the pathway of TTX bioaccumulation in marine ecosystems<sup>11</sup>.

Puffer fish poisoning is typical of warm waters and was regarded as a problem confined to Asian countries<sup>1,12</sup>, including Thailand<sup>5</sup>, Taiwan<sup>13</sup>, Singapore<sup>14</sup>, Cambodia<sup>15</sup>, Bangladesh<sup>16</sup>, India<sup>17,18</sup>. However, toxic puffer fish species have expanded to other regions, and there have been an increasing number of reports of incidences in the Mediterranean Sea, which has been attributed to the opening of the Suez Canal (the 'Lessepsian migration'), which resulted in the migration of species from the Red Sea to colonize the Mediterranean Sea<sup>19–22</sup>, the Aegean Sea<sup>23</sup>, the Adriatic Sea<sup>24</sup>, Oman<sup>25</sup> and there have also been reports of the incidence of tetrodotoxin in Australia<sup>26</sup>, and the United States<sup>27</sup>, highlighting the widespread distribution of the toxin.

Additionally, TTX has been recently found in shellfish, particularly in European countries such as the United Kingdom<sup>28</sup>, Greece<sup>29</sup>, the Netherlands<sup>30</sup>, Spain<sup>31</sup>, Italy<sup>32</sup>, and France<sup>33</sup>, although usually at very low concentrations. Therefore, it is now considered that TTX poses a major food safety risk even in non-endemic areas.

TTX is highly toxic. Puffer fish poisonings have revealed that ingestion of 0.18–0.2 mg of TTX might be near the minimum dose for developing TTX symptoms and 2 mg is a lethal dose<sup>34</sup>. In Japan, where puffer fish is considered a delicacy and highly consumed despite its potential toxicity, a limit of 2 mg TTX equiv./kg has been used as a criterion to judge the acceptability of puffer fish as food<sup>35</sup> and a guide with the edible parts and species of puffer fish that are allowed for consumption has been published<sup>36</sup>. In USA, strong restrictions exist for the import of pufferfish (FDA,2017)<sup>37</sup>. In Europe, fish of the family Tetraodontidae and products derived from them must not be placed on the markets (EC (European Commission), 2004a; 2004b)<sup>38,39</sup>. Regarding shellfish, no regulation exists. Nevertheless, the European Food Safety Authority (EFSA) has recently published that concentrations below 44 µg of TTX equiv./kg shellfish meat do not result in adverse effects in humans<sup>34</sup>.

There are about 30 TTX analogues<sup>40</sup>. Toxicity equivalency factors (TEFs) for these TTX analogues are essential for the evaluation of relative risk but, unfortunately, information on relative potencies of TTXs is limited. Although the use of different cell lines in toxicity assays has been questioned, it is evident that most analogues are much less toxic than TTX<sup>41,42</sup>. Additionally, the parent TTX is usually the most abundant<sup>34</sup>.

Bioassays, instrumental analysis and immunological methods are typically employed to detect TTXs in field samples, based on the toxic effects, physicochemical properties and antigenic specificity of the toxin, respectively<sup>43</sup>. Ethical concerns and low specificity of the mouse bioassay, the most frequently used method, encouraged the development of alternative strategies. Liquid chromatography coupled with mass spectrometry (LC-MS/MS)<sup>28,29</sup> has been widely exploited for TTX detection and it provides more sensitive, specific, and accurate results than bioassays. However, instrumental analysis techniques are expensive, time consuming, labor intensive and require sample pretreatment, trained personnel and significant laboratory

infrastructure. Immunological methods such as ELISA using specific TTX antibodies can provide quantitative and sensitive detection<sup>44,45</sup> and commercial ELISA kits are readily available. The small size of TTX requires the use of hapten-carrier protein bioconjugates for antibody development, requiring careful consideration in the preparation of these bioconjugates. The development of antibody pairs for sandwich assay development is hindered by the small size of the TTX, thus requiring the design of competitive assays<sup>46,47</sup>. Competitive immunoassays are more difficult to optimize, and the preparation of toxin-reporter molecule conjugates required for some types of immunoassays can also be challenging<sup>43</sup>. Nevertheless, antibody-based biosensors have been reported and are particularly useful for rapid screening purposes<sup>48–50</sup>.

Aptamers are biorecognition molecules considered as alternative to antibodies which are suitable for the detection of virtually any type of target<sup>51–53</sup>. Aptamers are single-stranded synthetic oligonucleotides which can bind their target molecule with high affinity and specificity owing to the specific structural conformations they adopt. Systematic Evolution of Ligands by Exponential enrichment, commonly known as SELEX, was developed for the generation of aptamers and it is based on iterative rounds of binding, partitioning and amplification<sup>54,55</sup>. Compared to antibodies, aptamers show several advantages for biosensing applications including *in vitro* selection, the possibility to bind any kind of target, high affinity and specificity, reproducible chemical synthesis, stability at various environmental conditions, reversible denaturation, and easy site-directed modification<sup>51,53</sup>.

The development of aptamers for small molecules is a challenging task<sup>52,56</sup>. One of the main hurdles is target immobilization on a solid matrix to allow selection through traditional SELEX approaches. Altering the native structure of the target to facilitate immobilization can prevent the aptamer from binding to the target in solution in its natural form, and an absence of functional groups can completely hinder immobilization as the small size of the targets also limits the availability of binding sites. An alternative selection strategy, termed capture-SELEX, based on library immobilization and use of the target in solution, was first reported by Stoltenburg *et al.*<sup>57</sup>. This approach is ideal for small molecules since the target molecule can be used in solution, and the potential structure-switching properties of the selected aptamers can be exploited for characterization and assay development<sup>52,56</sup>. The capture-SELEX strategy has been successfully used for several targets including aminoglycoside antibiotics<sup>57</sup>, cadmium<sup>58</sup>, penicillin<sup>59</sup>, quinolone<sup>60</sup>, and lipopolysaccharides<sup>61</sup>.

The path from aptamer discovery to assay development for small molecules is not trivial. The usual format is competitive assays which can be difficult to develop as discussed earlier in the case of antibodies. Sandwich assays are hindered by the small size of the targets and to the best of our knowledge, no sandwich aptamer assays have been reported for small molecules. Alternatively, split aptamers can be generated and have been exploited in a sandwich format for the detection of small molecules<sup>62</sup>. However, the trial-and-error nature of the process of generating split aptamers, possibly resulting in lower binding affinities of the individual fragments and further

requirements for modifications are among the factors discouraging researchers from undertaking this complex and costly task. In fact, to date, split aptamers have only been reported for 15 small molecules<sup>62</sup>. Hybrid antibody-aptamer sandwich systems on the other hand have emerged as an attractive alternative offering the best of both antibody and aptamer biorecognition molecules, together with the advantages of sandwich assays<sup>63</sup>. Even though several examples have been reported for the detection of protein targets using such hybrid systems, only a handful of examples exist for small molecules, including trinitrotoluene<sup>64</sup>, tetracycline<sup>65</sup> and aflatoxin B1<sup>66</sup>.

Two TTX aptamers have been reported, the first one by Shao et al.<sup>67</sup>, who did not provide details regarding the selection process or the aptamer affinity, and the second by Gu et al.<sup>68</sup> who used a variation of the capture-SELEX strategy with magnetic reduced graphene oxide to immobilize the ssDNA library and identified a TTX aptamer with high affinity ( $K_D$  of 44 nM). In this work we sought to apply the capture-SELEX strategy to develop novel TTX-binding aptamers and apply them for the detection of the toxin in puffer fish. Two selections were performed in parallel, using two different types of streptavidin-magnetic beads to facilitate library immobilization. Next Generation Sequencing of various pools from the selections enabled the identification of aptamer candidates and different approaches were used to evaluate their binding properties. Finally, a highly sensitive hybrid antibody-aptamer sandwich assay was developed and successfully exploited for the detection of TTX in puffer fish.

## 2.2. Experimental section

### 2.2.1. Materials

Tetrodotoxin of 98.8% purity (TTX) was purchased from Tocris Bioscience (Bristol, UK) and Latoxan (Valence, France) and standard solutions at 1 mg/mL were prepared in 0.1 M sodium acetate buffer pH 4.8. Certified reference materials of saxitoxin (STX) and domoic acid (DA) were obtained from the National Research Council of Canada (NRC, Halifax, Canada). The mouse monoclonal anti-TTX antibody (CABT-L3089, CD Creative Diagnostics) was obtained from Deltaclon S.L. (Spain). Sulfo-NHS-acetate, maleimide-activated microplate strip wells, Dynabeads M-270 streptavidin magnetic beads (Dynabeads SA-MB; 10 mg/mL, 2.8  $\mu$ m diameter, 200 pmol biotinylated oligonucleotide/mg particles binding capacity), DreamTaq DNA polymerase and lambda exonuclease were from Fisher Scientific (Spain). The DNA purification kits (Oligo Clean & Concentrator kit and DNA Clean & Concentrator kit) were from Ecogen (Spain). Okadaic acid potassium salt (OA) from *Prorocentrum concavum*, 11-amino-1-undecanethiol hydrochloride (MUAM), cysteamine, L-arginine, 1,6-anhydro- $\beta$ -D-mannopyranose and streptavidin-horseradish peroxidase (SA-HRP) were purchased from Merck (Spain). Maleimide-activated magnetic beads (30  $\mu$ m diameter, protein binding capacity  $\geq$  15 mg/ml) were from Cube Biotech (Germany) and SiMAG-streptavidin magnetic beads (SiMAG SA-MB; 10 mg/mL, 1  $\mu$ m diameter, 80 – 200 pmol

biotinylated oligonucleotide/mg particles binding capacity) from Chemicell (Germany). Streptavidin-polyHRP80 (SA-pHRP) was from Bionova (Spain) and the TMB Super Sensitive One Component HRP Microwell Substrate from Surmodics (USA). All oligonucleotides were synthesized by Biomers.net (Germany).

### 2.2.2. Capture-SELEX process

The library used for the selection was based on a previous report (5'-ATACCA GCTTAT TCAATT-N10-TGAGGC TCGATC-N40-AGATAG TAAGTG CAATCT-3')<sup>32</sup>. The docking site (5'- TGAGGCTCGATC-3', 12 nucleotides) was flanked by two random regions of 10 and 40 nucleotides. Library immobilization on streptavidin-magnetic beads (SA-MB) was achieved via hybridization of a docking probe (5'-biotin-TEG-GTC-HEGL-GATCGAGCCTCA-3', where TEG and HEGL are triethyleneglycol and hexanethyleneglycol spacers, respectively) with the docking site of the library. Two different types of SA-MB beads were used for two parallel selections, the Dynabeads M-270 streptavidin and the SiMAG-streptavidin. The binding buffer used was PBS with 1.5 mM MgCl<sub>2</sub>. A total of 23 selection rounds were performed using the TTX precursors L-arginine and 1,6-anhydro-β-D-mannopyranose as counter selection molecules during the last six rounds. Detailed description of the selections performed can be found in the Supplementary Information.

### 2.2.3. Next Generation Sequencing (NGS) and data analysis

Different rounds from the selections were chosen for NGS. Target elution fractions from rounds 6, 9, 16, 23 and counter elution fraction from round 23 for both selections were individually amplified with different forward primers (containing distinct barcode sequences) and a common reverse primer. The resulting dsDNA for each round was column-purified and sequenced using Ion Torrent NGS. The fastaq raw data was imported into the Galaxy web server (<https://usegalaxy.org/>) and the quality of the data was evaluated with the "FASTQC" tool which also provided general statistics. The format of the data was converted to fasta and datasets containing only library-length sequences (90-110 bp) were created. Each dataset was finally collapsed to identify unique sequences within the first megabyte of data. The 100 most abundant sequences from all the datasets were compared to identify the ones preferentially enriched in the target pools. Multiple sequence alignments were performed with Clustal Omega (<https://www.ebi.ac.uk/Tools/msa/clustalo/>) to determine sequence families, while sequence motif analysis was performed using MEME (<https://meme-suite.org/meme/tools/meme>). Ten aptamer candidates were finally selected, five from each selection, for further characterization.

#### 2.2.4. Determination of affinity dissociation constants ( $K_D$ )

Apta-PCR Affinity Assay (APAA)<sup>69</sup> The APAA was performed using TTX immobilized on maleimide-activated magnetic beads (TTX-beads) in combination with unmodified aptamer sequences. The preparation of the TTX-beads is described in the Supplementary Information. For the binding studies, 50  $\mu$ L of different concentrations of each aptamer (up to 600 nM in binding buffer) were incubated with 2  $\mu$ L of the TTX-beads for 30 min under rotation at ambient temperature. The supernatants were discarded, the beads were washed three times with 100  $\mu$ L of PBS with 0.05% v/v Tween-20 (PBST) and finally re-suspended with 20  $\mu$ L of binding buffer. Bound sequences were detected after PCR amplification using library-specific primers and agarose gel electrophoresis. Analysis was performed in duplicate for each concentration. The intensity of the DNA bands was estimated with the ImageJ software and the Gel Analysis option, plotted against aptamer concentration using GraphPad Prism 6 software and the  $K_D$  of each aptamer was finally determined using the “One site Specific binding with Hill slope” model.

Bead-Enzyme Linked Aptamer Assay (Bead-ELAA)<sup>70</sup> TTX-beads were used in combination with 5'-biotin-modified aptamers. TTX-beads (2  $\mu$ L) were mixed with different concentrations of each biotinylated aptamer in binding buffer (50  $\mu$ L of up to 450 nM) and incubated for 30 min at ambient temperature under rotation. The supernatants were discarded, and the beads were washed three times with 100  $\mu$ L of PBST. Next, 50  $\mu$ L of 50 ng/mL of SA-pHRP in PBST were added and incubated for 20 min. After a final washing step (five times with 100  $\mu$ L of PBST), 50  $\mu$ L of TMB substrate were added, and following a brief incubation at room temperature, an equal volume of 1 M  $H_2SO_4$  was added to stop color development. The supernatants were separated from the beads using a magnet, transferred to a 96-well microtiter plate and the absorbance was recorded at 450 nm. The  $K_D$  of the aptamers were calculated as described above. All measurements were carried out in duplicate.

#### 2.2.5. Hybrid antibody-aptamer sandwich assay for TTX determination

A sandwich assay was developed using an antibody for capture and an aptamer for detection of TTX. Specifically, 50  $\mu$ L of 5  $\mu$ g/mL anti-TTX monoclonal antibody in 50 mM carbonate buffer pH 9.4 were used to coat the wells of a MaxiSorp immunoassay plate overnight at 4°C. The wells were washed three times with 200  $\mu$ L of PBST, followed by blocking with 200  $\mu$ L of 1% w/v BSA in PBST for 30 min. The wells were washed again and incubated with 50  $\mu$ L of different concentrations of TTX in PBS for 1 h. After washing, 50  $\mu$ L of 500 nM biotinylated aptamer in binding buffer were added and let to incubate for 1 h, followed by washing. Fifty microliters of 100 ng/mL SA-HRP in PBST were then added, followed by a final incubation of 30 min and washing. TMB substrate (50  $\mu$ L) was added and color development proceeded for 6 min. Sulfuric acid (50  $\mu$ L of 1 M) was added to stop color development and the absorbance was recorded

at 450 nm. All incubation steps were performed at ambient temperature (22 – 25 °C) unless stated otherwise. All five aptamer candidates were initially screened in combination with the antibody at a constant TTX concentration (32 µg/mL = 100 nM) and the aptamer providing the highest signal was chosen for the final assay. A calibration curve was constructed using serial 2-fold dilutions of TTX in the range of 0.039 – 40 ng/mL (0.12 – 125 nM). Duplicate measurements were performed, and the data was fitted to a four-parameter sigmoidal model using Graph Pad Prism 6 software. The limit of detection (LOD) was interpolated from the curve as the bottom of the fitted curve plus three times its standard deviation (bottom + 3xSD<sub>bottom</sub>). The precision of the assay was evaluated using duplicate measurements of different concentrations of TTX analyzed on four different days. The inter-assay coefficients of variation (% CV) were calculated as the standard deviation for each measurement divided by the average. The cross-reactivity of the assay with possibly interfering marine toxins such as domoic acid, okadaic acid and saxitoxin was finally studied under the conditions detailed above using each toxin at 40 ng/mL.

#### 2.2.6. Fish samples and TTXs extraction

Fish extracts were obtained from a previous work<sup>71</sup>. One oceanic puffer fish (*Lagocephalus lagocephalus*, Linnaeus, 1758) (TTX-free individual) and one silver-cheeked toadfish (*Lagocephalus sceleratus*, Gmelin, 1789) (TTX-containing individual) were caught in 2014 in Alicante (Spain). Puffer fishes were dissected, and gonads, liver, skin and muscle were retrieved. A double TTX extraction was performed with 0.1% v/v acetic acid as previously described<sup>71</sup>. Extracts were obtained at a tissue concentration of 200 mg equiv./mL.

#### 2.2.7. Detection of TTX in puffer fish

The compatibility of the hybrid sandwich assay with field sample analysis was initially evaluated with a spiking experiment. The TTX-free extracts from the *L. lagocephalus* puffer fish organs (gonads, liver, skin and muscle) were spiked with TTX at 1.5 ng/mL and recoveries were calculated after interpolation in the TTX calibration curve constructed in PBS buffer as detailed above. The *L. sceleratus* TTX-containing fish extracts were then analyzed. The amount of TTX in these extracts was calculated after interpolation in the calibration curve constructed in PBS and also in calibration curves constructed in parallel using the respective extracts from the TTX-free *L. lagocephalus* puffer fish. The extracts were diluted 1/1000 with PBS for all experiments. For comparison, the extracts were also analyzed with a magnetic bead-based competitive immunoassay as detailed in the Supplementary Information.

## 2.3. Results and Discussion

### 2.3.1. Selections

TTX is a very small molecule with only one (amine) functional group (Figure 2.1A). Its covalent linking to a solid matrix to facilitate the partitioning of bound from unbound sequences with traditional aptamer selection approaches would significantly alter its structure and possibly complicate the recognition of the native molecule by the aptamers. Capture-SELEX was thus considered as the most appropriate selection strategy using the ssDNA library immobilized on magnetic beads and the target in solution, rendering the whole molecule accessible for aptamer binding. The design of the ssDNA library was based on a previous report<sup>57</sup>. Besides the primer annealing sites, the library contained two random regions separated by a docking sequence, which provided an immobilization site to streptavidin magnetic beads through its hybridization with a complementary biotinylated docking probe. Previous studies exploiting the capture-SELEX strategy reported the use of Dynabeads M-270 SA-MB<sup>59,60</sup> and the library design from the original study<sup>57</sup>. Different affinity media like streptavidin agarose beads and home-made avidin-magnetic beads were reported in other studies, in combination with libraries containing only one random region whose immobilization was achieved via a biotinylated complementary to one of the primer annealing sites<sup>58,61</sup>. The distribution of the random sequences on the SA-MB, which could be partially determined by the availability of immobilization sites on the beads and the specific three-dimensional structures of the sequences, could potentially affect the evolution of a selection based on the capture-SELEX strategy. In this work, two different types of streptavidin-magnetic beads were used to perform two parallel selections. Even though Dynabeads and SiMAG SA-MB differ in size (2.8  $\mu\text{m}$  and 1  $\mu\text{m}$ , respectively), their maximum binding capacity is almost identical. Taking into consideration the higher cost of the Dynabeads SA-MB as compared to the SiMAG ones, selections with both bead types were performed in an effort to reduce the overall selection costs and investigate the effect of the properties of the beads on their performance for capture-SELEX applications.

Two selections were performed using the conditions summarized in Table S1 (SI). Starting with 500  $\mu\text{M}$  of TTX and 2 h incubation steps (background and target elution steps), the gradual decrease of TTX concentration and duration of the incubation steps led to the completion of the selections after 23 rounds using 50  $\mu\text{M}$  of TTX and 30 min incubations. TTX precursors L-arginine and 1,6-anhydro- $\beta$ -D-mannopyranose<sup>72</sup> were added as counter selection molecules during the last seven selection rounds to improve the specificity of the selected sequences (Figure 2.1A). The evolution of the selections was monitored by PCR amplification of the background and target elution fractions (Figure 2.1B). Interestingly, when Dynabeads SA-MB were used, few sequences eluted in the presence of buffer alone resulting in lower intensity bands after PCR amplification, as opposed to SiMAG beads. This could be a consequence of a better distribution of the docking probe on the larger surface of the Dynabeads

facilitating a more efficient hybridization of the random sequences. By the end of the selections, where both the TTX concentration and incubation times were decreased 10-fold and 4-fold, respectively, as compared to the initial conditions, the pool from the Dynabeads selection appeared to be more enriched in TTX-specific sequences than the SiMAG one.

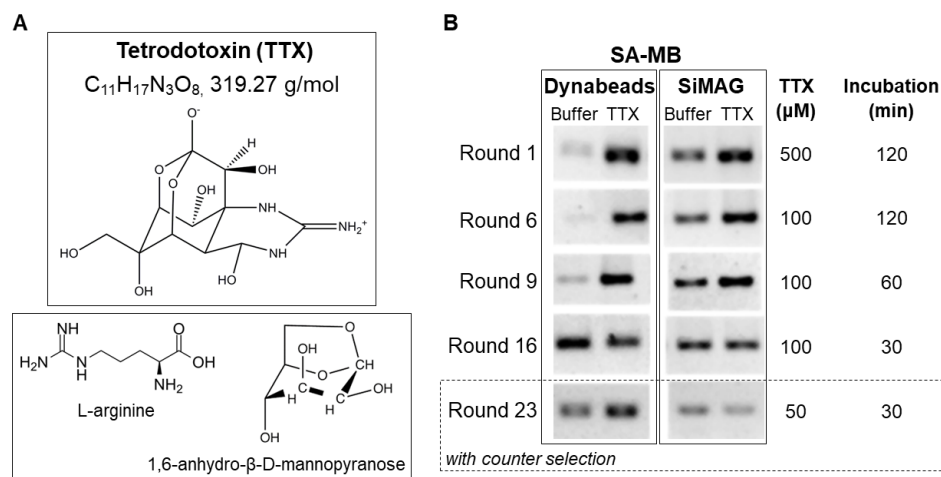


**Figure 2.1.** Selection of TTX-binding aptamers. (A) Structures of the target TTX (upper panel) and the counter selection molecules (lower panel). (B) Evolution of the selections using Dynabeads and SiMAG SA-MB. DNA eluting in the presence of buffer alone or TTX under the specific conditions from the selected rounds was detected after PCR amplification.

### 2.3.2. NGS and identification of aptamer candidates

High-throughput sequence analysis of multiple rounds from each selection was performed using Ion Torrent NGS. Five rounds were chosen from each selection, and these were rounds 6, 9, 16, 23 and 23-counter (Figure 2.1B). Rounds 6 and 16 were chosen because they were performed before a significant change in selection conditions such as duration of incubation steps (2 h in round 6  $\rightarrow$  1 h in round 7) or the concentration of TTX (100  $\mu\text{M}$  in round 16  $\rightarrow$  50  $\mu\text{M}$  in round 17). Additionally, in round 9, a significant enrichment in target-eluting sequences was observed by pilot PCR, especially when Dynabeads SA-MB were employed. Finally, round 23 was chosen as the last selection round. A comprehensive bioinformatics analysis was carried out using various tools from Galaxy webserver and other servers as detailed in the experimental section. General statistics can be found in Table 2.1.

**Table 2.1.** NGS data analysis of selected pools from the two selections.

Selection round	Total sequences	% GC	Sequences 90 – 110 bp	% Unique sequences
<b>(a) Selection with Dynabeads SA-MB</b>				
D6	43,188	42	41,225	99,5
D9	228,862	42	206,990	98,0
D16	82,059	43	76,140	78,2
D23	32,789	41	31,207	62,8
D23-counter	36,727	41	34,937	60,8
<b>(b) Selection with SiMAG SA-MB</b>				
C6	46,902	43	45,334	99,4
C9	54,139	42	50,880	99,2
C16	72,199	42	68,414	95,8
C23	81,705	41	58,299	73,7
C23-counter	111,076	41	76,770	71,5

Enrichment was observed by the end of both selections. The pools in round 6 were highly diverse containing more than 99% of unique sequences. By the end of round 23 though, the percentage of unique sequences decreased to 62.8% and 73.7% for the Dynabeads and SiMAG SA-MB selections, respectively. Furthermore, the enrichment of the counter selection pools from the last round for both selections was very similar to the respective target pools from the same rounds. Interestingly, faster enrichment was achieved when Dynabeads SA-MB were used as by round 16 the percentage of unique sequences dropped to 78.2% whereas it was 95.8% for the selection with the SiMAG beads. Favorable orientation and spacing between sequences on the Dynabeads SA-MB could potentially contribute to faster evolution.

Comparison of the composition of the target and counter selection pools in rounds 23 revealed the presence of most of the sequences in both datasets. This finding was not surprising since the counter selection molecules used were structurally almost identical to parts of the TTX molecule. Nevertheless, it was considered that sequences with lower affinity binding to small parts of the target structure could be eliminated during the successive rounds of counter selection/target selection. The evolution of the 20 most enriched sequences (highest counts per million, CPM) in the target pool datasets from rounds 23 was monitored and their distribution in the pools from rounds 16, 23 and 23-counter is shown in Table S2.2. A few sequences appeared to have been

selectively enriched in the TTX pools as compared to the counter selection pools and these were included in the analysis. Rounds 6 and 9 were excluded since low enrichment was observed.

A 7 to 89-fold enrichment was observed for the sequences selected with Dynabeads SA-MB which was calculated as the ratio of abundance in round 23 to round 16. The selection performed with the SiMAG beads exhibited 2 to 73-fold enrichment. This data again demonstrates that the Dynabeads-based selection appears to be more successful with a higher enrichment of selected sequences. A direct comparison of the datasets from the last selection rounds with TTX and the counter selection molecules revealed that the top 20 sequences were slightly more abundant in the counter selection dataset than in the target dataset when Dynabeads were used (Figure S2.1). The opposite was observed for the SiMAG-based selection (Figure S2.2). Notably, sequences selected with one type of beads were not found in the pools from the selection conducted with the other type of beads. Despite theoretically starting from the same initial library, and using the same selection conditions, each of the SELEX evolved differently, resulting in different sequences being selected, depending on the beads used for library immobilization. This can be explained in part, to be due to the fact that even though the starting aliquots are taken from the same initial library, each aliquot can contain a different combination of diverse sequences. Additionally, the size and nature of the beads can affect the number of docking probes, and thus individual sequences of the immobilized library, captured on its surface, and this can affect the accessibility of the target to the individual sequences.

Multiple sequence alignment of the 100 most abundant sequences in rounds 23 from both selections was also performed to identify possible sequence families. As can be seen in Figure S2.3 for the selection carried out with the Dynabeads, only one major cluster was observed and it contained the most abundant sequence in this dataset, identified as sequence 1, which constitutes 2.1% of the total unique sequences (Table S2). The second and third most abundant sequences, identified as sequences 2 and 3, were encountered at lower percentages (1.1 and 0.9%, respectively), did not appear to belong to any family. Only one major sequence family was also observed in the dataset from the SiMAG beads selection (Figure S2.4), containing the second most abundant sequence (sequence 2 at 1.8%). The first and third most enriched sequences (2.3 and 1.3%) do not appear to belong to any cluster.

The three most enriched sequences from the two selections were ultimately chosen for further characterization. These were annotated as D1, D2 and D3 for the Dynabeads and C1, C2 and C3 for the SiMAG selections. Additionally, two sequences identified in the two datasets from rounds 23 with preferential abundance in the target pools compared to the counter target pools (sequences 21 and 22 in Table S2.2 and Figures S2.3 and S2.4) were also selected and were annotated as D4, D5, C4 and C5. The sequences of all aptamer candidates are shown in Table S2.3.

### 2.3.3. Screening of the aptamer candidates

The ten selected aptamer candidates were initially evaluated under conditions mimicking the selection process to choose the most promising ones for further analysis. Each aptamer was immobilized on SA-MB via hybridization to biotinylated docking probe. Aptamer displacing to the solution after incubation with TTX was detected after PCR amplification and agarose gel electrophoresis as detailed in the Supplementary Information. Whilst displacement was observed for all the aptamer candidates, significant displacement in the presence of TTX was observed for aptamer candidates D3, D4, D5, C2 and C3 which were finally chosen for further evaluation (Figure S2.5). Moreover, the ssDNA-folding was observed in the predicted structures of the five selected TTX aptamers shown in Figure S2.7, using M-fold program (<http://www.unafold.org/mfold/applications/dna-folding-form.php>).

### 2.3.4. Binding properties of the aptamer candidates

Characterization of the binding properties of aptamers for small molecular weight targets like TTX using classical methods is usually hindered by the size of the molecules. A variety of approaches have been reported for affinity studies<sup>52,73</sup>, including microscale thermophoresis<sup>74,75</sup> and isothermal titration calorimetry<sup>49</sup> but these require specialized equipment not typically. Our group has previously reported the use of magnetic beads for the immobilization of small molecule targets and detection of aptamer binding by PCR and colorimetry<sup>69,70,75</sup>. We have developed microtiter plate-based assays using long-chain crosslinkers to spatially separate the target from the plate surface and facilitate aptamer binding<sup>69,70</sup>, and also used gold nanoparticle aggregation assays<sup>76</sup>. These methods are easy to perform and require material and equipment found in almost any laboratory.

For the TTX aptamers, three of these methods were exploited. The calculated  $K_D$  values are shown in Table 2.2 and the respective binding curves in Figure S2.6. For APAA, TTX was immobilized on magnetic beads whereas bound unmodified aptamer was detected after PCR amplification and gel electrophoresis. All aptamers demonstrated similar binding affinities with affinity dissociation constants in the range of 73 – 114 nM. Aptamers C2 and C3 selected using the SiMAG SA-MB showed slightly better  $K_D$  values compared to the ones selected with the Dynabeads SA-MB (D3, D4 and D5). Biotinylated aptamers were used for bead-ELAA in combination with TTX immobilized on magnetic beads. Colorimetric detection of bound aptamers was achieved using SA-pHRP and TMB substrate. As with APAA, all  $K_D$  values determined with bead-ELAA were calculated in the low nanomolar range (7 – 89 nM).

**Table 2.2.** Affinity dissociation constants of the aptamer candidates determined by APAA and bead-ELAA.

Aptamer	APAA		Bead-ELAA	
	$K_D$ (nM)	$R^2$	$K_D$ (nM)	$R^2$
<b>D3</b>	103 ± 24	0.9780	7 ± 1	0.9915
<b>D4</b>	96 ± 16	0.9827	29 ± 13	0.9811
<b>D5</b>	114 ± 46	0.9435	89 ± 58	0.9570
<b>C2</b>	77 ± 6	0.9729	25 ± 6	0.9859
<b>C3</b>	73 ± 12	0.9659	29 ± 7	0.9829

### 2.3.5. TTX detection with a hybrid antibody-aptamer sandwich assay

Once the binding properties of the five aptamer candidates were verified, the final objective was to design an aptamer assay for the detection of TTX in relevant samples. Detection of small molecules is usually accomplished with competitive-type assays since the size of the targets usually does not permit the simultaneous binding of more than one biorecognition elements. We have previously demonstrated competitive assays using the small molecule target immobilized on magnetic beads<sup>69</sup> or on microplate wells<sup>70</sup>, and here we pursued a robust hybrid antibody-aptamer sandwich microtiter plate assay. It was hypothesized that the unique cage-like structure of TTX could potentially allow the formation of an antibody-TTX-aptamer complex enabling the detection of TTX with a sandwich assay. Even though hybrid antibody-aptamer assays have been reported before for high molecular weight targets like proteins and cells<sup>63</sup>, examples for small molecule targets are rare. Nevertheless, these assays are very attractive because they combine the advantages of both types of biorecognition elements while at the same time providing the sensitivity/specificity of sandwich assay formats. Using a monoclonal anti-TTX IgG antibody to coat the wells of a microtiter immunoplate, the five TTX aptamers were initially screened in order to choose the most suitable one for sandwich assay development. Indeed, all aptamers were able to form a sandwich with the antibody and allow the detection of TTX (Figure S2.8). Aptamer D3 however was by far the most successful one leading to more than 2-fold higher signal compared to the signals obtained with the other aptamers and it was chosen for final assay development. The sensitivity of the hybrid assay employing the monoclonal TTX antibody for capture and the D3 aptamer for detection was then evaluated at concentrations of TTX ranging from 39 pg/mL – 40 ng/mL, equivalent to 122 pM – 125 nM. The assay was very sensitive with an LOD of 310 pg/mL (970 pM) and EC50 of 1.1 ng/mL or 3.4 nM (Figure 2.2A). Using TTX samples analyzed on different days, average inter-assay coefficients of variation (CV) of less than 5% were calculated,

demonstrating the high precision of the assay (Table S2.4). Finally, the high specificity of the assay was exhibited by the absence of interference from other marine toxins such as domoic acid (DA), okadaic acid (OA) or saxitoxin (STX) the latter sometimes simultaneously present in puffer fish<sup>77</sup> or shellfish<sup>32</sup> (Figure 2.2B). Various assays and biosensors have been reported in the literature for the detection of TTX and some are summarized in Table S5. To date, the two previously published TTX aptamers have been exploited for the development of fluorescence<sup>68,76,78</sup>, fluorescence combined with amplification<sup>53</sup> and electrochemical<sup>79</sup> assays and the LODs achieved ranged from 0.265 pg/mL to 319 ng/mL. Competitive immunoassays have also been reported using monoclonal TTX antibodies<sup>49,50,80</sup> and their sensitivity was 0.3 – 2.5 ng/mL. The performance of the assay developed in this work is therefore superior or at least comparable with many of the previously published assays employing aptamers or antibodies. Very importantly, the majority of previously reported assays are quite complicated to perform as opposed to the simple sandwich assay demonstrated in this work. Commercial TTX kits are available, and they are based on competitive immunoassays. Examples include the microplate kits from CD Creative Diagnostics and United Biotechnology with LODs of 1 – 10 ng/mL as well as the rapid lateral flow tests from CD Creative Diagnostics and UNIBIOTEST with a sensitivity of 0.1 – 2 µg/mL. It is thus evident that the hybrid antibody-aptamer format of the assay described herein has great potential for use in lateral flow tests, facilitating the facile and rapid on-site detection of TTX in field samples especially when combined with a simple method for sample preparation. It is also one of the rare examples of such hybrid assays for the detection of a small molecular weight analyte since there are reports for only three other targets, trinitrotoluene<sup>64</sup>, tetracycline<sup>65</sup> and aflatoxin B1<sup>66</sup>.

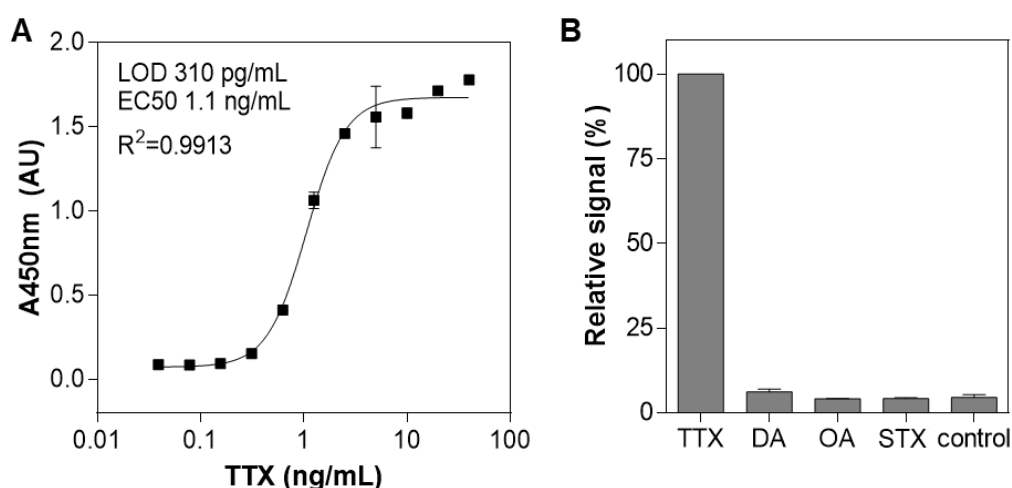


**Figure 2.2.** Hybrid antibody-aptamer assay for the detection of TTX. (A) TTX calibration curve with the monoclonal IgG antibody-D3 aptamer pair. (B) Specificity of the assay.

### 2.3.6. Application of the assay to puffer fish analysis

The hybrid antibody-aptamer sandwich assay was finally employed for the analysis of field samples. Extracts from different tissues (gonads, liver, skin and muscle) of a *L. lagocephalus* puffer fish were prepared as controls since our previous report showed the absence of TTX in these tissues<sup>71</sup>. The extracts were diluted, spiked with TTX and analyzed with the assay as explained in the Experimental Section. As shown in Table 3, excellent recoveries were achieved in the range of 93.5 – 109.1%, thus demonstrating the absence of matrix effects and the compatibility of the assay with such samples. Extracts from tissues of a *L. sceleratus* puffer fish previously shown to contain high levels of TTXs<sup>71</sup> were then analyzed. Since TTX may co-exist with several other naturally occurring TTX analogues, the hybrid sandwich assay is expected to provide a global TTX response (TTXs) depending on the specificity of both antibody and aptamer. The TTXs content was determined using calibration curves constructed both in PBS (afterwards applying the corresponding recovery factor) and in the respective tissue extract from the TTX-free puffer fish. As expected, TTXs contents with both strategies were very similar. High TTXs levels were observed, especially in the gonads and liver tissues where TTXs usually bioaccumulate (Table 2.3). The TTXs content in these tissues were 2.5 – 5-fold higher than the permissible levels in Japan (2 mg TTXs/kg). For comparison, the samples were analyzed in parallel with a competitive magnetic bead-based ELISA (detailed in the SI) which was previously developed and exploited a different monoclonal antibody<sup>23,81</sup>. Some differences were observed, which may derive from the specificity of the assays towards the different TTX analogues. It is necessary to take into account that the cross-reactivity factors for the different TTX analogues may vary according to the biorecognition molecule (which in the case of the hybrid sandwich assay are both the antibody and the aptamer) and also the format of the assay. Nevertheless, comparable results were obtained with both methods. Very good correlation was also observed with previous analysis carried out with LC-MS/MS<sup>71</sup>, the TTXs contents trend in the different tissues being the same: gonads > liver > skin > mussel (Table S6). The establishment of the cross-reactivity factors for the different TTX analogues present in these tissues would facilitate the comparison with LC-MS/MS results. However, pure TTX analogues are not commercially available, and their production is not an easy task. The elucidation of the TEFs alongside the cross-reactivity factors, which ideally should be similar, would certainly contribute to better manage the TTX risk.

**Table 2.3.** Detection of TTX in puffer fish extracts. Recovery (%) of TTX spiked in diluted extracts from a TTX-free fish (*L. lagocephalus*). TTXs content (mg TTX equiv./kg of tissue) in extracts from a TTX-containing fish (*L. sceleratus*) were determined using calibration curves constructed in PBS buffer and in the respective extract from the TTX-free fish.

Tissue	% TTX recovery ( <i>L. lagocephalus</i> )	TTXs content ( <i>L. sceleratus</i> ) (mg TTX equiv./ kg)		
		Hybrid antibody-aptamer sandwich assay		Competitive magnetic bead ELISA
		PBS	Extract	
Gonads	109.1	9.46	9.94	5.24
Liver	93.5	5.99	5.01	2.84
Skin	107.7	0.98	1.28	0.19
Muscle	96.3	0.86	0.82	0.42

## 2.4 Conclusions

TTX has emerged as a major food hazard because of its high neurotoxicity and its presence in seafoods found not only in Asian but also European waters. Traditionally, bioassays have been used to detect TTX, however instrumental analysis using liquid chromatography in combination with mass spectrometry is currently employed for monitoring of field samples. Microplate immunoassays and antibody-based biosensors can also provide the required sensitivity and specificity, provided that highly specific antibodies are used. Aptamers are cost-effective alternatives to monoclonal antibodies and since their discovery in the early 1990s, they have been used for the detection of not only large targets such as cells and proteins but also small molecular weight targets like toxins. To date, only two TTX specific aptamers have been reported and have been exploited for the development of fluorescence and electrochemical assays, which are quite elaborate and are not compatible with rapid and facile on-site analysis and have not been employed for the analysis of field samples. In this work, capture-SELEX technology in combination with high-throughput NGS analysis was exploited for the discovery of novel TTX aptamers. Assays using magnetic beads were developed for the verification of the binding properties of the selected aptamer candidates which exhibited  $K_D$  values in the low nanomolar range. The specific properties of the streptavidin magnetic beads used to immobilize the library and perform the two parallel selections appeared to affect the speed of evolution and the enrichment achieved even though the binding properties of the selected aptamers were not significantly affected.

Finally, a simple hybrid antibody-aptamer sandwich assay was demonstrated with high sensitivity, precision and specificity. Its sensitivity was superior or at least comparable to commercial kits based on competitive immunoassays and other existing aptamer and antibody-based assays and biosensors. The excellent performance of the assay was further demonstrated by the reliable determination of TTXs levels in puffer fish with an excellent degree of correlation with measurements obtained with a competitive magnetic bead-based immunoassay and liquid chromatography-mass spectrometry. This is the first demonstration of an assay employing an aptamer for the detection of TTX in puffer fish, and, in general, is one of the very few examples reported in the literature of such hybrid antibody-aptamer sandwich assay for small molecular weight analytes. The sandwich format of the assay is particularly attractive and ongoing work is focused on its transfer to a lateral flow assay to allow the rapid and facile analysis of samples at the point-of-need. The evaluation of cross-reactivity factors for different TTX analogues with this hybrid antibody-aptamer assay as well as its applicability to the analysis of shellfish, where the detection of lower TTXs contents is pursued, is also in progress.

## ACKNOWLEDGMENT

The authors are grateful to King Abdulaziz University, under the financing of the collaborative project “Cost-effective tools for mycotoxin testing” for funding. The research has also received funding from the Agencia Estatal de Investigación through the CELLECTRA projects (PID2020-112976RB-C21 and PID2020-112976RB-C22 / AEI /10.13039/501100011033).

## 2.5. References

- (1) Bane, V.; Lehane, M.; Dikshit, M.; O’Riordan, A.; Furey, A. Tetrodotoxin: Chemistry, Toxicity, Source, Distribution and Detection. *Toxins*. 2014, page .
- (2) Denac, H.; Mevissen, M.; Scholtysik, G. Structure, Function and Pharmacology of Voltage-Gated Sodium Channels. *Naunyn-Schmiedeberg’s Archives of Pharmacology*. 2000, page .
- (3) Hwang, D. F.; Noguchi, T. Tetrodotoxin Poisoning. *Advances in Food and Nutrition Research*. 2007, page .
- (4) Noguchi, T.; Ebesu, J. S. M. Puffer Poisoning: Epidemiology and Treatment. *Journal of Toxicology - Toxin Reviews*. 2001, page .
- (5) Chulanetra, M.; Sookrung, N.; Srimanote, P.; Indrawattana, N.; Thanongsaksrikul, J.; Sakolvaree, Y.; Chongsa-Nguan, M.; Kurazono, H.; Chaicumpa, W. Toxic Marine Puffer Fish in Thailand Seas and Tetrodotoxin They Contained. *Toxins (Basel)*. **2011**.
- (6) Jang, J.; Yotsu-Yamashita, M. Distribution of Tetrodotoxin, Saxitoxin, and Their Analogs among Tissues of the Puffer Fish *Fugu Pardalis*. *Toxicon* **2006**.
- (7) Sui, L. M.; Chen, K.; Hwang, P. A.; Hwang, D. F. Identification of Tetrodotoxin in Marine Gastropods Implicated in Food Poisoning. *J. Nat. Toxins* **2002**.

- (8) Yotsu-Yamashita, M.; Gilhen, J.; Russell, R. W.; Krysko, K. L.; Melaun, C.; Kurz, A.; Kaufenstein, S.; Kordis, D.; Mebs, D. Variability of Tetrodotoxin and of Its Analogues in the Red-Spotted Newt, *Notophthalmus Viridescens* (Amphibia: Urodela: Salamandridae). *Toxicon* **2012**.
- (9) Noguchi, T.; Jeon, J. kyun; Arakawa, O.; Sugita, H.; Deguchi, Y.; Shida, Y.; Hashimoto, K. Occurrence of Tetrodotoxin and Anhydrotetrodotoxin in *Vibrio* Sp. Isolated from the Intestines of a Xanthid Crab, *Atergatis Floridus*. *J. Biochem.* **1986**.
- (10) Magarlamov, T. Y.; Melnikova, D. I.; Chernyshev, A. V. Tetrodotoxin-Producing Bacteria: Detection, Distribution and Migration of the Toxin in Aquatic Systems. *Toxins*. 2017, page .
- (11) Khor, S.; Wood, S. A.; Salvitti, L.; Taylor, D. I.; Adamson, J.; McNabb, P.; Cary, S. C. Investigating Diet as the Source of Tetrodotoxin in Pleurobranchaea Maculata. *Mar. Drugs* **2014**.
- (12) Lago, J.; Rodriguez, L. P.; Blanco, L.; Vieites, J. M.; Cabado, A. G. Tetrodotoxin, an Extremely Potent Marine Neurotoxin: Distribution, Toxicity, Origin and Therapeutical Uses. *Mar. Drugs* **2015**.
- (13) Huang, Y. R.; Yin, M. C.; Hsieh, Y. L.; Yeh, Y. H.; Yang, Y. C.; Chung, Y. L.; Hsieh, C. H. E. Authentication of Consumer Fraud in Taiwanese Fish Products by Molecular Trace Evidence and Forensically Informative Nucleotide Sequencing. *Food Res. Int.* **2014**.
- (14) Ahasan, H. A. M. N.; Mamun, A. A.; Karim, S. R.; Bakar, M. A.; Gazi, E. A.; Bala, C. S. Paralytic Complications of Puffer Fish (Tetrodotoxin) Poisoning. *Singapore Med. J.* **2004**.
- (15) Ngy, L.; Taniyama, S.; Shibano, K.; Yu, C. F.; Takatani, T.; Arakawa, O. Distribution of Tetrodotoxin in Pufferfish Collected from Coastal Waters of Sihanouk Ville, Cambodia. *J. Food Hyg. Soc. Japan* **2008**.
- (16) Homaira, N.; Rahman, M.; Luby, S. P.; Rahman, M.; Haider, M. S.; Faruque, L. I.; Khan, D.; Parveen, S.; Gurley, E. S. Multiple Outbreaks of Puffer Fish Intoxication in Bangladesh, 2008. *Am. J. Trop. Med. Hyg.* **2010**.
- (17) Kaleshkumar, K.; Rajaram, R.; Purushothaman, P.; Arun, G. Morphological Variations in Marine Pufferfish and Porcupinefish (Teleostei: Tetraodontiformes) from Tamil Nadu, Southeastern Coast of India. *J. Threat. Taxa* **2018**.
- (18) Joseph, T. C.; Goswami, D. B.; Pradeep, M. A.; Anupama, T. K.; Parmar, E.; Renuka, V.; Remya, S.; Ravishankar, C. N. Pufferfish Poisoning from *Arothron Stellatus*: The First Confirmed Case in India with Exact Species Identification. *Toxicon* **2021**.
- (19) Bentur, Y.; Ashkar, J.; Lurie, Y.; Levy, Y.; Azzam, Z. S.; Litmanovich, M.; Golik, M.; Gurevych, B.; Golani, D.; Eisenman, A. Lessepsian Migration and Tetrodotoxin Poisoning Due to *Lagocephalus Sceleratus* in the Eastern Mediterranean. *Toxicon*. 2008, page .
- (20) Katikou, P.; Georgantelis, D.; Sinouris, N.; Petsi, A.; Fotaras, T. First Report on Toxicity Assessment of the Lessepsian Migrant Pufferfish *Lagocephalus Sceleratus* (Gmelin, 1789) from European Waters (Aegean Sea, Greece). *Toxicon* **2009**.
- (21) Kosker, A. R.; Özogul, F.; Durmus, M.; Ucar, Y.; Ayas, D.; Šimat, V.; Özogul, Y. First Report on TTX Levels of the Yellow Spotted Pufferfish (*Torquigener Flavimaculosus*) in the Mediterranean Sea. *Toxicon* **2018**.
- (22) Akbora, H. D.; Kunter, İ.; Erçetin, T.; Elagöz, A. M.; Çiçek, B. A. Determination of Tetrodotoxin (TTX) Levels in Various Tissues of the Silver Cheeked Puffer Fish (*Lagocephalus Sceleratus* (Gmelin, 1789)) in Northern Cyprus Sea (Eastern Mediterranean). *Toxicon* **2020**.

- (23) Leonardo, S.; Kiparissis, S.; Rambla-Alegre, M.; Almarza, S.; Roque, A.; Andree, K. B.; Christidis, A.; Flores, C.; Caixach, J.; Campbell, K.; Elliott, C. T.; Aligizaki, K.; Diogène, J.; Campàs, M. Detection of Tetrodotoxins in Juvenile Pufferfish *Lagocephalus Sceleratus* (Gmelin, 1789) from the North Aegean Sea (Greece) by an Electrochemical Magnetic Bead-Based Immunosensing Tool. *Food Chem.* **2019**.
- (24) Ujević, I.; Roje-Busatto, R.; Dragičević, B.; Dulčić, J. Tetrodotoxin in Invasive Silver-Cheeked Toadfish *Lagocephalus Sceleratus* (Gmelin, 1789) in the Adriatic Sea. In *Handbook of Environmental Chemistry*; 2021; page .
- (25) Alhatali, B.; Al Lawatia, S.; Khamis, F.; Kantur, S.; Al-Abri, S.; Kapil, V.; Thomas, J.; Johnson, R.; Hamelin, E. I.; Coleman, R. M.; Kazzi, Z. A Cluster of Tetrodotoxin Poisoning in Oman. *Clin. Toxicol.* **2021**.
- (26) Isbister, G. K.; Son, J.; Wang, F.; Maclean, C. J.; Lin, C. S. Y.; Ujma, J.; Balit, C. R.; Smith, B.; Milder, D. G.; Kiernan, M. C. Puffer Fish Poisoning: A Potentially Life-Threatening Condition. *Med. J. Aust.* **2002**.
- (27) Almeida, P.; Diaz, R.; Hernandez, F.; Ferrer, G. Blow: A Case of Pufferfish Intoxication in South Florida. *BMJ Case Rep.* **2019**.
- (28) Turner, A. D.; Powell, A.; Schofield, A.; Lees, D. N.; Baker-Austin, C. Detection of the Pufferfish Toxin Tetrodotoxin in European Bivalves, England, 2013 to 2014. *Eurosurveillance* **2015**.
- (29) Vlamis, A.; Katikou, P.; Rodriguez, I.; Rey, V.; Alfonso, A.; Papazachariou, A.; Zacharaki, T.; Botana, A. M.; Botana, L. M. First Detection of Tetrodotoxin in Greek Shellfish by UPLC-MS/MS Potentially Linked to the Presence of the Dinoflagellate *Prorocentrum Minimum*. *Toxins (Basel)*. **2015**.
- (30) Gerssen, A.; Bovee, T. H. F.; Klijnstra, M. D.; Poelman, M.; Portier, L.; Hoogenboom, R. L. A. P. First Report on the Occurrence of Tetrodotoxins in Bivalve Mollusks in the Netherlands. *Toxins (Basel)*. **2018**.
- (31) Leão, J. M.; Lozano-Leon, A.; Giráldez, J.; Vilariño, Ó.; Gago-Martínez, A. Preliminary Results on the Evaluation of the Occurrence of Tetrodotoxin Associated to Marine *Vibrio* Spp. in Bivalves from the Galician Rias (Northwest of Spain). *Mar. Drugs* **2018**.
- (32) Dell'Aversano, C.; Tartaglione, L.; Polito, G.; Dean, K.; Giacobbe, M.; Casabianca, S.; Capellacci, S.; Penna, A.; Turner, A. D. First Detection of Tetrodotoxin and High Levels of Paralytic Shellfish Poisoning Toxins in Shellfish from Sicily (Italy) by Three Different Analytical Methods. *Chemosphere* **2019**.
- (33) Hort, V.; Arnich, N.; Guérin, T.; Lavison-Bompard, G.; Nicolas, M. First Detection of Tetrodotoxin in Bivalves and Gastropods from the French Mainland Coasts. *Toxins (Basel)*. **2020**.
- (34) EFSA (European Food Safety Authority) (2017). Risks for Public Health Related to the Presence of Tetrodotoxin (TTX) and TTX Analogues in Marine Bivalves and Gastropods. *EFSA Journal*, 15(4), 4752.
- (35) Mahmud, Y.; Yamamori, K.; Noguchi, T. Occurrence of TTX in a Brackish Water Puffer "Midorifugu", *Tetraodon Nigroviridis*, Collected from Thailand. *J. Food Hyg. Soc. Japan* **1999**.
- (36) HP of Ministry of Health, Labour and Welfare of Japan, 2017. [http://www.mhlw.go.jp/topics/syokuchu/poison/animal\\_01.html](http://www.mhlw.go.jp/topics/syokuchu/poison/animal_01.html).
- (37) FDA (Food and Drug Administration), (2017). *Advisory on Puffer Fish. (2007)*. <https://www.fda.gov/food/resources-for-you/industry/Ucm085458.htm>; page .

- (38) EC (European Commission) (2004b). Regulation (EC) No. 853/2004 of the European Parliament and of the Council of 29 April 2004 Laying down Specific Hygiene Rules for Food of Animal Origin. *Official Journal of the European Union*, L139, 22–82.
- (39) EC (European Commission) (2004a). Regulation (EC) No 854/2004 of the European Parliament and of the Council of 29 April 2004 Laying down Specific Rules for the Organisation of Official Controls on Products of Animal Origin Intended for Human Consumption.
- (40) Katikou, P. Public Health Risks Associated with Tetrodotoxin and Its Analogues in European Waters: Recent Advances after the EFSA Scientific Opinion. *Toxins*. 2019, page .
- (41) Cembella, A. D.; Durán-Riveroll, L. M. Marine Guanidinium Neurotoxins: Biogenic Origins and Interactions, Biosynthesis and Pharmacology; 2021; page
- (42) Novelli, A.; Fernandez-Sanchez, M. T.; Aschner, M.; Costa, L. (Eds), Marine Neurotoxins. In *Advanced in Neurotoxicology*, Elsevier, Cambridge, 2021, 275-315. In *Advanced in Neurotoxicology*; Academic Press, Elsevier, Cambridge, 2021; pages .
- (43) Noguchi, T.; Mahmud, Y. Current Methodologies for Detection of Tetrodotoxin. *Journal of Toxicology - Toxin Reviews*. 2001, page .
- (44) Watabe, S.; Sato, Y.; Nakaya, M.; Hashimoto, K.; Enomoto, A.; Kaminogawa, S.; Yamauchi, K. Monoclonal Antibody Raised against Tetrodonic Acid, a Derivative of Tetrodotoxin. *Toxicon* **1989**.
- (45) Raybould, T. J. G.; Bignami, G. S.; Inouye, L. K.; Simpson, S. B.; Byrnes, J. B.; Grothaus, P. G.; Vann, D. C. A Monoclonal Antibody-based Immunoassay for Detecting Tetrodotoxin in Biological Samples. *J. Clin. Lab. Anal.* **1992**.
- (46) Neagu, D.; Micheli, L.; Palleschi, G. Study of a Toxin-Alkaline Phosphatase Conjugate for the Development of an Immunosensor for Tetrodotoxin Determination. In *Analytical and Bioanalytical Chemistry*; 2006; page .
- (47) Stokes, A. N.; Williams, B. L.; French, S. S. An Improved Competitive Inhibition Enzymatic Immunoassay Method for Tetrodotoxin Quantification. *Biol. Proced. Online* **2012**.
- (48) Li, Y.; Xu, X.; Liu, L.; Kuang, H.; Xu, L.; Xu, C. A Gold Nanoparticle-Based Lateral Flow Immunosensor for Ultrasensitive Detection of Tetrodotoxin. *Analyst* **2020**.
- (49) Reverté, L.; De La Iglesia, P.; Del Río, V.; Campbell, K.; Elliott, C. T.; Kawatsu, K.; Katikou, P.; Diogène, J.; Campàs, M. Detection of Tetrodotoxins in Puffer Fish by a Self-Assembled Monolayer-Based Immunoassay and Comparison with Surface Plasmon Resonance, LC-MS/MS, and Mouse Bioassay. *Anal. Chem.* **2015**.
- (50) Reverté, L.; Campàs, M.; Yakes, B. J.; Deeds, J. R.; Katikou, P.; Kawatsu, K.; Lochhead, M.; Elliott, C. T.; Campbell, K. Tetrodotoxin Detection in Puffer Fish by a Sensitive Planar Waveguide Immunosensor. *Sensors Actuators, B Chem.* **2017**.
- (51) Iliuk, A. B.; Hu, L.; Tao, W. A. Aptamer in Bioanalytical Applications. *Analytical Chemistry*. 2011, page .
- (52) Ruscito, A.; DeRosa, M. C. Small-Molecule Binding Aptamers: Selection Strategies, Characterization, and Applications. *Frontiers in Chemistry*. 2016, page .
- (53) Zhang, M.; Wang, Y.; Wu, P.; Wang, W.; Cheng, Y.; Huang, L.; Bai, J.; Peng, Y.; Ning, B.; Gao, Z.; Liu, B. Development of a Highly Sensitive Detection Method for TTX Based on a Magnetic Bead-Aptamer Competition System under Triple Cycle Amplification. *Anal. Chim. Acta* **2020**.
- (54) Tuerk, C.; Gold, L. Systematic Evolution of Ligands by Exponential Enrichment: RNA Ligands

- to Bacteriophage T4 DNA Polymerase. *Science (80-. ).* **1990**.
- (55) Ellington, A. D.; Szostak, J. W. In Vitro Selection of RNA Molecules That Bind Specific Ligands. *Nature* **1990**.
- (56) Spiga, F. M.; Maietta, P.; Guiducci, C. More DNA-Aptamers for Small Drugs: A Capture-SELEX Coupled with Surface Plasmon Resonance and High-Throughput Sequencing. *ACS Comb. Sci.* **2015**.
- (57) Stoltenburg, R.; Nikolaus, N.; Strehlitz, B. Capture-SELEX: Selection of DNA Aptamers for Aminoglycoside Antibiotics. *J. Anal. Methods Chem.* **2012**.
- (58) Wu, Y.; Zhan, S.; Wang, L.; Zhou, P. Selection of a DNA Aptamer for Cadmium Detection Based on Cationic Polymer Mediated Aggregation of Gold Nanoparticles. *Analyst* **2014**.
- (59) Paniel, N.; Istamboulié, G.; Triki, A.; Lozano, C.; Barthelmebs, L.; Noguier, T. Selection of DNA Aptamers against Penicillin G Using Capture-SELEX for the Development of an Impedimetric Sensor. *Talanta* **2017**.
- (60) Reinemann, C.; Freiin von Fritsch, U.; Rudolph, S.; Strehlitz, B. Generation and Characterization of Quinolone-Specific DNA Aptamers Suitable for Water Monitoring. *Biosens. Bioelectron.* **2016**.
- (61) Ye, H.; Duan, N.; Wu, S.; Tan, G.; Gu, H.; Li, J.; Wang, H.; Wang, Z. Orientation Selection of Broad-Spectrum Aptamers against Lipopolysaccharides Based on Capture-SELEX by Using Magnetic Nanoparticles. *Microchim. Acta* **2017**.
- (62) Qi, X.; Yan, X.; Zhao, Y.; Li, L.; Wang, S. Highly Sensitive and Specific Detection of Small Molecules Using Advanced Aptasensors Based on Split Aptamers: A Review. *TrAC - Trends in Analytical Chemistry.* 2020, page .
- (63) Jarczewska, M.; Malinowska, E. The Application of Antibody-Aptamer Hybrid Biosensors in Clinical Diagnostics and Environmental Analysis. *Analytical Methods.* 2020, page .
- (64) Sabherwal, P.; Shorie, M.; Pathania, P.; Chaudhary, S.; Bhasin, K. K.; Bhalla, V.; Suri, C. R. Hybrid Aptamer-Antibody Linked Fluorescence Resonance Energy Transfer Based Detection of Trinitrotoluene. *Anal. Chem.* **2014**.
- (65) Kim, S.; Lee, H. J. Gold Nanostar Enhanced Surface Plasmon Resonance Detection of an Antibiotic at Attomolar Concentrations via an Aptamer-Antibody Sandwich Assay. *Anal. Chem.* **2017**.
- (66) Kumar, Y. V. V. A.; Renuka, R. M.; Achuth, J.; Venkataramana, M.; Ushakiranmayi, M.; Sudhakar, P. Development of Hybrid IgG-Aptamer Sandwich Immunoassay Platform for Aflatoxin B1 Detection and Its Evaluation onto Various Field Samples. *Front. Pharmacol.* **2018**.
- (67) Shao, B.; Gao, X.; Yang, F.; Chen, W.; Miao, T.; Peng, J. Screening and Structure Analysis of the Aptamer Against Tetrodotoxin. *J. Chinese Inst. Food Sci. Technol.* **2012**.
- (68) Gu, H.; Duan, N.; Xia, Y.; Hun, X.; Wang, H.; Wang, Z. Magnetic Separation-Based Multiple SELEX for Effectively Selecting Aptamers against Saxitoxin, Domoic Acid, and Tetrodotoxin. *J. Agric. Food Chem.* **2018**.
- (69) Mairal Lerga, T.; Jauset-Rubio, M.; Skouridou, V.; Bashammakh, A. S.; El-Shahawi, M. S.; Alyoubi, A. O.; O'Sullivan, C. K. High Affinity Aptamer for the Detection of the Biogenic Amine Histamine. *Anal. Chem.* **2019**.
- (70) Jauset-Rubio, M.; Botero, M. L.; Skouridou, V.; Aktas, G. B.; Svobodova, M.; Bashammakh, A. S.; El-Shahawi, M. S.; Alyoubi, A. O.; O'Sullivan, C. K. One-Pot SELEX: Identification of

- Specific Aptamers against Diverse Steroid Targets in One Selection. *ACS Omega* **2019**.
- (71) Rambla-Alegre, M.; Reverté, L.; del Río, V.; de la Iglesia, P.; Palacios, O.; Flores, C.; Caixach, J.; Campbell, K.; Elliott, C. T.; Izquierdo-Muñoz, A.; Campàs, M.; Diogène, J. Evaluation of Tetrodotoxins in Puffer Fish Caught along the Mediterranean Coast of Spain. Toxin Profile of *Lagocephalus Sceleratus*. *Environ. Res.* **2017**.
- (72) Kotaki, Y.; Shimizu, Y. 1-Hydroxy-5,11-Dideoxytetrodotoxin, the First N-Hydroxy and Ring-Deoxy Derivative of Tetrodotoxin Found in the Newt *Taricha Granulosa*. *J. Am. Chem. Soc.* **1993**.
- (73) Pfeiffer, F.; Mayer, G. Selection and Biosensor Application of Aptamers for Small Molecules. *Frontiers in Chemistry*. 2016, page .
- (74) Entzian, C.; Schubert, T. Studying Small Molecule-Aptamer Interactions Using MicroScale Thermophoresis (MST). *Methods* **2016**.
- (75) Skouridou, V.; Jauset-Rubio, M.; Ballester, P.; Bashammakh, A. S.; El-Shahawi, M. S.; Alyoubi, A. O.; O'Sullivan, C. K. Selection and Characterization of DNA Aptamers against the Steroid Testosterone. *Microchim. Acta* **2017**.
- (76) Luan, Y.; Chen, J.; Li, C.; Xie, G.; Fu, H.; Ma, Z.; Lu, A. Highly Sensitive Colorimetric Detection of Ochratoxin A by a Label-Free Aptamer and Gold Nanoparticles. *Toxins (Basel)*. **2015**.
- (77) Zhu, H.; Sonoyama, T.; Yamada, M.; Gao, W.; Tatsuno, R.; Takatani, T.; Arakawa, O. Co-Occurrence of Tetrodotoxin and Saxitoxins and Their Intra-Body Distribution in the Pufferfish *Canthigaster Valentini*. *Toxins (Basel)*. **2020**.
- (78) Lan, Y.; Qin, G.; Wei, Y.; Wang, L.; Dong, C. Exonuclease I-Assisted Fluorescence Aptasensor for Tetrodotoxin. *Ecotoxicol. Environ. Saf.* **2020**.
- (79) Fomo, G.; Waryo, T. T.; Sunday, C. E.; Baleb, A. A.; Baker, P. G.; Iwuoha, E. I. Aptameric Recognition-Modulated Electroactivity of Poly(4-Styrenesulfonic Acid)-Doped Polyaniline Films for Single-Shot Detection of Tetrodotoxin. *Sensors (Switzerland)* **2015**.
- (80) Taylor, A. D.; Ladd, J.; Etheridge, S.; Deeds, J.; Hall, S.; Jiang, S. Quantitative Detection of Tetrodotoxin (TTX) by a Surface Plasmon Resonance (SPR) Sensor. *Sensors Actuators, B Chem.* **2008**.
- (81) Campàs, M.; Reverté, J.; Rambla-Alegre, M.; Campbell, K.; Gerssen, A.; Diogène, J. A Fast Magnetic Bead-Based Colorimetric Immunoassay for the Detection of Tetrodotoxins in Shellfish. *Food Chem. Toxicol.* **2020**.

## 2.6 Supplementary information

### 2.6.1. Selection process

For library immobilization on magnetic beads, the biotinylated docking probe was first captured on the streptavidin magnetic beads (SA-MB) according to the manufacturer's instructions, using a 1.5-fold molar excess of the docking probe over the theoretical

binding capacity of the beads. The library and the subsequent pools, prepared in binding buffer (BB, PBS with 1.5 mM MgCl<sub>2</sub>), were annealed (2 min at 95°C and slow cooling to 4°C) and then incubated overnight at 22°C under rotation for immobilization on the SA-MB/docking probe complexes. For the first round, 100 µL of SA-MB were used for the immobilization of 0.2 nmol of the library whereas for subsequent rounds, 20 – 40 µL of SA-MB were required according to the amount of ssDNA pool prepared at the end of each round. Unbound oligonucleotides were removed by extensive washing of the beads (5 x 500 µL of binding buffer) and the SA-MB/docking probe/library complexes were finally resuspended with binding buffer to 10 mg/mL. Selection was initiated with a temperature pre-elution step for 15 min at 28°C under gentle agitation. After removal of the supernatant, the beads were resuspended in the same volume of binding buffer and a background elution step was performed. Finally, the beads were resuspended in the same volume of binding buffer containing tetrodotoxin for the target elution step, which was performed under the same conditions as the background elution to select sequences eluting in the presence of the target molecule. During the last six rounds, tetrodotoxin precursors L-arginine and 1,6-anhydro-beta-d-mannopyranose were included during the background elution step as counter-selection molecules. A total of 23 rounds were performed and the specific conditions used for each round are shown in Table S2.1 (Supplementary Information). The supernatants from the three elution steps were collected via magnetic separation and were used for pilot PCR experiments to monitor the progress of the selections. To this end, 2 µL of each fraction (pre-elution, background elution and target elution) were added to 10 µL of PCR master mix containing library-specific forward and phosphorylated reverse primers. Pilot PCR was performed using an initial denaturation step of 2 min at 95°C followed by 6 – 16 cycles of (15 sec at 95°C, 15 sec at 55°C, 30 sec at 72°C). For the preparation of ssDNA for succeeding rounds, PCR reactions were performed using the optimal number of amplification cycles found by pilot PCR, followed by asymmetric PCR and lambda exonuclease digestion. For asymmetric PCR, the PCR master mix contained only the forward primer and 20 µL of PCR reaction per 100 µL of master mix and amplification was performed for 12 cycles. Remaining dsDNA in the asymmetric PCR reaction was digested by lambda exonuclease for 1.5 h at 37°C, followed by enzyme deactivation for 10 min at 80°C and column purification of the generated ssDNA for use in subsequent rounds of selection.

**Table S2.1.** Conditions used for the selections.

Selection round	Duration* (min)	Tetrodotoxin ( $\mu\text{M}$ )	Counter-selection
R1 – R4	120	500	no
R5	120	100	no
R6	120	100	no
R7 – R13	60	100	no
R14 – R16	30	100	no
R17 – R23	30	50	yes **

\* background, counter and target elution steps

\*\* *L-arginine* and *1,6-anhydro- $\beta$ -D-mannopyranose*

## 2.6.2. NGS analysis

**Table S2.2** Distribution (%) of highly abundant sequences in the different pools from the two selections. Sequences were ranked according to their abundance in the TTX pool from round 23.

Sequence		Dynabeads SA-MB			SiMAG SA-MB		
		R23	R23-counter	R16	R23	R23-counter	R16
Most abundant	1	2.125	2.373	0.095	2.321	1.438	0.041
	2	1.138	1.351	0.063	1.825	1.478	0.061
	3	0.884	0.873	0.197	1.308	1.062	0.040
	4	0.477	0.492	0.016	0.985	0.841	0.014
	5	0.436	0.435	0.137	0.768	0.371	0.020
	6	0.359	0.381	0.051	0.666	0.448	0.009
	7	0.314	0.321	0.035	0.535	0.474	0.056
	8	0.311	0.332	0.034	0.459	0.363	0.017
	9	0.285	0.366	0.007	0.359	0.259	0.005
	10	0.263	0.298	0.012	0.354	0.284	0.034

	11	0.250	0.289	0.102	0.277	0.211	0.012
	12	0.244	0.384	0.007	0.270	0.231	0.003
	13	0.228	0.335	0.007	0.268	0.175	0.000
	14	0.224	0.226	0.009	0.235	0.109	0.011
	15	0.192	0.163	0.003	0.228	0.135	0.002
	16	0.192	0.160	0.028	0.191	0.165	0.000
	17	0.179	0.232	0.003	0.184	0.122	0.026
	18	0.179	0.169	0.060	0.184	0.150	0.023
	19	0.176	0.166	0.009	0.163	0.126	0.006
	20	0.176	0.143	0.021	0.158	0.113	0.008
<b>More abundant in target pool</b>	21	0.087	0.031	0.007	0.028	0.007	0.000
	22	0.026	0.000	0.000	0.026	0.005	0.000

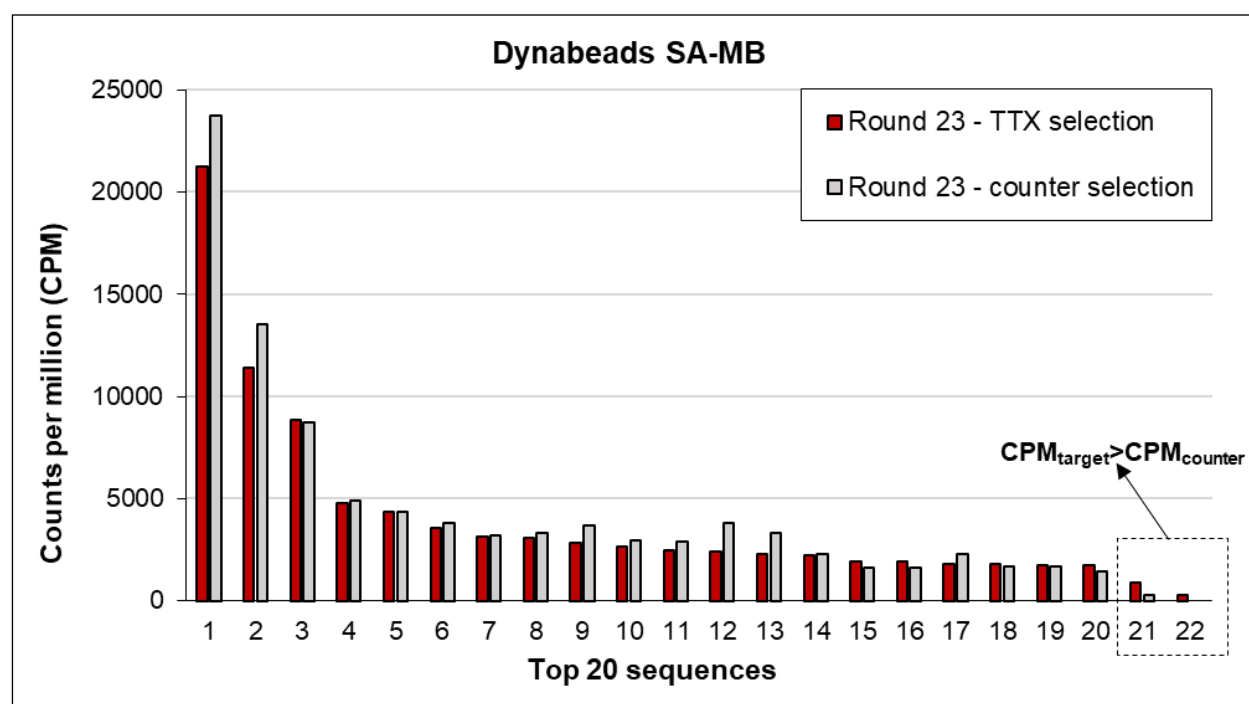


**Figure S2.1.** Abundance of highly abundant sequences in the last selection round of the target and counter selection molecules pools using Dynabeads SA-MB for library immobilization

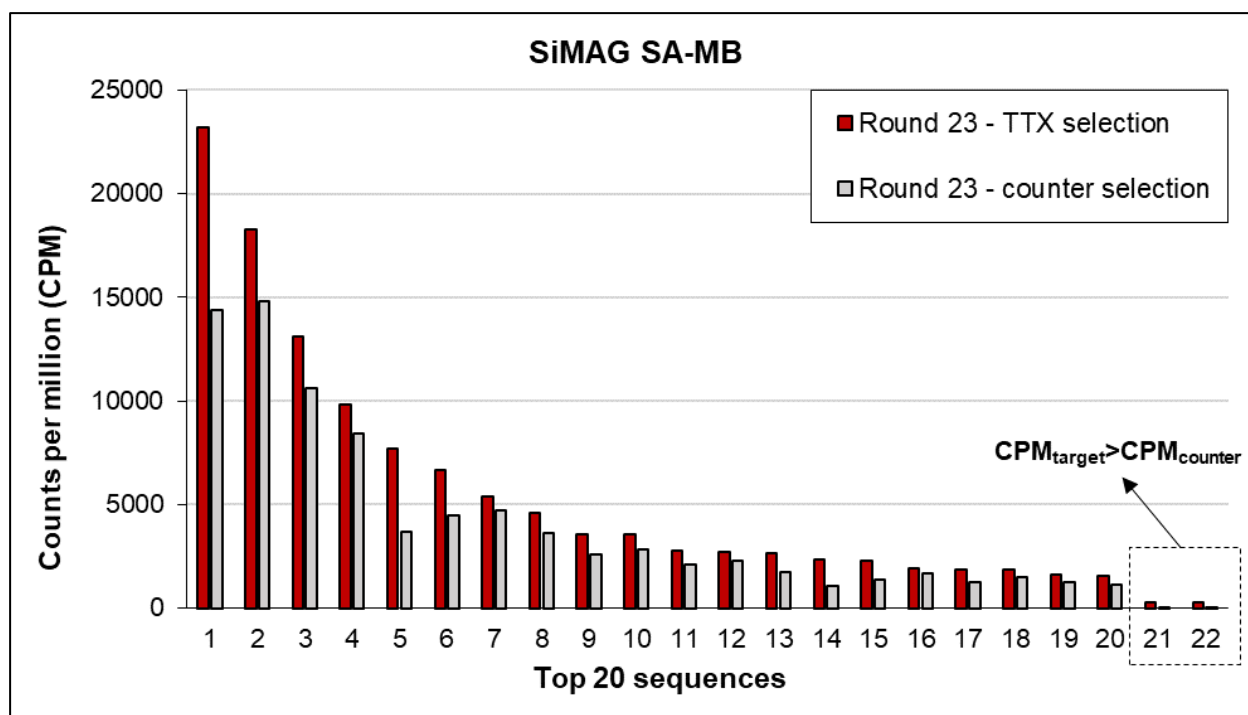


**Figure S2.2.** Abundance of highly abundant sequences in the last selection round of the target and counter selection molecules pools using SiMAG SA-MB for library immobilization.

	Forward primer ATACCGCTTATTCAATT	Docking site TGAGGCTCGATC	Reverse primer AGATAGTAAGTGCAATCT
46	ATACCGCTTATTCAATTCAAGCGGTTGAGGCTCAATCAAGGTTAGAAGAGAGTA--TTGTGAGTATAGAAATATGG	GAGATAGTAAGTGCAATCT	
35	ATACCGCTTATTCAATTTAGCGGGAGTGAGACTCGATCGTACGGCCGATCAAGGATAGTATGAAAGTCAATGAGGT	GAGATAGTAAGTGCAATCT	
63	ATACCGCTTATTCAATTTGCGGGATATGAGGCTTGATCTGCGCAAGCGATGG--TGAAGTTTTATTTATTAGAGGT	GAGATAGTAAGTGCAATCT	
76	ATACCGCTTATTCAATTTGAGATATAGGCTCGATTAATCGAAAGAAAT--CACAGCGTATAGGTAAAGGGG	GAGATAGTAAGTGCAATCT	
84	ATACCGCTTATTCAATTTGAGAGTATGAGACTCGATCAACTGAGAGAGGCT--TTCAAGTTAGCCAAATAAGGT	GAGATAGTAAGTGCAATCT	
4	ATACCGCTTATTCAATTTCAAGATATGAGGCTCGATCTCTGGAGAGATG--TATAAGTATGATATTCAGAGAGGG	GAGATAGTAAGTGCAATCT	
82	ATACCGCTTATTCAATTTCAAGCAACATGAGGCTCGATCGCTCCAAAGAC--TGGATCGTTGATAGTATAAGAGGG	GAGATAGTAAGTGCAATCT	
17	ATACCGCTTATTCAATTTCAACACAAATGGGCTCGATCTAGGATCGAGATGT--AGCTGTATAAAAAA--CCAGAGGC	GAGATAGTAAGTGCAATCT	
22	ATACCGCTTATTCAATTTCAACACAAATGGGCTCGATCTAGGATCGAGATGT--AGCTGTATAAAAAA--CCAGAGGC	GAGATAGTAAGTGCAATCT	
77	ATACCGCTTATTCAATTTCCAGGAAATGAGGCTCGATCAAGCGCGTGTGTC--AGCTGTATATAAAGAAAGAGGT	GAGATAGTAAGTGCAATCT	
41	ATACCGCTTATTCAATTTGAAGGTAGGTGAGGCTCGATCCGTTCCGATAC--AGGAAAAA--CTTGAATAAAGAGGT	GAGATAGTAAGTGCAATCT	
81	ATACCGCTTATTCAATTTGAGCGTGTAGTGGGCTCGATCCGGTAGCGTATAGC--GTCTAAAGCTTTTACAGAGGG	GAGATAGTAAGTGCAATCT	
75	ATACCGCTTATTCAATTTAAGAGGGGATGAGGCTCGATCGCCAGGGAACCTGA--TCGAAAAAAGCGGGTCGTATAC	AGATAGTAAGTGCAATCT	
30	ATACCGCTTATTCAATTTAGCGGGAGTGGGCTCGATCGGCCGCTTAAGGC--GTGACGGAAATATAGTATGGGGC	AGATAGTAAGTGCAATCT	
57	ATACCGCTTATTCAATTTAGGTGGATGAGGCTCGATCGAGGACTTGGAAC--GAGAGAAGAACAATAAGTTAAGGC	AGATAGTAAGTGCAATCT	
96	ATACCGCTTATTCAATTTGGGTGGGATGAGGCTCGGTCGTAGACTATAAT--AATATAGCAAGATGGTTTAGAGGC	AGATAGTAAGTGCAATCT	
95	ATACCGCTTATTCAATTTGGAGGAATGAGGCTTGATCAAAAGACATAT--AAAAAGAGCTTATCAAAAGGGA	AGATAGTAAGTGCAATCT	
58	ATACCGCTTATTCAATTTCAAGAGAGGTGAGGCTCGATCCGAGGGAACTCCG--AACGAGTAGATATATAAAGAAGC	AGATAGTAAGTGCAATCT	
9	ATACCGCTTATTCAATTTGGGCGGATGAGGCTTGATCCCAAGCGAACAANA--AAGGGCAGTAGCGTAAACAAGCC	AGATAGTAAGTGCAATCT	
59	ATACCGCTTATTCAATTTGGTGAAGTGGGCTCGATCCGAAACGTAGCAT--BAGGAGAAAGATTAAGAGAGGGG	AGATAGTAAGTGCAATCT	
33	ATACCGCTTATTCAATTTGAGGGTTGAGGCTCGATCGTAGATTACAGC--AGGGAGAATAAAGCGTCGAGAGGG	AGATAGTAAGTGCAATCT	
52	ATACCGCTTATTCAATTTGAGCGGATGAGGCTTGATCTTACACCGTAGT--AGTACAACCAAGCTCAAAAGAGGG	AGATAGTAAGTGCAATCT	
61	ATACCGCTTATTCAATTTGAGCGGATGAGGCTTGATCTTACACCGTAGT--AGTACAACCAAGCTCAAAAGAGGG	AGATAGTAAGTGCAATCT	
6	ATACCGCTTATTCAATTTCAAGTGGATGAGGCTCGATCCGATCCAGCTAAAGT--TGGAATAAAGGGAGATAAGAC	AGATAGTAAGTGCAATCT	
56	ATACCGCTTATTCAATTTGGCAGATATGAGGCTCGATCAACAGCGCTTATCCA--TGATGAGTAAATGGAAAGAGGGCC	AGATAGTAAGTGCAATCT	
12	ATACCGCTTATTCAATTTGACAAATGTGGGCTCGATCCAGCAATCAAT--TAGCGGGATGTGAGGGCAACAGAGGG	AGATAGTAAGTGCAATCT	
97	ATACCGCTTATTCAATTTGTCAGATATGAGGCTCGATCTACAGGCTGAGGA--AAGCTGAAAGAAAGTGGGGCTC	AGATAGTAAGTGCAATCT	
40	ATACCGCTTATTCAATTTGATAAATGAGGCTCGATCTTATCTATATAATA--TAGATACAGTAGGTAAATGAGGA	AGATAGTAAGTGCAATCT	
36	ATACCGCTTATTCAATTTGAGCGAAGTGGGCTCGATCCCAAGCTTAAAG--AACCAACCGGAGCTTTCCTGAGGG	AGATAGTAAGTGCAATCT	
98	ATACCGCTTATTCAATTTGAGGCAATGAGGCTCGAAAACAAAAGTAGAAG--AAGAA-----AGTGGAAATGAGGG	AGATAGTAAGTGCAATCT	
93	ATACCGCTTATTCAATTTGAGGCAATGAGGCTCGAAAACAAAAGTAGAAG--AAGAA-----AGTGGAAATGAGGG	AGATAGTAAGTGCAATCT	
80	ATACCGCTTATTCAATTTGAGGCAATGAGGCTCGAAAACAAAAGTAGAAG--AAGAA-----AGTGGAAATGAGGG	AGATAGTAAGTGCAATCT	
68	ATACCGCTTATTCAATTTGAGGCAATGAGGCTCGAAAACAAAAGTAGAAG--AAGAA-----AGTGGAAATGAGGG	AGATAGTAAGTGCAATCT	
54	ATACCGCTTATTCAATTTGAGGCAATGAGGCTCGAAAACAAAAGTAGAAG--AAGAA-----AGTGGAAATGAGGG	AGATAGTAAGTGCAATCT	
39	ATACCGCTTATTCAATTTGAGGCAATGAGGCTCGAAAACAAAAGTAGAAG--AAGAA-----AGTGGAAATGAGGG	AGATAGTAAGTGCAATCT	
1	ATACCGCTTATTCAATTTGAGGCAATGAGGCTCGAAAACAAAAGTAGAAG--AAGAA-----AGTGGAAATGAGGG	AGATAGTAAGTGCAATCT	
15	ATACCGCTTATTCAATTTGAGGCAATGAGGCTCGAAAACAAAAGTAGAAG--AAGAA-----AGTGGAAATGAGGG	AGATAGTAAGTGCAATCT	
53	ATACCGCTTATTCAATTTGCGAGTAAGTGGGCTCGATCTATAGGTGTTATG--AAAGAGAAAAAAGATATAGGAGGT	AGATAGTAAGTGCAATCT	
62	ATACCGCTTATTCAATTTGACAAAGTGGGCTCGATCCCAATTCAGCG--TAGGTTGAGGATGTAATATAGAGGG	AGATAGTAAGTGCAATCT	
34	ATACCGCTTATTCAATTTGACAAAGTGGGCTCGATCCCAATTCAGCG--TAGGTTGAGGATGTAATATAGAGGG	AGATAGTAAGTGCAATCT	
66	ATACCGCTTATTCAATTTGACCACTGTGGGCTCGATCTAAGGACTAGC--AGATGAAAGCAATTAACAATGAGGT	AGATAGTAAGTGCAATCT	
86	ATACCGCTTATTCAATTTGAGGAGATGAGGCTCGATCGAGAGAAAGTATG--TGTAAAAG--AGGCAGAGAGGT	AGATAGTAAGTGCAATCT	
71	ATACCGCTTATTCAATTTGCGGGACATGAGGCTCGATCCGACGGAGTGGAGTGTGGAT--AT--AGGTAGTAGAGGC	AGATAGTAAGTGCAATCT	
10	ATACCGCTTATTCAATTTGGGATAGTGGGCTCGATCTAAAATAAGAGTG--TAAAAGT--GAAATGAGAGGGC	AGATAGTAAGTGCAATCT	
99	ATACCGCTTATTCAATTTGAGTGGAAATGAGGCTCGATCTCGAATAAGGATAGC--AAAAGTTAA--AAGTATGAGGGC	AGATAGTAAGTGCAATCT	
72	ATACCGCTTATTCAATTTGAGGCTGAGGCTCAATCCGAACCTAGGAAACAGAT--TAAAAG--AAAATCCAGGGC	AGATAGTAAGTGCAATCT	
47	ATACCGCTTATTCAATTTCAAGCAAGTGGGCTCGATCCATAGAGATTAATG--GTGGGTAT--CAAGAAATGAGGC	AGATAGTAAGTGCAATCT	
89	ATACCGCTTATTCAATTTCAAGCAAGTGGGCTCGATCCATAGAGATTAATG--GTGGGTAT--CAAGAAATGAGGC	AGATAGTAAGTGCAATCT	
26	ATACCGCTTATTCAATTTGACCGTGAAGTGGCTC--GATCTACAGAGAAAGTAAAGCCGACAG--TGACATGAGAGGC	AGATAGTAAGTGCAATCT	
20	ATACCGCTTATTCAATTTGCGGGATGAGGCTCAATCAATATATGTCTAAGAG--GGTCGT--CAATTTAGTGGT	AGATAGTAAGTGCAATCT	
87	ATACCGCTTATTCAATTTGAGGATGAGGCTCGATCCAGTATGACGATA--TCCGGATAAT--GCAATGAGGGC	AGATAGTAAGTGCAATCT	
5	ATACCGCTTATTCAATTTGAGGCTGAGGCTCAATCCGTCGATTTACTTATCACTA--ATTAAATAAGGGC	AGATAGTAAGTGCAATCT	
79	ATACCGCTTATTCAATTTGCGAAAAGTGGGCTCGATCTCAATTCAGAGT--TGGAAGAAATAA--TAGGCTAATG	AGATAGTAAGTGCAATCT	
14	ATACCGCTTATTCAATTTGCGTAGG--ATGCTC--GATCTCAGAGGAATAAGCGTAAATGAGA--GTATAAATGAGGG	AGATAGTAAGTGCAATCT	
90	ATACCGCTTATTCAATTTGCGTAGG--ATGCTC--GATCTCAGAGGAATAAGCGTAAATGAGA--GTATAAATGAGGG	AGATAGTAAGTGCAATCT	
94	ATACCGCTTATTCAATTTGAGCGAGGCTGAGACTCGATCCAGAACCAACAGATAT--AAAAGTAA--AGTACAGGCT	AGATAGTAAGTGCAATCT	
74	ATACCGCTTATTCAATTTGCGGTA--TGTGAGGCTCAATCCAACTGCTAGGAAAT--AAGGATCC--ACAGAAATG	AGATAGTAAGTGCAATCT	
19	ATACCGCTTATTCAATTTGAGAAATAATGAGGCTTGATCCGAAAAGATGTTAG--TGAGATGTA--AAGAGGCCAATA	AGATAGTAAGTGCAATCT	
65	ATACCGCTTATTCAATTTGAGAAAGTGGGCTCGATTAAGGATGACAAAG--G-----GA--GAATATTAGG	AGATAGTAAGTGCAATCT	
85	ATACCGCTTATTCAATTTGAGCGGCTGAGGCTCGATCCAGGATCA--TAGTAGCTAGAGAAAGAA--AAA--CA	AGATAGTAAGTGCAATCT	
37	ATACCGCTTATTCAATTTGCAAAATGAGGCTCAATCACTAAACCTCTTCA--AGGCTACCTC--AAGAAATAGGGC	AGATAGTAAGTGCAATCT	
100	ATACCGCTTATTCAATTTGCGGAAAGTGGGCTCGATCCAGGATTTTATTCAAG--CAACAGCA--AAAGAAATATGGC	AGATAGTAAGTGCAATCT	
73	ATACCGCTTATTCAATTTGAGGAGGATGAGGCTCAATCAATAAGGAGCTTCTG--AAGGTGTA--AATCAAGAGGGC	AGATAGTAAGTGCAATCT	
55	ATACCGCTTATTCAATTTGGCGGGTGTGAGGCTCGATCTGTAGTCCAGAAAT--TGGTATAGAA--GATTAATGAGT	AGATAGTAAGTGCAATCT	
11	ATACCGCTTATTCAATTTGCGCAAGTGGGCTCGATCCGAACTCGCAAAAGACAATA--AGAATAATCAGGGC	AGATAGTAAGTGCAATCT	
7	ATACCGCTTATTCAATTTGAGGATATGAGGCTCAATCAATAAATGAGAAAG--AAGAAACG--ATATATGAGGCT	AGATAGTAAGTGCAATCT	
38	ATACCGCTTATTCAATTTGAGGGGATGAGGCTCGATCCGAAATGTAAGAGAG--GAAATAAG--ACGTAAAGGGC	AGATAGTAAGTGCAATCT	
8	ATACCGCTTATTCAATTTGGCGGGTGTGAGGCTCGATCCCGGATCGGATATAACCTATAA--A--AGTGAAGAGGC	AGATAGTAAGTGCAATCT	
67	ATACCGCTTATTCAATTTGGCGGGTGTGAGGCTCGATCCCGGATCGGATATAACCTATAA--A--AGTGAAGAGGC	AGATAGTAAGTGCAATCT	
29	ATACCGCTTATTCAATTTGAGGGATGAGGCTCGATCCGTTAAGCGAAGGATCA--CGAAAGTA--AAGAAAGGGC	AGATAGTAAGTGCAATCT	
21	ATACCGCTTATTCAATTTGAGGGGATGAGGCTCGATCCGAAATGTAAGAGAG--GAAATAAG--ACGTAAAGGGC	AGATAGTAAGTGCAATCT	
44	ATACCGCTTATTCAATTTGAGGGGACATGAGGCTCGATCCGAAATTTGG--GCTAGGGTAGAAAG--A--CAAGAGGAGT	AGATAGTAAGTGCAATCT	
60	ATACCGCTTATTCAATTTGCGGGAGATGAGGCTCGATCCGGCGAGTGGCCGAT--CACAAAGAT--GGACATATTAATG	AGATAGTAAGTGCAATCT	
24	ATACCGCTTATTCAATTTGAGGGGAGGAGGCTCGATCCGGGCGGGCAGAGAGTAAAT--CAATAAAGGAGGT	AGATAGTAAGTGCAATCT	
50	ATACCGCTTATTCAATTTGATGGGATGAGGCTCAATCACTAGACTGACAAAT--GTAAAGT--GGCAGATCAGGT	AGATAGTAAGTGCAATCT	
3	ATACCGCTTATTCAATTTAATCCGGGCTGAGGCTCAATCAAGGAAAGATATAGTA--GCCAAAAG--GTC--AACCAAGGC	AGATAGTAAGTGCAATCT	
1	ATACCGCTTATTCAATTTAATCCGGGCTGAGGCTCAATCAAGGAAAGATATAGTA--GCCAAAAG--GTC--AACCAAGGC	AGATAGTAAGTGCAATCT	
45	ATACCGCTTATTCAATTTGACAAAGTGGGCTCGATCCGTTGAGATCGATTAATAA--AAGC--GTGAGGAGGGC	AGATAGTAAGTGCAATCT	
83	ATACCGCTTATTCAATTTGAGAGAACCGGAGGCTCGATCAACAGTACAGAG--AATGATGCT--ATTTATTAGGGC	AGATAGTAAGTGCAATCT	
32	ATACCGCTTATTCAATTTGAGAGAACCGGAGGCTCGATCAACAGTACAGAG--AATGATGCT--ATTTATTAGGGC	AGATAGTAAGTGCAATCT	
92	ATACCGCTTATTCAATTTGGGTGGGTTGAGGCTCGATCCGATCGTAAAC--CGTAAAATAA--G--GGCT--GTC--TG	AGATAGTAAGTGCAATCT	

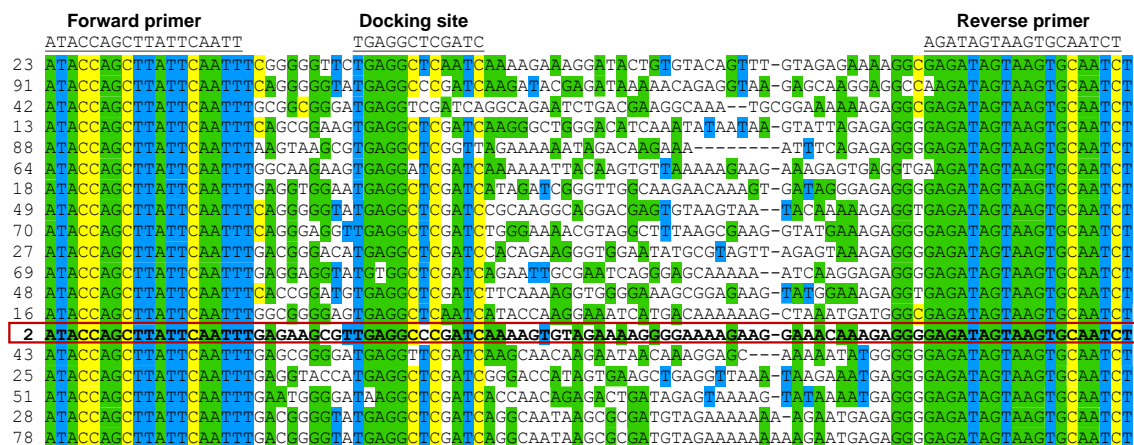


**Figure S2.3.** Multiple sequence alignment of the 100 most abundant sequences in the TTX target pool from round 23 of the selection performed with the Dynabeads SA-MB. Identical bases are shaded, and the three most enriched sequences selected for characterization are in boxes.



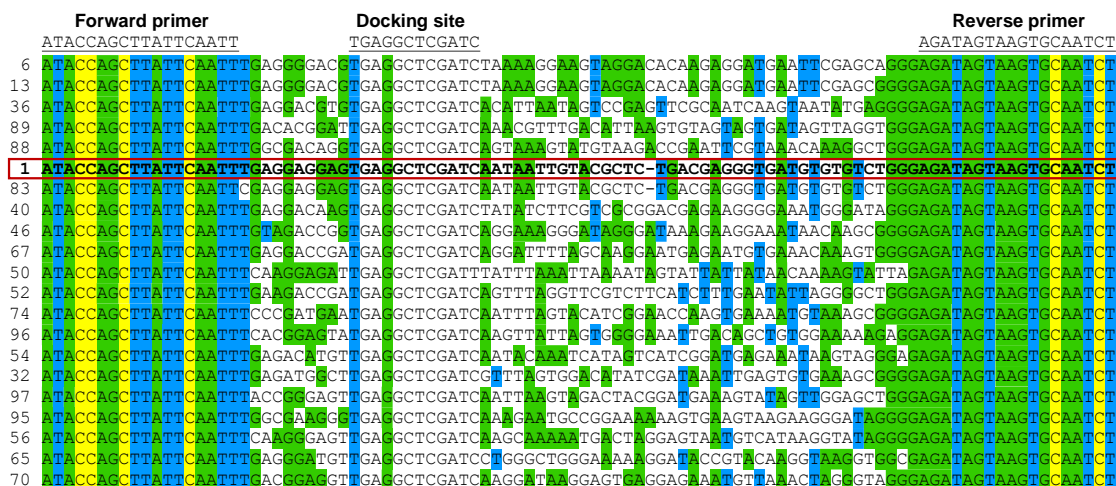


**Figure S2.4.** Multiple sequence alignment of the 100 most abundant sequences in the TTX target pool from round 23 of the selection performed with the SiMAG SA-MB. Identical bases are shaded and the three most enriched sequences selected for characterization are in boxes.

**Table S2.3.** Sequences of the selected aptamer candidates. D sequences were identified from the selection with Dynabeads and C sequences with the SiMAG SA-MB.

ID	Sequence (5'-3')	Length (nt)	GC (%)
D1	ATACCAGCTTATTCAATTTGAAGGCATATGAGGCTCGAAAACAAA AAGTAGAAGAAGAAAGTGGAAATGAGGGGAGATAGTAAAGTGA TCT	92	37.0
D2	ATACCAGCTTATTCAATTTGAGAAGCGTTGAGGCCCGATCAAAG TGTAGAAAAGGGGAAAAGAAGGAAACAAAGAGGGGAGATAGTAA GTGCAATCT	98	40.8
D3	ATACCAGCTTATTCAATTTAATGCGGGGTGAGGCTCAATCAAGGA AAGATATAAGTAAGCAAAAAGGTCAAACAAGGGCGAGATAGTAA GTGCAATCT	98	38.8
D4	ATACCAGCTTATTCAATTTGAGGAGGTATGTGGCTCGATCAGAAT TGCGAATCAGGGAGCAAAAATCAAGGAGAGGGGAGATAGTAAAG TGCAATCT	97	42.3
D5	ATACCAGCTTATTCAATTTGAGCGTGGGTGAGGCTTGATCCGAG GGTAGTTAGCGTAGCGAAGGAAGAAAAAAGAGGGGAGATAGTAA AGTGAATCT	98	44.9
C1	ATACCAGCTTATTCAATTTGAGGAGGAGTGAAGGCTCGATCAATAA TTGTACGCTCTGACGAGGGTGTGTGTGTCTGGGAGATAGTAAAG TGCAATCT	97	44.3

C2	ATACCAGCTTATTCAATTTGAGAAAATATGAGGCTCGATAAAAAAT AATAGTATAGAAATATATAAAGTGGTATTTTGGAGATAGTAAGTGCA ATCT	96	26.0
C3	ATACCAGCTTATTCAATTTGAGGAACATGAGGCTCGATCCTATAT AGAGATGACGAAGAATGATAGAAAGCGTAGGTGAAGATAGTAAG TGCAATCT	97	38.1
C4	ATACCAGCTTATTCAATTTACGGGGGGTGAGGCTCGATCTGTAA TTAAGAGTGCAAGGGGAAGTGAGATGAAAGTTGGGAGATAGTAA GTGCAATCT	98	43.9
C5	ATACCAGCTTATTCAATTTGAGGCGAGGTGAGGCTCGATCAATAG AAAAACCGAGGCGAAAATGAGAAAAAGGGACTGGGAGATAGTAA GTGCAATCT	98	42.9

### 2.6.3. Characterization of aptamer candidates

#### 2.6.3.1 Immobilization of TTX on magnetic beads for affinity assays

TTX was immobilized on magnetic as follows: maleimide-activated magnetic beads (10  $\mu$ L of 250 mg/mL suspension) were washed with washing buffer (PBST: 0.1 M PBS, 0.05 % v/v Tween-20, pH 7.2), resuspended in 500  $\mu$ L of 1 mM MUAM in binding buffer (0.1 M PBS, pH 7.2, 10 % v/v ethanol) and incubated for 3 h at room temperature under tilt rotation. The beads were washed again with PBST, followed by resuspension with 500  $\mu$ L of TTX (25  $\mu$ g/mL in 0.1 M PBS, 10 % v/v formaldehyde). After overnight incubation at ambient temperature (22-25°C) under tilt rotation, the beads were washed again and blocked with 500  $\mu$ L of sulfo-NHS-acetate (1 mM in 0.1 M PBS) for 1 h. After a final washing step, the TTX-beads were resuspended in 100  $\mu$ L of PBS (final suspension of 25 mg/mL). Immobilization of TTX on the beads was verified with a bead-ELISA using a monoclonal anti-TTX antibody as described previously<sup>1</sup>.

#### 2.6.3.2 Initial screening of the aptamer candidates

A displacement assay was designed to screen the aptamer candidates under conditions similar to the ones used during the selection process. Specifically, SiMAG SA-MB/docking probe complexes were prepared as described in the “Capture-SELEX process” section of the manuscript and used to immobilize the individual aptamer candidates (100 nM). The aptamer-magnetic beads were then incubated with TTX (1  $\mu$ M) or binding buffer alone for 30 min at room temperature under tilt rotation. The supernatant was recovered by magnetic separation and was used for PCR

amplification to detect eluted sequences. The PCR reactions were analyzed by agarose gel electrophoresis as shown in Figure S2.5. The candidates preferentially eluting in the presence of TTX compared to buffer alone were selected for characterization of their binding properties.

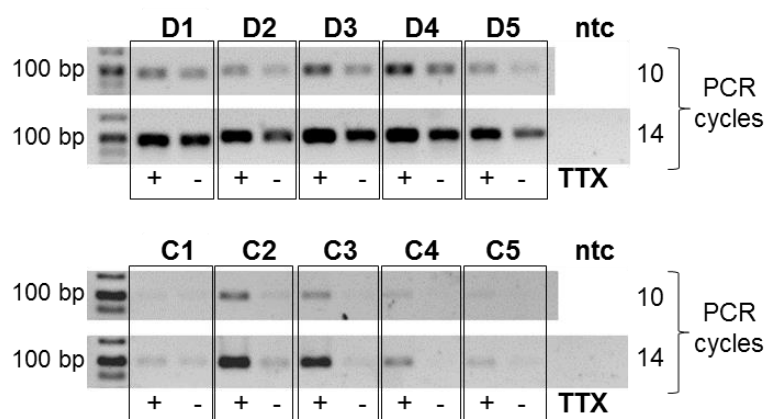


**Figure S2.5.** Screening of the aptamer candidates with a displacement assay. Aptamer candidates immobilized on docking probe-streptavidin magnetic beads complexes were incubated with 100  $\mu$ M TTX (+) or only binding buffer (-). Aptamer displacing to the solution was detected by PCR amplification and agarose gel electrophoresis. ntc: PCR no template control.

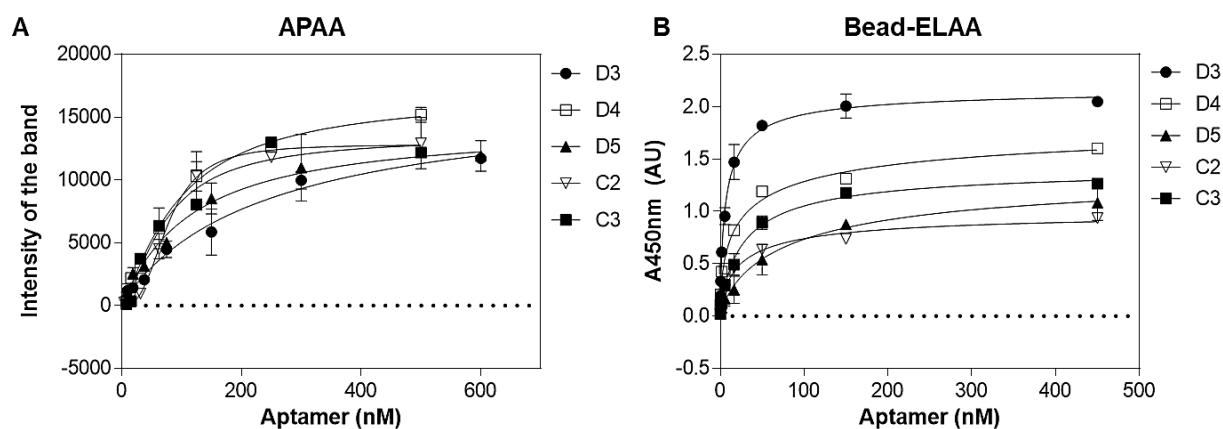


**Figure S2.6.** Binding curves of the aptamers determined by (A) APAA and (B) bead-ELAA

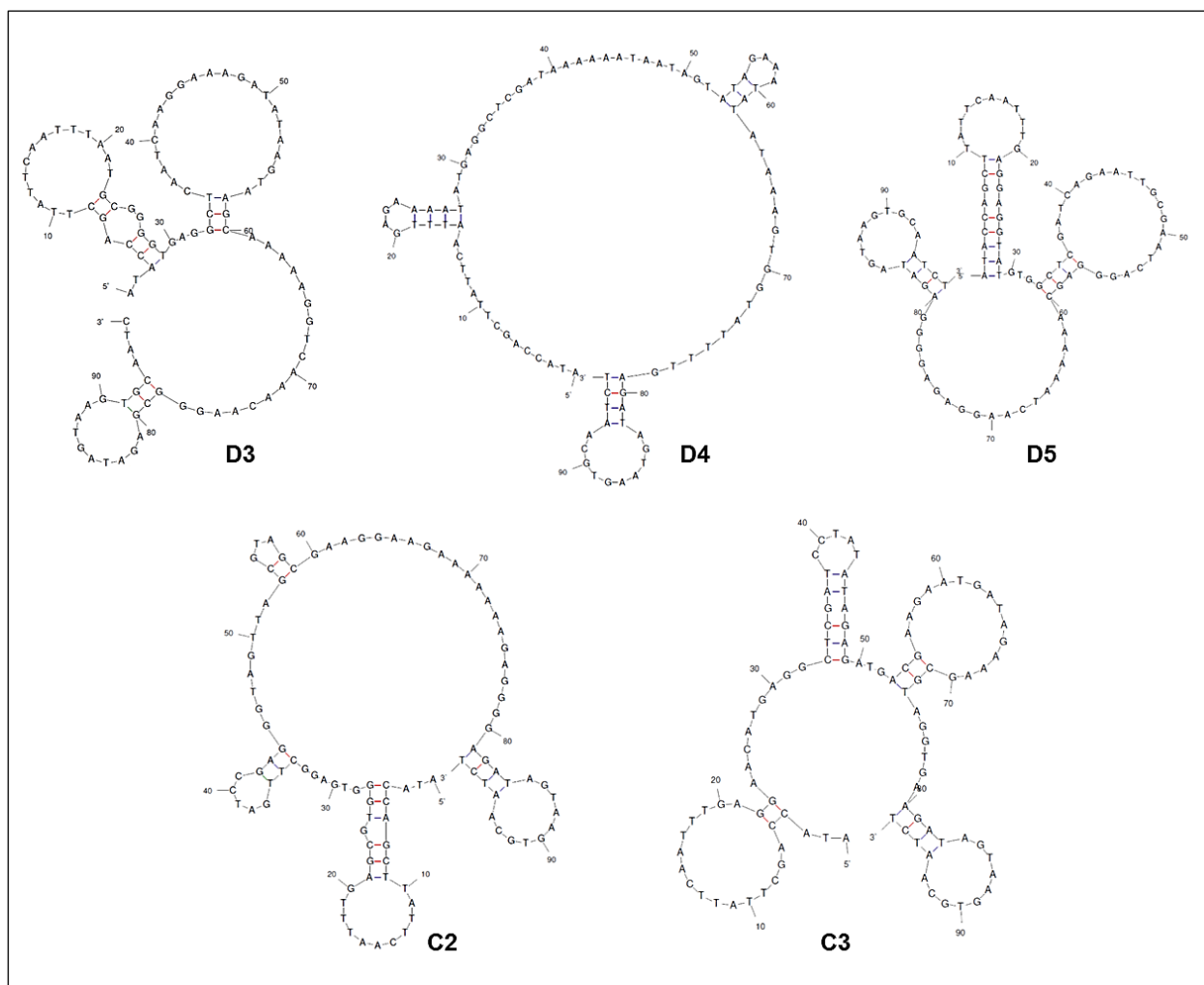


Figure S2.7. Predicted structures of the five selected TTX aptamers.

### 2.6.4. TTX detection

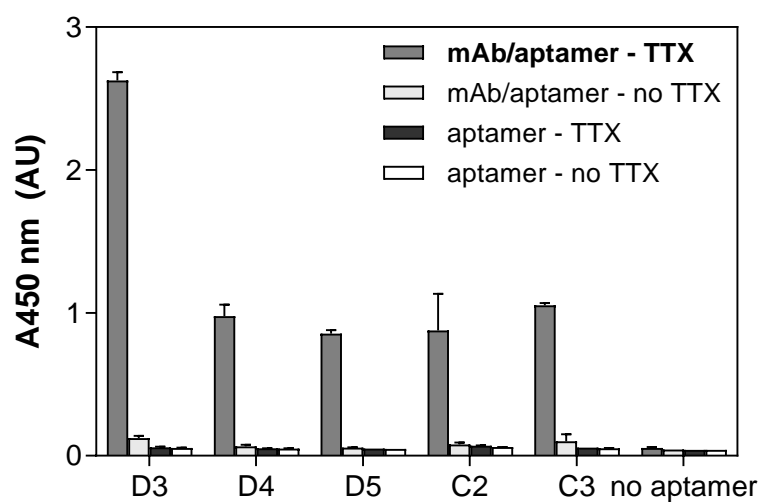


Figure S2.8. Screening of antibody-aptamer pairs for sandwich assay development.

**Table S2.4.** Hybrid antibody-aptamer assay precision. Inter-assay coefficients of variation (% CV) were calculated from duplicate samples using solutions of different TTX concentration measured on four different days (n=4).

Sample	Concentration (ng/mL)	MV $\pm$ SD	% CV	Average % CV
1	1.25	2.420 $\pm$ 0.077	3.2	2.8
		2.416 $\pm$ 0.003	0.1	
		2.357 $\pm$ 0.069	2.9	
		2.334 $\pm$ 0.112	4.8	
2	0.625	1.371 $\pm$ 0.064	4.9	3.3
		1.702 $\pm$ 0.007	0.4	
		1.219 $\pm$ 0.057	4.7	
		1.615 $\pm$ 0.055	3.4	
3	0.3125	0.443 $\pm$ 0.009	2.0	4.3
		0.782 $\pm$ 0.014	1.8	
		0.361 $\pm$ 0.002	0.5	
		0.436 $\pm$ 0.056	12.8	
4	0.039	0.157 $\pm$ 0.001	0.6	2.9
		0.160 $\pm$ 0.011	6.7	
		0.095 $\pm$ 0.004	4.1	
		0.145 $\pm$ 0.000	0.2	

#### 2.6.4.1 Magnetic bead-based colorimetric immunoassay for TTX detection

The MB-based colorimetric immunoassay protocol was similar to that described<sup>2</sup> and optimized<sup>3</sup> in our previous works. Briefly: (1) 10  $\mu$ L of maleimide-activated MBs were rinsed three times with washing buffer (0.1 M PBS, 0.05 % v/v Tween-20, pH 7.2) under vigorous mixing; (2) 1 mL of 1 mM cysteamine in binding buffer (0.1 M PBS, 10 mM EDTA, pH 7.2) was added and incubated for 2 h at room temperature; (3) after washing, 1 mL of TTX solution (25  $\mu$ g/mL) in binding buffer containing 10 % v/v formaldehyde was added and incubated overnight at 4°C; (4) the washed TTX-coated MBs were resuspended in 1 mL of binding buffer. When amounts of MB varied, volumes were adjusted proportionally. Once the MB-TTX conjugate had been prepared, (5) 200  $\mu$ L of the conjugate was taken, the supernatant was removed and 100  $\mu$ L of the TTX standard solution or fish extract and 100  $\mu$ L of anti-TTX mAb at 1/2000 dilution in 1 % w/v BSA-binding buffer were added and incubated for 30 min at room temperature; (6) after washing, 200  $\mu$ L of 1/1000 IgG-HRP dilution in 1 % w/v BSA-binding buffer was incubated for 30 min at room temperature; (7) the washed immunocomplex was resuspended in 200  $\mu$ L of binding buffer; (8) 50  $\mu$ L of immunocomplex was transferred to a new tube and after supernatant removal, 125  $\mu$ L of TMB liquid substrate was added and incubated for 10 min; (9) the tube was placed

on the magnetic separation stand and 100  $\mu$ L of TMB liquid substrate was collected for colorimetric measurement at 620 nm in a microtiter plate. All incubation steps were performed under agitation. Measurements were performed in triplicate.

**Table S2.5.** Assays and biosensors reported in the literature for TTX detection.

Platform	Sensitivity (LOD)	Reference
Fluorescence assay with aptamer	1 $\mu$ M (319 ng/mL)	4
Electrochemical impedance spectroscopy biosensor with aptamer immobilized on glassy carbon electrode	200 pg/mL	5
Fluorescence assay with aptamer and berberine	0.074 nM (24 pg/mL)	6
Fluorescence assay with aptamer, berberine and exonuclease I	11 pM (3.5 pg/mL)	7
Fluorescence assay with FAM-labeled aptamer and magnetic reduced graphene oxide	1.21 ng/mL	8
Competitive assay with aptamer immobilized on magnetic beads, strand displacement amplification with catalytic hairpin assembly and fluorescence detection	0.265 pg/mL	9
Microplate competitive immunoassay	2.28 ng/mL	10
Competitive planar wavelength immunosensor	2.5 ng/mL	11
Inhibition immunoassay with surface plasmon resonance sensor	0.3 ng/mL	12
Hybrid antibody-aptamer sandwich assay	310 pg/mL (970 pM)	This work

**Table S2.6.** TTX and analogues contents (mg TTX or analogue/kg tissue) in *L. sceleratus* by LC-MS/MS.

	TTX	4-epiTTX	11-norTTX-6(R)-ol	11-norTTX-6(S)-ol	4,9-anhydroTTX	5-deoxyTTX	11-deoxyTTX	5,11-dideoxyTTX/6,11-dideoxyTTX	5,6,11-trideoxyTTX
Gonads	21.8	4.3	1.1	16.3	0.5	0.9	1.1	0.4	94.3
Liver	2.3	0.7	0.3	1.3	0.2	-	0.2	0.2	12.4
Skin	1.2	0.3	0.1	1.1	-	-	0.1	-	1.8
Muscle	0.7	0.3	0.2	0.6	0.1	-	0.1	0.1	1.2

## 2.6.5. References

1. Skouridou, V.; Jauset-Rubio, M.; Ballester, P.; Bashammakh, A. S.; El-Shahawi, M. S.; Alyoubi, A. O.; O'Sullivan, C. K. Selection and Characterization of DNA Aptamers Against the Steroid Testosterone. *Microchim. Acta* **2017**, *184*, 1631-1639.
2. Leonardo, S.; Kiparissis, S.; Rambla-Alegre, M.; Almarza, S.; Roque, A.; Andree, K.B.; Christidis, A.; Flores, C.; Caixach, J.; Campbell, K.; Elliott, C.T.; Aligizaki, K.; Diogène, J.; Campàs, M. Detection of tetrodotoxins in juvenile pufferfish *Lagocephalus sceleratus* (Gmelin, 1789) from the North Aegean Sea (Greece) by an electrochemical magnetic bead-based immunosensing tool. *Food Chem.* **2019**, *290*, 255–262.
3. Campàs, M.; Reverté, J.; Rambla-Alegre, M.; Campbell, K.; Gerssen, A.; Diogène, J. A fast magnetic bead-based colorimetric immunoassay for the detection of tetrodotoxins in shellfish. *Food Chem. Toxicol.* **2020**, *140*, 111315.
4. Shao, B. Y.; Chen, B.; Chen, W.B.; Yang, F.; Miao, T.Y.; Peng J. Preparation and Application of Tetrodotoxin DNA Aptamer. *J. Food Sci.*, **2014**, *35*, 205-208.
5. Fomo, G.; Waryo, T.; Sunday, C.; Baleg, A. A.; Baker, P.; Iwuoha, E. Aptameric Recognition-Modulated Electroactivity of Poly(4-Styrenesulfonic Acid)-Doped Polyaniline Films for Single-shot Detection of Tetrodotoxin. *Sensors* **2015**, *15*, 22547-22560.
6. Lan, Y.; Qin, G.; Wei, Y.; Dong, C.; Wang, L. Highly Sensitive Analysis of Tetrodotoxin Based on Free-Label Fluorescence Aptamer Sensing System. *Spectrochim. Acta A Mol. Biomol. Spectrosc.* **2019**, *219*, 411-418.
7. Lan, Y.; Qin, G.; Wei, Y.; Wang, L.; Dong, C. Exonuclease I-assisted Fluorescence Aptasensor for Tetrodotoxin. *Ecotoxicol. Environ. Saf.* **2020**, *194*, 110417.
8. Gu, H.; Duan, N.; Xia, Y.; Hun, X.; Wang, H.; Wang, Z. Magnetic Separation-based Multiple SELEX for Effectively Selecting Aptamers Against Saxitoxin, Domoic acid and Tetrodotoxin. *J. Agric. Food Chem.* **2018**, *66*, 9801-9809.
9. Zhang, M.; Wang, Y.; Wu, P.; Wang, W.; Cheng, Y.; Huang, L.; Bai, J.; Peng, Y.; Ning, B.; Gao, Z.; Liu, B. Development of a highly sensitive detection method for TTX based on a magnetic bead-aptamer competition system under triple cycle amplification. *Anal. Chim. Acta* **2020**, *1119*, 18-24.
10. Reverté, L.; de la Iglesia, P.; del Río, V.; Campbell, K.; Elliott, C. T.; Kawatsu, K.; Katikou, P.; Diogène, J.; Campàs, M. Detection of Tetrodotoxins in Puffer Fish by a Self-Assembled Monolayer-Based Immunoassay and Comparison with Surface Plasmon Resonance, LC-MS/MS, and Mouse Bioassay. *Anal. Chem.* **2015**, *87*, 10839-10847.
11. Reverté, L.; Campàs, M.; Yakes, B. J.; Deeds, J. R.; Katikou, P.; Kawatsu, K.; Lochhead, M.; Elliott, C. T.; Campbell, K. Tetrodotoxin Detection in Puffer Fish by a Sensitive Planar Waveguide Immunosensor. *Sens. Actuators B Chem.* **2017**, *253*, 967-976.
12. Taylor, A. D.; Ladd, J.; Etheridge, S.; Deeds, J.; Hall, S.; Jiang, S. Quantitative detection of tetrodotoxin (TTX) by a surface plasmon resonance (SPR) sensor. *Sens. Actuators B Chem.* **2008**, *130*, 120-128.



# Chapter 3

---

## **Dipstick antibody-aptamer assay for detection of tetrodotoxin in puffer fish**

## Chapter 3

### Abstract

Tetrodotoxin (TTX), is a low molecular weight, highly toxic neurotoxin found in pufferfish and various shellfish. Here we describe the development of a dipstick for the sensitive detection of tetrodotoxin (TTX) in puffer fish. The dipstick exploits a hybrid sandwich assay, using a monoclonal antibody generated against TTX as the capture molecule immobilized on the test line and a gold nanoparticle functionalized aptamer as the reporter molecule, with an oligonucleotide complementary to the aptamer sequence immobilized on the control line. The dipstick is highly sensitive and reproducible, capable of detecting as low as 3ng/mL TTX, with the assay completed within 20 minutes. The specificity of the assay was demonstrated by a complete lack of interaction with other marine toxins such as domoic acid (DA), okadaic acid (OA) or saxitoxin (STX). The excellent performance of the dipstick was further demonstrated by the reliable determination of TTXs levels in puffer fish extracts (gonads, muscle, liver, and skin) with the results obtained in agreement with measurements obtained with a competitive magnetic bead-based immunoassay and liquid chromatography-mass spectrometry. The developed dipstick is the first example of a sandwich assay based rapid test for the detection of TTX in pufferfish, as well as being the first to use an aptamer, and furthermore a hybrid aptamer-antibody sandwich.

### 3.1. Introduction

Tetrodotoxin (TTX) is a neurotoxin with a low-molecular weight of approximately 319.27 g/mol<sup>1</sup> that is found and associated with a variety of species including puffer fish, octopuses, seashells, and xanthid crabs<sup>2</sup>. Beside this, TTX has been reported in terrestrial species including newts, frogs and toads<sup>3,4</sup>. Its paralytic toxic effects derive from its selective binding to voltage-gated sodium channels, thereby blocking the generation of neuronal action potentials and impulse conduction. Even a low dose of TTX poisoning results in severe neurological symptoms including ataxia, cardiac arrhythmias, seizures, respiratory failure, and death<sup>5,6</sup>. The toxin is approximately 1200 times more poisonous than cyanide<sup>7</sup>.

Although TTX-poisoning is typical of warm waters and it was regarded as a problem confined to Asian countries, in the last decade, due to the worldwide increase in water temperature<sup>8,9</sup>, TTX has been found also in the European waters through the possible migration of these toxic species from the Red Sea to Mediterranean Sea through the Suez Canal (Lessepsian migration)<sup>10</sup>. TTX has been detected in seafood harvested in the United Kingdom, Portugal, Spain, Greece and the Netherlands<sup>10-12</sup>.

Different approaches are used for TTX detection based on the physicochemical properties of the toxin, its antigen specificity and neurotoxic effect. The initial method used for TTX detection was the mouse bioassay (MBA). A mouse bioassay (MBA) involves aliquots of sample extract being injected into mice and the median death times used to calculate the toxicity (in mouse units; MU)<sup>13</sup>. MBA has frequently been used but due to a lack of specificity and high individual variability across experimental animals, the method suffers from accuracy, and furthermore due to ethical concerns, it is banned in most developed countries<sup>14</sup>. Moreover, positive results could also be caused by the presence of saxitoxin-group toxins as both exhibit the same symptomology in mice. The tissue culture bioassay (TCBA) was thus developed as an alternative to MBA<sup>15</sup>.

Currently, liquid chromatography (LC) is widely used for the analysis of TTX, with the LC being combined with fluorescence detection (HPLC-FLD)<sup>16</sup>, or tandem mass spectrometry (LC-MS/MS)<sup>9,17</sup>. These chromatographic methods are more sensitive, specific, and accurate than the bioassays, but they are time and solvent-consuming, labor-intensive and cannot be employed at the point-of-need.

Enzyme-Linked Immunosorbent Assays (ELISA) using antibodies against TTX, which provide quantitative and sensitive detection have been developed<sup>18,19</sup>. ELISA kits are now commercially available and mainly exploit indirect competitive assay formats, with immobilized BSA-TTX<sup>20,21</sup>. Antibodies against TTX have also been exploited in diverse assays and sensor formats and can potentially be used for rapid screening purposes<sup>22-24</sup>. Immunochromatographic assays exploiting gold nanoparticles (AuNPs), have garnered increasing attention due to their advantages in terms of sensitivity, rapidity, portability, robustness and ease-of-use. Thattiyaphong et al., proposed a rapid test for the detection of TTX in pufferfish tissues, using a BSA-TTX conjugate immobilized at the test line and a monoclonal antibody labelled with AuNPs and a competitive assay format, with the higher the level of TTX in the sample the lower the intensity of the band at the test line. The assay was successfully applied to the analysis of samples from 750 pufferfish, achieving 94.0% sensitivity and 92.4% specificity, as compared to LC/MS-MS<sup>25</sup>. Subsequently Shen et al., described a rapid test for the detection of TTX, which was coined a "turn-on competitive, lateral-flow immunochromatographic strip". Monoclonal antibodies against TTX were labelled with gold nanoflowers, whilst at the test line there was a mixture of BSA-TTX and BSA linked with quantum dots (BSA-QD), and just BSA-QD at the control line. In the absence of TTX in the sample, the gold labelled antibodies bound at both the test and control line, with the gold label acting to quench the fluorescence of the QD. Thus, in this approach, increasing levels of TTX resulted in an increasing intensity of the band at the test line, a preferred approach in rapid tests in general. Using spiked pufferfish muscle samples, a good degree of correlation was achieved with a commercial ELISA test kit<sup>18</sup> Li et al., produced their own monoclonal antibodies and pursued an approach similar to that of Thattiyaphong, using AuNP labelled monoclonal antibody and a BSA-TTX bioconjugate, achieving a detection limit of 10 ng/mL. Using spiked crucian and clam matrices, a reasonable degree of correlation was observed with LC/MS-MS<sup>28</sup>.

Whilst the results obtained with these rapid tests are very positive, competitive immunoassays are more difficult to optimize, and the preparation of toxin-reporter molecule conjugates, required for some types of immunoassays, can also be challenging<sup>14</sup>. Sandwich assays are more robust, with all reagents in excess, and due to this have longer shelf-lives, and often are more sensitive and specific.

Aptamers are single-stranded, synthetic oligonucleotides (DNA or RNA) which fold into 3-dimensional shapes capable of binding non-covalently and with high affinity to a target molecule. They are generated through the process known as Systematic Evolution of Ligands by Exponential enrichment (SELEX)<sup>26</sup>. The SELEX method is a repetitive process allowing the identification of unique RNA/DNA molecules from thousands of random oligonucleotides that bind to the target molecule with high affinity and specificity. Once the SELEX process is complete, the aptamer sequence can be validated, and unlimited amounts of the aptamer can be subsequently prepared using chemical synthesis.

Aptamers have been successfully applied as an alternative to antibodies in lateral flow assays<sup>30,31</sup>, and whilst there are several examples of lateral flow assays using dual aptamers for the detection of target molecules in sandwich formats<sup>32-38</sup>, or using split-aptamer formats<sup>39</sup>. Whilst aptamers have been selected against many small molecules, it is not trivial to identify dual aptamers that bind to different sites of a small target molecule, which have limited binding domains for aptamer recognition. To address this issue, the possibility of using split aptamers<sup>40</sup> or hybrid antibody-aptamer assays for the detection of small molecules has been reported<sup>41-43</sup>.

We recently selected high affinity aptamers against TTX and demonstrated that the unique cage-like structure of TTX facilitated the formation of an antibody-TTX-aptamer complex enabling the detection of TTX with a sandwich assay<sup>44</sup>. Here we report the implementation of the developed sandwich assay in a dipstick format for the detection of TTX in puffer fish. The tests is based on the use of a capture monoclonal antibody immobilized at the test line, and a AuNP labelled aptamer as the reporter molecule, with an oligonucleotide sequence partially complementary to the aptamer sequence immobilised at the control line. The dipstick was applied to the detection of a range of concentrations of TTX and the approximate detection limit established. The reproducibility of the dipstick performance was investigated, and the assay applied to the analysis of potentially interfering marine toxins. Finally, the assay was used for the detection of TTX in extracts from contaminated and noncontaminated puffer fish.

## **3.2. Materials and methods**

### **3.2.1. Chemicals and reagents**

Tetrodotoxin (TTX) was purchased from Latoxan (Valence, France) and standard solutions at 1 mg/mL were prepared in 0.1 M sodium acetate buffer pH 4.8. Certified reference materials of saxitoxin (STX) and domoic acid (DA) were obtained from the National Research Council of Canada (NRC, Halifax, Canada). Okadaic acid potassium salt (OA) was from *Prorocentrum concavum*. The mouse monoclonal anti-TTX antibody (CABT-L3089, CD Creative Diagnostics) was obtained from Deltaclon S.L. (Spain), and Streptavidin (*Streptomyces avidinii*) were purchased from Merck (Spain). All oligonucleotides were synthesized by Biomers.net (Germany).

### 3.2.2 Oligonucleotide sequences

Biotin-modified TTX aptamer:

5'-biotin-ATA CCA GCT TAT TCA ATT TAA TGC GGG GTG AGG CTC AAT CAA GGA AAG ATA TAA GTA AGC AAA AAG GTC AAA CAA GGG CG AGAT AGT AAG TGC AAT CT-3'

Aminated-modified reverse primer:

5'-NH<sub>2</sub>-TTTTTTTTTTTTTTAGTA TTG CAC TTA CTA TC T-3'

The specific TTX aptamer sequence had previously been chosen as the best aptamer, in terms of specificity and affinity, from an in-house capture SELEX previously carried out<sup>27</sup>. This selected aptamer was biotinylated and linked to streptavidin coated gold nanoparticles (described below). The oligonucleotide sequence immobilized at the control line was partially complementary to the selected aptamer sequence.

### 3.2.3 Development of the dipstick assay for TTX

The strip was constructed using 3 different components: the nitrocellulose membrane (FF120HP Whatman, Germany), the PVC backing card, and the absorbent pad (Whatman, England). The test and control lines were manually placed on the nitrocellulose membrane using an Eppendorf tip containing the biomolecule to be deposited. Aminated reverse primer sequence (100 µM diluted in water) was linked via ultraviolet (UV) cross-linking to the control line on the nitrocellulose via exposure to 254 nm wavelength for 15 minutes. Monoclonal antibody generated against TTX (1.5 mg/mL in PBS) was immobilized on test line via adsorption at 37 °C for 2 hours. Blocking of the nitrocellulose membrane was achieved using 5% w/v skimmed milk powder, 0.5% v/v Empigen detergent, and carbonate buffer (200 mM, pH 9.4) for 15 min, under rotation conditions. The membrane was then left to dry at 37°C for approximately 2 h and then assembled with the backing card, with the absorbent pad overlapping the nitrocellulose membrane by 2mm to ensure correct wicking. Following assembly, the strips were placed in a sealed bag containing dessicant and then stored in the fridge until use.

### 3.2.4 Preparation of gold nanoparticle labelled reporter aptamer conjugates

Gold nanoparticles (AuNPs) with an optical density of 1 and a diameter of 40 nm were mixed with Streptavidin (SA) and concentrated to OD-50 for use with the aptamer reporter molecules in the dipstick assay. Streptavidin, (12.5  $\mu$ L of 5 mg/mL in PBS) was primarily incubated with 5 mL AuNP solution for 30 min under tilt rotation at room temperature (RT), followed by the addition of 500  $\mu$ L (10% BSA w/v), for 30 min under tilt rotation at RT for AuNPs blocking. After the blocking step, the conjugate was washed 3 times by centrifugation and resuspension using Buffer A (boric acid (100mM), sucrose and bovine serum albumin (BSA)), each step for 30 min, in centrifuge at 15000 rpm, at 4 °C. Finally the conjugate was resuspended in the Buffer A and stored at 4°C until use. UV-Vis measurement confirmed the formation of the complex between -AuNPs and SA and the concentration of the conjugate to have an OD of 50.

### 3.2.5 Calibration Curve

The dipstick assay optimized in this work was evaluated by testing a range of TTX standard solutions at concentrations of 200, 100, 50, 25, 12.5, 6.2, 3.1, 1.5, and 0.7 ng/mL prepared in PBS, and for the control strip was used just PBS buffer. After the preparation of all the strips (as described above), in a parallel experiment were used 20 strips for analysis of each TTX concentration in duplicate samples. In the first step, dipstick was dip in a well containing 20  $\mu$ L of TTX (200-0.7 ng/mL) in PBS. Subsequently, after all TTX solution run through the membrane, the strip was transfer to a new well containing 20  $\mu$ L of 2  $\mu$ M biotinylated aptamer in Binding buffer (PBS with 1.5 mM MgCl<sub>2</sub>). In the third step, all the strips were dipped in 20  $\mu$ L AuNPs-SA conjugate (OD-10) prepared in PBS-Tween and let to run until all the solution in the well was absorbed. Finally, a washing step of the strips with 20  $\mu$ L PBS-Tween was performed and picture of all strips (duplicate samples) was capture using a Smartphone camera.

### 3.2.6 Sensitivity and specificity of the dipstick assay

The specificity of the dipstick assay was evaluated by the analysis of other potentially interfering marine toxins including domoic acid (DA), okadaic acid (OA) or saxitoxin (STX) which can be potentially co-detected in pufferfish. All toxins were analyzed at 50 ng/mL concentration and the image per each strip was captured by a Smartphone camera.

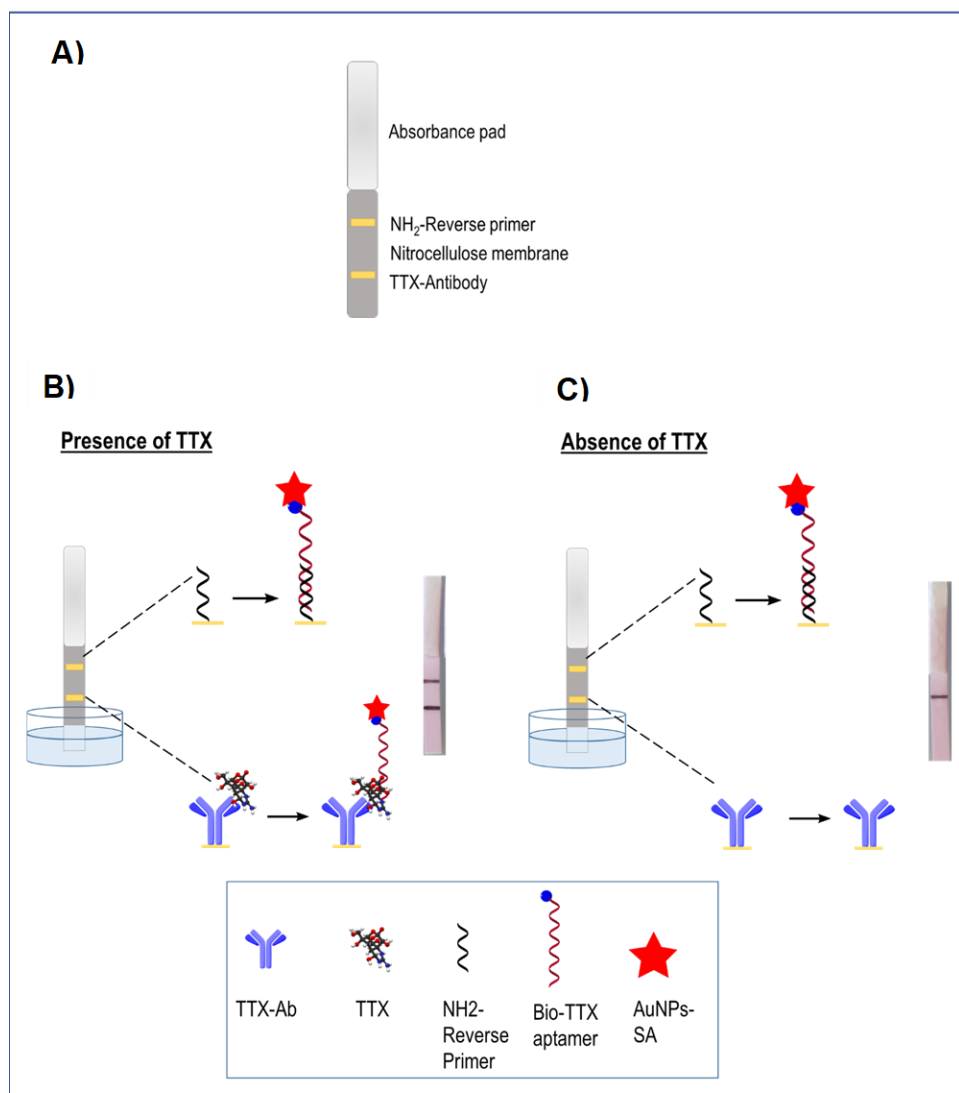
### 3.2.7 Fish extracts for TTX detection

For the validation of the dipstick assay, extracts from 2 different species were analysed, an oceanic puffer fish (*Lagocephalus lagocephalus*, Linnaeus, 1758) (TTX-free) and a silver-cheeked toadfish (*Lagocephalus sceleratus*, Gmelin, 1789) (TTX-contaminated). Puffer fish were dissected, and the gonads, liver, skin and muscle were retrieved (45). A double TTX extraction was performed with 0.1% v/v acetic acid as previously described<sup>28</sup>. Extracts were obtained at a tissue concentration of 200 mg equiv./mL.

## 3.3. Results and discussions

### 3.3.1 Optimization of the dipstick assay

For the optimization of the dipstick assay, experimental parameters such as DNA length on control line, TTX antibody concentration, TTX concentration and the OD of AuNPs-SA were investigated. The TTX aptamer that we used was selected from the Capture-SELEX selection<sup>44</sup> by immobilization of ssDNA on streptavidin magnetic beads through the aid of a bio-docking probe complementary to ssDNA sequences by 12 nucleotides<sup>44</sup>. Using this advantage, aminated docking probe was linked via UV cross-linking to the nitrocellulose membrane for the control line, aiming its complementary binding to TTX aptamer. The length of the complementary DNA probe is a key factor as it can affect the interaction with the aptamer. If the sequence of the DNA probe is too short, the complementary hybridization to the aptamer can be weak, conversely, if the DNA probe is too long, the complementary hybridization can be too strong, resulting in false-positive results<sup>29</sup>. As the complementary region between the aptamer and the docking probe was only 12 bases, in this experiment, TTX aptamer didn't bind to the docking probe, so no control line was observed (Figure 3.2A). In the next experiment, aminated reverse primer complementary to TTX aptamer was linked via UV cross-linking to the nitrocellulose membrane. There is a perfect hybridization between the amine-reverse primer and the bio-aptamer for TTX (Figure 3.2B). After this, the next step was the preparation of the dipstick membrane with the amine-reverse primer and TTX-Antibody. Different concentrations and solution volumes were used to obtain the best spots on the test line, but in later experiment we used a line form instead of the spot one. For paper-based assays, the most common immobilization method is direct, physical adsorption of the affinity reagent to the assay nitrocellulose membrane. As it is shown in Figure 3.3 the spots diameter differs in size between DNA probe and TTX antibody. This difference comes as these molecules are quite different, one is a DNA and the other one a protein, consequently the adsorption through the membrane will be different.



**Scheme 3.1.** Schematic illustration of the dipstick assay for the simple and rapid detection of TTX. (A) Structure of the dipstick strip (B) TTX present in the sample is capture by monoclonal TTX antibody in the test line where later is captured by biotinylated aptamer and AuNPs-SA, while the excess of biotin-aptamer and SA-AuNPs is captured through complementary hybridization on reverse primer immobilized in the control line, resulting in two red lines. (C) When TTX is not present, there is no binding on monoclonal TTX antibody on the test line and the biotin-aptamer with AuNPs-SA run along the nitrocellulose membrane by capillary action and are captured by the reverse primer immobilized on the control line resulting in one red line. Dipstick assay results for positive tests (left) and for negative test (right).

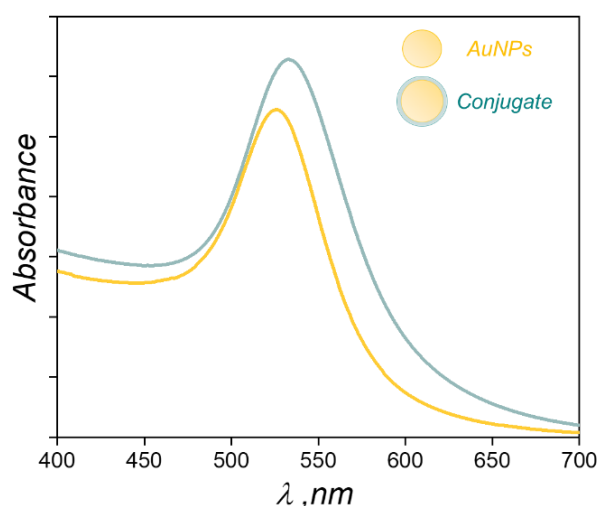


**Figure 3.1.** UV-visible spectrum of pure AuNPs and AuNPs-SA conjugate



**Figure 3.2.** Optimization of control line DNA probe. In this experiment 0.4  $\mu\text{L}$  (100  $\mu\text{M}$ ) of each aminated probe was directly immobilized on control line via UV-crosslinking (A) Using aminated docking probe. and (B) Using aminated reverse prime.

The dipstick assay developed in this work, was based on a sandwich assay using an immobilized monoclonal anti-TTX antibody as a capture molecule and a AuNP-labelled aptamer as a reporter molecule (Scheme 3.1).

For optimization of the dipstick parameters, the dipstick was first dipped in a well of a microtiter plate, containing TTX standards where complete wicking of the membrane is observed. The dipstick was then placed in a microtiter well containing the AuNP-labelled reporter aptamer that wicks across the membrane, forming complexes at the test line (in the case of the presence of TTX) and at the control line.

To elucidate the optimal parameters of the AuNPs-SA conjugate, three different OD (10, 15, 20) were tested using different concentrations of target TTX (0-1-10-100 ng/mL). As can be seen in Figure 3.3 the intensity of the test and control lines for the same target concentration using aptamer-AuNP bioconjugates of different OD, are very similar and there was no significant increase in the line intensity, and an OD of 10 for AuNPs-SA-aptamer conjugate was considered optimal and used in all further experiments.

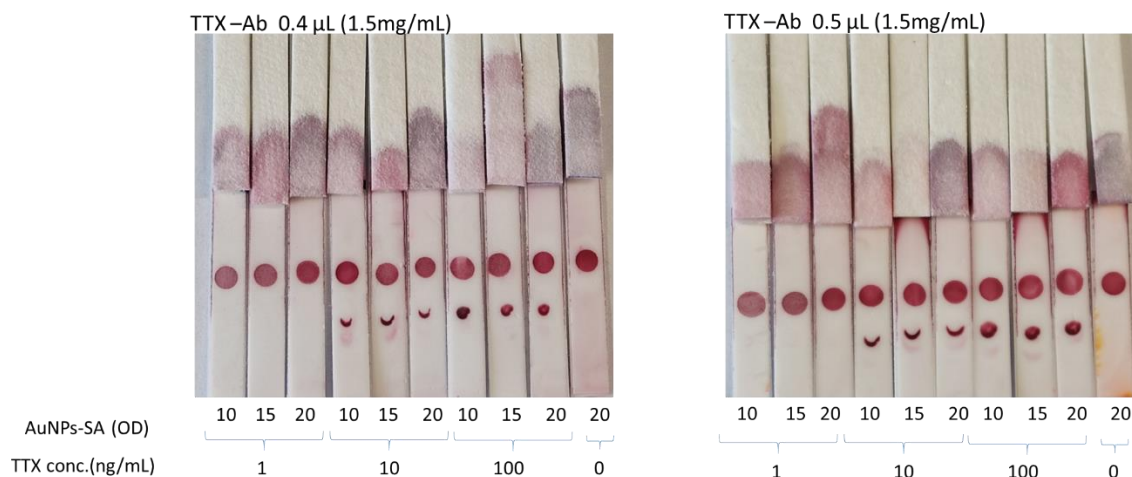


**Figure 3.3.** Optimization of AuNPs-SA OD in dipstick format for control and test line. Three different OD (10,15,20) of AuNPs-SA were analyzed in order to obtain the best visual intensity spot on the test and control line. Moreover, to increase the specificity of the dipstick format 2 different concentration of monoclonal TTX antibody were tested, 0.4 uL (of 1.5mg/mL stock) (left) and 0.5 uL (of 1.5mg/mL stock)(right).As it is shown here there is no significant difference between the different OD used for the same concentration of TTX samples, but there is an improvement of the assay sensitivity when using higher volume of monoclonal TTX antibody.

In order to test the sensitivity of the assay, a wide range of TTX concentrations (0–200 ng/mL) was analyzed using 1 in 2 dilutions of TTX concentration. With all concentrations tested, a red colour of deep intensity was observed at the control line, indicative of a successful wicking across the nitrocellulose membrane and hybridization of the oligonucleotide at the control line with the aptamer-AuNP conjugate. As the dipstick assay is based on a sandwich format, the intensity of the band at the control line is directly proportional to the concentration of the TTX. A Smartphone camera was used to take an image of all the strips and the colour of the red bands can easily be seen by the naked eye (Figure 3.4).

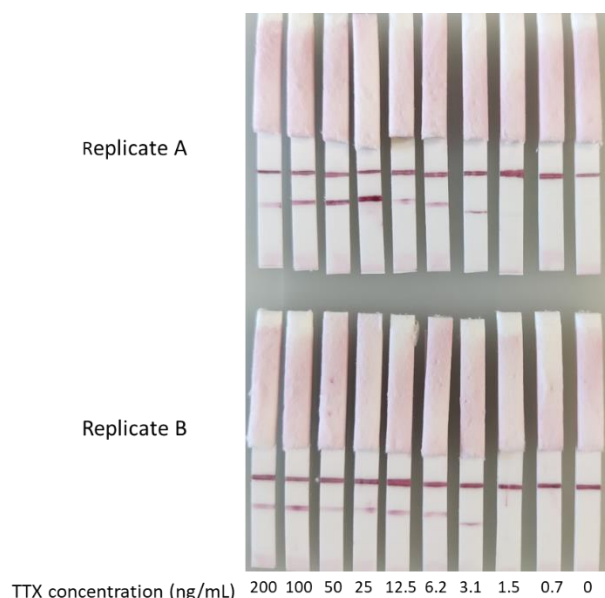


**Figure 3.4.** Image of the dipstick strips demonstrate the sensitivity of the assay using a range of TTX concentration starting from 200 ng/ml to 0.7 ng/mL using 1 in 2 dilutions and the control strip (0 ng/mL TTX) step.

### 3.3.2 Cross-reactivity studies.

The specificity of the assay was evaluated using 50 ng/mL of each of domoic acid (DA), okadaic acid (OA) and saxitoxin (STX). In this study saxitoxin is the most relevant as this toxin is often found with tetrodotoxin in pufferfish, and as it is hydrophilic, is often co-extracted with the tetrodotoxin and is also a neurotoxin. Okadaic acid, a diarrhetic toxin, can also be found in pufferfish, but as it is lipophilic, it would possible not be extracted using the method of extraction for tetrodotoxin, and is thus not expected to be as potentially problematic in terms of false positives, as saxitoxin. Due to the high specificity of the hybrid aptamer-antibody sandwich, no cross-reactivity, or non-specific binding with the other marine toxins studied, was observed (Figure 4.5)



**Figure 4.5.** Cross-reactivity experiment for the dipstick experiment using 4 different marine toxins (OA, STX, DA, and TTX).

### 3.3.2 Analysis of TTX in puffer fish samples

The dipstick was finally employed for the analysis of fish samples. Extracts from different tissues (gonads, liver, skin and muscle) of *Lagocephalus lagocephalus*, Linnaeus, 1758 (TTX-free) and one silver-cheeked toadfish, *Lagocephalus sceleratus*, Gmelin, 1789 (TTX-containing) were diluted 1 in 25 in PBS. As can be seen in Figure 6 the developed dipstick was able to detect TTX in all four positive extracts whilst giving no false positives with the negative extracts, highlighting not only the absence of any matrix effects, but also the sensitivity of the dipstick for the detection of TTX in pufferfish (Figure 4.6).

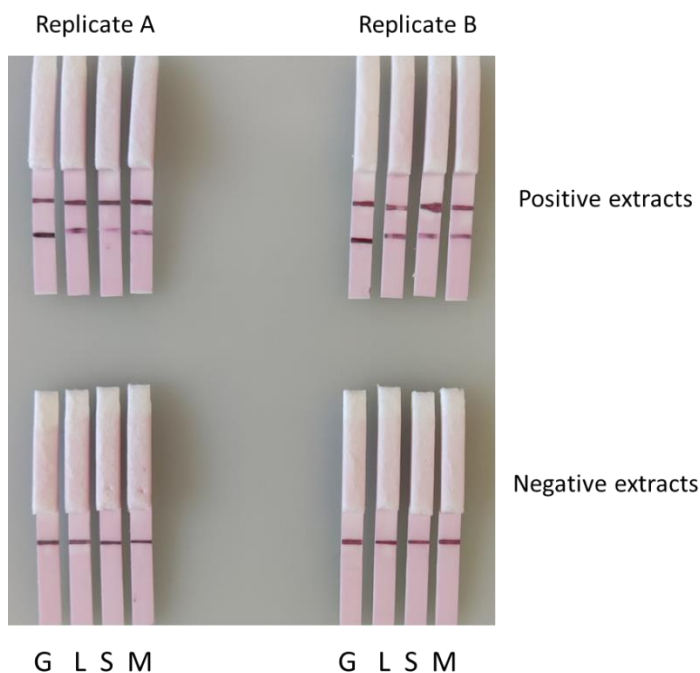


**Figure 4.6.** The successful application of the dipstick assay was evaluated by analysing 4 different fish extracts, gonads (G), liver (L), skin (S), and muscle (M).

### 3.4. Conclusions

To best of our knowledge, we have presented the first report of a dipstick based on a hybrid antibody-aptamer for the detection of TTX in extracts from puffer fish. The ease-of-use and high-sensitivity of this paper-based format facilitates the rapid, on-site, cost-effective detection of TTX in field samples. The developed dipstick was demonstrated to be specific, able to detect as low as 3ng/mL, with the assay being complete within 20 minutes and with no need for trained personnel. Ongoing work is focused on integrating the dipstick into an integrated lateral flow assay, evaluating the long-term stability of this LFA and the optimal storage conditions, and developing a facile and rapid methodology for the extraction of TTX from pufferfish, in order to realise a rapid test that can truly be deployed to and implemented at the point-of-need.

### 3.5. References

- 1) Bane, V.; Lehane, M.; Dikshit, M.; O'Riordan, A.; Furey, A. Tetrodotoxin: chemistry, toxicity, source, distribution and detection. *Toxins*, 2014, 6, 693-755.
- 2) Sui, L. M.; Chen, K.; Hwang, P. A.; Hwang, D. F. Identification of tetrodotoxin in marine gastropods implicated in food poisoning. *J. Nat. Toxins* 2002, 11, 213-220.
- 3) Yotsu-Yamashita M.; Tateki E.; First report on toxins in the Panamanian toads *Atelopus limosus*, *A. glyphus* and *A. certus*. *Toxicon* 2010, 55, 153-156.
- 4) Kim Y. H.; Brown G. B.; Mosher H. S.; Fuhrman F. A. Tetrodotoxin: Occurrence in atelopid frogs of Costa Rica. *Science* 1975, 189, 151-152.
- 5) Hwang, D. F.; Noguchi, T. Tetrodotoxin poisoning. *Adv. Food. Nutr. Res.* 2007, 52, 141-236.
- 6) Noguchi, T.; Ebesu, J. S. M. Puffer poisoning: epidemiology and treatment. *J. Toxicol. Toxin Rev.* 2001, 20, 1-10.
- 7) Lago, J.; Rodriguez, L. P.; Blanco, L.; Vieites, J. M.; Cabado, A. G. Tetrodotoxin, an extremely potent marine neurotoxin: distribution, toxicity, origin and therapeutical uses. *Mar. Drugs* 2015, 13, 6384-6406.
- 8) Noguchi T.; Arakawa O. Tetrodotoxin-distribution and accumulation in aquatic organisms, and cases of human intoxication. *Mar. Drugs* 2008, 6, 220-242.
- 9) Vlamis A.; Katikou P.; Rodriguez I.; Rey V.; Alfonso A.; Papazachariou A.; Zacharaki, T.; Botana A. M.; Botana, L. M. First detection of tetrodotoxin in greek shellfish by UPLC-MS/MS potentially linked to the presence of the dinoflagellate *prorocentrum minimum*. *Toxins* 2015, 7, 1779-1807.
- 10) Bentur, Y.; Ashkar, J.; Lurie, Y.; Levy, Y.; Azzam, Z. S.; Litmanovich, M.; Golik, M.; Gurevych, B.; Golani, D.; Eisenman, A. Lessepsian migration and tetrodotoxin poisoning due to *Lagocephalus Sceleratus* in the eastern mediterranean. *Toxicon*, 2008, 52, 964-968.
- 11) Katikou, P.; Georgantelis, D.; Sinouris, N.; Petsi, A.; Fotaras, T. First report on toxicity assessment of the lessepsian migrant pufferfish *Lagocephalus Sceleratus* (Gmelin, 1789) from European waters (Aegean Sea, Greece). *Toxicon* 2009, 54, 50-55.
- 12) Zaki M.A.; Wahab A. E.; Mossa A. Red Sea puffer fish poisoning: emergency diagnosis and management of human intoxication. *Egypt. J. Aquat. Res.* 2005, 31, 370-378.
- 13) Hungerford J. M. Committee on Natural Toxins and Food Allergens. Marine and freshwater toxins. *J. AOAC Int.* 2006, 89, 248-269.
- 14) Noguchi, T.; Mahmud, Y. Current methodologies for detection of tetrodotoxin. *J. Toxicol. Toxin Rev.* 2001, 20, 35-50.
- 15) Kogure K.; Do H.; Thuesen E.; Nanba K.; Ohwada K.; Simidu U. Accumulation of tetrodotoxin in marine sediment. *Mar. Ecol. Prog. Ser.* 1988, 45, 303-305.
- 16) Pires O. R.; Sebben A.; Schwartz E. F.; Morales R. A. V.; Bloch C.; Schwartz C. A. Further report of the occurrence of tetrodotoxin and new analogues in the Anuran family *Brachycephalidae*. *Toxicon* 2005, 45, 73-79.
- 17) Turner, A. D.; Powell, A.; Schofield, A.; Lees, D. N.; Baker-Austin, C. Detection of the pufferfish toxin tetrodotoxin in european bivalves, England, 2013 to 2014. *Euro Surveill.* 2015, 20, 21009-21016.
- 18) Asakawa M.; Gomez-Delan G.; Tsuruda S.; Shimomura M.; Shida Y.; Taniyama S.; Quilantang, M. B.; Shindo, J. Toxicity assessment of the xanthid crab *dementia cultripes* from Cebu Island, Philippines. *J. Toxicol.* 2010, 2010, 172367-172374.
- 19) Watabe, S.; Sato, Y.; Nakaya, M.; Hashimoto, K.; Enomoto, A.; Kaminogawa, S.; Yamauchi, K. Monoclonal antibody raised against tetrodonic acid, a derivative of tetrodotoxin. *Toxicon* 1989, 27, 265-268.
- 20) Raybould, T. J. G.; Bignami, G. S.; Inouye, L. K.; Simpson, S. B.; Byrnes, J. B.; Grothaus, P. G.; Vann, D. C. A monoclonal antibody-based immunoassay for detecting tetrodotoxin in biological samples. *J. Clin. Lab. Anal.* 1992, 6, 65-72.

- 21) Neagu, D.; Micheli, L.; Palleschi, G. Study of a toxin-alkaline phosphatase conjugate for the development of an immunosensor for tetrodotoxin determination. *Anal. Bioanal. Chem.* 2006, 385, 1068-1074.
- 22) Stokes, A. N.; Williams, B. L.; French, S. S. An improved competitive inhibition enzymatic immunoassay method for tetrodotoxin quantification. *Biol. Proced. Online* 2012, 14, 3-8.
- 23) <https://www.creative-diagnostics.com/TTX-EIA-Kit-258614-499.html>
- 24) Reverté, L.; De La Iglesia, P.; Del Río, V.; Campbell, K.; Elliott, C. T.; Kawatsu, K.; Katikou, P.; Diogène, J.; Campàs, M. Detection of tetrodotoxins in puffer fish by a self-assembled monolayer-based immunoassay and comparison with surface plasmon resonance, LC-MS/MS, and mouse bioassay. *Anal. Chem.* 2015, 87, 10839-10847.
- 25) Reverté, L.; Campàs, M.; Yakes, B. J.; Deeds, J. R.; Katikou, P.; Kawatsu, K.; Lochhead, M.; Elliott, C. T.; Campbell, K. Tetrodotoxin detection in puffer fish by a sensitive planar waveguide immunosensor. *Sens. Actuators B Chem.* 2017, 253, 967-976.
- 26) Thattiyaphong A.; Unahalekhaka J.; Mekha N.; Nispa W.; Kluengklangdon P.; Rojanapantip L. Efficiency of a rapid test for detection of tetrodotoxin in puffer fish. *J. Immunoass. Immunochem.* 2014, 35, 111-119.
- 27) Shen H.; Xu F.; Xiao M.; Fu Q.; Cheng Z.; Zhang S.; Huang, C.; Tang, Y. A new lateral-flow immunochromatographic strip combined with quantum dot nanobeads and gold nanoflowers for rapid detection of tetrodotoxin. *Analyst* 2017, 142, 4393-4398.
- 28) Li, Y.; Xu, X.; Liu, L.; Kuang, H.; Xu, L.; Xu, C. A. Gold nanoparticle-based lateral flow immunosensor for ultrasensitive detection of tetrodotoxin. *Analyst* 2020, 145, 2143-2151.
- 29) Tuerk, C.; Gold, L. Systematic evolution of ligands by exponential enrichment: RNA ligands to bacteriophage T4 DNA polymerase. *Science* 1990, 249, 505-510.
- 30) Jauset-Rubio. M.; El-Shahawi, M. S.; Bashammakh, A. S.; Alyoubi, A. O.; Ciara K. O'Sullivan, C. K. Advances in aptamers-based lateral flow assays, *Trend. Anal. Chem.* 2017, 97, 385-398.
- 31) Wang T.; Chen L.; Chikkanna A.; Chen S.; Brusius I.; Sbu N.; Veedu, R. N. Development of nucleic acid aptamer-based lateral flow assays: A robust platform for cost-effective point-of-care diagnosis. *Theranostics* 2021, 11, 5174-5196.
- 32) Bruno, J. G.; Carrillo, M. P.; Richarte, A. M.; Phillips, T.; Andrews, C.; Lee, J. S. Development, screening, and analysis of DNA aptamer libraries potentially useful for diagnosis and passive immunity of arboviruses, *BMC Res. Notes* 2012, 5, 63-75.
- 33) Bruno, J. G. Application of DNA aptamers and quantum dots to lateral flow test strips for detection of foodborne pathogens with improved sensitivity versus colloidal gold, *Pathog.* 2014, 3, 341-355.
- 34) Raston, N. H. A.; Nguyen, V. T.; Gu, M. B. A new lateral flow strip assay (LFSA) using a pair of aptamers for the detection of Vaspin, *Biosens. Bio-electron* 2017, 93, 21-25.
- 35) Minagawa, H.; Onodera, K.; Fujita, H.; Sakamoto, T.; Akitomi, J.; Kaneko, N.; Shiratori, I.; Kuwahara, M.; Horii, K.; Waga, I. Selection, characterization and application of artificial DNA aptamer containing appended bases with sub- nanomolar affinity for a salivary biomarker, *Sci. Rep.* 2017, 7, 42716-42725.
- 36) Shen G.; Zhang S.; Hu X. Signal enhancement in a lateral flow immunoassay based on dual gold nanoparticle conjugates. *Clin. Biochem.* 2013, 46, 1734-1738.
- 37) Adhikari, M.; Strych, U.; Kim, J.; Goux, H.; Dhamane, S.; Poongavanam, M. V.; Hagstoëm, A. E. V.; Kourentzi, K.; Conrad, J. C.; Willson, R. C. Aptamer-phage reporters for ultrasensitive lateral flow assays, *Anal. Chem.* 2015, 87, 11660-11665.
- 38) Liu G.; Mao X.; Phillips J. A.; Xu H.; Tan W.; Zeng L. Aptamer-nanoparticle strip biosensor for sensitive detection of cancer cells. *Anal. Chem.* 2009, 81, 10013-10018.
- 39) Zhu, C.; Zhao, Y.; Yan, M.; Huang, Y.; Yan, J.; Bai, W.; Chen, A. A sandwich dipstick assay for ATP detection based on split aptamer fragments, *Anal. Bioanal. Chem.* 2016, 408, 4151-4158.
- 40) Qi, X.; Yan, X.; Zhao, Y.; Li, L.; Wang, S. Highly sensitive and specific detection of small molecules, *Trend. Anal. Chem.* 2020, 133, 116069-116087.

- 41) Sabherwal, P.; Shorie, M.; Pathania, P., Chaudhary, S.; Bhasin, K. K.; Bhalla, V.; Suri, C. R. Hybrid aptamer-antibody linked fluorescence resonance energy transfer based detection of trinitrotoluene. *Anal. Chem.* 2014, 86, 7200-7204.
- 42) Kim, S.; Lee, H. J. Gold nanostar enhanced surface plasmon resonance detection of an antibiotic at attomolar concentrations via an aptamer-antibody sandwich assay. *Anal. Chem.* 2017, 89, 6624-6630.
- 43) Kumar, Y. V. V. A.; Renuka, R. M.; Achuth, J.; Venkataramana, M.; Ushakiranmayi, M.; Sudhakar, P. Development of hybrid IgG-aptamer sandwich immunoassay platform for aflatoxin B1 detection and its evaluation onto various field samples. *Front. Pharmacol.* 2018, 9, 271-282.
- 44) Shkempi, X.; Skouridou, V.; Svobodova, M.; Leonardo, S.; Bashammakh, A. S.; Alyoubi, A. O.; Campàs, M.; O'Sullivan, C. K. Hybrid antibody-aptamer assay for detection of tetrodotoxin in puffer fish, Manuscript under review.
- 45) Rambla-Alegre M.; Reverté L.; del Río V.; de la Iglesia P.; Palacios O.; Flores C.; Caixach, J.; Campbell, K.; Elliott, C. T.; Izquierdo-Muñoz, A.; Campàs, M.; Diogène, J. Evaluation of tetrodotoxins in puffer fish caught along the Mediterranean coast of Spain. Toxin profile of *Lagocephalus sceleratus*. *Environ Res.* 2017, 158, 1-6.
- 46) Kotaki Y.; Shimizu Y. 1-Hydroxy-5,11-dideoxytetrodotoxin, the first n-hydroxy and ring-deoxy derivative of tetrodotoxin found in the Newt *Taricha granulosa*. *J. Am. Chem. Soc.* 1993, 115, 827-830.
- 47) Hu J.; Wang S. Q.; Wang L.; Li F.; Pingguan-Murphy B.; Lu T. J.; Tian Jian Lu, T. J.; Xu, F. Advances in paper-based point-of-care diagnostics. *Biosens. Bioelectron.* 2014, 54, 585-597.

# Chapter 4

---

## **Novel nandrolone aptamer for rapid colorimetric detection of anabolic steroids**

## Chapter 4

### Abstract

The illicit use of anabolic androgenic steroids (AAS) as performance-enhancing drugs remains a global issue threatening not only the credibility of competitive sports but also public health because of the well-documented adverse effects they elicit. Despite the existence of strict rules and continuous anti-doping controls, doping scandals continue to surface, suggesting that the fight against doping is far from over. AAS abuse however is not restricted only to professional sports, but it also extends to recreational athletes and adolescents as well as in livestock production as growth-promoting agents. Testosterone and nandrolone are among the AAS most frequently exploited for these purposes. Gas chromatography-mass spectrometry is the reference method for AAS detection, but it is strictly laboratory-based and cannot be performed on-site. The great potential of aptamers in bioanalytical applications and specifically for the development of simple biosensors suitable for on-site analysis has been well demonstrated. In this report, we describe the selection and identification of aptamers binding nandrolone exhibiting affinity dissociation constants in the low nanomolar range and cross-reactivity with testosterone. A label-free colorimetric assay was finally developed using one of these novel aptamers for AAS detection based on gold nanoparticles and their aggregation in the presence of target molecules after salt addition. The assay could be deployed for rapid on-site screening of suspicious samples and provide qualitative visual results with a red to purple/blue color change to indicate the presence of both nandrolone and testosterone as doping biomarkers.

### 4. 1. Introduction

Anabolic androgenic steroids (AAS) are synthetic derivatives of testosterone, the main male sex hormone, with clinical and illicit uses. Their anabolic effects are related to their ability to increase lean body mass, muscle size and strength, and to improve protein and bone metabolism<sup>1</sup>. On the other hand, their androgenic properties cause masculinization. Clinically, AAS, and especially testosterone, have been traditionally prescribed to treat male hypogonadism<sup>2</sup>. However, the potential benefits of their anabolic properties to certain patient populations have encouraged the therapeutic use of AAS for several conditions including growth impairment, infertility and depression as well as to treat cachexia related to chronic diseases such as HIV, burns, renal failure, pulmonary disorders, muscular dystrophies, breast cancer and anemia<sup>3-6</sup>. Unfortunately, the illicit use of AAS as performance-enhancement drugs, a practice commonly known as doping, has also been known for many decades<sup>1</sup>. Doping has been reported among not only competing athletes but also amateurs and recreational athletes as well as adolescents with the main objective to increase muscle mass and improve bodily appearance<sup>4, 7, 8</sup>. However, a plethora of adverse effects have been associated with AAS use/abuse including hypertension, hepatic damages, reproductive disorders as well as neuropsychiatric and behavioral disorders<sup>1, 4, 8</sup>. The use of AAS is prohibited in professional sports and the World Anti-Doping Agency (WADA) publishes a

yearly list with prohibited substances, in- and out-of-competition, in an effort to contain the abuse<sup>9</sup>.

Nandrolone is among these substances whose use in sports as well as in horse racing is prohibited at all times<sup>10</sup>. Nandrolone (19-nortestosterone) is a synthetic testosterone analogue and one of the most frequently abused AAS together with testosterone, stanozolol and methandienone<sup>7,8</sup>. Its anabolic properties though are more potent than those of testosterone, since it exhibits an anabolic:androgenic ratio of 10 compared to 1 for testosterone<sup>1,11</sup>. Besides its potential therapeutic uses as an AAS, nandrolone has also been used as a growth promoting agent in livestock intended for human consumption<sup>12,13</sup>. Its use however for this purpose is banned in the EU<sup>14</sup>. On the other hand, several studies report the presence of nandrolone in dietary supplements as a cross-contaminant and consumption of such supplements could lead to accidental doping<sup>15-17</sup>. It is therefore evident that monitoring the presence of nandrolone in human and animal biological fluids, meat products and nutritional supplements is essential to protect public health and discourage doping practices in sports.

According to WADA regulations, gas chromatography-mass spectrometry (GC-MS) and gas chromatography-isotope ratio mass spectrometry (GC-IRMS) are the official methods for the detection of endogenous (such as testosterone)<sup>18</sup> and exogenous AAS (like nandrolone)<sup>19</sup>, respectively. Indeed, gas chromatography combined with mass spectrometry has been widely exploited in the literature as well to analyze different types of samples potentially containing AAS<sup>16, 20-23</sup>. The use of other techniques has also been reported, such as ultra-high-performance liquid chromatography coupled with mass spectrometry (UHPLC-MS) which is garnering increased interest<sup>24,25</sup>, high-performance thin-layer chromatography (HPTLC)-densitometry<sup>26</sup> and nuclear magnetic resonance (NMR)<sup>27</sup>. These techniques, even though highly accurate, are expensive and laboratory-based requiring significant infrastructure, specific equipment and trained personnel. Immunoassays have also been developed as simpler, lower cost and more user-friendly alternatives to the above-mentioned techniques<sup>10, 28-32</sup>. Due to the small size of the steroids, the ELISAs are typically performed in an indirect competitive format, and they require the preparation of haptens for animal immunization and antibody production or for signal generation. Depending on their specific design, ELISAs can be very sensitive with limits of detection (LOD) in the (sub)nanomolar range. For example, an LOD of 4 pg/mL (~ 15 pM) was reported when a linker-optimized biotin derivative of nandrolone was used in conjunction with avidin as an immobilized competitor<sup>32</sup>. ELISA kits are also available in the market for various AAS with LODs in the low picomolar range. The high sensitivity and specificity demonstrated by immunoassays emphasize the potential of biorecognition molecules in AAS detection and their compatibility with anti-doping drug testing.

Aptamers are biorecognition molecules considered as the chemical alternatives to antibodies. They are single stranded DNA or RNA molecules with specific three-dimensional structures able to bind their cognate targets with high affinity and specificity. Starting from highly diverse oligonucleotide libraries, specific sequences binding to target molecules are identified using an *in vitro* repetitive process called Systematic Evolution of Ligands by Exponential

Enrichment (SELEX)<sup>33,34</sup>. Advantages of aptamers such as facile and reproducible chemical synthesis, straightforward modification, reversible denaturation, small size and stability have expanded their application to bioanalytical applications for the detection of a plethora of targets<sup>35</sup> including small molecules<sup>36</sup>. In fact, there are a few reports in the literature regarding the selection of aptamers binding steroids, such as estradiol<sup>37-39</sup>, progesterone<sup>39, 40</sup>, cortisol<sup>41</sup> and testosterone<sup>39,42</sup>. There is no report though demonstrating the selection of aptamers binding nandrolone. There is only one study in which a previously reported estradiol aptamer was split in two fragments and repurposed for the detection of nandrolone in a sandwich fluorescence resonance energy transfer (FRET) assay<sup>43</sup>. In this work, we describe the first selection designed for the identification of nandrolone aptamers. Using Next Generation Sequencing to analyze the last selection round, aptamer candidates were selected and their binding affinity for nandrolone was verified using different assays. Finally, a homogenous colorimetric assay was developed using gold nanoparticles (AuNPs) with a red-to-blue color change to indicate the presence of nandrolone as a proof-of-concept of an assay suitable for fast screening of suspicious samples.

## 4. 2. Experimental

### 4. 2. 1 Materials

Nandrolone (NAND), trenbolone (TREN), 17 $\beta$ -estradiol (ESTR), 17 $\beta$ -estradiol-6-one 6-(O-carboxymethyloxime) (ESTR-CMO), progesterone (PROG), progesterone-3-(O-carboxymethyl)oxime (PROG-CMO), testosterone (TEST), testosterone-3-(O-carboxymethyl)oxime (TEST-CMO), 11-amino-1-undecanethiol hydrochloride (MUAM), O-(carboxymethyl)hydroxylamine hemihydrochloride and rabbit anti-mouse-HRP conjugate were purchased from Merck (Spain). Nortestosterone Sepharose 6B (10-14  $\mu$ mole/mL, NAND-resin) was obtained from Polysciences (Germany). Epoxy-activated sepharose 6B, 1-ethyl-3-(3-dimethylaminopropyl)carbodiimide hydrochloride (EDC), N-hydroxysuccinimide (NHS), sulfo-NHS-acetate, maleimide-activated microtiter plates, DreamTaq DNA polymerase and lambda exonuclease were from Fisher Scientific (Spain). The DNA purification kits (Oligo Clean & Concentrator kit and DNA Clean & Concentrator kit) were from Zymo Research (supplied by Ecogen, Spain). Monoclonal antibodies to ESTR (clone 9F9), PROG (clone 9F44) and TEST (clone 5E801) were provided from US Biological Life Sciences (acquired through VWR, Spain). Streptavidin-polyHRP80 was purchased from SDT-Reagents (supplied by Bionova, Spain) and TMB Super Sensitive One Component HRP Microwell Substrate from Surmodics (USA). The ssDNA library (5'-TAGGGAAGAGAAGGACATATGAT-N40-TTGACTAGTACATGACCACTTGA-3', 86 nt) was obtained from TriLink Biotechnologies (USA) whereas all other oligonucleotides were synthesized by Biomers.net (Germany). All other reagents were obtained from Fisher Scientific (Spain), Scharlau (Spain) and Sigma (Spain). MilliQ-grade water was used for all experiments.

#### 4. 2. 2 *In vitro* selection

Commercially available nandrolone sepharose 6B resin (NAND-resin) was used for the positive selection. Epoxy-activated sepharose 6B was used to prepare control-resin for the negative selection and counter-selection resins with each of the four counter selection steroids (PROG, ESTR, TEST, TREN) as detailed in the Supplementary Information. For the first round, 300 pmol of the ssDNA library containing a 40 nucleotide-long random region was dissolved in 100  $\mu$ L of selection buffer (10 mM Tris-HCl pH 7.5, 100 mM NaCl, 2 mM MgCl<sub>2</sub>), heated for 5 min at 95 °C and cooled slowly to room temperature. The ssDNA library was then transferred to a microspin column containing 20  $\mu$ L of the NAND-resin to perform the first selection round. For the second and third rounds, the ssDNA pool was first incubated with 20  $\mu$ L of control-resin before incubation with the NAND-resin. Rounds 4 – 7 were performed with sequential incubations with the control-resin, PROG-resin, ESTR-resin, TEST-resin, TREN-resin and finally the NAND-resin. All selection rounds were performed using 30 min incubation steps at room temperature under rotation. For the counter selection steps, 20  $\mu$ L of each resin was used for round 4 whereas 10  $\mu$ L were used for rounds 5 – 7. At the end of each selection round, unbound sequences from each resin were removed by centrifugation for 30 sec at 10,000 rpm followed by washing four times with 400  $\mu$ L of water and four times with 400  $\mu$ L of selection buffer. The resins were resuspended in 50  $\mu$ L of water and stored for further experiments, whereas ssDNA bound on the NAND-resin was used for the preparation of ssDNA for succeeding rounds. This was achieved by the amplification of resin-bound sequences using library-specific forward and phosphorylated reverse primers and a combination of asymmetric PCR with lambda exonuclease digestion. The evolution of the selection was monitored during the selection by PCR to ensure enrichment in sequences binding the target NAND-resin. After PCR amplification of resin-bound sequences and agarose gel electrophoresis, the intensity of the bands was estimated with the ImageJ software using the gel analysis option.

#### 4. 2.3 Next Generation Sequencing (NGS) and identification of aptamer candidates

The ssDNA pool from the last selection round (round 7) was amplified and sequenced by Ion Torrent Next Generation Sequencing (Centre for Omic Sciences, Eurecat Technology Centre, Reus, Spain). The Galaxy web server was used for the analysis of the raw data. The length of the sequences was constrained to library-length (80 – 95 nt) and the filtered sequences were collapsed in order to identify unique sequences. The 100 most abundant sequences were aligned for the identification of sequence families using the Clustal Omega multiple sequence alignment tool (<https://www.ebi.ac.uk/Tools/msa/clustalo/>). Sequence motifs within these sequences were also identified using the MEME tool (<https://meme-suite.org/meme/tools/meme>). The UNAFold webserver was finally used to predict potential secondary structures of the selected aptamer candidates adjusting the conditions to the ones used during selection (100 mM NaCl, 2 mM MgCl<sub>2</sub>, 25°C) and the RNAComposer 3D

modeling server (<http://rnacomposer.cs.put.poznan.pl/>) to build three-dimensional models of aptamers.

#### 4. 2. 4 Apta-PCR affinity assay (APAA)

The binding properties of the aptamer candidates were first evaluated by APAA. To this end, nandrolone was immobilized on magnetic beads (NAND-beads) as described in the Electronic Supplementary Material (ESM). NAND-beads (1.5  $\mu\text{L}$  of 30 mg/mL) were incubated with 50  $\mu\text{L}$  of the desired concentration of each aptamer candidate (10 nM down to 15.6 pM performing serial two-fold dilutions in selection buffer) for 30 min at room temperature under rotation. The beads were thoroughly washed with selection buffer and finally resuspended in 10  $\mu\text{L}$  of water. The amount of bound aptamer was determined after PCR amplification, agarose gel electrophoresis and analysis of the intensity of the bands using the ImageJ program and the gel analysis option. Duplicate measurements were performed for all samples. The relative band intensities were plotted against the aptamer concentration using the GraphPad software. The “One site - specific binding with Hill slope” model was finally used to construct the binding curves and calculate the affinity dissociation constants ( $K_D$ ).

#### 4. 2. 5 Bead-Enzyme Linked Aptamer Assay (bead-ELAA)

NAND-beads (1.5  $\mu\text{L}$  of 30 mg/mL) were incubated with 50  $\mu\text{L}$  of each biotinylated aptamer candidate (100 nM down to 6.4 pM performing serial five-fold dilutions in selection buffer) for 15 min at room temperature under rotation. For the motif sequence, a range of concentrations from 400 nM to 1.6 nM were prepared with serial two-fold dilutions. The beads were washed with PBS containing 0.05 % Tween-20 (PBST), resuspended in 50  $\mu\text{L}$  of 0.05  $\mu\text{g}/\text{mL}$  streptavidin-polyHRP in PBST and incubated for 15 min. Finally, the beads were thoroughly washed with PBST and resuspended in 50  $\mu\text{L}$  of TMB substrate solution. Color development was terminated by the addition of 50  $\mu\text{L}$  of 1 M  $\text{H}_2\text{SO}_4$  and absorbance was read at 450 nm. The  $K_D$  values were calculated as described above in the “APAA” section, by plotting the absorbance at 450 nm against aptamer concentration. Duplicate samples were analyzed for each concentration. To evaluate the specificity of the aptamers, 2  $\mu\text{L}$  of each bead type (NAND-beads, TEST-beads, TREN-beads, PROG-beads, ESTR-beads or control-beads, prepared as detailed in the ESM) were incubated with 50  $\mu\text{L}$  of 0.5 nM of Nand1 or Nand2 aptamer, 1 nM of Nand3 aptamer or 100 nM of the motif sequence in binding buffer for 30 min at room temperature under rotation. Detection of bound aptamers was performed as described above.

#### 4. 2. 6 Enzyme Linked Aptamer Assay (ELAA)

For this assay, nandrolone was immobilized on microtiter plates as detailed in the ESM employing maleimide activated microplates and MUAM crosslinker. Solutions with different concentrations of the biotinylated aptamers (50  $\mu\text{L}$  of 20 nM down to 10 pM, two-fold serial

dilutions in selection buffer) were added to the wells and incubated for 15 min at room temperature under mild agitation and then washed with PBST. Then, 50  $\mu\text{L}$  of 0.05  $\mu\text{g}/\text{mL}$  streptavidin-polyHRP in PBST were added for another 15-min incubation. The wells were finally washed with PBST and 50  $\mu\text{L}$  of TMB solution were added, followed by the addition of 50  $\mu\text{L}$  of 1 M  $\text{H}_2\text{SO}_4$  after approximately 5 min to stop color development. Absorbance was read at 450 nm and the  $K_D$  values were determined as described above.

#### 4. 2. 7 Gold nanoparticles (AuNPs)-aptamer assay for NAND detection

AuNPs (diameter of  $\sim 16$  nm) were synthesized with the sodium citrate reduction method as previously described [44]. AuNPs (50  $\mu\text{L}$  of OD 2) were incubated with the aptamer (15  $\mu\text{L}$ ) for 30 min under rotation at room temperature. Then, 10  $\mu\text{L}$  of solutions containing different concentrations of NAND were added and the mixtures were incubated further for 15 min. Finally, 25  $\mu\text{L}$  of NaCl were added and after 1 min, the spectra of the samples were acquired in the range of 350 – 750 nm. The concentrations of the aptamer and NaCl in the final 100  $\mu\text{L}$  mixtures were initially optimized in the absence of NAND, using the aptamer at 0 – 300 nM and NaCl at 0 – 200 mM. A narrower range of concentrations of the aptamer (100 – 200 nM) and NaCl (50 – 150 mM) was then studied in the absence and presence of NAND (200  $\mu\text{M}$ ). Optimized conditions were finally used for the construction of a calibration curve using NAND in the range of 0.2 – 200  $\mu\text{M}$ . The absorbance ratio of aggregated/dispersed AuNPs was plotted against the logarithm of NAND concentration using the GraphPad Prism software and a four-parameter sigmoidal model was used to fit the data. The limit of detection (LOD), defined as the bottom of the fitted curve plus three times its standard deviation (bottom +  $3 \times \text{SD}_{\text{bottom}}$ ), was finally calculated after interpolation from the calibration curve.

### 4. 3. Results and Discussion

#### 4. 3. 1 Selection process

The selection of nandrolone aptamers was based on the use of nandrolone-sepharose affinity resin (NAND-resin) and a highly diverse ssDNA library with a 40 nucleotide-long random region. The selection was completed in seven rounds and a summary of the conditions used can be seen in Figure 4. 1A. Commercially available NAND-resin was employed for the positive selections, whereas control sepharose resin was used for the negative selections as well as for the preparation of counter selection resins with each of the four counter-SELEX molecules, progesterone (PROG), estradiol (ESTR), testosterone (TEST) and trenbolone (TREN). The structures of the target nandrolone and the other steroids used in the selection can be seen in Figure S4.1 of the ESM. The immobilization of these steroids on sepharose resin is described in the ESM (Figure S4.2). For the first round, the ssDNA library was incubated with the NAND-resin (Figure S4.1B) and bound sequences were amplified and used for the preparation of ssDNA for the next round. For the second round, the ssDNA pool prepared from the first round was first incubated with the control-resin to remove any

sequences binding non-specifically to the matrix (sepharose resin). Unbound ssDNA was recovered and incubated with the NAND-resin for the positive selection. The amount of target-bound sequences during the second round decreased compared to the first one as a consequence of the negative selection which effectively removed part of the ssDNA pool interacting non-specifically with the control-resin (Figure 4.1B). After completion of the third round, which was performed in the same way as the second one, the ssDNA pool appeared to be enriched in NAND-resin-binding sequences with insignificant binding to the control-resin. Counter selection molecules were thus introduced in the following selection round 3. After a negative selection step, sequential incubations with the PROG-resin, ESTR-resin, TEST-resin and TREN-resin were performed for counter-SELEX followed by the positive selection with the NAND-resin. This procedure was followed for rounds 4 – 7, with the only difference being the use of less resin per counter selection molecule in rounds 5 – 7 compared to round 4 (Figure 4.1A). By the final round 7, PCR amplification of bound sequences to each resin type followed by agarose gel electrophoresis showed the specific binding of the enriched ssDNA pool to the NAND-resin and no binding to the other steroid-resins (Figure 4.1C).

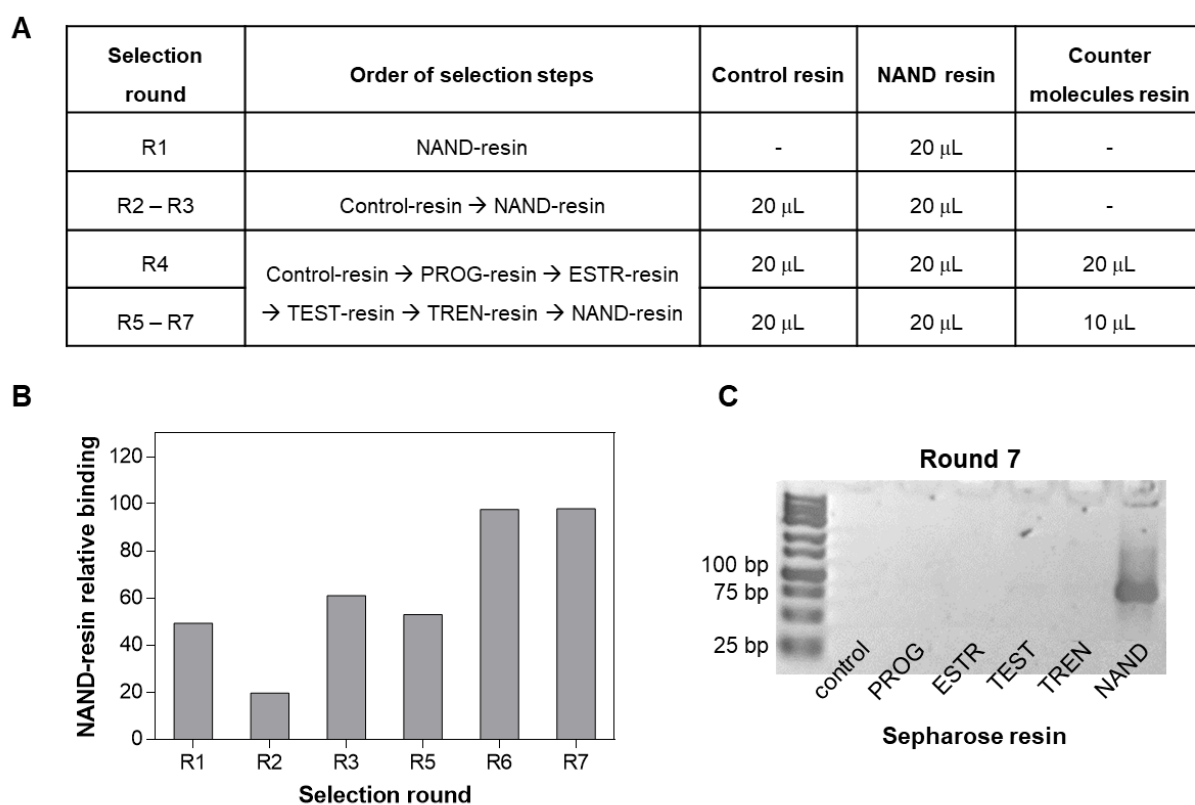


**Figure 4.1.** Selection strategy and evolution of the process. (A) Conditions used for SELEX. (B) Evolution of the selection. (C) Specificity of the last selection round.

#### 4. 3. 2 NGS and identification of aptamer candidates

The last selection round was analyzed by Ion Torrent Next Generation Sequencing to identify aptamer candidates. The raw data was imported in the Galaxy webserver and the length of

sequences was constrained to library length (80 – 95 nt) to remove artefacts resulting from PCR amplification and sequencing. Unique sequences were then identified after collapsing the filtered dataset. Out of the 117225 total reads, 54.5 % were sequences with library length and approximately half of those (51.5 %) were unique (Figure 4.2A). The ranking and copy number of the 100 most abundant unique sequences, corresponding to 16.3 % of the total unique sequences (Figure 4.2B), can be found in Table S1. The next step was to perform multiple sequence alignment of these 100 sequences using Clustal Omega as well as analyze them with MEME for sequence motif discovery. No sequence families were identified as it can be seen in Figure S4.3. Interestingly, a short sequence motif of 11 nt was identified in 52 of the 100 most abundant unique sequences (Figure S4.3 and S4.4). It was also found in 50 % of the 500 most over-represented sequences (data not shown). The first three most abundant sequences were denoted as Nand1, Nand2 and Nand3 and they constituted 5.9, 4.1 and 3.9 %, respectively of the top 100 most over-represented sequences dataset (Figure 4.2B). These sequences together with the sequence motif were finally chosen for further characterization and their sequences can be found in Table S4.2.

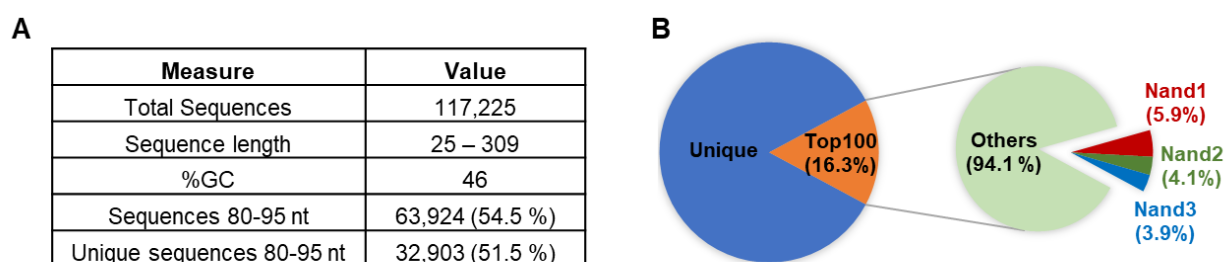


**Figure 4.2.** NGS analysis of round 7 from the nandrolone selection. (A) General statistics. (B) Composition of the top 100 most abundant unique sequences.

#### 4. 3. 3 Affinity and specificity of the aptamers

Once the aptamer candidates were identified, different assays were performed to evaluate their binding properties. APAA, bead-ELAA and ELAA were employed, based on the use of magnetic beads and maleimide-activated microtiter plates to immobilize nandrolone. We have previously reported the use of these three assays for the characterization of aptamers binding to small molecules like steroids [39, 42, 45] and biogenic amines [46]. They are easy to perform in any laboratory as opposed to more sophisticated methods like MicroScale Thermophoresis (MST) and isothermal titration calorimetry (ITC) which require special equipment and trained personnel. For APAA and bead-ELAA, a carboxyl-derivative of nandrolone (NAND-CMO) was directly conjugated to magnetic beads. The beads were modified with amine groups through a short hydrophilic linker and cross-linking was achieved using classic carbodiimide chemistry via EDC/NHS. On the other hand, an 11 carbon-long crosslinker (MUAM) was used as a spacer to facilitate the immobilization of NAND-CMO on maleimide-activated microtiter plates and perform the ELAA. For APAA, unmodified aptamers were used whereas biotinylated aptamers (with a biotin added to the 5' end of the aptamers)

were required for bead-ELAA and ELAA. The binding curves of the aptamers obtained from each of the assays are shown in Figure 4.3A-C and the affinity dissociation constants ( $K_D$ s) in Figure 4.3D. All three assays verified the high binding affinity of the three full length aptamers (Nand1, Nand2 and Nand3) with  $K_D$ s in the low (sub)nanomolar range. The use of different surfaces for NAND immobilization, the length of the spacer used to spatially separate NAND from the surface, or the modification of the aptamers did not appear to affect their binding properties.

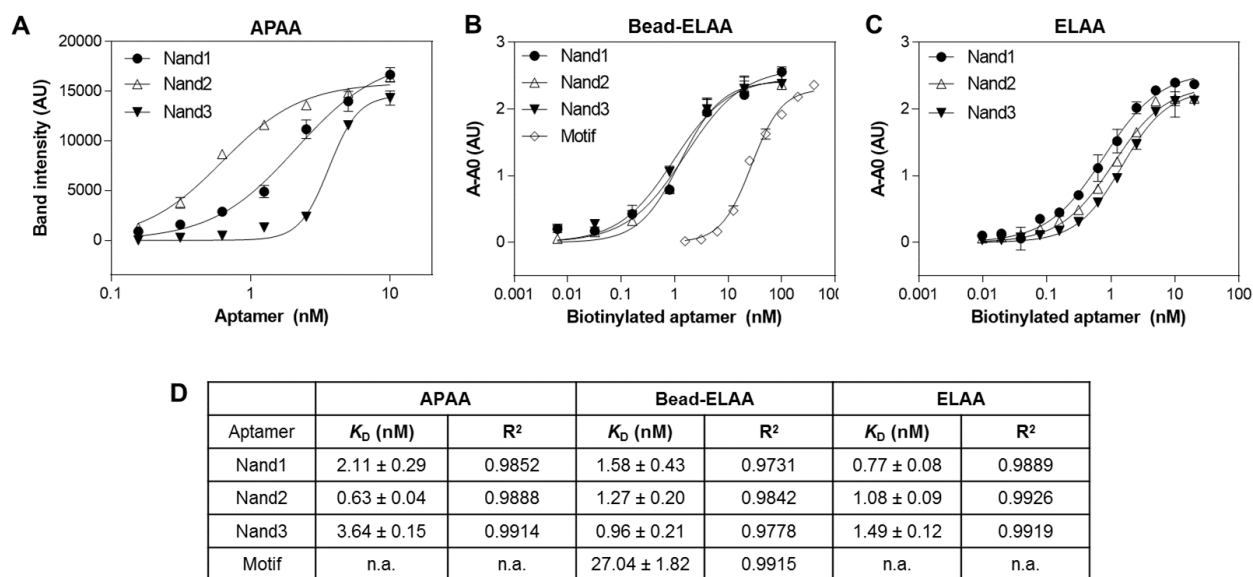


**Figure 4.3.** Evaluation of the affinity of the aptamer candidates for nandrolone. Binding curves obtained by (A) APAA, (B) bead-ELAA and (C) ELAA. (D) Affinity dissociation constants.

The motif, which is present in the sequences of the Nand2 and Nand3 candidates but not in Nand1, was analyzed next (Figure S4.5). A DNA-based spacer (T15) was introduced at the 5'-end of this 11-mer motif sequence to provide more structural flexibility and prevent any potential interference of the biotin added to facilitated detection on NAND-motif complex formation. A  $K_D$  of 27 nM was calculated for the motif by bead-ELAA (Figure 4.3B and 4.3D). As mentioned earlier, this sequence was found in 52 % of the top 100 and in half of the top 500 sequences from the last selection round, indicating that the selection process resulted in the enrichment of this sequence as a NAND binding motif. Considering the small size of the steroids, a binding pocket formed in a three-dimensional structure of the motif predicted using the RNAComposer webserver could potentially accommodate NAND binding (Figure S4.6).

The specificity of the aptamers was finally studied by bead-ELAA. This assay is very easy to perform and is quite useful in evaluating the binding properties of aptamers. It must be commented though that variations in the immobilization level of each steroid on the magnetic beads could potentially affect the accuracy of the assay when evaluating aptamer specificity. Naturally occurring steroids like testosterone, progesterone and estradiol, as well as the synthetic anabolic steroid trenbolone were immobilized on magnetic beads and bound aptamers were detected via the biotin modification introduced at the 5' end of the aptamers

as detailed earlier. As shown in Figure 4.4, the three full-length aptamers as well as the motif showed preferential binding to both NAND and TEST, while lower binding was observed to the other steroids. Certain level of cross-reactivity of the aptamers with other steroids is reasonable considering the extremely high structural similarities these molecules exhibit (Figure S4.1). Regardless, taking into account that PROG and ESTR are encountered in low (sub)nanomolar concentrations in biological samples, their presence is not expected to affect the analysis of doping-related samples.

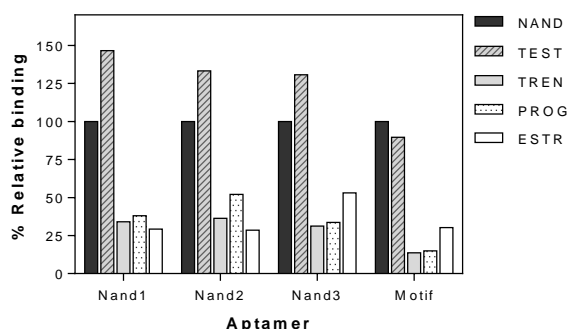


**Figure 4.4** Specificity of the aptamers using bead-ELAA.

#### 4. 3. 4 AuNP-aptamer assay for NAND detection

A label-free colorimetric assay employing the Nand3 aptamer and gold nanoparticles (AuNPs) was finally designed for the detection of NAND and its principle is demonstrated in Fig. 5A. The negatively charged ssDNA (unmodified) aptamer is adsorbed on the surface of the AuNPs, resulting in the stabilization of the particles and prevention of aggregation after the addition of NaCl salt and the increase of the ionic strength of the suspension. The AuNPs are thus maintained well-dispersed and exhibit their characteristic red wine color. When the target molecule is added to the suspension though, the folding of the aptamer changes provoking its desorption from the particles and displacement to the solution phase to bind the target. In this case, when salt is added, the AuNPs aggregate since their surface is no longer protected by the aptamer and the color of the suspension changes to purple/blue. This assay has been widely exploited for small molecule detection because of the several advantages it provides; it is facile and rapid, provides a clear visual result with a red-to-purple/blue color change to indicate target presence, does not require any labels to generate signal, the aptamer is used unmodified (thus maintaining its binding properties) and as a homogenous assay performed in a single tube does not require any separation/washing steps<sup>44, 47, 48</sup>. There are already a few studies in the literature using this assay for steroid detection, such as cortisol<sup>41</sup>, estradiol<sup>49</sup> and progesterone<sup>50</sup>.

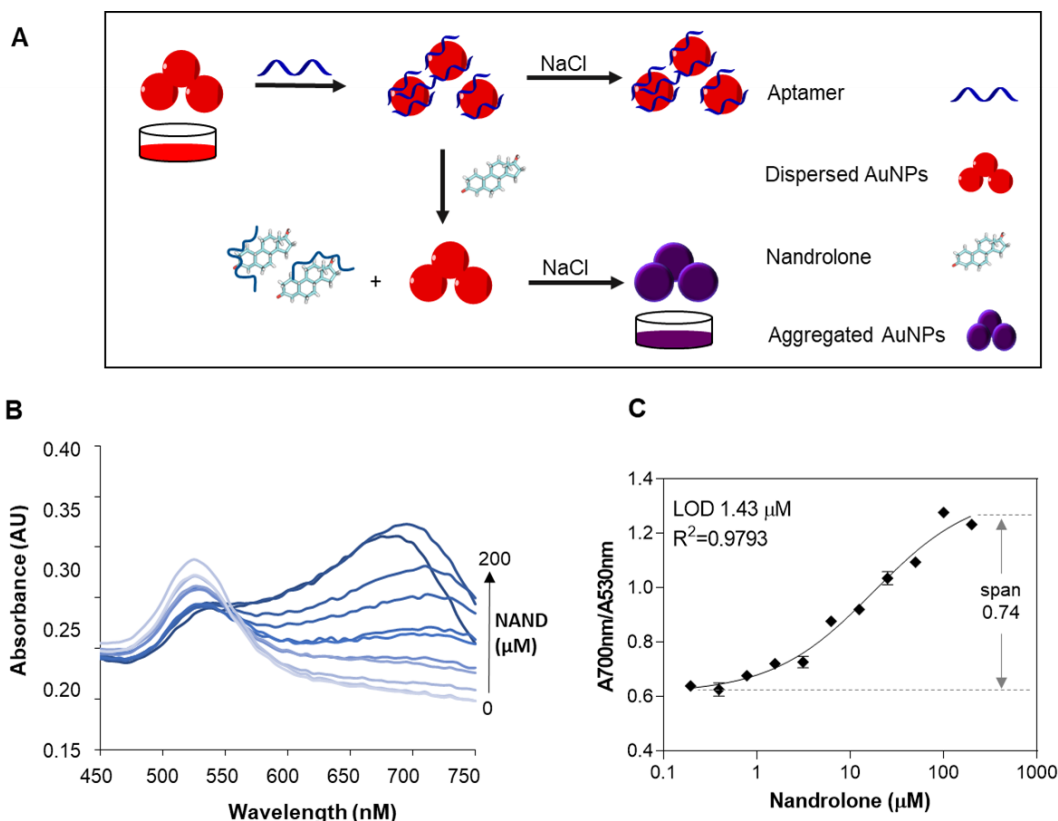


**Figure 4.5.** AuNP-aptamer assay for NAND detection. (A) Principle of the assay. (B) Representative spectra of samples containing different concentrations of NAND. (C) Calibration curve for NAND quantification.

Herein we sought to apply the novel aptamers to NAND detection using this AuNP-based assay. The concentrations of the Nand3 aptamer, which was chosen for assay development, and NaCl were optimized to enhance assay performance. Initially the assay was performed without NAND to evaluate the conditions providing better discrimination of the AuNPs with and without aptamer. These were found to be 100 – 200 nM of Nand3 aptamer and 50 – 150 mM of NaCl (Fig. S7A). These conditions were further explored in the presence of NAND which was better detected after the addition of 75 mM and 100 mM of NaCl (Fig. S7B). The sensitivity of the assay was then evaluated for different combinations of concentrations of aptamer and NaCl. As shown in Table S3, 200 nM of Nand3 aptamer with 100 mM NaCl was the most successful combination resulting in the lowest limit of detection (LOD of 1.1  $\mu\text{M}$ ) and wider span (absorbance ratio of aggregated to dispersed AuNPs), which can improve the analytical sensitivity of the assay. Representative images of samples containing increasing concentrations of NAND showing the red-to-purple/blue color change can be found in Fig. S8. Finally, a range of NAND concentrations (0.2 – 200  $\mu\text{M}$ ) were analyzed with the assay under the optimized conditions. The spectra acquired are shown in Fig. 5B and the calibration curve constructed using the absorbance ratios of aggregated to dispersed AuNPs in Fig. 5C. The LOD of the assay was calculated at 1.4  $\mu\text{M}$  NAND. The relatively low sensitivity of the assay might be attributed to the length of the aptamer (86 nt) limiting its efficient displacement to the solution phase. Truncation of the aptamer to remove non-essential bases could

potentially improve assay performance, a strategy previously demonstrated for a bisphenol A aptamer<sup>51</sup>. In that work, > 250-fold improvement of the LOD was achieved with an equivalent AuNP-based assay when the aptamer length was reduced from 63 nt to 38 nt. Additionally, removing certain parts of the sequence potentially forming secondary structures with low free energy could also improve the assay sensitivity as shown previously for an estradiol aptamer<sup>52</sup>. Truncations were not pursued in this work as this process was not within the scope of the study. The alternative use of the short 11-mer motif sequence for this assay was evaluated. However, it was not considered compatible since high concentrations of the sequence were required to efficiently protect the particles from salt-induced aggregation which are expected to decrease assay sensitivity (data not shown). As mentioned earlier, there is only one study in the literature demonstrating the use of an aptamer for nandrolone detection<sup>43</sup>. Using a split estradiol aptamer modified with a fluorophore and a quencher in each fragment, a FRET assay was developed with an LOD of 5  $\mu\text{M}$ . The sensitivity of the assay developed in this work is in the same low micromolar range as the one previously described. Even though not optimal, the assay can serve as an example of an aptamer-based rapid homogenous assay suitable for on-site monitoring of AAS levels in suspicious samples.

#### 4. 5. Conclusions

Doping refers to the illicit use of prohibited substances with the objective of gaining competitive advantage especially in professional sports. Anabolic androgenic steroids (AAS) are one category of these substances including testosterone and one of its synthetic derivatives called nandrolone. AAS abuse though poses serious health concerns because of the numerous adverse effects they can cause, and international organizations are dedicated to improving global monitoring and prevention strategies to manage the problem. Even though highly sensitive gas chromatographic-mass spectroscopic methods have been established for the specific detection of these substances, they are limited to laboratory use and they cannot be deployed on-site for fast screening of suspicious samples. The numerous advantages of aptamers as alternative biorecognition elements successfully applied for the detection of a plethora of small molecules make them particularly attractive for the development of an assay for AAS detection suitable for on-site analysis. In this work, we report the first selection performed for the identification of nandrolone aptamers assisted by next generation sequencing. Three aptamer candidates and a highly enriched 11-mer sequence motif were chosen for characterization and their specific binding to nandrolone was verified with different assays. Their affinity dissociation constants were calculated in the low (sub)nanomolar range, and all sequences exhibited cross-reactivity with testosterone but not with other potentially interfering steroids. Finally, a facile and rapid colorimetric assay was developed as a proof-of-concept employing one of the full-length aptamers and gold nanoparticles, allowing the detection of 1.4  $\mu\text{M}$  of nandrolone. Considering the high cross-reactivity of the novel nandrolone aptamers with testosterone, the assay could serve as a simple on-site screening tool with the red-to-purple/blue color change to indicate the potential presence of both nandrolone and testosterone in the sample as doping biomarkers.

Nandrolone can only be found in a sample when it is administered exogenously (doping) whereas  $> 0.7 \mu\text{M}$  (200 ng/mL) of testosterone in urine samples are considered suspicious for doping according to WADA regulations. Taking into account that the normal endogenous levels of testosterone are low ( $< 42 \text{ nM}$ ) and are not expected to interfere with the assay, only samples with significantly higher amounts of the two AAS can produce a positive result and suggest doping practices. Further analysis by GC-MS/GS-IRMS can finally confirm the steroid(s) in the sample, their concentration and source. Future work will focus on the improvement of the sensitivity of the assay (e.g. by aptamer truncation and/or splitting) and evaluation of its performance with appropriate real samples.

## Acknowledgments

This work was funded through King Abdulaziz University, under the financing of the collaborative project "Selection and application of aptamers against anabolic steroids".

## 4.6 References

- (1) Evans N.A. (2004). Current concepts in anabolic-androgenic steroids. *The American Journal of Sports Medicine*, <https://doi.org/10.1177/0363546503262202>.
- (2) Kumar P., Kumar N., Thakur D.S., Patidar A. (2010). Male hypogonadism: symptoms and treatment. *Journal of Advanced Pharmaceutical Technology & Research*, <https://doi.org/10.4103/0110-5558.72420>.
- (3) Basaria S., Wahlstrom J.T., Dobs A.S. (2001). Anabolic-androgenic steroid therapy in the treatment of chronic diseases. **The Journal of Clinical Endocrinology & Metabolism**, <https://doi.org/10.1210/jcem.86.11.7983>.
- (4) Hartgens F., Kuipers H. (2004). Effects of androgenic-anabolic steroids in athletes. *Sports Medicine*, <https://doi.org/10.2165/00007256-200434080-00003>.
- (5) Woerdeman J., de Ronde W. (2011). Therapeutic effects of anabolic androgenic steroids on chronic diseases associated with muscle wasting. *Expert Opinion on Investigational Drugs*, <https://doi.org/10.1517/13543784.2011.544651>.
- (6) Hill S.A., Waring W.S. (2019). Pharmacological effects and safety monitoring of anabolic androgenic steroid use: differing perceptions between users and healthcare professionals. *Therapeutic Advances in Drug Safety*, <https://doi.org/10.1177/2042098619855291>.
- (7) Sjöqvist F., Garle M., Rane A. (2008). Use of doping agents, particularly anabolic steroids, in sports and society. *The Lancet*, [https://doi.org/10.1016/S0140-6736\(08\)60801-6](https://doi.org/10.1016/S0140-6736(08)60801-6).
- (8) Sessa F., Salerno M., Di Mizio G., Bertozzi G., Messina G., Tomaiuolo B., Pisanelli D., Maglietta F., Ricci P., Pomara C. (2018). Anabolic androgenic steroids: searching new molecular biomarkers. *Frontiers in Pharmacology*, <https://doi.org/10.3389/fphar.2018.01321>.
- (9) WADA, <https://www.wada-ama.org/en/content/what-is-prohibited>. Accessed 2021/07/26.
- (10) Jiang J., Zhang H., Li G., Wang Z., Wang J., Zhao H. (2011). Preparation of anti-nortestosterone antibodies and development of an indirect heterologous competitive enzyme-linked immunosorbent assay to detect nortestosterone residues in animal urine. *Analytical Letters*, <https://doi.org/10.1080/00032719.2010.551694>.

- (11) Pan M.M., Kovac J.R. (2016). Beyond testosterone cypionate: evidence behind the use of nandrolone in male health and wellness. *Translational Andrology and Urology*, <https://doi.org/10.21037/tau.2016.03.03>.
- (12) Scarth J., Akre C., van Ginkel L., Le Bizec B., De Brabander H., Korth W., Points J., Teale P., Kay J. (2009). Presence and metabolism of endogenous androgenic-anabolic steroid hormones in meat-producing animals: a review. *Food Additives & Contaminants: Part A*, <https://doi.org/10.1080/02652030802627160>.
- (13) Yunin M.A., Metalnikov P.S., Komarov A.A., Panin A.N. (2015). Development of a rapid method for the analysis of trenbolone, nortestosterone, and zeranol in bovine liver using liquid chromatography tandem mass spectrometry. *Analytical and Bioanalytical Chemistry*, <https://doi.org/10.1007/s00216-014-8346-y>.
- (14) Commission of the European Communities, Council Directive 96/22/EC (1996).
- (15) Geyer H., Parr M.K., Koehler K., Mareck U., Schänzer W., Thevis M. (2008). Nutritional supplements cross-contaminated and faked with doping substances. *Journal of Mass Spectrometry*, <https://doi.org/10.1002/jms.1452>.
- (16) Dahmani H., Louati K., Hajri A., Bahri S., Safta F. (2018). Development of an extraction method for anabolic androgenic steroids in dietary supplements and analysis by gas chromatography-mass spectrometry: application for doping-control. *Steroids*, <https://doi.org/10.1016/j.steroids.2018.08.001>.
- (17) Walpurgis K., Thomas A., Geyer H., Mareck U., Thevis M. (2020). Dietary supplement and food contaminations and their Implications for doping controls. *Foods*, <https://doi.org/10.3390/foods9081012>.
- (18) WADA (2021). Technical Document TD2021EAAS. Measurement and Reporting of Endogenous Anabolic Androgenic Steroid (EAAS) Markers of the Urinary Steroid Profile. <https://www.wada-ama.org/en/resources/science-medicine/td2021eaas-0>. Accessed 2021-07-26.
- (19) WADA (2021). Technical Document TD2021IRMS. Detection of Synthetic Forms of Prohibited Substances by GC/C/IRMS. <https://www.wada-ama.org/en/resources/science-medicine/td2021irms-0>. Accessed 2021-07-26.
- (20) Gosetti F., Mazzucco E., Gennaro M.C., Marengo E. (2013). Ultra high performance liquid chromatography tandem mass spectrometry determination and profiling of prohibited steroids in human biological matrices. A review. *Journal of Chromatography B*, <https://doi.org/10.1016/j.jchromb.2012.12.003>.
- (21) Piper T., Schänzer W., Thevis M. (2016). Revisiting the metabolism of 19-nortestosterone using isotope ratio and high resolution/high accuracy mass spectrometry. *Journal of Steroid Biochemistry and Molecular Biology*, <https://doi.org/10.1016/j.jsbmb.2015.12.013>.
- (22) Abushareeda W., Lyris E., Kraiem S., Wahaibi A.A., Alyazidi S., Dbes N., Lommen A., Nielen M., Horvatovich P.L., Alsayrafi M., Georgakopoulos C. (2017). Gas chromatographic quadrupole time-of-flight full scan high resolution mass spectrometric screening of human urine in antidoping analysis. *Journal of Chromatography B*, <https://doi.org/10.1016/j.jchromb.2017.08.019>.
- (23) Alladio E., Amante E., Bozzolino C., Seganti F., Salomone A., Vincenti M., Desharnais B. (2020). Effective validation of chromatographic analytical methods: the illustrative case of androgenic steroids. *Talanta*, <https://doi.org/10.1016/j.talanta.2020.120867>.
- (24) Badoud F., Boccard J., Schweizer C., Pralong F., Saugy M., Baume N. (2013). Profiling of steroid metabolites after transdermal and oral administration of testosterone by ultra-high pressure liquid chromatography coupled to quadrupole time-of-flight mass spectrometry. *Journal of Steroid Biochemistry and Molecular Biology*, <https://doi.org/10.1016/j.jsbmb.2013.05.018>.
- (25) Genangeli M., Caprioli G., Cortese M., Laus F., Petrelli R., Ricciutelli M., Sagratini G., Sartori S., Vittori S. (2019). Simultaneous quantitation of 9 anabolic and natural steroidal hormones in equine urine by UHPLC-MS/MS triple quadrupole. *Journal of Chromatography B*, <https://doi.org/10.1016/j.jchromb.2019.04.002>.

- (26) Dolowy M., Pyka-Pajak A., Jampílek J. (2019). Simple and accurate HPTLC-densitometric method for assay of nandrolone decanoate in pharmaceutical formulation. *Molecules*, <https://doi.org/10.3390/molecules24030435>.
- (27) de Moura Ribeiro M.V., Boralle N., Felipe L.G., Pezza H.R., Pezza L. (2018). <sup>1</sup>H NMR determination of adulteration of anabolic steroids in seized drugs. *Steroids*, <https://doi.org/10.1016/j.steroids.2018.07.002>.
- (28) Hungerford N.L., Sortais B., Smart C.G., McKinney A.R., Ridley D.D., Stenhouse A.M., Suann C.J., Munn K.J., Sillence M.N., McLeod M.D. (2005). Analysis of anabolic steroids in the horse: development of a generic ELISA for the screening of 17 $\alpha$ -alkyl anabolic steroid metabolites. *Journal of Steroid Biochemistry and Molecular Biology*, <https://doi.org/10.1016/j.jsbmb.2005.03.007>.
- (29) Tort N., Salvador J.P., Marco M.P. (2012). Multiplexed immunoassay to detect anabolic androgenic steroids in human serum. *Analytical and Bioanalytical Chemistry*, <https://doi.org/10.1007/s00216-012-5904-z>.
- (30) Holubova B., Goselova S., Sevcikova L., Vlach M., Blazkova M., Lapcik O., Fukal L. (2013). Rapid immunoassays for detection of anabolic nortestosterone in dietary supplements. *Czech Journal of Food Sciences*, <https://doi.org/10.17221/507/2012-CJFS>.
- (31) Peng C.F., Liu C.L., Song S.S., Liu L.Q. (2014). Highly sensitive nano-ELISA for detecting 19-nortestosterone in beef. *Food and Agricultural Immunology*, <https://doi.org/10.1080/09540105.2013.821599>.
- (32) Jurasek M., Goselova S., Miksatkova P., Holubova B., Vysatova E., Kuchar M., Fukal L., Lapcik O., Drasar P. (2015). Highly sensitive avidin-biotin ELISA for detection of nandrolone and testosterone in dietary supplements. *Drug Testing and Analysis*, <https://doi.org/10.1002/dta.2005>.
- (33) Tuerk C., Gold L. (1990). Systematic Evolution of Ligands by Exponential Enrichment: RNA ligands to bacteriophage T4 DNA polymerase. *Science*, <https://doi.org/10.1126/science.2200121>.
- (34) Ellington A.D., Szostak J.W. (1990). In vitro selection of RNA molecules that bind specific ligands. *Nature*, <https://doi.org/10.1038/346818a0>.
- (35) Toh S.Y., Citartan M., Gopinath S.C.B., Tang T.H. (2015). Aptamers as a replacement for antibodies in enzyme-linked immunosorbent assay. *Biosensors and Bioelectronics*, <http://doi.org/10.1016/j.bios.2014.09.026>.
- (36) Ruscito A., DeRosa M.C. (2016). Small-molecule binding aptamers: selection strategies, characterization, and applications. *Frontiers in Chemistry*, <https://doi.org/10.3389/fchem.2016.00014>.
- (37) Kim Y.S., Jung H.S., Matsuura T., Lee H.Y., Kawai T., Gu M.B. (2007). Electrochemical detection of 17 $\beta$ -estradiol using DNA aptamer immobilized gold electrode chip. *Biosensors and Bioelectronics*, <https://doi.org/10.1016/j.bios.2006.10.004>.
- (38) Alsager O.A., Kumar S., Willmott G.R., McNatty K.P., Hodgkiss J.M. (2014). Small molecule detection in solution via the size contraction response of aptamer functionalized nanoparticles. *Biosensors and Bioelectronics*, <https://doi.org/10.1016/j.bios.2014.02.004>.
- (39) Jauset-Rubio M., Botero M.L., Skouridou V., Aktas G.B., Svobodova M., Bashammakh A.S., El-Shahawi M.S., Alyoubi A.O., O'Sullivan C.K. (2019). One-Pot SELEX: identification of specific aptamers against diverse steroid targets in one selection. *ACS Omega*, <https://doi.org/10.1021/acsomega.9b02412>.
- (40) Contreras-Jiménez G., Eissa S., Ng A., Alhadrami H., Zourob M., Siaj M. (2015). Aptamer-based label-free impedimetric biosensor for detection of progesterone. *Analytical Chemistry*, <https://doi.org/10.1021/ac503639s>.
- (41) Martin J.A., Chavez J.L., Chushak Y., Chapleau R.R., Hagen J., Kelley-Loughnane N. (2014). Tunable stringency aptamer selection and gold nanoparticle assay for detection of cortisol. *Analytical and Bioanalytical Chemistry*, <https://doi.org/10.1007/s00216-014-7883-8>.

- (42) Skouridou V., Jauset-Rubio M., Ballester P., Bashammakh A.S., El-Shahawi M.S., Alyoubi A.O., O'Sullivan C.K. (2017). Selection and characterization of DNA aptamers against the steroid testosterone. *Microchimica Acta*, <https://doi.org/10.1007/s00604-017-2136-0>.
- (43) Bai W., Zhu C., Liu J., Yan M., Yang S., Chen A. (2016). Split aptamer-based sandwich fluorescence resonance energy transfer assay for 19-nortestosterone. *Microchimica Acta*, <https://doi.org/10.1007/s00604-016-1905-5>.
- (44) Mairal Lerga, T.; Skouridou, V.; Bermudo, M. C.; Bashammakh, A. S.; El-Shahawi, M. S.; Alyoubi, A. O.; O'Sullivan, C. K. Gold nanoparticle aptamer assay for the determination of histamine in foodstuffs. *Microchim. Acta* **2020**, *187*, 452.
- (45) Svobodova M., Skouridou V., Botero M.L., Jauset-Rubio M., Schubert T., Bashammakh A.S., El-Shahawi M.S., Alyoubi A.O., O'Sullivan C.K. (2017). The characterization and validation of 17 $\beta$ -estradiol binding aptamers. *Journal of Steroid Biochemistry and Molecular Biology*, <https://doi.org/10.1016/j.jsbmb.2016.09.018>.
- (46) Mairal Lerga T., Jauset-Rubio M., Skouridou V., Bashammakh A.S., El-Shahawi M.S., Alyoubi A.O., O'Sullivan C.K. (2019). High affinity aptamer for the detection of the biogenic amine histamine. *Analytical Chemistry*, <https://doi.org/10.1021/acs.analchem.9b00075>.
- (47) Miron-Merida V.A., Gonzalez-Espinosa Y., Collado-Gonzalez M., Gong Y.Y., Guo Y., Goycoolea F.M. (2021). Aptamer-target-gold nanoparticle conjugates for the quantification of fumonisin B1. *Biosensors*, <https://doi.org/10.3390/bios11010018>.
- (48) Zahra Q.u.A., Luo Z., Ali R., Khan M.I., Li F., Qiu B. (2021). Advances in gold nanoparticles-based colorimetric aptasensors for the detection of antibiotics: an overview of the past decade. *Nanomaterials*, <https://doi.org/10.3390/nano11040840>.
- (49) Liu J., Bai W., Niu S., Zhu C., Yang S., Cheng A. (2014). Highly sensitive colorimetric detection of 17 $\beta$ -estradiol using split DNA aptamers immobilized on unmodified gold nanoparticles. *Scientific Reports*, <https://doi.org/10.1038/srep07571>.
- (50) Du G., Zhang D., Xia B., Xu L., Wu S., Zhan S., Ni X., Zhou X., Wang L. (2016). A label-free colorimetric progesterone aptasensor based on the aggregation of gold nanoparticles. *Microchimica Acta*, <https://doi.org/10.1007/s00604-016-1861-0>.
- (51) Jia M., Sha J., Li Z., Wang W., Zhang H. (2020). High affinity truncated aptamers for ultra-sensitive colorimetric detection of bisphenol A with label-free aptasensor. *Food Chemistry*, <https://doi.org/10.1016/j.foodchem.2020.126459>.
- (52) Chang C.C., Yeh C.Y. (2021). Using simple-structured split aptamer for gold nanoparticle-based colorimetric detection of estradiol. *Analytical Sciences*, <https://doi.org/10.2116/analsci.20SCP07>.

## 4.6 Supplementary information

### 4.6.1. Materials and methods

#### 4.6.1.1 Structures of the molecules

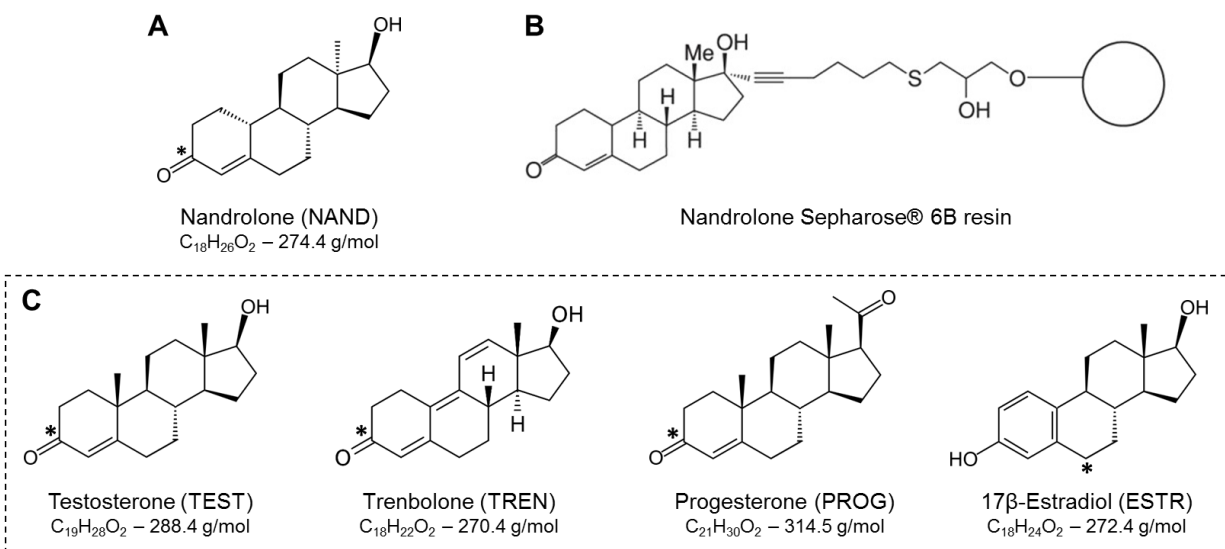


**Figure S4.1.** Structures of the steroids used in this work. (A) The target steroid nandrolone. (B) Nandrolone-sepharose® 6B resin used for SELEX. (C) Other steroids used for counter-SELEX. The asterisks (\*) denote the carbon atoms on the steroid structures carrying the carboxymethyloxime (CMO) modification facilitating steroid immobilization on amine-modified magnetic beads.

#### 4.6.1.2 Preparation of carboxymethyloxime (CMO) derivatives of steroids

Carboxymethyloxime derivatives of nandrolone (NAND) and trenbolone (TREN) were prepared according to a previous report <sup>1</sup>. Briefly, each steroid (100 mg) and O-(carboxymethyl) hydroxylamine hemihydrochloride (113 mg) were dissolved in 10.2 mL of anhydrous pyridine under argon atmosphere and the mixtures were heated at 50°C for two days. Pyridine was then removed under vacuum and the crude solids were dissolved in a mixture of ethyl acetate and water (20 mL each). Following, HCl (10 %) was added until pH 1 was achieved yielding two phases. The lower ethyl acetate layers were separated and washed two times with water (20 mL per wash) and then dried over sodium sulfate. Finally, they were filtered and concentrated under vacuum yielding light yellow solids.

#### 4.6.1.3 Preparation of sepharose media for negative and counter selection steps

Epoxy-activated sepharose 6B resin (~ 143 mg) was transferred in a micro-spin column and washed three times with water (1 mL per wash) by resuspending the resin in the appropriate volume followed by centrifugation for 30 sec at 10,000 rpm. Next, the resin was resuspended in 30  $\mu$ L of 25 mg/mL of each steroid solution [progesterone (PROG), estradiol (ESTR), testosterone (TEST) or trenbolone (TREN), prepared in DMSO] and 470  $\mu$ L of PBS for the preparation of the counter-selection media or in plain coupling buffer for the negative selection resin (control-resin). The resins were incubated overnight at room temperature under rotation, followed by washing and blocking of any remaining active groups with 1 mM of sulfo-NHS-acetate in PBS for 2 h at room temperature under rotation. Finally, the resins were washed with water and resuspended in 2 mL of water. The immobilization of the steroids on the resins was confirmed by bead-ELISA. Specifically, 50  $\mu$ L of each steroid-sepharose resin were incubated with 50  $\mu$ L of 5  $\mu$ g/mL of the respective steroid antibody in PBS for 30 min at room temperature under rotation. The TEST antibody was used to detect both TEST and TREN. The resins were washed three times with 200  $\mu$ L of water, resuspended in 50  $\mu$ L of rabbit anti-mouse-HRP antibody conjugate (~ 3  $\mu$ g/mL) in PBST followed by a 30-minute incubation at room temperature under rotation. Finally, the resins were washed and resuspended in 50  $\mu$ L of TMB solution. After 2 minutes, color development was stopped by the addition of 50  $\mu$ L of 1 M H<sub>2</sub>SO<sub>4</sub> and absorbance of the supernatants was read at 450 nm. The results are shown in Figure S4.2.

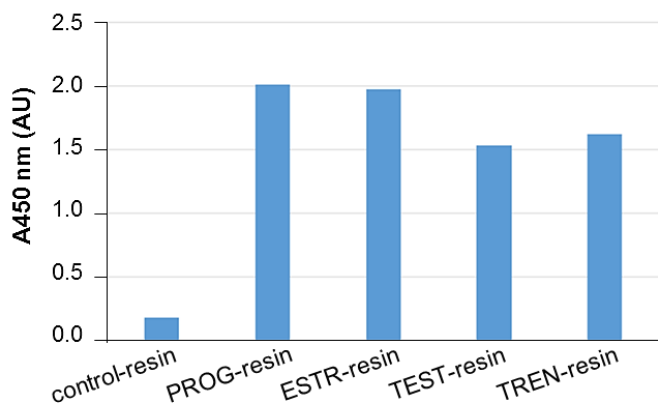


**Figure S4.2.** Confirmation of the immobilization of various steroids on sepharose resin.

#### 4.6.1.4 Preparation of steroid-magnetic beads

Immobilization of steroids on magnetic beads was performed as previously described [2]. Amine-activated magnetic beads (200  $\mu$ L of Dynabeads M-270 Amine, 30 mg/mL) were washed with 100 mM MES pH 5.3 and then resuspended in 40  $\mu$ L of 25 mg/mL NAND-CMO, TEST-CMO, TREN-CMO, PROG-CMO or ESTR-CMO (in DMSO), 40  $\mu$ L of 10 mg/mL EDC, 40  $\mu$ L of 75 mg/mL NHS, 80  $\mu$ L of 100 mM MES pH 5.3 and 10  $\mu$ L of ethanol. The suspensions were incubated overnight at room temperature under rotation. The beads were then washed with PBS and blocked with 5 % skim milk in PBST for 1 h at room temperature under rotation. Finally, the beads were blocked with 1 mM sulfo-NHS-acetate in PBS for 1 h, washed with PBST and resuspended in 200  $\mu$ L of PBS. The control-beads were prepared in the same manner by using only DMSO instead of the steroid. The modified magnetic beads were kept at 4°C until use. The immobilization of the steroids on the magnetic beads was verified by bead-ELISA as detailed above for the sepharose resins. The ESTR antibody was used for the detection of ESTR and NAND, the TEST antibody for TEST and TREN and the PROG antibody for PROG.

#### 4.6.1.5 Immobilization of nandrolone on microtiter plates for binding studies

The preparation of nandrolone-functionalized microtiter plates was based on a previous report [3]. Maleimide-activated microtiter plate strips were washed with PBS and then incubated with 50  $\mu$ L of 100  $\mu$ M of 11-amino-1-undecanethiol hydrochloride (MUAM, in PBS) overnight at 4°C. The plates were washed with PBS and 50  $\mu$ L of a mixture of NDR-CMO (300  $\mu$ M, in PBS), EDC (4 mM, equivalent to 0.62 mg/mL) and NHS (1 mM, equivalent to 0.115 mg/mL) was added to the wells and let to incubate for 3 h at room temperature. After washing, any remaining active groups were blocked with 50  $\mu$ L of sulfo-NHS-acetate (1 mM in PBS) for 1 h. The plates were finally washed with PBS and kept dry at 4°C until use.

## 4.6. 2. Next Generation Sequencing for aptamer identification

**Table S4.1** Abundance (%) of the 100 most over-represented unique sequences.

Sequence	%	Sequence	%	Sequence	%	Sequence	%
1	5,94	26	1,08	51	0,73	76	0,58
2	4,07	27	1,05	52	0,71	77	0,58
3	3,86	28	1,05	53	0,71	78	0,54

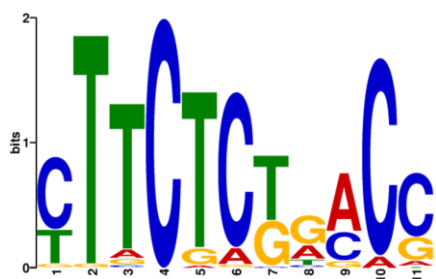
4	2,56	29	1,01	54	0,71	79	0,54
5	2,11	30	0,99	55	0,69	80	0,52
6	2,04	31	0,97	56	0,69	81	0,52
7	1,96	32	0,97	57	0,69	82	0,50
8	1,89	33	0,95	58	0,69	83	0,50
9	1,87	34	0,93	59	0,67	84	0,50
10	1,87	35	0,91	60	0,67	85	0,50
11	1,85	36	0,91	61	0,65	86	0,50
12	1,76	37	0,91	62	0,63	87	0,50
13	1,66	38	0,91	63	0,63	88	0,49
14	1,51	39	0,90	64	0,63	89	0,49
15	1,49	40	0,90	65	0,63	90	0,49
16	1,46	41	0,86	66	0,63	91	0,49
17	1,34	42	0,86	67	0,63	92	0,47
18	1,31	43	0,82	68	0,63	93	0,47
19	1,31	44	0,82	69	0,62	94	0,47
20	1,31	45	0,80	70	0,60	95	0,47
21	1,19	46	0,78	71	0,60	96	0,45
22	1,19	47	0,77	72	0,60	97	0,45
23	1,18	48	0,77	73	0,60	98	0,45
24	1,16	49	0,75	74	0,60	99	0,45
25	1,10	50	0,75	75	0,58	100	0,45

**Figure S4.3.** Multiple sequence alignment of the 100 most abundant unique sequences of library-length (80 – 95 bp) using Clustal Omega <sup>4</sup>. The first number denotes the ranking of the sequence and the second one the number of copies. The common sequence motif is underlined.

14-81 TAGGGAAGAGAAGGACATATGATGTACTGAGCGACCGTTTGGGCATGGTGTAAACCGTGCTAGTTTGACTAGTACATGACCACTTGA  
56-37 TAGGGAAGAGAAGGACATATGATGTACTTCCCTGACCTGAGGTTCATATCGCGAAGCGATGTACGTTGACTAGTACATGACCACTTGA  
68-34 TAGGGAAGAGAAGGACATATGATGTACCCTCTTACACCCCTGGCATGCGGAAGCGTACTGTCTTGACTAGTACATGACCACTTGA  
88-26 TAGGGAAGAGAAGGACATATGATGGACTACTATGACCGTGCCAACGTGGTGGGAGCCAGGTATTGACTAGTACATGACCACTTGA  
35-49 TAGGGAAGAGAAGGACATATGATCGGATATGTGCACAGGATGGTGCCTTCACTGACCGGGTCTTGACTAGTACATGACCACTTGA  
69-33 TAGGGAAGAGAAGGACATATGATGAGCCACATATGCTGAAAGCGTTCGCTTCGATGACCGGGTCTTGACTAGTACATGACCACTTGA  
93-25 TAGGGAAGAGAAGGACATATGATCGTCCAACGTCTTAAGTTTTCGCTGACCGAGATGGGGTCTTGACTAGTACATGACCACTTGA  
64-34 TAGGGAAGAGAAGGACATATGATGTCGCCATGTGTTCCACGGCCTGCTCTGACCACGAGGGAATTGACTAGTACATGACCACTTGA  
50-40 TAGGGAAGAGAAGGACATATGATGAACAGAACATGTGCGAAGCCTGATCGACCGAATGCGTCTTGACTAGTACATGACCACTTGA  
71-32 TAGGGAAGAGAAGGACATATGATGGCCGCTGGTAACTACGCAGCTTCTCGACCGAATGCGGCATTGACTAGTACATGACCACTTGA  
18-70 TAGGGAAGAGAAGGACATATGATATACGTC AATGGGAACCATTTCTTCTCGACCGATCGGTGTCTTGACTAGTACATGACCACTTGA  
45-43 TAGGGAAGAGAAGGACATATGATCCGCTATATGTGCGGAAGCCTTCTCGACCGTGAACGGTCTTGACTAGTACATGACCACTTGA  
58-37 TAGGGAAGAGAAGGACATATGATCAACGAGCATAGGGGCTTGCGTAGCCTCTTCTTAGGGCTTGACTAGTACATGACCACTTGA  
92-25 TAGGGAAGAGAAGGACATATGATCATGTGCAATAAACCATTTGCCTCTGTGACCGTGTGGGATTGACTAGTACATGACCACTTGA  
51-39 TAGGGAAGAGAAGGACATATGATGTCAAGATGAAATAACATCTTCTTCGATGACCGTGTGGAATTGACTAGTACATGACCACTTGA  
99-24 TAGGGAAGAGAAGGACATATGATGTCGTGGCGAATGCTCACCTTCTTTCCGAAATCAGGGAATTGACTAGTACATGACCACTTGA  
77-31 TAGGGAAGAGAAGGACATATGATGTCGTGAGGTACTCACTTCTCACGTACGTTTCCCTCTTGAATTGACTAGTACATGACCACTTGA  
34-50 TAGGGAAGAGAAGGACATATGATAATCATGGATCGCACTCCGCGCTAGCGTTCGCGTTCCCGTTGGCATTGACTAGTACATGACCACTTGA  
54-38 TAGGGAAGAGAAGGACATATGATCAGTGTGGCCAGACGTCGCTTCTCGACCGTGGGGTTTGACTAGTACATGACCACTTGA  
62-34 TAGGGAAGAGAAGGACATATGATGTGGCCGAGGTGTGTAGCCCTTCTTCTCGACCGATGTGGCTTGACTAGTACATGACCACTTGA  
97-24 TAGGGAAGAGAAGGACATATGATGTACTTGGGAAGCCTCTGACCAAGCCGGTGGCATACTTCTTGACTAGTACATGACCACTTGA  
60-36 TAGGGAAGAGAAGGACATATGATGTATGGCCACATCGTAAGTATGTTCTCTGACCACTGTCATTGACTAGTACATGACCACTTGA  
12-94 TAGGGAAGAGAAGGACATATGATGACCTTGAAGCTGTTCCAGCTTCTTCCAGGTGGTATGTTGACTAGTACATGACCACTTGA  
63-34 TAGGGAAGAGAAGGACATATGATGGCCTTCCGATGTCATAGCGCTTCCCGTCTCAATGGTTTTGACTAGTACATGACCACTTGA  
24-62 TAGGGAAGAGAAGGACATATGATCCCTTCTGCGATGGATTGCGCTTCCCTCGTGGCCCATGCATTGACTAGTACATGACCACTTGA  
55-37 TAGGGAAGAGAAGGACATATGATAATGTCTCGTAGTTGACGACTTCTCTTGGCGACCGCCCT-TGACTAGTACATGACCACTTGA  
6-109 TAGGGAAGAGAAGGACATATGATAATGTCTCGTAGTTGACGACTTCTCTTGGCGACCGCCCTTGACTAGTACATGACCACTTGA  
8-101 TAGGGAAGAGAAGGACATATGATAATGTCTCGTAGTTGACGACTTCTCTTGGCGACCGCCCTTGACTAGTACATGACCACTTGA  
70-32 TAGGGAAGAGAAGGACATATGATGGTACTTCTGCGATTTCTCGAATCTGCCTTCCCGTGTGGGTTGACTAGTACATGACCACTTGA  
49-40 TAGGGAAGAGAAGGACATATGATACATGTCCCGCGAGCGTCTCTGACCGGTCGCTAGTTGACTAGTACATGACCACTTGA  
47-41 TAGGGAAGAGAAGGACATATGATAATACGTGCGGATCGCGAATCCCTGAACGACCGATGGGCTTGACTAGTACATGACCACTTGA  
5-113 TAGGGAAGAGAAGGACATATGATTATGTGCGTAAAACGCCCTTCTCTGACCGATGGGAATGGTTGACTAGTACATGACCACTTGA  
36-49 TAGGGAAGAGAAGGACATATGATCATGTCCAGCATTGCTGTTCTCTGACCAACCGGTTGGCATTGACTAGTACATGACCACTTGA  
40-48 TAGGGAAGAGAAGGACATATGATTAAT--TGTGCTTAGCCTACTCTGACCGCAGTGTGGAATTGACTAGTACATGACCACTTGA  
96-24 TAGGGAAGAGAAGGACATATGATGTTGAAAGCCCTATCAATGGTTCGCGAGTATCGCATGTAAGTTGACTAGTACATGACCACTTGA  
28-56 TAGGGAAGAGAAGGACATATGATAATAGCGTCCACGTAAGTTTCTCGACCGGCGAGTTGGGAGTTGACTAGTACATGACCACTTGA  
2-218 TAGGGAAGAGAAGGACATATGATGGCCACGTTAGTTTCTCTGACCGCAATTACAAGTGTGAGTTGACTAGTACATGACCACTTGA  
27-56 TAGGGAAGAGAAGGACATATGATGGCCACGAAAGTTTCTCTGACCGTCCGAAAGCAGCACTAGGTTGACTAGTACATGACCACTTGA  
100-24 TAGGGAAGAGAAGGACATATGATGGCCCCGAAAGGTTCTCTTACCGGCTTTAGGAAGTACTCGTTGACTAGTACATGACCACTTGA  
87-27 TAGGGAAGAGAAGGACATATGATCTCGGACCGGAGGCTGACCGAAGTGAGGAATTCGTACCTATTGACTAGTACATGACCACTTGA  
94-25 TAGGGAAGAGAAGGACATATGATCT--CGACCGGAGGTTGACCGAAGTGAGGAATTCGTACCTATTGACTAGTACATGACCACTTGA  
39-48 TAGGGAAGAGAAGGACATATGATAAATCATGCTTCTCCGCTACGTTGTTTGCCTTCCCTTGAAGTTGACTAGTACATGACCACTTGA  
33-51 TAGGGAAGAGAAGGACATATGATTATATGCTCTGCTCCTTCTCTCGCACTATATTGCTTCCCTTGACTAGTACATGACCACTTGA  
16-78 TAGGGAAGAGAAGGACATATGATGGCCATCGGACCGGATTTCTCTTCCATTAATAAGAGGGGCTTGACTAGTACATGACCACTTGA  
17-72 TAGGGAAGAGAAGGACATATGATCATAGTACGGAACGCTTCTCTGACCCATTAACCTGCGGCTTGACTAGTACATGACCACTTGA  
75-31 TAGGGAAGAGAAGGACATATGATTGGCCACTACAGCAGCTGGAAGTTTCTCGTACCGGCGGCTTGACTAGTACATGACCACTTGA  
80-28 TAGGGAAGAGAAGGACATATGATTGGCCACTGGAACAGTTTCTCTTCCATATTTGGTGGTATTGACTAGTACATGACCACTTGA  
91-26 TAGGGAAGAGAAGGACATATGATGACGCTCTGACCTGGTCATTGCGAAAGCAGTACCTATCTTTGACTAGTACATGACCACTTGA  
76-31 TAGGGAAGAGAAGGACATATGATATTGGCCGTAACACCGTTACTTCTCTGACCTTCATGTTACTTGACTAGTACATGACCACTTGA  
41-46 TAGGGAAGAGAAGGACATATGATCAATCATGGCAGTTAGTCTTCTGGGTTCCCTTGCCTGGTGGTTGACTAGTACATGACCACTTGA

13-89 TAGGGAAGAGAAGGACATATGATCCGACATCTGACCACGGGGAATGCCAGAGGCGTACTATGCTTGACTAGTACATGACCACTTGA  
95-25 TAGGGAAGAGAAGGACATATGATAATATGCGATAGCGTCTCTTCGGGTTACCTACAATGTGGATTGACTAGTACATGACCACTTGA  
7-105 TAGGGAAGAGAAGGACATATGATGTCGCGCACAGGAGCCCTTCGACGGGCCCTAAAGTGTGCTTGACTAGTACATGACCACTTGA  
46-42 TAGGGAAGAGAAGGACATATGATACGTCACACCTGGCACAGGTTTTCTCTTCATGCGTGGTTCCTTGACTAGTACATGACCACTTGA  
1-318 TAGGGAAGAGAAGGACATATGATGTCCTTCACTGTATGCTATACGCATTACTCCCTAAGTGGCATTGACTAGTACATGACCACTTGA  
85-27 TAGGGAAGAGAAGGACATATGATGTC AATGTGTACACATTCTCTCCGACC GG TAGTGTAGGCTTGACTAGTACATGACCACTTGA  
81-28 TAGGGAAGAGAAGGACATATGATGGCCGCCGTTAATAACGGCTTCTCTGACC GTAGT CAGGGCTTGACTAGTACATGACCACTTGA  
20-70 TAGGGAAGAGAAGGACATATGATAAGATGTCGCCGTAGGCCCTCTCGCACACTATACTGGGCTTGACTAGTACATGACCACTTGA  
30-53 TAGGGAAGAGAAGGACATATGATATCATATGCGTTAGCGTCTTCTTCGACCCTAACATGGGCTTGACTAGTACATGACCACTTGA  
3-207 TAGGGAAGAGAAGGACATATGATGTCAAATGTGGAACATTTCTTCTCTGACCATCGGTGGCGCTTGACTAGTACATGACCACTTGA  
53-38 TAGGGAAGAGAAGGACATATGATGTCAACTGCGTAGAAGTTCTGCTCGGACC ACTGAGGGGTATTGACTAGTACATGACCACTTGA  
19-70 TAGGGAAGAGAAGGACATATGATACTTCTCGACCCGCGGGAATTGCATCCGAGTACTGTCCATTGACTAGTACATGACCACTTGA  
15-80 TAGGGAAGAGAAGGACATATGATCCTTGTCAAATTAATCCATTGACCTCTTCCGGGTGTTCAATTGACTAGTACATGACCACTTGA  
67-34 TAGGGAAGAGAAGGACATATGATCCTTCTGCCATCCTTGGAGGTGGGCCTTCCCACGTGCTCATTGACTAGTACATGACCACTTGA  
43-44 TAGGGAAGAGAAGGACATATGATCCTGAACGCCCGGT CATACGATGTAATCGTGTACGGTACTTGACTAGTACATGACCACTTGA  
11-99 TAGGGAAGAGAAGGACATATGATGGCCCGGGAACCGTTCCTCTGAGCCAAGCTGGGTACGTCGATTGACTAGTACATGACCACTTGA  
57-37 TAGGGAAGAGAAGGACATATGATGAGCCTTACTCTGCGGGACAGGCCCCCGCTCCCTAGGTCACTTGACTAGTACATGACCACTTGA  
4-137 TAGGGAAGAGAAGGACATATGATCCAGAGGTAATATGCGTAGCGTCCGATCTTCACATCGTGGTTGACTAGTACATGACCACTTGA  
83-27 TAGGGAAGAGAAGGACATATGATGTCGCGTAAGCCTTCTCGACCTTCTTCAGCGTTATCGTGGTTGACTAGTACATGACCACTTGA  
59-36 TAGGGAAGAGAAGGACATATGATGGTCCACGGGGAATCCTCGTTTTCGTTTCCAACAATGGGATTGACTAGTACATGACCACTTGA  
23-63 TAGGGAAGAGAAGGACATATGATGGCCAACCGGTATCCGGAAGTTTCTCTGACC ACTGGTGGTTGACTAGTACATGACCACTTGA  
29-54 TAGGGAAGAGAAGGACATATGATGGCCAAGTAAACCTTACTTTCTCGCACCGAACATGTGGTTGACTAGTACATGACCACTTGA  
98-24 TAGGGAAGAGAAGGACATATGATTAATAGTCCGGTTTAGCCGCTTCTCGACCCGCTTTGTGGTTGACTAGTACATGACCACTTGA  
73-32 TAGGGAAGAGAAGGACATATGATAATATGGATGCGTAATCCGCTTCTTCTCGGACC ACCGTTGGTTGACTAGTACATGACCACTTGA  
79-29 TAGGGAAGAGAAGGACATATGATAGTCCAGCGCGT GAGCATGCTTTCTCGACCCGCTTTGTGGTTGACTAGTACATGACCACTTGA  
52-38 TAGGGAAGAGAAGGACATATGATGTCGCCCTCGACCGATAGTGGGAATGAGTTTATCTCGTACTTGACTAGTACATGACCACTTGA  
82-27 TAGGGAAGAGAAGGACATATGATACAACAATGTGCTTCACGGTAGTCTTCCCTGTGTGCGTCTTGACTAGTACATGACCACTTGA  
9-100 TAGGGAAGAGAAGGACATATGATCCATATGTGCGAAGCACGTC CGATCTCCCTAACCGGTGGCTTGACTAGTACATGACCACTTGA  
31-52 TAGGGAAGAGAAGGACATATGATAACATGTCTCGGGATAGGCCGACTTCTCTGACCCTTGTCATTGACTAGTACATGACCACTTGA  
84-27 TAGGGAAGAGAAGGACATATGATCCGCACTCGCAATGGAGAACCGTAATGCTTCCCGTGTGGTTGACTAGTACATGACCACTTGA  
42-46 TAGGGAAGAGAAGGACATATGATCCGAAGCTTCCCGCGGGTCAATTGGTAAACCAAGTACTATCTTGACTAGTACATGACCACTTGA  
22-64 TAGGGAAGAGAAGGACATATGATCCTCTCCATCGCTCGTAGTGCATGTTCCCTTCGTGGCATTGACTAGTACATGACCACTTGA  
48-41 TAGGGAAGAGAAGGACATATGATGGCCGCGATCGTACCCCTGGGCATCAACAGAGTTGGTACTTGACTAGTACATGACCACTTGA  
61-35 TAGGGAAGAGAAGGACATATGATCCGCGGCTTCCCTGGTCAATGCACAATTACAGTGTGCGTACTTGACTAGTACATGACCACTTGA  
78-29 TAGGGAAGAGAAGGACATATGATGTCGCGTTGGTAGGCGCCTTCTCTGGACTGAGATGGTTTGTGACTAGTACATGACCACTTGA  
32-52 TAGGGAAGAGAAGGACATATGATCATACGTCAAGCGCAATCGTCTTCTCGATGACC GGCTCTGTTGACTAGTACATGACCACTTGA  
72-32 TAGGGAAGAGAAGGACATATGATGTCACCGCAGGCTTCTCGCATCCGAGGTTGTAGGGGTTGTTGACTAGTACATGACCACTTGA  
10-100 TAGGGAAGAGAAGGACATATGATGGCCGCAACTTGTGTGCTTCCGATGACC CGCAAGTCGGAATGTTTGGACTAGTACATGACCACTTGA  
44-44 TAGGGAAGAGAAGGACATATGATCCGGCTCTGAACCAGGGTGTACATACCAGGCTCTGGTACTTGACTAGTACATGACCACTTGA  
25-59 TAGGGAAGAGAAGGACATATGATTCTCTGACCGAGTGTATCATCACAAGTATGGTATCTGGTTGACTAGTACATGACCACTTGA  
65-34 TAGGGAAGAGAAGGACATATGATGTCGCACAAGGTGCCCTTACTCGACCGTAACGGTGGTAATATTGACTAGTACATGACCACTTGA  
86-27 TAGGGAAGAGAAGGACATATGATATGTCGCTGCACCGT CAGCCTTCTCGACCGAGGTTAATGTTTGGACTAGTACATGACCACTTGA  
89-26 TAGGGAAGAGAAGGACATATGATGTCGTCGTCGCTTACCTTCTCGACCCCGGTATGTGGTTGACTAGTACATGACCACTTGA  
26-58 TAGGGAAGAGAAGGACATATGATCCAATATGACGAAGT CGTCTTCTCGGACC GCGGTGGCGTTGACTAGTACATGACCACTTGA  
74-32 TAGGGAAGAGAAGGACATATGATGGACTGTGATTTTACTATCACTCTCTGACCGCACGTTGGCTTGACTAGTACATGACCACTTGA  
21-64 TAGGGAAGAGAAGGACATATGATGACCGAGCGAACC GTGGATGGTCCCAACGCATTTGGATGTATTGACTAGTACATGACCACTTGA  
90-26 TAGGGAAGAGAAGGACATATGATGTCAGGCACCGCTCTTCTCTGACCGGCTTTGGGAAATAGTTGACTAGTACATGACCACTTGA  
38-49 TAGGGAAGAGAAGGACATATGATGGCCGCCGATGCCCTGGGT CATCCCATAAGGGGTACAAGTTGACTAGTACATGACCACTTGA  
37-49 TAGGGAAGAGAAGGACATATGATATGTCGCGGAAGCCTTCGCTTCTACTAATCGTGGGACCTGTTGACTAGTACATGACCACTTGA  
66-34 TAGGGAAGAGAAGGACATATGATCTGTCACGGTTAATGCCGCTCTTCTCTGAA CCGCTGTGGGATTGACTAGTACATGACCACTTGA

**Figure S4.4.** Sequence motif encountered in 52 % of the 100 most abundant sequences using the MEME tool of the MEME Suite <sup>5</sup>.



### 4.6.3. Aptamer characterization

**Table S4.2** Sequences of the selected aptamer candidates and the motif sequence.

	Sequence (5' to 3')	Length (nt)
<b>Nand1</b>	TAGGGAAGAGAAGGACATATGATGTCTTCACTGTATGCTATACGCATTACTCC CTAAGTGGCATTGACTAGTACATGACCACTTGA	86
<b>Nand2</b>	TAGGGAAGAGAAGGACATATGATGGCCACGTTAGTTTCTCTGACCGACAATT ACAAGTGTGAGTTGACTAGTACATGACCACTTGA	86
<b>Nand3</b>	TAGGGAAGAGAAGGACATATGATGTCAAATGTGGAACATTTCTTCTCTGACCA TCGGTGGCGCTTGACTAGTACATGACCACTTGA	86
<b>Motif</b>	CTTCTCTGACC	11

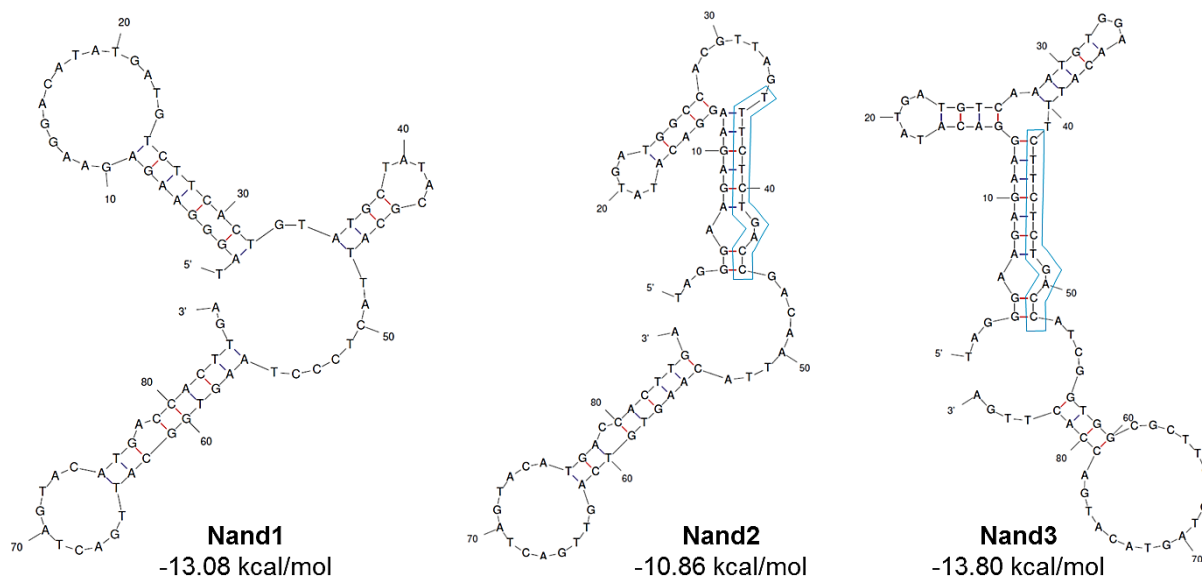


**Figure S4.5.** Secondary structures of the nandrolone aptamer candidates predicted by the UNAFold webserver [6] (100 mM NaCl and 2 mM MgCl<sub>2</sub>, at 25°C). The sequence motif encountered in Nand2 and Nand3 sequences is boxed.

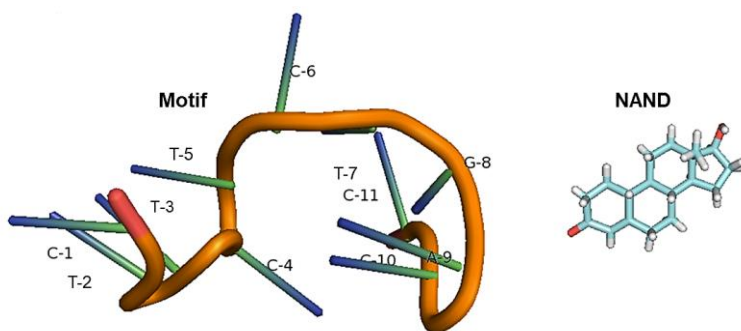


**Figure S4.6.** Predicted structure of the motif sequence and comparison of its size with NAND. The motif structure was predicted with the RNAComposer webserver <sup>7</sup>.

#### 4.6.4 AuNPs-aptamer assay for NAND detection

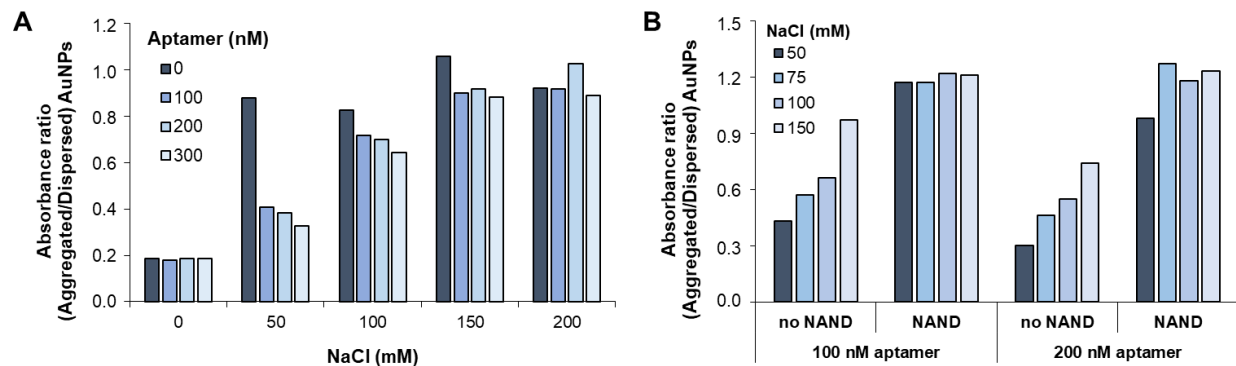


**Figure S4.7.** Optimization of Nand3 aptamer and NaCl concentrations. (A) Nand3 aptamer (0 – 300 nM) was used in combination with NaCl (0 – 200 mM) in the absence of NAND. (B) The aptamer (100 and 200 nM) was used in combination with NaCl (50 – 150 mM) in the absence and presence of NAND (200  $\mu$ M).

**Table S4.3** Sensitivity of the AuNP-aptamer assay for NAND detection using different concentrations of aptamer and NaCl.

Nand3 aptamer (nM)	75 mM NaCl			100 mM NaCl		
	LOD ( $\mu$ M)	R <sup>2</sup>	Span	LOD ( $\mu$ M)	R <sup>2</sup>	Span
100	3.4	0.9810	0.62	0.8	0.9935	0.41
150	3.5	0.9868	0.81	4.8	0.9701	0.42
200	13.4 *	0.9834	na	1.1	0.9940	0.50

\* ambiguous fit of the calibration curve; n.a.: not available



**Figure S4.8.** Color change of samples containing increasing concentration of nandrolone analyzed with the AuNPs-Nand3 aptamer assay.

#### 4.6.5 References

- (1) Jiang J., Zhang H., Li G., Wang Z., Wang J., Zhao H. (2011). Preparation of anti-nortestosterone antibodies and development of an indirect heterologous competitive enzyme-linked immunosorbent assay to detect nortestosterone residues in animal urine. *Analytical Letters*, <https://doi.org/10.1080/00032719.2010.551694>.
- (2) Skouridou V., Jauset-Rubio M., Ballester P., Bashammakh A.S., El-Shahawi M.S., Alyoubi A.O., O'Sullivan C.K. (2017). Selection and characterization of DNA aptamers against the steroid testosterone. *Microchimica Acta*, <https://doi.org/10.1007/s00604-017-2136-0>.
- (3) Jauset-Rubio M., Botero M.L., Skouridou V., Aktas G.B., Svobodova M., Bashammakh A.S., El-Shahawi M.S., Alyoubi A.O., O'Sullivan C.K. (2019). One-Pot SELEX: identification of specific aptamers against diverse steroid targets in one selection. *ACS Omega*, <https://doi.org/10.1021/acsomega.9b02412>.
- (4) Madeira F., Park Y.M., Lee J., Buso N., Gur T., Madhusoodanan N., Basutkar P., Tivey A.R.N., Potter S.C., Finn R.D., Lopez R. (2019). The EMBL-EBI search and sequence analysis tools APIs in 2019. *Nucleic Acids Research*, <https://doi.org/10.1093/nar/gkz268>.
- (5) Bailey T.L., Bodén M., Buske F.A., Frith M., Grant C.E., Clementi L., Ren J., Li W.W., Noble W.S. (2009). MEME SUITE: tools for motif discovery and searching. *Nucleic Acids Research*, <https://doi.org/10.1093/nar/gkp335>.
- (6) Zuker M. (2003). Mfold web server for nucleic acid folding and hybridization prediction. *Nucleic Acids Research*, <https://doi.org/10.1093/nar/gkg595>.
- (7) Popena M., Szachniuk M., Antczak M., Purzycka K.J., Lukasiak P., Bartol N., Blazewicz J., Adamiak R.W. (2012). Automated 3D structure composition for large RNAs. *Nucleic Acids Research*, <https://doi.org/10.1093/nar/gks339>.

## **List of Figures**

**Figure 1.1.** Number of publications as a function of the years involving the research in aptamers. (Data extracted from PubMed).

**Figure 1.2.** (A) stem-loop/ bulge (RNA ligand for ATP), (B) G-quartet (DNA ligand for thrombin), (C) Pseudoknot (RNA ligand for HIV-1 reverse transcriptase), (D) hairpin (RNA ligand for Bacteriophage T4 polymerase).

**Figure 1.3.** A schematic diagram of ssDNA oligonucleotide.

**Figure 1.4.** Schematic overview of SELEX cycle.

**Figure 1.5.** A chart that represents the selected aptamer per each target type.

**Figure 1.6.** Schematic representation of Magnetic bead-based SELEX.

**Figure 1.7.** Schematic representation of GO-SELEX.

**Figure 1.8.** Schematic representation of Capture-SELEX.

**Figure 2.1.** Selection of TTX-binding aptamers. (A) Structures of the target TTX (upper panel) and the counter selection molecules (lower panel). (B) Evolution of the selections using Dynabeads and SiMAG SA-MB. DNA eluting in the presence of buffer alone or TTX under the specific conditions from the selected rounds was detected after PCR amplification.

**Figure 2.2.** Hybrid antibody-aptamer assay for the detection of TTX. (A) TTX calibration curve with the monoclonal IgG antibody-D3 aptamer pair. (B) Specificity of the assay.

**Figure S2.1.** Abundance of highly abundant sequences in the last selection round of the target and counter selection molecules pools using Dynabeads SA-MB for library immobilization

**Figure S2.2.** Abundance of highly abundant sequences in the last selection round of the target and counter selection molecules pools using SiMAG SA-MB for library immobilization.

**Figure S2.3.** Multiple sequence alignment of the 100 most abundant sequences in the TTX target pool from round 23 of the selection performed with the Dynabeads SA-MB. Identical bases are shaded, and the three most enriched sequences selected for characterization are in boxes.

**Figure S2.4.** Multiple sequence alignment of the 100 most abundant sequences in the TTX target pool from round 23 of the selection performed with the SiMAG SA-MB. Identical bases are shaded and the three most enriched sequences selected for characterization are in boxes.

**Figure S2.5.** Screening of the aptamer candidates with a displacement assay. Aptamer candidates immobilized on docking probe-streptavidin magnetic beads complexes were incubated with 100  $\mu$ M TTX (+) or only binding buffer (-). Aptamer displacing to the solution was detected by PCR amplification and agarose gel electrophoresis. ntc: PCR no template control.

**Figure S2.6.** Binding curves of the aptamers determined by (A) APAA and (B) bead-ELAA

**Figure S2.7.** Predicted structures of the five selected TTX aptamers.

**Figure S2.8.** Screening of antibody-aptamer pairs for sandwich assay development.

*Scheme 3.1.* Schematic illustration of the dipstick assay for the simple and rapid detection of TTX. (A) Structure of the dipstick strip (B) TTX present in the sample is capture by monoclonal TTX antibody in the test line where later is captured by biotinylated aptamer and AuNPs-SA, while the excess of biotin-aptamer and SA-AuNPs is captured through complementary hybridization on reverse primer immobilized in the control line, resulting in two red lines. (C) When TTX is not present, there is no binding on monoclonal TTX antibody on the test line and the biotin-aptamer with AuNPs-SA run along the nitrocellulose membrane by capillary action and are captured by the reverse primer immobilized on the control line resulting in one red line. Dipstick assay results for positive tests (left) and for negative test (right).

**Figure 3.1.** UV-visible spectrum of pure AuNPs and AuNPs-SA conjugate.

**Figure 3.2.** Optimization of control line DNA probe. In this experiment 0.4  $\mu$ L (100  $\mu$ M) of each aminated probe was directly immobilized on control line via UV-crosslinking (A) Using aminated docking probe. and (B) Using aminated reverse prime.

**Figure 3.3.** Optimization of AuNPs-SA OD in dipstick format for control and test line. Three different OD (10,15,20) of AuNPs-SA were analyzed in order to obtain the best visual

intensity spot on the test and control line. Moreover, to increase the specificity of the dipstick format 2 different concentration of monoclonal TTX antibody were tested, 0.4 uL (of 1.5mg/mL stock) (left) and 0.5 uL (of 1.5mg/mL stock)(right).As it is shown here there is no significant difference between the different OD used for the same concentration of TTX samples, but there is an improvement of the assay sensitivity when using higher volume of monoclonal TTX antibody.

**Figure 3.4.** Image of the dipstick strips demonstrate the sensitivity of the assay using a range of TTX concentration starting from 200 ng/ml to 0.7 ng/mL using 1 in 2 dilutions and the control strip (0 ng/mL TTX) step.

**Figure 3.5.** Cross-reactivity experiment for the dipstick experiment using 4 different marine toxins (OA, STX, DA, and TTX).

**Figure 3.6.** The successful application of the dipstick assay was evaluated by analysing 4 different fish extracts, gonads (G), liver (L), skin (S), and muscle (M).

**Figure 4.1.** Selection strategy and evolution of the process. (A) Conditions used for SELEX. (B) Evolution of the selection. (C) Specificity of the last selection round.

**Figure 4.2.** NGS analysis of round 7 from the nandrolone selection. (A) General statistics. (B) Composition of the top 100 most abundant unique sequences.

**Figure 4.3.** Evaluation of the affinity of the aptamer candidates for nandrolone. Binding curves obtained by (A) APAA, (B) bead-ELAA and (C) ELAA. (D) Affinity dissociation constants.

**Figure 4.4.** Specificity of the aptamers using bead-ELAA.

**Figure 4.5.** AuNP-aptamer assay for NAND detection. (A) Principle of the assay. (B) Representative spectra of samples containing different concentrations of NAND. (C) Calibration curve for NAND quantification.

**Figure S4.1.** Structures of the steroids used in this work. (A) The target steroid nandrolone. (B) Nandrolone-sepharose® 6B resin used for SELEX. (C) Other steroids used for counter-SELEX. The asterisks (\*) denote the carbon atoms on the steroid structures carrying the carboxymethyloxime (CMO) modification facilitating steroid immobilization on amine-modified magnetic beads.

**Figure S4.2.** Confirmation of the immobilization of various steroids on sepharose resin.

**Figure S4.3.** Multiple sequence alignment of the 100 most abundant unique sequences of library-length (80 – 95 bp) using Clustal Omega. The first number denotes the ranking of the sequence and the second one the number of copies. The common sequence motif is underlined.

**Figure S4.4.** Sequence motif encountered in 52 % of the 100 most abundant sequences using the MEME tool of the MEME Suite.

**Figure S4.5.** Secondary structures of the nandrolone aptamer candidates predicted by the UNAFold webserver<sup>6</sup> (100 mM NaCl and 2 mM MgCl<sub>2</sub>, at 25°C). The sequence motif encountered in Nand2 and Nand3 sequences is boxed.

**Figure S4.6.** Predicted structure of the motif sequence and comparison of its size with NAND. The motif structure was predicted with the RNAComposer webserver.

**Figure S4.7.** Optimization of Nand3 aptamer and NaCl concentrations. (A) Nand3 aptamer (0 – 300 nM) was used in combination with NaCl (0 – 200 mM) in the absence of NAND. (B) The aptamer (100 and 200 nM) was used in combination with NaCl (50 – 150 mM) in the absence and presence of NAND (200 μM).

**Figure S4.8.** Color change of samples containing increasing concentration of nandrolone analyzed with the AuNPs-Nand3 aptamer assay.

## **List of Tables**

**Table 1.1.** Characteristics for antibodies and aptamers.

**Table 1.2.** List of some modified SELEX methods which are commonly used.

**Table 1.3.** Commercially available chemically modified matrixes used for the immobilization of small molecules for their aptamer selection.

**Table 1.4.** Example of different specific aptamers selected via Capture SELEX.

**Table 1.5.** The advantages and limitations of lateral flow assay.

**Table 1.6.** Aptamers in lateral flow (adapted from reference 324)

**Table 2.1.** NGS data analysis of selected pools from the two selections.

**Table 2.2.** Affinity dissociation constants of the aptamer candidates determined by APAA and bead-ELAA.

**Table 2.3.** Detection of TTX in puffer fish extracts. Recovery (%) of TTX spiked in diluted extracts from a TTX-free fish (*L. lagocephalus*). TTXs content (mg TTX equiv./kg of tissue) in extracts from a TTX-containing fish (*L. scleratus*) were determined using calibration curves constructed in PBS buffer and in the respective extract from the TTX-free fish.

**Table S2.1.** Conditions used for the selections.

**Table S2.2.** Distribution (%) of highly abundant sequences in the different pools from the two selections. Sequences were ranked according to their abundance in the TTX pool from round 23.

**Table S2.3.** Sequences of the selected aptamer candidates. D sequences were identified from the selection with Dynabeads and C sequences with the SiMAG SA-MB.

**Table S2.4.** Hybrid antibody-aptamer assay precision. Inter-assay coefficients of variation (% CV) were calculated from duplicate samples using solutions of different TTX concentration measured on four different days (n=4).

**Table S2.5.** Assays and biosensors reported in the literature for TTX detection.

**Table S2.6.** TTX and analogues contents (mg TTX or analogue/kg tissue) in *L. scleratus* by LC-MS/MS.

**Table S4.1.** Abundance (%) of the 100 most over-represented unique sequences.

**Table S4.2.** Sequences of the selected aptamer candidates and the motif sequence.

**Table S4.3.** Sensitivity of the AuNP-aptamer assay for NAND detection using different concentrations of aptamer and NaCl.

## **Abbreviations**

SELEX	Systematic Evolution of Ligands by EXponential Enrichment
K <sub>D</sub>	Dissociation constants
FDA	Food and Drug Administration

AMD	Age-related Macular Degeneration
PEG	Polyethylene glycol
ELISA	Enzyme-Linked Immunosorbent Assay
EGFR	Epidermal growth factor receptor
Bn-dU	2-deoxyuridine
Nap-dU	5-[N-(1-naphthylmethyl) carboxamide]-2-deoxyuridine
PKC	Protein kinase C
bFGF	basic Fibroblast Growth Factor
VEGF	Vascular Endothelial Growth Factor
HNE	Human Neutrophil Elastase
IL-1	Inhibit Interleukin-1
ASO	Antisense Oligonucleotide
AML	Acute Myeloid Leukemia
AMV RT	Avian Myeloblastosis Virus reverse transcriptase
A	Adenine
T	Thymine
G	Guanine
C	Cytosine
OTA	Ochratoxin
G4	G-quadruplex
SDS	Sodium Dodecyl Sulfate
EDTA	Ethylenediaminetetraacetic acid
dsDNA	Double stand DNA
HEGL	Hexaethylene Glycol
poly A	adenine nucleotides
SPR	Surface Plasmon Resonance
ELONA	Enzyme-Linked Oligonucleotide Assay
EMSA	Electrophoretic Mobility Shift Assay
FACS	Fluorescence-Activated Cell Sorting
PCR-RFLP	PCR-restriction, fragment length polymorphism
NMR	Nuclear Magnetic Resonance
NGS	Next Generation Sequence
MST	MicroScale Thermophoresis
GO-SELEX	Graphene Oxide-SELEX
CE	Capillary Electrophoresis
NECEEM	Non-Equilibrium Capillary Electrophoresis of Equilibrium Mixtures
ECEEM	Equilibrium capillary electrophoresis of equilibrium mixtures
FFE	Free Flow Electrophoresis
M-SELEX	Microfluidic SELEX

HTS	high-throughput-sequencing
CRC	intrahepatic colorectal cancer
BSA	Bovine serum albumin
OVA	Ovalbumin
KLH	Keyhole limpet hemocyanin
NHS	N-hydroxy succinimide
GO	Graphene oxide
PAGE	Polyacrylamide gel electrophoresis
OA	Okadaic acid
PAT	Patulin
APAA	Apta-PCR affinity assay
ELAA	Enzyme linked aptamer assay
ITC	isothermal titration calorimetry
TTMB	Tetramethylbenzidine
OD	Optical density
DON	Deoxynivalenol
IgE	Human immunoglobulin E
MST	Microscale Thermophoresis
ATP	Adenosine triphosphate
APPA	Apta-PCR affinity assay
ITC	Isothermal Titration Calorimetry
$K_D$	equilibrium binding constant
$\Delta H$	Enthalpy
$\Delta S$	Entropy
BLI	Bi-layer interferometry
CCD	Charge coupled device
cAMP	Cyclic monophosphate
QDs	Quantum dots
FRET	Fluorescence resonance energy transfer
AuNPs	Gold nanoparticles
FRET	Fluorescence resonance energy transfer
Cy5/FAM	Cy5/Fluorescein Amidite
RQ/BHQ	Low Black Hole Quencer
TAMRA	Carboxytetramethylrhodamine
GMPs	Gold capped magnetic nanoparticles
CNTs	Carbon nanotubes
CPs	Conducting polymers
MNPs	Metal nanoparticles
SPE	Screen-printed electrode

GNPs-GNSs	Gold nanoparticles-graphene nanosheets
EFSA	European Food Safety Authority
TEF	Toxicity equivalency factors
LC-MS/MS	Liquid chromatography coupled with mass spectrometry
SA-MB	Streptavidin-magnetic beads
DA	Domoic acid
STX	Saxitoxin
APAA	Apta-PCR Affinity Assay
MBA	Mouse bioassay
TCBA	Tissue culture bioassay
AAS	Anabolic androgenic steroids
WADA	World Anti-Doping Agency
GC-MS	Gas chromatography-mass spectrometry
GC-IRMS	Gas chromatography-isotope ratio mass spectrometry
UHPLC-MS	Ultra-high-performance liquid chromatography coupled with mass spectrometry
HPTLC	High-performance thin-layer chromatography
LOD	Limits of detection
TEST	Testosterone
TREN	Trenbolone
NAND	Nandrolone
ITC	Isothermal titration calorimetry

## **List of publication**

### **1. Aptasensors for mycotoxin detection: A review**

Xhensila Shkembi, Marketa Svobodova Vasso Skouridou Abdulaziz S. Bashammakh  
Abdulrahman O. Alyoubi Ciara K. O'Sullivan

### **2. Hybrid antibody-aptamer assay for detection of tetrodotoxin in puffer fish**

Xhensila Shkembi, Vasso Skouridou, Marketa Svobodova, Sandra Leonardo, Abdulaziz  
S. Bashammakh, Abdulrahman O. Alyoubi, Mònica Campàs, Ciara K. O'Sullivan (in  
review)

### **3. Dipstick antibody-aptamer assay for detection of tetrodotoxin in puffer fish**

Xhensila Shkembi, Vasso Skouridou, Marketa Svobodova, Sandra Leonardo, Abdulaziz  
S. Bashammakh, Abdulrahman O. Alyoubi, Mònica Campàs, Ciara K. O'Sullivan (in  
preparation)

### **4. Novel nandrolone aptamer for rapid colorimetric detection of anabolic steroids**

Xhensila Shkembi, Mary Luz Botero , Vasso Skouridou , Miriam Jauset-Rubio , Marketa  
Svobodova , Pablo Ballester , Abdulaziz S. Bashammakh , Mohammad S. El-Shahawi ,  
Abdulrahman O. Alyoubi , Ciara K. O'Sullivan (in preparation)



UNIVERSITAT  
ROVIRA i VIRGILI